WAVES SERIES

# Introduction to Quantum Mechanics 1

## Thermal Radiation and Experimental Facts Regarding the Quantization of Matter

Ibrahima Sakho

iSTE

WILEY

# Introduction to Quantum Mechanics 1

*I dedicate this book to my son Abdallah*
*and to his mother Mariama Diallo*

# Introduction to Quantum Mechanics 1

## *Thermal Radiation and Experimental Facts Regarding the Quantization of Matter*

Ibrahima Sakho

iSTE

WILEY

First published 2019 in Great Britain and the United States by ISTE Ltd and John Wiley & Sons, Inc.

ISTE Ltd
27-37 St George's Road
London SW19 4EU
UK

www.iste.co.uk

John Wiley & Sons, Inc.
111 River Street
Hoboken, NJ 07030
USA

www.wiley.com

Library of Congress Control Number: 2019944514

British Library Cataloguing-in-Publication Data
A CIP record for this book is available from the British Library
ISBN 978-1-78630-487-2

# Contents

# Foreword

Founded in 1925 and 1926 by Werner Heisenberg, Erwin Schrödinger and Paul Dirac, quantum mechanics is nearly 100 years old. Being the basis of modern technology, it has given rise to countless applications in physics, chemistry and even biology. The relevant literature is very rich, counting works written in many languages and from various perspectives, addressing a broad audience, from beginner students and teachers to expert researchers in the field.

Professor Sakho has chosen the former as the target audience of this book, connecting the quarter of a century that preceded the initiation of quantum mechanics and its first results. The book is organized in two volumes. The first deals with thermal radiation and the experimental facts that led to the quantization of matter. The second volume focuses on the Schrödinger equation and its applications, Hermitian operators and Dirac notations.

The clear and detailed presentation of the notions introduced in this book reveals its constant didactic concern. A particular element of originality of this book is the broad range of approaches used throughout its chapters:

– the course includes many solved exercises, which complete the presentation in a concrete manner;

– the presentation of experimental devices goes well beyond idealized schematic representations and illustrates the nature of laboratory work;

– more advanced notions (semiconductors, relativistic effects in hydrogen, Lamb shift, etc.) are briefly introduced, always in relation with more fundamental concepts;

– the biographical boxes give the subject a human touch and invite the reader to anchor the development of a theory in its historical context.

The book concludes with a list of references and a detailed index.

Science is a key element of contemporary culture. Researchers’ efforts to write the books required for students’ education are praiseworthy. Undergraduate students and teachers will find this work especially beneficial. We wish it a wide distribution.

Louis MARCHILDON
Professor Emeritus of Physics
University of Quebec at Trois-Rivières
July 2019

# Preface

Quantum mechanics or the physics of the infinitely small (microcosm) is often contrasted with classical mechanics or the physics of macroscopic bodies (macrocosm). This book, whose title is *Introduction to Quantum Mechanics 1*, aims to equip the reader with the basic tools that are essential for a good understanding of the physical properties of atoms, nuclei, molecules, lasers, solid bodies and electronic materials, in short all that is infinitely small. Introductory courses on quantum mechanics generally focus on the *study of the interaction between matter and radiation and the quantum states of matter*. This book emphasizes the various experiments that led to discoveries within the set of physical phenomena related to the properties of quantum systems. Consequently this book is composed of seven chapters organized in two volumes. Each chapter starts with a presentation of the general objective, followed by a list of specific objectives and finally by a list of prerequisites essential for a good understanding of the concepts introduced. Furthermore, the introduction of each law follows a simple application. Each chapter ends with a collection of various exercises and solutions that facilitate the assimilation of all the concepts presented. Moreover, brief biographies of all the thinkers who contributed to the discovery of the studied physical laws or phenomena are given separately, as the chapter unfolds. The reader can this way acquire a sound scientific culture related to the evolution of scientific thought during the elaboration of quantum mechanics. Due to its structuring and didactic approach, this work is a modern and very original book. Volume 1 covers the study of the first four chapters related to *thermal radiation* and the *experimental facts* that revealed the *quantization of matter*.

Chapter 1 deals with the study of the characteristics of *thermal radiation.* The study of the black body radiation spectrum makes it possible to establish the *fundamental laws of radiation*, namely *Lambert's law*, *Kirchhoff's laws*, the *Stefan–Boltzmann law*, *Wien's laws*, the *Rayleigh–Jeans law* and *Planck's law*. The statement of these laws is an opportunity to introduce the main *energy-related* *quantities* characterizing thermal radiation such as *radiance*, *light intensity*, *total radiant exitance* and *monochromatic radiant exitance*. Chapter 2 is dedicated to the *wave and particle aspects* of light. *Light interferences*, highlighting the wave nature of light, as well as the *photoelectric effect* and the *Compton effect*, evidencing the particle nature of light, are studied. The chapter is completed by the study of the *wave–particle duality*, combining wave and particle properties of light as a flow of photons. Chapter 3 reviews the main experiments leading to the discovery of the four *quantum numbers* of the electron. This chapter studies in particular *Bohr's model of the atom*, which introduces the *main quantum number*, *Sommerfeld's model of the atom*, which introduces the *angular momentum quantum number,* as well as the *magnetic quantum number* using the interpretation of the *normal Zeeman effect*. This is followed by the study of the *Stern-Gerlach experiment* and *Uhlenbeck and Goudsmit* hypothesis, which led to the introduction of *electron spin*. The chapter ends with an introduction of the *spectroscopic notation* of quantum states based on the properties of the *total quantum number* of the electron. This spectroscopic notation makes it possible to explain the *fine structure* of the energy levels arising from the *spin-orbit coupling* and also to interpret the *anomalous (*or *complex) Zeeman effect*. Chapter 4 focuses on the study of *de Broglie's wave theory* based on the notion of *matter waves* and on *Heisenberg's uncertainty principle*, which facilitated the elaboration of quantum mechanics.

Volume 2 is dedicated to three chapters dealing with the study of Schrödinger's equation and applications, Hermitian operators and Dirac notations, respectively.

The book ends with a set of five appendices that help the reader gain in-depth knowledge on the physical phenomena studied in this work. Appendix 1 relates to a demonstration of *Planck's law* that can be used to introduce *photon gas*, *photon spin* through the *Sadovsky effect*, and the notions of *photon polarization,* and to study the principle of decomposition of the electromagnetic radiation field into a sum of *virtual harmonic oscillators*. Appendix 2 is dedicated to the study of the link between Planck's law and *Einstein's theory*. This study makes it possible to describe the main processes of *interaction between optical radiation and matter* in relation to light *absorption* and *stimulated and spontaneous emission*, introduces *Einstein coefficients* and establishes the relations between them. Appendix 3 focuses on establishing *Stefan's law* using the thermodynamic approach and then the theoretical approach according to the procedure used by Boltzmann. Appendix 4 relies on a brief study of *Dirac's relativistic theory* that makes it possible to define the *fine structure perturbing Hamiltonian*, express the energy of weakly relativistic *hydrogen-like systems* and study the effects of the fine structure perturbing Hamiltonian on the levels of energy of the hydrogen atom. Appendix 5 describes *fine structure* and *hyperfine structure* phenomena. Topics such as *Lamb shift*, the notion of *physical vacuum*, *nuclear spin*, the *lifetime* of excited states, the *anomalous Zeeman effect* and *the broadening of spectral lines* due to the *Doppler* *effect* are properly covered in this appendix. A list of references and an index can be found at the end of the book.

I wish to thank Chrono Environnement Laboratory at the Université Franche Comté de Besançon for their hospitality during my stay from September 1 to November 2, 2018, as Visiting Professor. Many pages of this book were written during this period, which proved very favorable to this endeavor, both in terms of logistics and documentation. I would like to make a special mention to Jean-Emmanuel Groetz, Senior Lecturer at Chrono Environnement Laboratory, who was in charge of my visiting professor request file. I wish to express my warmest thanks to Elie Belorizky, Professor of Physics at Université Joseph Fourier de Grenoble (France) for his critical remarks and suggestions, which made a great contribution to improving the scientific quality of this work. Many corrections brought to this book were made via telephone exchanges during my stay at the Université Franche Comté de Besançon. I express here my deep appreciation for him gracefully bearing the inherent expenses for the telephone calls related to this book review. Finally, I wish to address my deepest gratitude to Louis Marchildon, Professor Emeritus of Physics at the University of Quebec at Trois-Rivières (Canada), who spared no effort to review the entire book, and whose comments have enhanced the scientific quality of this work, of which the preface bears his signature. We started our collaboration in 2013, when he invited me to host a conference at the Hydrogen Research Institute (HRI). I am deeply grateful for his kind and very fruitful collaboration.

All human endeavor being subject to improvement, I remain open to and interested in critical remarks and suggestions that my readers can send me at the email address below.

Ibrahima SAKHO
aminafatima_sakho@yahoo.fr
July 2019

# 1

# Thermal Radiation

## *General objective*

Gain knowledge on energy-related quantities and the laws of thermal radiation.

## *Specific objectives*

On completing this chapter, the reader should be able to:

- define thermal radiation;
- know the origin of thermal radiation;
- know the relations between energy, photon wavelength and frequency;
- distinguish between black body and gray body;
- define the energy-related quantities (flux, exitance, radiance and intensity);
- apply the law of conservation of radiant flux;
- state Lambert's, Kirchhoff's, Stefan-Boltzmann and Wien's laws;
- provide an interpretation of Planck's law;
- apply the laws of thermal radiation;
- find the useful spectrum from a given isotherm of the black body.

## *Prerequisites*

- structure of matter;

---

For color versions of the figures in this book, see www.iste.co.uk/sakho/quantum1.zip.

*Introduction to Quantum Mechanics 1: Thermal Radiation and Experimental Facts*
*Regarding the Quantization of Matter,* First Edition. Ibrahima Sakho.

– modes of energy transfer;

– range of electromagnetic waves.

## 1.1. Radiation

### 1.1.1. *Definition*

An object at temperature $T$ can emit or absorb *light waves* of several frequencies [PÉR 86, PER 11, SAK 12]. The distribution of the energy exchanged by the object with its external environment depends on the temperature $T$. When two objects at different temperatures are in contact, thermal energy (heat) is transferred from the hot object to the cold object. By contrast, radiation is energy that is carried by an electromagnetic wave. In this case, energy is transferred by emission and absorption of light waves. Hence, by definition, *thermal radiation* is the *electromagnetic radiation* emitted by any object at non-zero temperature $T$.

### 1.1.2. *Origin of radiation*

In 1900, **Max Planck** laid the foundations of quantum physics by studying the *black body emission spectrum* within the theory of quanta [BRO 25, PAI 82, PLO 16]. He formulated the fundamental hypothesis according to which *the energy generated by a periodic movement of frequency $\nu$ (rotation or vibration) has, similar to matter, a discontinuous structure. Consequently, radiant energy can only exist as bundles or quanta of energy $h\nu$*. The number $h$ is a universal constant known as the *Planck constant*. In 1905, **Albert Einstein** stated that light is made of particles subsequently called photons, each of which has an energy $h\nu$. Radiation results from *electronic transitions* between discrete levels of atomic or molecular systems. The energy exchanged during these transitions corresponds to *photon absorption and emission processes*. The energy $E$, angular frequency $\omega$, *frequency* $\nu$ and *wavelength* $\lambda$ of the photon are related by the following relations:

$$\begin{cases} E = h\nu = \hbar\omega \\ E = \dfrac{hc}{\lambda} \end{cases} \Rightarrow \begin{cases} \nu = \dfrac{\omega}{2\pi} = \dfrac{c}{\lambda} \\ \hbar = \dfrac{h}{2\pi} \end{cases} \qquad [1.1]$$

In relations [1.1], $E$ is expressed in joules (J), $\nu$ in hertz (Hz), $\omega$ in radian per second (rad · $s^{-1}$) and $\lambda$ in meters (m). The quantity $c$ designates the *speed of light* in a vacuum and $\hbar$ is the *h-bar* (or *reduced*) *Planck constant*.

## Numerical expression:

$$h = 6.62606896\ (33) \times 10^{-34}\ \text{J} \cdot \text{s};\ \hbar = 1.054571628\ (53) \times 10^{-34}\ \text{J} \cdot \text{s}.$$

$$c = 299792458\ \text{m} \cdot \text{s}^{-1}\ \text{(exact value)}.$$

The figures designate the absolute errors $\Delta X$ (uncertainties) of the given values of the measured $X$ quantity. For example, $h = (6.626\ 068\ 96 \pm 0.000\ 000\ 33) \times 10^{-34}$ J · s.

This means an absolute error $\Delta h = (0.000\ 000\ 33) \times 10^{-34}$ J · s.

At the microscopic scale, it is convenient to use the *electronvolt* (eV) as a unit of energy:

$$1\ \text{eV} = 1.602179487 \times 10^{-19}\ \text{J}.$$

Photon absorption and emission processes are illustrated in Figure 1.1.

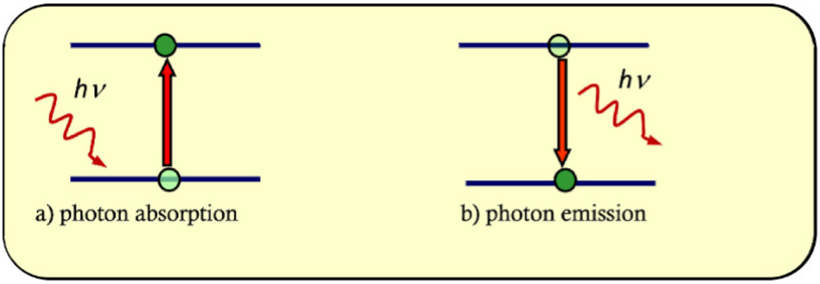

**Figure 1.1.** *Electronic transition between two discrete levels*

**APPLICATION 1.1.–**

A He-Ne laser in a laboratory emits radiation whose wavelength is 633 nm. Calculate the energy $E$, frequency $\nu$ and angular frequency $\omega$ of a photon of this radiation. Express $E$ in eV.

*Given data.* $h = 6.63 \times 10^{-34}$ J · s; $c = 3.0 \times 10^{8}$ m · s$^{-1}$; 1 eV = $1.60 \times 10^{-19}$ J.

**Solution.** $E = 1.96$ eV; $\nu = 4.74 \times 10^{14}$ Hz; $\omega = 2.98 \times 10^{15}$ rad · s$^{-1}$.

Max Planck, in full Max Karl Ernst Ludwig Planck, was a German physicist. He founded quantum physics in 1900 with his fundamental hypothesis on the theory of quanta. He was awarded the Nobel Prize for physics in 1918 for his essential contribution to the theory of quanta. Planck is also one of the founding fathers of quantum mechanics. He is also well known for his law giving monochromatic radiant exitance, which makes it possible to interpret the experimental observations related to black body isotherms.

**Box 1.1.** *Planck (1854–1947)*

### 1.1.3. *Classification of objects*

Objects susceptible to exchange energy are classified into three categories:

– *transparent objects* that allow radiation to pass through without attenuation. This is the case with glass, transparent plastic material, etc.;

– *opaque objects* that absorb radiation and get heated. This is the case with solid bodies (metals, rocks, etc.), cardboard and some viscous liquids, such as paint;

– *translucent objects* that absorb a part of the radiation and allow the rest to pass through. For these objects, radiation propagation is accompanied by absorption that increases the energy of the medium. A familiar example is that of oil.

## 1.2. Radiant flux

### 1.2.1. *Definition of radiant flux, coefficient of absorption*

By definition, *radiant flux* denoted by $\Phi$ is the power emitted by a source throughout the space in which it can radiate. Radiant flux is expressed in Watts (W).

Let us consider an object receiving an incident energy flux $\Phi_\mathrm{i}$. The surface of the object is chosen to allow radiation reflection, absorption and transmission (Figure 1.2).

According to the law of conservation of energy, we have:

$$\Phi_\mathrm{i} = \Phi_r + \Phi_a + \Phi_t. \qquad [1.2]$$

In this relation, $\Phi_\mathrm{r}$ is the *reflected radiant flux*, $\Phi_\mathrm{a}$ designates the *absorbed radiant flux* and $\Phi_\mathrm{t}$ represents the *transmitted radiant flux*. Let us consider $\rho$, $\alpha$ and $\tau$ as the *coefficients* of *reflection*, *absorption* and *transmission*, respectively, of the radiant flux. Their expressions are given as:

$$\rho = \frac{\Phi_r}{\Phi_i} \quad ; \quad \alpha = \frac{\Phi_a}{\Phi_i} \quad ; \quad \tau = \frac{\Phi_t}{\Phi_i} \qquad [1.3]$$

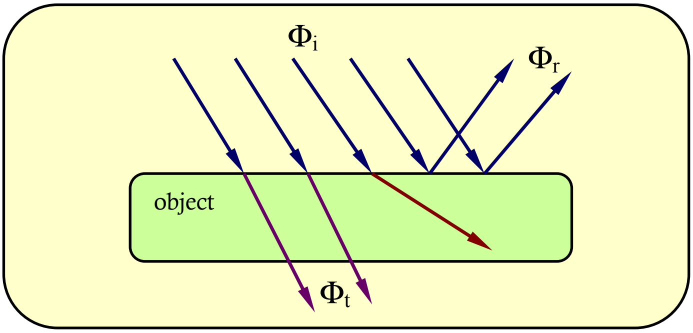

**Figure 1.2.** *Decomposition of an incident radiant flux $\Phi_i$ at the contact with the surface of an object*

Implementing relations [1.3] in [1.2], the *conservation of energy* can be written as:

$$\rho + \alpha + \tau = 1. \qquad [1.4]$$

Coefficients $\rho$, $\alpha$ and $\tau$ characterize the behavior of an object that is subjected to radiation. It is worth noting that the absorption coefficient $\alpha$ is the most important parameter. This coefficient measures the proportion in which incident electromagnetic radiation is converted into thermal energy.

**APPLICATION 1.2.–**

> Let us consider an arbitrary process of reflection, absorption and transmission of an incident radiant flux. Calculate the absorbed flux.
>
> *Given data*. $\rho = 30$ %; $\tau = 20$ %; transmitted flux: 200 W.
>
> **Solution.** $\Phi_a = 500$ W.

### 1.2.2. *Black body and gray body*

There are two types of bodies:

– *gray bodies* for which $\alpha < 1$;

– *black bodies* for which $\alpha = 1$.

By definition, a *black body* is an ideal (therefore fictitious) object that has the specific property of perfectly absorbing the radiations of the visible spectrum irrespective of their frequency. The adjective “black” highlights only the fact that the object absorbs all the radiations of the visible spectrum so that it appears to be black. A black body can be actually realized by piercing a small orifice in the wall of a temperature-controlled cavity (whose walls are brought to a given temperature $T$). No radiation entering this cavity can escape. Hence the orifice behaves as a black body. It is nevertheless worth noting that an insignificant amount of thermal radiation leaves the cavity, but it is not sufficient to perturb the thermal equilibrium established in the cavity (but it is sufficient to be studied experimentally). Black velvet and black ink are simple examples of black bodies. Let us finally note that a *gray body* is not necessarily gray. This term designates any object whose absorption coefficient is $\alpha < 1$.

## 1.3. Black body emission spectrum

### 1.3.1. *Isotherms of a black body: experimental facts*

By definition, the *electromagnetic energy density* denoted by $du$ in the band of angular frequency between $\omega$ and $\omega + d\omega$ (or of wavelength between $\lambda$ and $\lambda + d\lambda$) is given by the expression:

$$du = u(\omega)\, d\omega = u(\lambda)\, d\lambda \qquad [1.5]$$

In relations [1.5], the physical quantity $u(\omega)$ or $u(\lambda)$ is called the *spectral density of electromagnetic energy*. $u(\omega)$ is expressed in $\mathrm{J \cdot rad^{-1} \cdot s}$ and $u(\lambda)$ in $\mathrm{J \cdot m^{-1}}$.

Let us study the variation of the spectral density of electromagnetic energy depending on wavelength $\lambda$ for each temperature $T$ of the black body. Experience shows that these are asymmetrical curves known as *black body isotherms*. For each temperature value $T$, there is a corresponding curve that reaches a maximum for a specific wavelength value denoted as $\lambda_{\max}$ (Figure 1.3). It should be kept in mind that $\lambda_{\max}$ does not correspond to the maximal value of the wavelength of an isotherm taking place at temperature $T$ of the black body. It is rather the wavelength corresponding to the peak of each isotherm. For example, for the isotherm at 5,500 K, $\lambda_{\max} \approx 520$ nm.

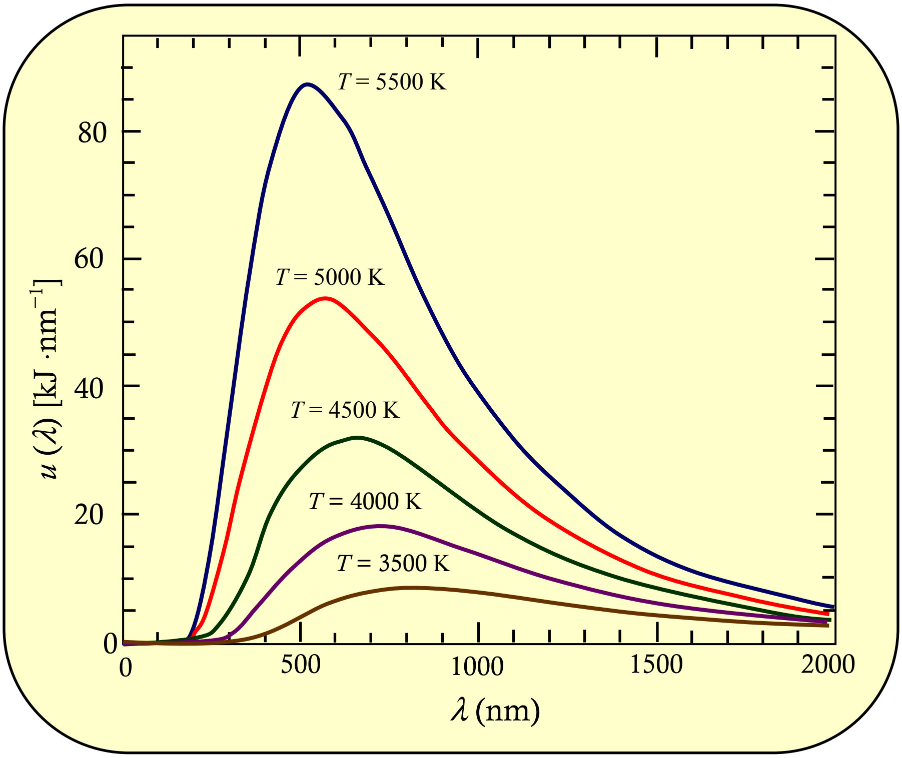

**Figure 1.3.** *Black body isotherm curves*

### 1.3.2. *Solid angle*

An angle $\theta$ (in radian) is defined as the length $l$ of the arc cut off from a circle, centered at the vertex of the angle, divided by the radius $R$ of this circle, which is $\theta = l/R$. By analogy, the *solid angle* denoted as Ω (expressed in *steradian*) of a cone is defined as the area $S$ cut off by this cone on a sphere centered at its vertex divided by the squared radius of the sphere (Figure 1.4), which is:

$$\Omega = \frac{S}{R^2} \qquad [1.6]$$

– For the whole space, $S = 4\pi R^2 \Rightarrow \Omega = 4\pi$ steradian.

– For a half-space, $S = 2\pi R^2 \Rightarrow \Omega = 2\pi$ steradian.

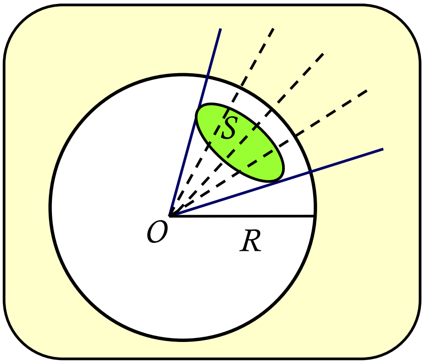

**Figure 1.4.** *Surface S cut off by a cone on a sphere of radius R*

The solid angle under which an elementary area *dS*, whose dimensions are small compared to its distance $r$ to point $O$, and whose normal makes an angle $\theta$ with the direction of the unit vector $\vec{e}_r$ (Figure 1.5), can be seen from a point $O$ is very often interesting to consider. This elementary solid angle is present, for example, in the definition of the flux of a field of vectors through an elementary area *dS*. By definition, the *elementary solid angle* is given by the following relation:

$$d\Omega = \frac{\overrightarrow{dS} \cdot \vec{e}_r}{r^2} = \frac{dS \cos\theta}{r^2} \qquad [1.7]$$

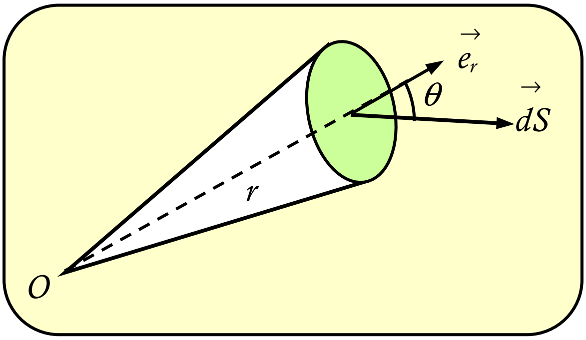

**Figure 1.5.** *Area dS seen from a point O at a distance r*

Let us finally express the solid angle of a *cone of revolution* of vertex $O$ and half-angle at vertex $\theta$. Let us consider for this purpose two cones of the same vertex $O$ and the same axis, and half-angles $\alpha$ and $\alpha + d\alpha$ (Figure 1.6).

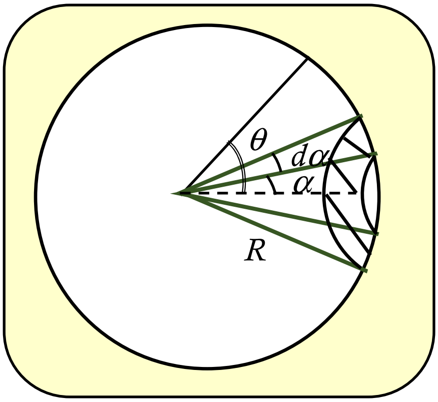

**Figure 1.6.** *Cones of half-angles at vertex $\alpha$ and $\alpha + d\alpha$*

The (hatched) surface cut off from the sphere of radius $R$ by the interval between the two cones is given by the relation:

$$dS = 2\pi R\sin\alpha R d\alpha = 2\pi R^2 \sin\alpha d\alpha$$

The corresponding elementary solid angle $d\Omega$ is then:

$$d\Omega = \frac{dS}{R^2} = 2\pi \sin\alpha d\alpha \qquad [1.8]$$

The solid angle $\Omega$ of a cone of revolution of vertex $O$ and half-angle at the vertex $\theta$ is obtained by integration of equation [1.8] between the limits 0 and $\theta$. This leads to:

$$\Omega = 2\pi \int_0^\theta \sin\alpha d\alpha = 2\pi(1-\cos\theta) \qquad [1.9]$$

– For the entire space, $\theta = \pi \Rightarrow \Omega = 4\pi$ steradian.

– For a half-space, $\theta = \pi/2 \Rightarrow \Omega = 2\pi$ steradian.

### 1.3.3. *Lambert's law, radiance*

Let us consider an emissive surface $S$. The fraction of flux $d^2\Phi$ contained in the cone of solid angle $d\Omega$ in direction $Ox$ making an angle $\theta$ with the normal $N$ to the surface $dS$ (Figure 1.7) is given by the relation:

$$d^2\Phi = A dS d\Omega \qquad [1.10]$$

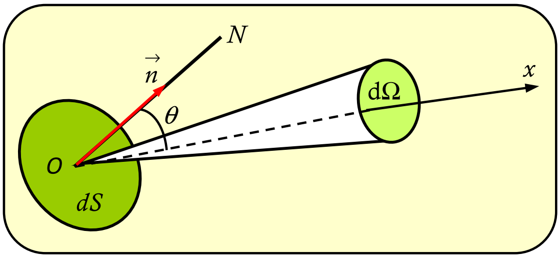

**Figure 1.7.** *Solid angle seen from a point O, center of an emissive surface S*

Surface $dS$ follows Lambert's law if $A = L\cos\theta$. The fraction of flux [1.10] is then written as:

$$d^2\Phi = L\cos\theta dS d\Omega \qquad [1.11]$$

The energy-related quantity $L$ is known as the *radiance* of the emissive object. As relation [1.11] shows, radiance is by definition equal to the *flux radiated by a solid angle unit and by a surface unit* perpendicular to $Ox$. $L$ is expressed in $\mathrm{W \cdot m^{-2} \cdot sr^{-1}}$. According to *Lambert's law*, the radiance of an object is independent of the direction of axis $Ox$. Radiance depends only on temperature $T$ and on the nature of the object surface (color, roughness, etc.). Moreover, total radiant intensity $dI$ is equal to the fraction of the flux radiated in direction $Ox$ (Figure 1.7) per unit solid angle $d\Omega$, which is:

$$dI = AdS = L\cos\theta dS \qquad [1.12]$$

Total radiant intensity is expressed in Watt per steradian ($\mathrm{W \cdot sr^{-1}}$).

### 1.3.4. *Kirchhoff's laws*

There are two *Kirchhoff's laws* on thermal radiation. They explain the black body isotherms and the relation between radiance $L$ of the gray body and radiance $L_0$ of the black body. Kirchhoff's laws can be stated as follows:

– *first law*: all black bodies at the same temperature have the same radiance;

– *second law*: among all the objects brought to the same temperature, the black body is the most luminous.

Considering a gray body of coefficient of absorption $\alpha$, the mathematical expression of Kirchhoff's second law leads to the relation between radiance $L$ of the gray body and radiance $L_0$ of the black body, which is:

$$L = \alpha L_0 \qquad [1.13]$$

**Johann Heinrich Lambert** was a Swiss mathematician and astronomer. He is considered as one of the founders of photometry. He is well known in this field for the law that introduces the radiance of an emissive object and for the Beer–Lambert law stating that the decrease in light intensity is proportional to the number of particles absorbing light.

**Gustav Robert Kirchhoff** was a German physicist. He is well known especially for his laws related to the conservation of currents and charges in electrical circuits. Kirchhoff is also known for his laws related to thermal radiation, which he formulated in 1859.

**Box 1.2.** *Lambert (1728–1777); Kirchhoff (1824–1887)*

### 1.3.5. *Stefan–Boltzmann law, total energy exitance*

By definition, *total energy exitance M* is equal to the power radiated by the unit surface in all directions. Its relation with radiance is:

$$M = \int L \cos\theta \, d\Omega = 2\pi L \int_0^{\pi/2} \cos\theta \sin\theta \, d\theta.$$

Considering $x = \cos\theta$, this leads to:

$$M = -2\pi L \int_1^0 \cos\theta \, d\cos\theta = -2\pi L \int_1^0 x dx$$

or:

$$M = \pi L. \qquad [1.14]$$

$M$ is expressed in $\mathrm{W \cdot m^{-2}}$.

For the black body, total radiant exitance denoted by $M^0$ is, according to [1.14]:

$$M^0 = \pi L_0 \qquad [1.15]$$

Given the Stefan–Boltzmann law, total radiant exitance $M^0$ of the black body is proportional to the fourth power of its temperature $T$ or (see demonstration in Appendix A.3):

$$M^0 = \sigma T^4 \qquad [1.16]$$

In this relation, $\sigma$ is *Stefan–Boltzmann constant*.

### Numerical expression:

$$\sigma = 5.66897 \times 10^{-8}\ \mathrm{W \cdot m^{-2} \cdot K^{-4}}$$

Using relations [1.15] and [1.16], the radiance $L_0$ of the black body can be written as:

$$L_0 = \frac{\sigma}{\pi} T^4 \qquad [1.17]$$

There is no need to memorize expression [1.17] of the radiance $L_0$. It can be deduced, when needed. Only the laws and the definitions of the energy-related quantities studied in this section and in the following sections should be retained.

**APPLICATION 1.3.–**

> Calculate the radiance and the radiant exitance of a gray body at temperature 3000 K whose coefficient of absorption is 85%.
>
> *Given data*. Stefan–Boltzmann constant: $\sigma = 5.67 \times 10^{-8}\ \mathrm{W \cdot m^{-2} \cdot K^{-4}}$.
>
> **Solution.** $L = 1.24\ \mathrm{MW \cdot m^{-2} \cdot sr^{-1}}$; $M = 3.9\ \mathrm{MW \cdot m^{-2}}$.

**Joseph Stefan** was an Austrian physicist. He is especially renowned for his work published in 1879 on the radiation of the black body in which he stated the law that bears his name. Based on this law, Stefan determined the Sun's surface temperature (5430°C). Then his student Boltzmann offered a theoretical justification for the Stefan law. This is why this law is commonly known as the Stefan–Boltzmann law (for Boltzmann, see Box A.3).

**Box 1.3.** *Stefan (1835–1893)*

## 1.3.6. *Wien's laws, useful spectrum*

The two Wien's laws give the abscissa $\lambda_{\max}$ of the wavelength and the ordinate $M^0_{\max}$ of the maximum *monochromatic exitance* for each temperature $T$ of the black body (Figure 1.8).

### *Wien's first law*

The wavelength $\lambda_{\max}$ at an isotherm peak shifts toward short wavelengths when temperature $T$ increases according to the law:

$$\lambda_{\max} T = \sigma_{\mathrm{w}} \qquad [1.18]$$

In this relation, $\sigma_W$ designates the *Wien constant*: $\sigma_W = 2.898 \times 10^{-3}\ \text{m} \cdot \text{K}$.

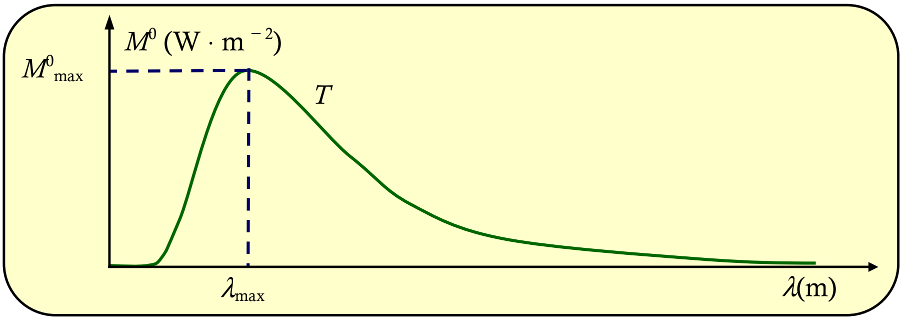

**Figure 1.8.** *Isotherm curve of the black body at temperature T*

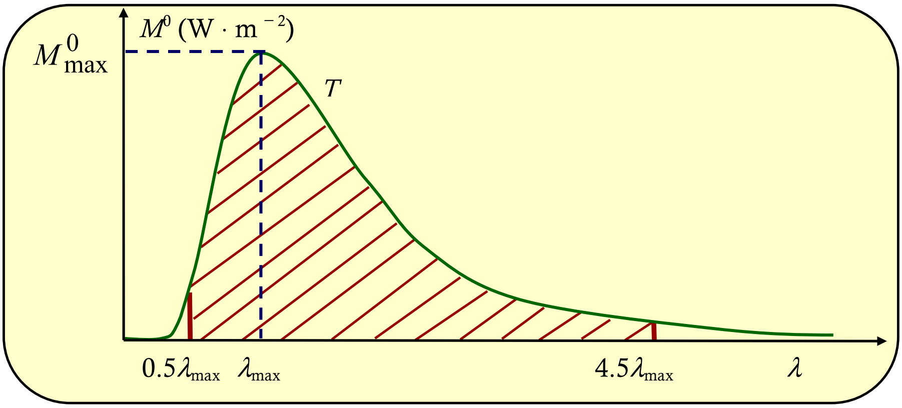

**Figure 1.9.** *Useful spectrum (hatched part of the isotherm curve)*

Wien's law [1.19] shows that the value of $\lambda_{max}$ shifts toward short wavelengths when the temperature $T$ increases.

### *Wien's second law*

The ordinate $M^0_{\lambda\max}$ of the maximum monochromatic exitance is proportional to the fifth power of temperature, which is:

$$M^0_{max} = BT^5 \qquad [1.19]$$

In relation [1.19], $M^0_{\max}$ is expressed in $\mathrm{W \cdot m^{-3}}$ (if the wavelength $\lambda_{\max}$ is expressed in m) or in $\mathrm{W \cdot m^{-2} \cdot \mu m^{-1}}$ (if $\lambda_{\max}$ is expressed in micrometers); the units of constant $B$ depend on the unit of wavelength $\lambda_{\max}$.

$$B = 1.28 \times 10^{-5}\,[\mathrm{W \cdot m^{-3} \cdot K^{-5}}] \text{ if } \lambda_{\max} \text{ is expressed in m.}$$

$$B = 1.28 \times 10^{-11}\,[\mathrm{W \cdot m^{-2} \cdot \mu m^{-1} \cdot K^{-5}}] \text{ if } \lambda_{\max} \text{ is expressed in } \mu\text{m.} \qquad [1.20]$$

Moreover, experience shows that when the wavelength of radiation is such that $\lambda < 0.5\lambda_{\max}$, there is practically no more radiated energy (approximately 1%) [PER 11].

Furthermore, there is practically no more radiated energy when $\lambda > 4.5\lambda_{\max}$. By definition, the wavelength range $0.5\lambda_{\max} < \lambda < 4.5\lambda_{\max}$ is called the *useful spectrum* of the considered isotherm (hatched part in Figure 1.9).

**APPLICATION 1.4.–**

Let us consider an isotherm at the surface temperature of the Sun, which is assimilated to a black body. Find the useful spectrum corresponding to $T = 6{,}000$ K.

*Given data*. $\sigma_W = 2.898 \times 10^{-3}$ m · K.

**Solution.** Useful spectrum: $0.5\lambda_{\max} < \lambda < 4.5\lambda_{\max} \Rightarrow (241.5 < \lambda < 2{,}173.5)$ nm.

NOTE.– The useful spectrum contains radiations from ultraviolet to infrared. Therefore it contains all the radiations of the visible spectrum.

**APPLICATION 1.5.–**

What is the maximal monochromatic exitance of the isotherm of the black body at wavelength $\lambda_{\max} = 1.184$ µm at $T = 2{,}500$ K?

*Given data*. $B = 1.28 \times 10^{-11}\ \mathrm{W \cdot m^{-2} \cdot \mu m^{-1} \cdot K^{-5}}$.

**Solution.** $M^0_{\lambda\max} = 1.25\ \mathrm{MW \cdot m^{-2} \cdot \mu m^{-1}}$.

**Wilhelm Wien** was a German physicist. He is well known for the laws published in 1896 that give the spectral distribution of the black body radiation for short wavelengths.

**Box 1.4.** *Wien (1864–1928)*

### 1.3.7. *The Rayleigh–Jeans law, "ultraviolet catastrophe"*

Let us consider a black body at thermodynamic equilibrium. The *density of modes* $n(\omega)$ (or the number of types of oscillators) in the angular frequency range $[\omega, \omega + d\omega]$ is given by the following relation (see demonstration in Appendix A.1):

$$n(\omega) = \frac{\omega^2}{\pi^2 c^3} \qquad [1.21]$$

In this relation, $c$ designates the speed of light in a vacuum.

The *spectral energy density* is equal to the product of the density of modes $n(\omega)$ and the average energy $\langle E_\omega \rangle (T)$ of the field of a single mode:

$$u(\omega) = n(\omega) \times \langle E_\omega \rangle (T) \qquad [1.22]$$

For a *classical oscillator*, the average energy is $\langle E_\omega \rangle (T) = kT$. Hence using [1.21], the classical formula of the Rayleigh–Jeans can be written as:

$$u(\omega) = \frac{\omega^2}{\pi^2 c^3} \times kT \qquad [1.23]$$

Expression [1.23] shows that *spectral energy density* $u(\omega)$ is a parabolic arc. Let us draw the graphical representation of the variation of $u(\omega)$ as a function of angular frequency $\omega$ compared to experimental observations. The resulting curves are represented in Figure 1.10.

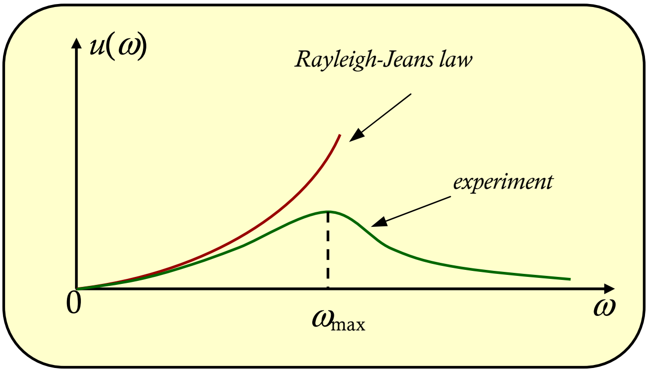

**Figure 1.10.** *Comparison of the classical Rayleigh–Jeans law with experimental observations*

Figure 1.10 shows that the *classical Rayleigh–Jeans law* is in agreement with the experimental observations for low frequencies $\nu\,(\nu = \omega/2\pi)$ or for long wavelengths $\lambda\,(\omega = 2\pi c/\lambda)$. On the other hand, it corresponds to an infinitely wide field of energy for high angular frequencies or for short wavelengths. This shift of the spectrum toward the ultraviolet region when angular frequency increases is known as "*ultraviolet catastrophe*".

**John William Strutt Rayleigh** was a British physicist. In 1900, he applied the laws of classical statistical mechanics to the field of radiation to establish the law expressing the distribution of the energy radiated by the black body depending on frequency. A factor 8 error, due to erroneous counting in the phase space, was corrected in 1905 by Jeans [TAI 08].

**James Hopwood Jeans** was a British physicist, mathematician and astronomer. He had significant scientific contributions to several fields of physics, such as thermal radiation, in which he co-authored with Rayleigh the law bearing their names.

**Box 1.5.** *Rayleigh (1842–1919); Jeans (1877–1946)*

### 1.3.8. *Planck's law, monochromatic radiant exitance*

In order to establish the quantum law of radiation by a generalization of the classical law [1.23] within the *theory of quanta* [BRO 25], Planck assimilated the black body cavity to a set of *virtual harmonic oscillators*. The problem posed is then to express the average energy of each of these oscillators. Considering that the average energy $\langle E_\omega \rangle\,(T)$ of a mode is determined by the quotient of the discrete sum energies of the set of elementary oscillators by the total number of oscillators, the result is (see Exercise 1.4.3 for the demonstration):

$$\langle E_\omega \rangle (T) = \frac{\hbar\omega}{(e^{\hbar\omega/kT} - 1)} \qquad [1.24]$$

Using results [1.21] and [1.24], the quantum expression of the spectral density of electromagnetic energy known as *Planck's law* is obtained:

$$u(\omega) = \frac{\hbar\omega^3}{\pi^2 c^3} \times \frac{1}{(e^{\hbar\omega/kT} - 1)} \qquad [1.25]$$

NOTE.– Depending on frequency $\nu\,(\omega = 2\pi\nu)$, Planck's law can be written as:

$$u(\nu) = \frac{8\pi h\nu^3}{c^3} \times \frac{1}{(e^{h\nu/kT} - 1)} \qquad [1.26]$$

Figure 1.11 shows an illustration of classical [1.23] and quantum [1.26] predictions compared to experimental observations. It is worth noting that Planck's quantum law is perfectly corroborated by experimental observations for all frequencies. Moreover, as indicated in Figure 1.11, the classical (*Rayleigh–Jeans law*) and quantum (*Planck's law*) curves overlap for low values of angular frequency. This shows that Planck's law is actually a generalization of the Rayleigh–Jeans' law (see Application 1.6).

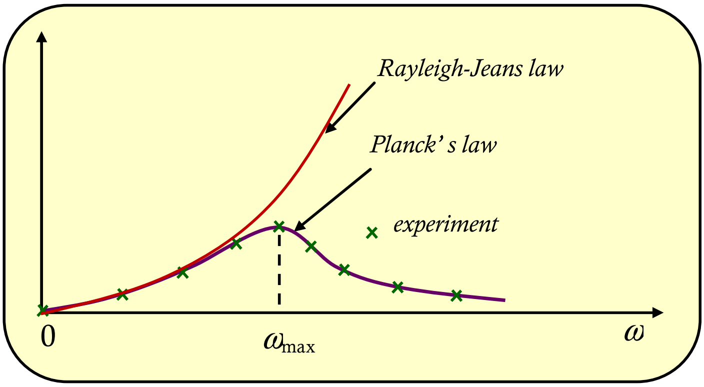

**Figure 1.11.** *Comparison of classical and quantum predictions with experimental observations*

Moreover, there is another formulation of Planck's law expressing the *monochromatic exitance* $M_\lambda^0$ of the black body as a function of wavelength $\lambda$ and its absolute temperature $T$. This formulation can be written as:

$$M_\lambda^0 = \frac{C_1 \lambda^{-5}}{(e^{C_2/\lambda T} - 1)} \qquad [1.27]$$

In [1.27], $C_1$ and $C_2$ are constants: $C_1 = 2\pi hc^2$ and $C_2 = hc/k$, where $h$ designates the Planck constant, $c$ designates the speed of light in a vacuum and $k$ denotes the Boltzmann constant. Planck's law [1.25] makes it possible to find Wien's first law [1.19] (see Application 1.6) and deduce from it the theoretical expression of the Wien constant.

### APPLICATION 1.6.–

> Use Planck's law [1.25] to find the Rayleigh–Jeans law.
>
> **Solution.** For low frequencies such that $\hbar\omega \ll kT$, Planck's law [1.25] gives:

$$u(\omega) \approx \frac{\hbar\omega^3}{\pi^2 c^3}\frac{1}{(\hbar\omega/kT - 1)} \Rightarrow u(\omega) \approx \frac{\omega^2}{\pi^2 c^3}kT$$

which actually corresponds to the classical Rayleigh–Jeans law [1.23].

## 1.4. Exercises

### 1.4.1. *Exercise 1 – Calculation of the Stefan–Boltzmann constant*

Let us consider a surface element $dS$ of a black body. $d^2\Phi$ is the power emitted by this element in the wavelength range $[\lambda, \lambda + d\lambda]$.

(1) Express $d^2\Phi$ and the total exitance $M^0$ of the black body.

(2) Deduce the expression of the Stefan–Boltzmann law.

(3) Calculate the Stefan–Boltzmann constant.

*Given data.*

– $h = 6.62606896 \times 10^{-34}$ J · s; $k = 1.3806504 \times 10^{-23}$ J · K$^{-1}$.

– $c = 2.99792458 \times 10^8$ m · s$^{-1}$.

– Spectral radiance of the black body:

$$L_\lambda^0 = \frac{2hc^2}{\lambda^5} \times \frac{1}{e^{hc/\lambda kT} - 1}$$

For all practical purposes, the following integral is given:

$$\int_0^\infty \frac{x^3}{e^x - 1} = \frac{\pi^4}{15}$$

### 1.4.2. *Exercise 2 – Calculation of the Sun's surface temperature*

The Sun, of radius $R$ and surface area $S$, is assimilated to a black body at temperature $T$. The part of solar radiation reaching the Earth situated at distance $d$ from the Sun is considered. $P_0$ designates the solar power received by the Earth disc of surface area $S_0$ and radius $R_0$. Throughout the exercise, the Earth is assimilated to a gray body.

(1) Express the power $P$ radiated by the solar surface $S$ as a function of $R$, $T$ and $\sigma$ (Stefan–Boltzmann constant).

(2) Draw a schematic representation of the relative positions of the Sun and Earth. Indicate on it the radii $R$ and $R_0$, surfaces $S$ and $S_0$ and the sphere of solar radiation of radius $d$ and surface $S'$. Express $P_0$ as a function of $R$, $R_0$, $T$, $d$ and $\sigma$.

(3) Find the expressions of power $P_a$ absorbed by the Earth and of power $P_r$ radiated through its entire spherical surface of radius $R_0$.

(4) Express the temperature $T$ of the Sun's surface as a function of $T_0$, $d$ and $R$. Make the numerical application.

*Given data.*

– Ratio of the Sun's radius R to the Earth–Sun distance $d = R/d = 200$.

– Stefan–Boltzmann constant: $\sigma = 5.670 \times 10^{-8}$ W $\cdot$m$^{-2}\cdot$K$^{-4}$.

### 1.4.3. *Exercise 3 – Average energy of a quantum oscillator, Planck's formula*

According to Planck's approach to black body radiation, the oscillations of an electromagnetic field can be assimilated to a set of elementary oscillators. Let us consider that $E_n$ is the energy of an elementary mode constituted of a number $n$ of photons.

(1) Establish the relation between $E_n$ and $\omega$ using Planck's hypothesis.

(2) At thermodynamic equilibrium, the number $N_n$ of elementary oscillators obeys Boltzmann's distribution law, which is:

$$N_n = N_0\, e^{-\beta E_n}$$

In this expression, $\beta = 1/kT$, where $k$ is Boltzmann constant.

Find the physical significance of $N_0$.

(3) Knowing that the average energy $\langle E_\omega \rangle (T)$ of a mode can be calculated by the quotient of the discrete sum of energies of the set of elementary oscillators to the total number of oscillators, express $\langle E_\omega \rangle (T)$ as a function of $N_n$ and $E_n$.

(4) Considering $a = \hbar\omega$ and $x = e^{-\beta a}$, show that $\langle E_\omega \rangle (T)$ can be written as:

$$\langle E_\omega \rangle (T) = \frac{a}{x^{-1} - 1}$$

(5) Use this result to deduce the expression of energy $\langle E_\omega \rangle (T)$ as a function of $\hbar$, $\omega$ and $T$.

(6) Find Planck's formula. The expression of mode density is:

$$n(\omega) = \omega^2 / \pi^2 c^3$$

## 1.4.4. *Exercise 4 – Deduction of Wien's first law from Planck's formula*

Given Planck's formula, the spectral exitance $M_\lambda$ (or spectral radiant exitance) can be written as follows (in vacuum):

$$M_\lambda = \frac{2hc^2}{\lambda^5} \frac{1}{e^{hc\beta/\lambda} - 1}$$

(1) Express the spectral exitance in a medium of refractive index $n_\lambda$.

(2) What is spectral exitance at the peak of light emission of the black body and at temperature $T$?

(3) Use the previous results to deduce Wien's first law. Consider $x = hc\beta/\lambda$.

(4) Estimate the Sun's surface temperature corresponding to a maximum emission at a wavelength of 500 nm.

*Given data.*

– Unique positive solution of the equation: $e^{-x} + \frac{1}{5}x - 1 = 0$ : $x_0 = 4.965$.

– $k = 1.3806504 \times 10^{-23}$ J·K$^{-1}$; h = $6.62606896 \times 10^{-34}$ J·s; c = $2.99792458 \times 10^8$ m · s$^{-1}$.

– Wien constant $\sigma_W = 2.898 \times 10^{-3}$ m · K.

## 1.4.5. *Exercise 5 – Total electromagnetic energy radiated by the black body*

Let us consider a black cavity within which there is along all directions a light radiation emitted by the cavity walls at temperature $T$. Let us consider on the walls an emissive surface $dS$ that obeys Lambert's law. Let us denote $d^2\Phi$ the flux contained in the cone of solid angle $d\Omega$ and direction $Ox$ that makes an angle $\theta$ with the normal $N$ to the surface $dS$.

(1) Use Lambert's law to find the expression of $d^2\Phi$. Deduce from it the electromagnetic energy $d^3E$ exiting a black surface orifice of cross-section $dS$ in the solid angle $d\Omega$ for a duration $dt$ along the normal $N$.

(2) The electromagnetic radiation is considered to be contained in a cylinder of height $h = cdt$ and base surface area $dS$. Express the energy density per unit volume $du$ as a function of $d\Omega$, $L_0$ and $c$ (speed of light in a vacuum).

(3) Show that the total energy per unit volume $U(T)$ radiated by the black body can be written as $U(T) = \sigma^* \times T^4$, where $\sigma^*$ is a constant. Calculate $\sigma^*$.

(4) Calculate $U(T)$ at $T = 6{,}000$ K.

*Given data.* $\sigma = 5.670400 \times 10^{-8}$ W · m$^{-2}$ · K$^{-4}$. The values of other constants are among the given data in Exercise 1.5.3.

## 1.5. Solutions

### 1.5.1. *Solution 1 – Calculation of the Stefan–Boltzmann constant*

(1) *Expression of flux and total exitance of the black body*

An emissive surface following Lambert's law radiates the light intensity:

$$d^2\Phi = \pi L dS \qquad [1.28]$$

The total exitance is $M = d^2\Phi/dS$. Hence for the black body:

$$M^0 = \pi L_0 \qquad [1.29]$$

(2) *Expression of Stefan–Boltzmann law*

In the wavelength range $[\lambda, \lambda + d\lambda]$, radiance $L_0$ of the black body is given by the integral of spectral radiance $L_\lambda^0(T)$ on all the wavelengths, which is:

$$L_0 = \int_0^\infty L_\lambda^0(T)d\lambda \qquad [1.30]$$

Using [1.29], the total exitance $M^0$ of the black body is written as:

$$M^0 = \pi\int_0^\infty L_\lambda^0(T)d\lambda \qquad [1.31]$$

The spectral radiance is given by the following expression:

$$L_{\lambda}^{0}(T) = \frac{2hc^2}{\lambda^5} \cdot \frac{1}{e^{hc/\lambda kT} - 1}$$

Equation [1.31] becomes:

$$M^0 = 2\pi hc^2 \int_0^\infty \frac{1}{\lambda^5} \cdot \frac{1}{e^{hc/\lambda kT} - 1} d\lambda \qquad [1.32]$$

Let us consider: $x = hc/\lambda kT \Rightarrow dx = -(hc/\lambda^2 kT) d\lambda$. After simplification, [1.32] gives:

$$M^0 = \frac{2\pi}{h^3 c^2} k^4 T^4 \int_0^\infty \frac{x^3}{e^x - 1} dx \qquad [1.33]$$

Taking the following result into account:

$$\int_0^\infty \frac{x^3}{e^x - 1} dx = \frac{\pi^4}{15}$$

leads to:

$$M_0 = \frac{2\pi^5 k^4}{15 h^3 c^2} T^4 = \sigma T^4 \qquad [1.34]$$

(3) *Calculation of the Stefan–Boltzmann constant*

According to [1.34], the Stefan–Boltzmann constant can be written as:

$$\sigma = \frac{2\pi^5 k^4}{15 h^3 c^2} \qquad [1.35]$$

N.A.– $\sigma = 5.67040400 \times 10^{-8}\ \mathrm{W \cdot m^{-2} \cdot K^{-4}}$.

The accepted value of the Stefan–Boltzmann constant is actually found: $\sigma = 5.670400 \times 10^{-8}\ \mathrm{W \cdot m^{-2} \cdot K^{-4}}$. Therefore, the result [1.34] corresponds to the Stefan–Boltzmann law.

### 1.5.2. *Solution 2 – Calculation of the Sun's surface temperature*

(1) *Expression of the power P radiated by a solar surface*

The power radiated by the solar surface $S = 4\pi R^2$ per unit time is $P = SM_0$, or according to the Stefan–Boltzmann law [1.17]:

$$P = 4\pi R^2 \sigma T^4 \qquad [1.36]$$

(2) *Schematization and expression of the power $P_0$ received by the Earth disc*

– *Schematization*: see Figure 1.12.

– *Expression of power $P_0$.*

The total power [1.36] is radiated in the sphere of radius $d$ and surface $S'$ (Figure 1.12). The power $P_0$ received by the Earth disc of surface $S_0$ is ($P \to S'$; $P_0 \to S_0$):

$$P_0 = P \times \frac{S_0}{S'} \qquad [1.37]$$

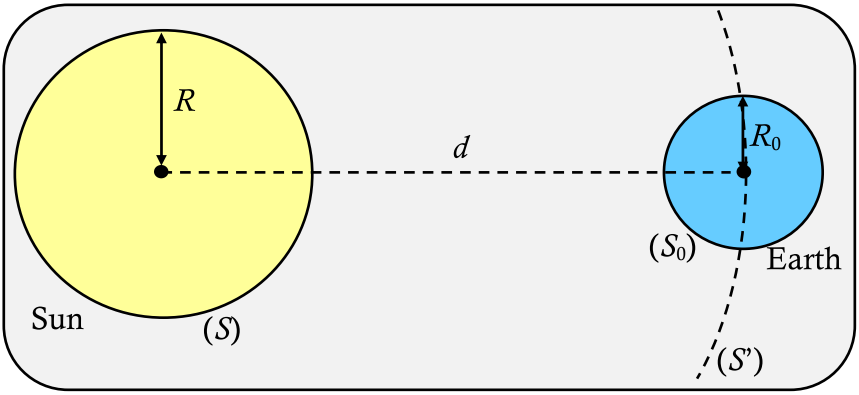

**Figure 1.12.** *Solar radiation sphere of radius d and surface S'*

Taking [1.36] into account and knowing that $S' = 4\pi d^2$, relation [1.37] can be written as:

$$P_0 = R^2 \sigma T^4 \times \frac{\pi R_0^2}{d^2} \qquad [1.38]$$

(3) *Expressions of absorbed power $P_a$ and radiated power $P_r$*

– *Expression of absorbed power*

The Earth is assimilated to a gray body whose coefficient of absorption is $\alpha < 1$. Hence, it only absorbs a fraction of power [1.38]. Let us consider: $P_a = \alpha P_0$. Using [1.38] leads to:

$$P_0' = \alpha \pi R^2 \sigma T^4 \times \frac{R_0^2}{d^2} \qquad [1.39]$$

– *Expression of radiated power*

If the Earth is brought to constant temperature $T_0$, the power radiated throughout its spherical surface of radius $R_0$ is:

$$P_r = \alpha 4\pi R_0^2 \sigma T_0^4 \qquad [1.40]$$

(4) *Expression of the Sun's surface temperature, application*

When in thermodynamic equilibrium, the Earth radiates as much as it absorbs. Hence $P_a = P_r$. Placing expressions [1.39] and [1.40] in this equality leads, after simplification, to:

$$T = \left(4\frac{d^2}{R^2}\right)^{\frac{1}{4}} \times T_0 = \sqrt{2\frac{d}{R}} \times T_0 \qquad [1.41]$$

N.A.– T = 6,000 K.

In fact, the temperature of the solar surface (photosphere) is slightly below 6,000 K. Its precise value is 5,800 K.

### 1.5.3. *Solution 3 – Average energy of a quantum oscillator, Planck's formula*

(1) *Relation between $E_n$ and $\omega$*

According to Planck's hypothesis, the energy of a quantum oscillator can only take discrete values:

$$E_n = n\hbar\omega \qquad [1.42]$$

In this relation, $n = 0, 1, 2, \ldots$ and $\hbar\omega$ is the energy of a quantum of energy.

(2) *Physical significance* $N_0$

– *Expression of* $\langle E_\omega \rangle (T)$

At thermodynamic equilibrium, the number $N_n$ of elementary oscillators of angular frequency $\omega$ follows the Boltzmann distribution law or, using [1.42]:

$$N_n = N_0 \, e^{-n\beta\hbar\omega} \qquad [1.43]$$

$$\beta = 1/kT$$

In relation [1.43], $N_0$ designates the number of elementary oscillators of angular frequency $\omega$ at ground state of energy $E_0 = 0$ ($n = 0$) of the black body cavity.

(3) *Expression of* $\langle E_\omega \rangle (T)$ *as a function of* $N_n$ *and* $E_n$

The average energy $\langle E_\omega \rangle (T)$ of a mode can be calculated by the quotient of the discrete sum of energies of the set of elementary oscillators to the total number of oscillators:

– energy of the set of elementary oscillators:

$$\sum_{n=0}^{\infty} N_n \times E_n$$

In this expression, $N_n$ is given by relation [1.43]:

– total number of oscillators:

$$\sum_{n=0}^{\infty} N_n$$

Hence, the average energy of the set of modes can be written as:

$$\langle E_\omega \rangle (T) = \frac{\sum_{n=0}^{\infty} N_n \times E_n}{\sum_{n=0}^{\infty} N_n} \qquad [1.44]$$

(4) *Demonstration*

Using [1.43] and considering $a = \hbar\omega$, expression [1.44] becomes:

$$\langle E_\omega \rangle (T) = \hbar\omega \frac{\sum_{n=0}^{\infty} n\, e^{-n\beta\hbar\omega}}{\sum_{n=0}^{\infty} e^{-n\hbar\omega\beta}} = a \frac{\sum_{n=0}^{\infty} n\, x^n}{\sum_{n=0}^{\infty} x^n} \qquad [1.45]$$

Since $x < 1$, we have at infinity:

$$\frac{1}{(1-x)} = 1 + x + x^2 + x^3 + x^4 ..... + x^n + O(x^{n+1})$$

Hence:

$$\frac{d}{dx}\left(\frac{1}{1-x}\right) = 1 + 2x + 3x^2 + 4x^3 + .... = \frac{1}{(1-x)^2}$$

Taking these results into account, expression [1.45] is written as:

$$\langle E_\omega \rangle (T) = a \times \frac{x + 2x^2 + 3x^3 + 4x^4 + ........}{1 + x + x^2 + x^3 + x^4 ..........} = a \times x \frac{1 + 2x + 3x^2 + 4x^3 + ........}{1 + x + x^2 + x^3 + x^4 .........} \qquad [1.46]$$

Using these last relations, [1.46] can be written as:

$$\langle E_\omega \rangle (T) = a \times x \frac{(1-x)}{(1-x)^2} = a \times \frac{x}{(1-x)}$$

or by multiplying the numerator and denominator by $x^{-1}$:

$$\langle E_\omega \rangle (T) = \frac{a}{x^{-1} - 1} \qquad [1.47]$$

(5) *Expression of* $\langle E_\omega \rangle (T)$ *as a function of* $\omega$, $\hbar$ *and* $T$

Let us consider: $a = \hbar\omega$, $x = e^{-\beta a}$, $\beta = 1/kT$. The average energy of the set of quantum oscillators is then written according to [1.47]:

$$\langle E_\omega \rangle (T) = \frac{\hbar\omega}{\left(e^{\hbar\omega/kT} - 1\right)} \qquad [1.48]$$

Moreover, spectral energy density is given by the following relation:

$$u(\omega) = n(\omega) \times \langle E_\omega \rangle (T) \qquad [1.49]$$

(6) *Planck's law*

The density of modes is given by the relation $n(\omega) = \omega^2 / \pi^2 c^3$. Planck's law is written as:

$$u(\omega) = \frac{\hbar\omega^3}{\pi^2 c^3} \times \frac{1}{\left(e^{\hbar\omega/kT} - 1\right)} \qquad [1.50]$$

### 1.5.4. *Solution 4 – Deduction of Wien's law from Planck's law*

Using Planck's formula, spectral exitance $M_\lambda$ (or spectral radiance exitance) can be written (for a vacuum) in the form [1.51]:

$$M_\lambda = \frac{2hc^2}{\lambda^5} \frac{1}{e^{hc\beta/\lambda} - 1}$$

(1) *Expression of spectral exitance*

In a medium of refractive index $n_\lambda$, spectral exitance $M_\lambda$ can be written as:

$$M_\lambda = \frac{2hc_\lambda^2}{\lambda^5} \frac{1}{e^{hc_\lambda \beta/\lambda} - 1} \qquad [1.52]$$

with $c_\lambda = c/n_\lambda$, where $c$ is the speed of light in a vacuum, $n_\lambda = 1$. This leads to [1.51].

(2) *Spectral exitance at the peak of light emission of the black body*

At the peak of emission of the black body, spectral exitance is maximal. To put it differently, for $\lambda = \lambda_{\max}$, $M_\lambda$ = constant. This is mathematically expressed by the following relation:

$$\left.\frac{dM_\lambda}{d\lambda}\right|_{\lambda=\lambda_{\max}} = 0 \qquad [1.53]$$

(3) *Deduction of Wien's law*

Let us consider $x = hc\beta/\lambda$. In this case, Planck's law [1.51] can be written as:

$$M_\lambda = \frac{2}{h^4c^3\beta^5} \times \frac{x^5}{e^x - 1} \qquad [1.54]$$

Differentiating expression [1.54] and applying condition [1.53] lead to the required result. It is however simpler to differentiate the inverse of spectral exitance:

$$\frac{d}{d\lambda}\left(\frac{1}{M_\lambda}\right) = \frac{h^4c^3\beta^5}{2} \times \frac{d}{d\lambda}\left(\frac{e^x - 1}{x^5}\right) = \frac{h^4c^3\beta^5}{2} \times \left(\frac{x^5e^x - 5x^4(e^x - 1)}{x^{10}}\right)$$

If the result obtained is minimized with respect to $\lambda$, this leads to:

$$\frac{x^5e^x - 5x^4(e^x - 1)}{x^{10}} = 0 \Rightarrow xe^x - 5(e^x - 1) = 0$$

The division by $e^x / x^5$ leads to:

$$e^{-x} + \frac{1}{5}x - 1 = 0$$

This equation has a unique solution $x_0 = 4.9651$. Knowing that $x = hc\beta/\lambda$, then:

$$x_0 = \frac{hc\beta}{\lambda_{\max}} = \frac{hc}{kT\lambda_{\max}}$$

or:

$$\lambda_{\max}T = \frac{hc}{kx_0} = \text{Cst} \qquad [1.55]$$

Let us find the value of constant Cst in [1.55].

Given $k = 1.3806504 \times 10^{-23}$ J · K$^{-1}$, $h = 6.62606896 \times 10^{-34}$ J · s and $c = 2.99792458 \times 10^{8}$ m · s$^{-1}$, the result is: Cst = 2.89776802 × 10$^{-3}$m · K.

But the Wien constant is $\sigma_W$ = 2,898 × 10$^{-3}$ m · K. It can be noted that Cst ≈ $\sigma_W$.

Hence, relation [1.55] can be written as:

$$\lambda_{\max} T = \sigma_W.$$

which actually corresponds to Wien's first law [1.18].

(4) *Estimation of Sun's surface temperature*

Using Wien's first law [1.18] leads to:

$$T = \frac{\sigma_W}{\lambda_{\max}}. \qquad [1.56]$$

N.A.– $\lambda_{\max}$= 5 × 10$^{-7}$ m; $\sigma_W$ = 2.898 × 10$^{-3}$ m · K. This leads to: $T$ = 5,798 K.

### 1.5.5. *Solution 5 – Total electromagnetic energy radiated by the black body*

(1) *Expression of the flux $d^2\Phi$ and the electromagnetic energy $d^3E$*

The flux contained in the solid angle dΩ and of direction *Ox* making an angle $\theta$ with the normal $\vec{n}$ to the surface *dS* is given by the following relation:

$$\mathrm{d}^2\Phi = AdSd\Omega \qquad [1.57]$$

As the surface *dS* follows Lambert's law, then $A = L\cos\theta$. Hence [1.57] can be written as:

$$\mathrm{d}^2\Phi = L\cos\theta dSd\Omega \qquad [1.58]$$

In this relation, *L* designates the radiance of the emissive surface.

For an elementary duration *dt*, the energy $d^3E$ exiting an orifice of area section *dS* of black surface in the solid angle $d\Omega$ is such that $d^3E = \mathrm{d}^2\Phi dt$. Or considering [1.58] this leads to:

$$d^3E = L_0\cos\theta dSd\Omega dt \qquad [1.59]$$

Along the normal to the orifice ($\theta = 0$), we have:

$$d^3E = L_0 dSd\Omega dt \qquad [1.60]$$

(2) *Expression of the energy density per unit volume*

Electromagnetic radiation is constituted by photons moving at speed $c$. Light energy [1.60] is contained in an elementary cylinder of height $h = cdt$ and volume $d\tau = dSh = cdSdt$. Energy density per unit volume $du$ is then given by the following relation:

$$d^3E = dud\tau = ducdSdt \qquad [1.61]$$

Equalization of [1.60] and [1.61] leads to:

$$du = \frac{d\Omega}{c} L_0 \qquad [1.62]$$

(3) *Demonstration, calculation of* $\sigma^*$

Over the whole space, $\int d\Omega = 4\pi$. Knowing that $L_0$ depends on temperature, the total energy per unit volume $U(T)$ radiated by the black body can be written according to [1.62]:

$$U(T) = \frac{4\pi}{c} L_0 \qquad [1.63]$$

According to the Stefan–Boltzmann law, the total energy exitance of the black body is $M^0 = \pi L_0 = \sigma T^4$. Black body radiance is expressed as a function of temperature as follows:

$$L_0 = \frac{\sigma}{\pi} T^4 \qquad [1.64]$$

Putting [1.64] in [1.63], total energy per unit volume $U(T)$ radiated by the black body can be written as:

$$U(T) = \frac{4\pi}{c} \times \frac{\sigma}{\pi} T^4 \Rightarrow U(T) = \frac{4\sigma}{c} T^4 = \sigma^* T^4 \qquad [1.65]$$

with:

$$\sigma^* = \frac{4\sigma}{c} \qquad [1.66]$$

– *Calculation of constant* $\sigma^*$

$$c = 2.99792458 \times 10^{8}\ \mathrm{m \cdot s^{-1}};\ \sigma = 5.670400 \times 10^{-8}\ \mathrm{W \cdot m^{-2} \cdot K^{-4}}$$

Hence according to [1.66]: $\sigma^* = 7.565767 \times 10^{-16}\ \mathrm{W \cdot s \cdot m^{-3} \cdot K^{-4}} = 7.565767 \times 10^{-16}\ \mathrm{J \cdot m^{-3} \cdot K^{-4}}$.

(4) *Calculation of the total energy per unit volume radiated by the black body*

Using [1.65] leads to the numerical result $T = 6000$ K: $U = 0.98$ J.

## 2

# Wave and Particle Aspects of Light

### *General objective*

Gain knowledge on the wave and particle properties of light.

### *Specific objectives*

On completing this chapter, the reader should be able to:

- define coherent sources;
- describe Young's experimental set-up;
- define the interference field;
- provide an interpretation of how interference fringes form;
- define the path difference;
- define the order of interference;
- determine the spacing between fringes;
- describe the experimental set-up for observing the photoelectric effect;
- define the photoelectric effect;
- provide an interpretation of the photoelectric effect;
- use Einstein relation;
- define the photoelectric threshold;
- express the stopping potential;
- define the saturation current;

---

For color versions of the figures in this book, see www.iste.co.uk/sakho/quantum1.zip.

*Introduction to Quantum Mechanics 1: Thermal Radiation and Experimental Facts Regarding the Quantization of Matter,* First Edition. Ibrahima Sakho.

- determine the quantum efficiency of a photoelectric cell;
- define the sensitivity of a photoelectric cell;
- experimentally determine Planck constant;
- describe the experimental set-up for observing the Compton effect;
- define the Compton effect;
- provide an interpretation of the Compton effect;
- define the Compton wavelength of the electron;
- establish the Compton shift in wavelength;
- express Planck–Einstein relations combining the wave and particle properties of light.

*Prerequisites*

- plane electromagnetic wave;
- light diffraction;
- photon characteristics;
- energy and linear momentum of a relativistic particle.

## 2.1. Light interferences

### 2.1.1. *Elongation of a light wave*

Light propagates in an arbitrary medium through vibrations of *plane electromagnetic waves* [STA 08, SAK 18]. These are transverse waves since the electric and magnetic fields are perpendicular to one another and to the propagation direction, which is given by the direction of the wave vector $\vec{k}$. Let us consider a light wave that propagates along *Ox* and whose period is *T*. The *elongation of the wave* is given by the following expression:

$$a(x,t) = A\sin(\omega t - kx + \varphi) \qquad [2.1]$$

In this relation:

- $A$ is the amplitude of the wave, which is essentially positive: maximal value of $a(x, t)$;
- $\omega$ designates the angular frequency of the wave: $\omega = 2\pi/T = 2\pi f$, $f$ is the wave frequency;

– $k$ is the norm of the wave vector: $k = 2\pi/\lambda$, $\lambda$ is the spatial period of the wave and $\varphi$ represents the phase of the wave.

In the international system of units $\omega$ is expressed in radian per second (rad · $s^{-1}$); $T$ in seconds (s), $f$ in hertz (Hz), $k$ in meters to negative 1 power ($m^{-1}$); $\lambda$ in meters (m) and $\varphi$ in radians (rad). Figure 2.1 indicates the principle of measurement of the *temporal period T* and the *spatial period λ* (*wavelength*) of a light wave whose elongation is given by [2.1].

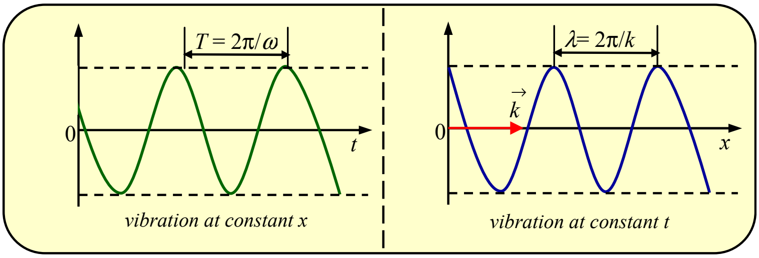

**Figure 2.1.** *Temporal period T and spatial period λ of a light wave*

## 2.1.2. *Total elongation of synchronous light sources*

Let us consider two *synchronous* (same period $T$) light sources $S_1$ and $S_2$ whose waves propagate along $Ox$ axis. Their respective elongations $a_1(x, t)$ and $a_2(x, t)$ are given by the following relations:

$$a_1(x,t) = A\sin(\omega t - kx + \varphi_1) \quad [2.2]$$

$$a_2(x,t) = A\sin(\omega t - kx + \varphi_2) \quad [2.3]$$

According to the *principle of superposition*, the sum of the two elongations is:

$$a(x,t) = A\sin(\omega t - kx + \varphi_1) + A\sin(\omega t - kx + \varphi_2) \quad [2.4]$$

Using the trigonometric relation:

$$\sin\alpha + \sin\beta = 2\sin\frac{\alpha+\beta}{2}\cos\frac{\alpha-\beta}{2} \quad [2.5]$$

and considering:

$$\alpha = (\omega t - kx + \varphi_1)\ ;\ \beta = (\omega t - kx + \varphi_2)$$

Relation [2.4] can be written as:

$$a(x,t) = A\left[2\sin\frac{(\omega t - kx + \varphi_1) + (\omega t - kx + \varphi_2)}{2}\cos\frac{(\omega t - kx + \varphi_1) - (\omega t - kx + \varphi_2)}{2}\right]$$

which is:

$$a(x,t) = 2A\left[\sin\left(\omega t - kx + \frac{\varphi_1 + \varphi_2}{2}\right)\cos\frac{\varphi_1 - \varphi_2}{2}\right] \qquad [2.6]$$

The *phase shift* between two sources $S_1$ and $S_2$ is the phase difference $\Delta\varphi$ given by the relation: $\Delta\varphi = \varphi_1 - \varphi_2$. By definition, two sources are known as coherent if they are synchronous (they have the same period) and if their phase shift is constant in time ($\Delta\varphi$ = constant). The two sources $S_1$ and $S_2$ are in phase if the phase shift is zero:

$$\Delta\varphi = \varphi_1 - \varphi_2 = 0 \Rightarrow \varphi_1 = \varphi_2 = \varphi$$

In this case, elongation [2.6] is written as:

$$a(x,t) = 2A\sin(\omega t - kx + \varphi) \qquad [2.7]$$

In practice, two coherent sources can be obtained from a single source of monochromatic light using *Young's experimental set-up*.

## 2.1.3. *Young's experimental setup*

A schematic diagram of Young's experimental setup, which is used for studying light interferences, is presented in Figure 2.2. In brief, this setup is composed of a light source $S$ (*main source*) and a thin sheet pierced by two small slits $S_1$ and $S_2$, referred to as *Young's slits* (*secondary sources*), so that $SS_1 = SS_2$. The main source light is a monochromatic radiation generated by a laser beam [SAK 16].

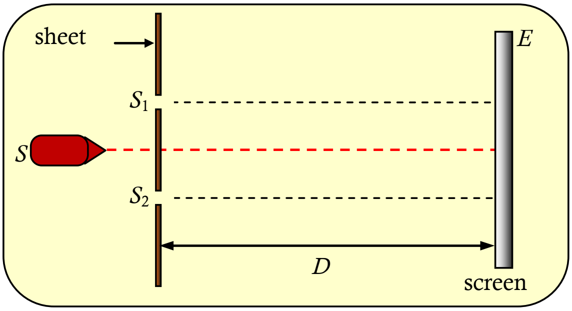

**Figure 2.2.** *Young's experimental setup for observing light interferences*

$S_1S_2$ is a distance of the order of several dozens of millimeters. A screen ($E$) parallel to the sheet is placed at a distance $D$ from the latter.

### 2.1.4. *Interference field, fringes of interference*

A monochromatic light source $S$ (*laser source*) lights the slits $S_1$ and $S_2$. The waves emerging from the two slits overlap in a space known as *interference field*. The screen ($E$) shows *light* or *bright bands* and *dark* or *obscure bands* known as *fringes of interference* (Figure 2.3). The physical phenomenon observed on the screen is called *interference*. Light interference occurs, provided that the two waves that superpose in a propagation medium are emanated by two coherent sources.

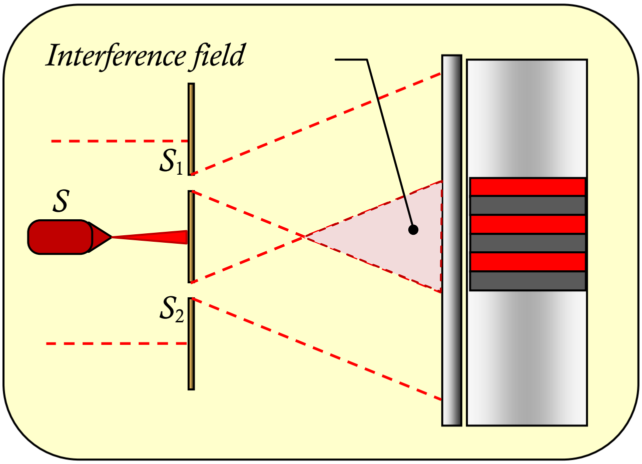

**Figure 2.3.** *Light interference fringes*

### 2.1.5. *Interpretation, interference as concept*

Light coming from source $S$ undergoes *diffraction* when it reaches slits $S_1$ and $S_2$. Diffracted waves overlap in the interference field. The points where the amplitude of vibrations is *maximal* and those where the amplitude of vibrations is *minimal* are distributed on surfaces called *hyperboloids* and form the fringes of interference. These fringes should appear as curved. But given that the interference phenomenon is observed in a very limited region of the screen and at a distance $D$ from sources $S_1$ and $S_2$ that is very long compared to the space between them ($D >> S_1S_2$), the curve of fringes cannot be perceived. Parallel and equally spaced fringes are observed at the intersection of the mediating plane of the two sources with the screen. Light diffraction due to secondary sources $S_1$ and $S_2$ and the formation of fringes of interference support the *wave aspect* of light.

Let us now adopt a mathematical perspective and analyze the interference phenomenon using the complex notation of waves [STA 08, PÉR 86]. Given $\Psi_1(x, t)$ and $\Psi_2(x, t)$, waves that propagate along the same axis $Ox$ and emanate from slits $S_1$ and $S_2$, respectively, the following relations can be written as:

$$\Psi_1(x,t) = \Psi_{01} e^{i(kx-\omega t+\varphi_1)} \qquad [2.8]$$

$$\Psi_2(x,t) = \Psi_{02} e^{i(kx-\omega t+\varphi_2)} \qquad [2.9]$$

At any point $M$ of the interference field, the global wave function $\Psi(x, t)$ results from the superposition of waves $\Psi_1(x, t)$ and $\Psi_2(x, t)$, which can be written as:

$$\Psi(x,t) = \Psi_{01} e^{i(kx-\omega t+\varphi_1)} + \Psi_{02} e^{i(kx-\omega t+\varphi 2)} \qquad [2.10]$$

By definition, *light intensity* $I$ is equal to the average value in time of the squared module $|\Psi(x, t)|^2 = \Psi(x, t)\ \Psi^*(x, t)$ of the wave function $\Psi(x, t)$, which is:

$$I = \langle \Psi(x,t)\Psi^*(x,t) \rangle_t = \left\langle [\Psi_1(x,t)+\Psi_2(x,t)] \times [\Psi_1^*(x,t)+\Psi_2^*(x,t)] \right\rangle_t \qquad [2.11]$$

Using [2.11], this gives:

$$I = \left\langle \Psi_1(x,t)\Psi_1^*(x,t) + \Psi_2(x,t)\Psi_1^*(x,t) + \Psi_1(x,t)\Psi_2^*(x,t) + \Psi_2(x,t)\Psi_2^*(x,t) \right\rangle_t$$

Hence:

$$I = \left\langle |\Psi_1(x,t)|^2 + |\Psi_2(x,t)|^2 + \Psi_1(x,t)\Psi_2^*(x,t) + \Psi_2(x,t)\Psi_1^*(x,t) \right\rangle_t \qquad [2.12]$$

Considering expressions [2.8] and [2.9], relation [2.12] can be written as:

$$I = \left\langle \Psi_{01}^2 + \Psi_{02}^2 + \Psi_{01}\Psi_{02} e^{i(\varphi_1-\varphi_2)} + \Psi_{02}\Psi_{01} e^{-i(\varphi_1-\varphi_2)} \right\rangle_t$$

which is:

$$I = \left\langle \Psi_{01}^2 + \Psi_{02}^2 + \Psi_{01}\Psi_{02}[\cos(\varphi_1-\varphi_2) + i\sin(\varphi_1-\varphi_2) + \cos(\varphi_1-\varphi_2) - i\sin(\varphi_1-\varphi_2)] \right\rangle_t$$

or:

$$I = \Psi_{01}^2 + \Psi_{02}^2 + 2\Psi_{01}\Psi_{02}\cos(\varphi_1-\varphi_2)$$

Knowing that partial intensities are $I_1 \equiv \Psi_{01}^2$ and $I_2 \equiv \Psi_{02}^2$, this finally leads to:

$$I = I_1 + I_2 + 2\sqrt{I_1 I_2}\cos\varphi = I_1 + I_2 + 2I_{12} \qquad [2.13]$$

Result [2.13] shows that the intensity $I$ of the wave resulting from the superposition of light waves from secondary sources $S_1$ and $S_2$ is not the sum of partial intensities $I_1$ and $I_2$. The third term $I_{12} = 2\sqrt{I_1 I_2}\cos\varphi$ containing the phase difference between the two waves $\varphi = (\varphi_1 - \varphi_2)$ is known as *interference term*.

As sources $S_1$ and $S_2$ are identical in all respects (originating from the same main source $S$ and being symmetrical with respect to the mediating plane containing the central fringe, see Figure 2.2), then $I_1 = I_2$. Hence [2.13] can be written as:

$$I = 2I_0 + 2I_0\cos\varphi = 2I_0(1+\cos\varphi) \qquad [2.14]$$

Relation [2.14] has two extremely important consequences:

– when $\varphi = 0$, the two waves are *in phase* and $I = 4I_0$: in this case, interferences are *constructive*. *Bright fringes* or fringes of *maximal amplitude* are obtained;

– when $\varphi = \pi$, the two waves are *out of phase* and $I = 0$: the result is darkness. Interferences are *destructive*. This corresponds to *dark fringes* or to fringes of *zero amplitude*. In this case, "light added to light" results in darkness. This supports the purely wave-like character of light.

**APPLICATION 2.1.–**

Let us consider two non-polarized (non-coherent) sources $S_1$ and $S_2$, whose light intensities are $I_1 = 10\ \mathrm{W \cdot m^{-2}}$ and $I_1 = 20\ \mathrm{W \cdot m^{-2}}$, respectively. Find intensity $I$ at point $M$ where the waves coming from $S_1$ and $S_2$ meet.

**Solution.** Being non-polarized and non-coherent, the two sources $S_1$ and $S_2$ do not interfere. The interference term $I_{12}$ is therefore zero. Hence: $I = 30\ \mathrm{W \cdot m^{-2}}$.

### 2.1.6. *Path difference*

Let $M$ be a point on the screen in the interference field (Figure 2.4). By definition, the *path difference* denoted $\delta$ between the light rays emitted by the two secondary sources $S_1$ and $S_2$ is given by the relation:

$$\delta = |MS_2 - MS_1| \qquad [2.15]$$

where $MS_1$, $MS_2$ and $\delta$ are expressed in meters.

Let $\lambda$ be the wavelength of light radiations emitted by the monochromatic source $S$.

– Interferences are *constructive* if, in $M$, $\delta = k\lambda$; $k$ is a natural integer.

– Interferences are *destructive* if, in $M$, $\delta = (k + \frac{1}{2})\lambda = k\,\lambda + \frac{\lambda}{2}$; $k$ is a natural integer.

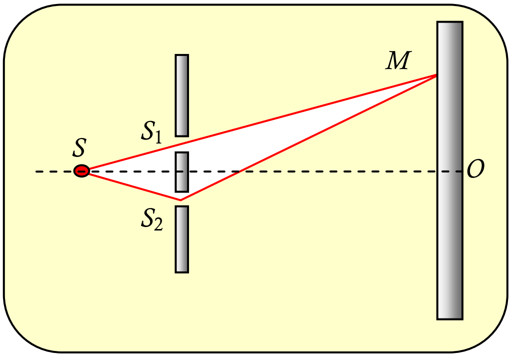

**Figure 2.4.** *Definition of the path difference $\delta$ = |MS2 – MS1|*

For $k = 0$, $\delta = |MS_2 - MS_1| = 0 \Rightarrow |MS_1| = |MS_2|$: this corresponds to the *bright central fringe* contained in the mediating plane of $S_1S_2$ passing through point $O$ (Figure 2.4). In order to obtain the expression of the path difference, let us consider Figure 2.5.

The path difference can be deduced from relation [2.15] if we find the expressions of lengths $MS_1 = r_1$ and $MS_2 = r_2$. According to Figure 2.5:

$$r_1^2 = D^2 + \left(x - \frac{a}{2}\right)^2 \;;\; r_2^2 = D^2 + \left(x + \frac{a}{2}\right)^2 \qquad [2.16]$$

Using [2.16] leads to:

$$\left|r_1^2 - r_2^2\right| = \left|r_1 - r_2\right| \times \left|r_1 + r_2\right| = \left|D^2 + \left(x - \frac{a}{2}\right)^2 - D^2 - \left(x + \frac{a}{2}\right)^2\right|$$

which is:

$$|r_1 - r_2| \times (r_1 + r_2) = \left|\left(x^2 + \frac{a^2}{4} - ax\right) - \left(x^2 + \frac{a^2}{4} + ax\right)\right| = 2ax \qquad [2.17]$$

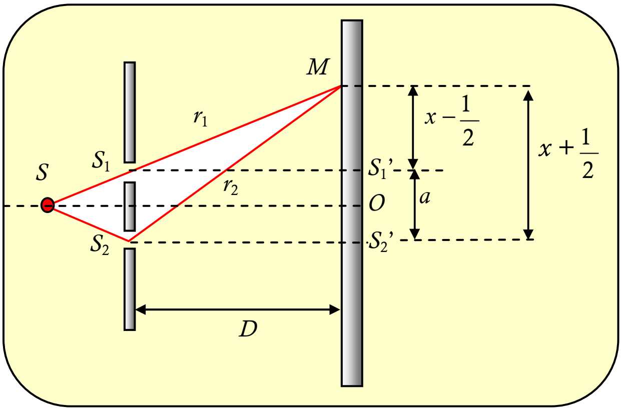

**Figure 2.5.** *Finding the expression of the path difference*

Young's experimental setup is such that $(r_1 + r_2) \approx 2D$. Then relation [2.17] can be written as:

$$2D|r_1 - r_2| = 2ax \Rightarrow |r_1 - r_2| = \frac{ax}{D} \qquad [2.18]$$

A comparison between result [2.18] and relation [2.15] leads to the expression of the path difference, which is:

$$\delta = \frac{ax}{D} \qquad [2.19]$$

### 2.1.7. *Fringe spacing, order of interference*

By definition, *fringe spacing* denoted by *i* is the distance between two fringes of the same nature. The principle of measurement of fringe spacing is shown in Figure 2.6. Fringe spacing can be determined by measuring the *spacing between the midpoints of two consecutive fringes of the same nature* (*in practice, the length l filled by a large number of fringe spacings is measured, to minimize measurement errors, for example: l =10i*).

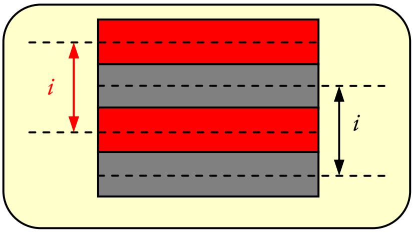

**Figure 2.6.** *Principle of measurement of fringe spacing i*

Moreover, the term *order of interference* (or *order of an interference fringe*) designates the integer $k$ involved in path difference calculation.

– For a bright fringe of order $k$:

$$\delta_k = \frac{a}{D} x_k = k\,\lambda \Rightarrow x_k = k\frac{\lambda D}{a} \qquad [2.20]$$

– For a dark fringe of order $k$:

$$\delta_k = \frac{a}{D} x_k = \left(k + \frac{1}{2}\right)\lambda \Rightarrow x_k = \left(k + \frac{1}{2}\right)\frac{\lambda D}{a}. \qquad [2.21]$$

By definition, fringe spacing $i$ is given by the relation:

$$i = x_{k+1} - x_k \qquad [2.22]$$

Using [2.20] or [2.21] leads to the same result:

$$i = \frac{\lambda D}{a} \qquad [2.23]$$

Relation [2.23] shows that fringe spacing $i$ is proportional to the wavelength $\lambda$ of light waves. Therefore, the measurement of $i$ makes it possible to determine $\lambda$.

**APPLICATION 2.2.–**

> Let us consider a point $M$ located at a distance $x$ from the center $O$ of a screen displaying interference fringes. The radiation used has a wavelength of 633 nm. What is the distance between point $O$ and the dark fringe of order 9?
>
> *Given data*. $a = 500$ µm; $D = 2.0$ m

**Solution.** Dark fringes result from zero-amplitude vibrations. Their positions are given by relation [2.21], which yields:

$$x_k = \left(k + \frac{1}{2}\right)\frac{\lambda D}{a} \Rightarrow x_9 = \frac{19}{2} \times \frac{\lambda D}{a}$$

N.A.– x9 = 0.024054 m = 2.4 cm

**Thomas Young** was a British physicist, physician and Egyptologist. In physics, he is well-known for his double slit experiment in optics, known as Young's double slit experiment, in his honor. In 1801, Young sent a light beam through two parallel slits and observed its projection on a screen. Light is diffracted when passing through the slits and produces alternating bright and dark bands on the screen, known as interference fringes. Young offered an interpretation of the observed phenomenon, which supported the wave-like nature of light.

**Box 2.1.** *Young (1773–1829)*

### APPLICATION 2.3.–

A light interference experiment is set up using a He-Ne laser source. For a spacing between slits $a$ = 350 µm and a screen located at distance $D$ = 4 m, the experimentally measured value of the fringe spacing is $i$ = 7.2 mm. Find the wavelength of the laser beam used. Compare the result with the manufacturer specification: $\lambda_0$ = 632.8 nm.

**Solution.** Relation [2.23] is used to deduce the expression of the wavelength. This gives:

$$\lambda = i\frac{a}{D} \qquad [2.24]$$

N.A.– $\lambda = 630.0$ NM.

The experimental value is $\lambda_{exp}$ = 630.0 nm. This value is close to the wavelength specification $\lambda_0$ = 632.8 nm provided by the manufacturer. Relative deviation is approximately 0.44%.

## 2.2. Photoelectric effect

### 2.2.1. *Experimental setup, definition*

The *photoelectric effect* was first observed by **Heinrich Hertz** in 1887, when exposing an initially negatively charged zinc plate to ultraviolet (UV) radiation [PÉR 86, DUA 08, SAK 12, PAR 15, SAK 16]. He noted a discharge inside an electroscope connected to the zinc plate. The experimental set-up currently used for the observation of the photoelectric effect is schematically shown in Figure 2.7.

A freshly etched zinc plate amalgamated with mercury is placed on a negatively charged *electroscope*. The plate is lighted by a halogen lamp with quartz crystal envelope (*UV-rich light*). Rapid discharge of the electroscope can be noted, which proves that *electrons are removed* from the *lighted* zinc plate: this is referred to as photoelectric effect.

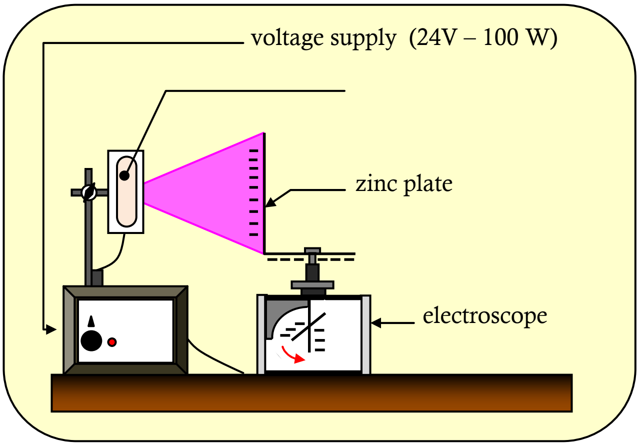

**Figure 2.7.** *Experimental setup for the observation of the photoelectric effect*

If light passes through a glass plate that fully absorbs ultraviolet radiations, the electroscope does not discharge; this proves that the removal of electrons due to photoelectric effect requires *short wavelength light*. By definition, p-hotoelectric effect is the extraction of electrons from a metal exposed to adequate (UV-rich) light. Electrons removed by light are known as *photoelectrons*.

### 2.2.2. *Interpretation, photon energy*

The photoelectric effect is explained within Einstein's *photon theory*. Light is a set of particles called photons. Therefore, the photoelectric effect results from a collision between a *photon* of light radiation and an *electron* of the lighted metal. Two outcomes are possible:

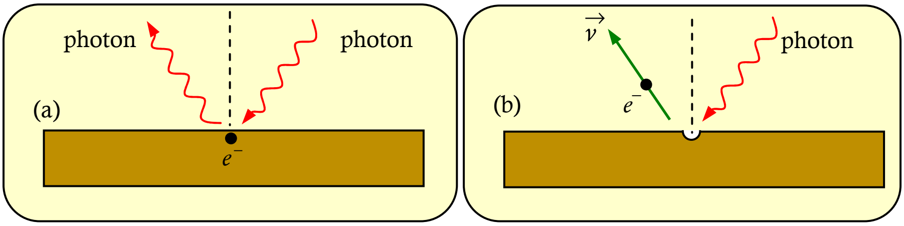

**Figure 2.8.** *Interpretation of the photoelectric effect: photonelectron collision*

– if photon energy is not sufficient (*long wavelength light*), the photon rebounds off the metal and the electron is not removed (Figure 2.8(a));

– if photon energy is sufficient (*short wavelength light*), the photon is absorbed by the metal, which absorbs all its energy: one electron is then removed and set in motion with maximal speed $v$ (Figure 2.8(b)).

In conclusion, the photoelectric effect supports the *particle nature of light*.

**Heinrich Rudolf Hertz** was a German engineer and physicist. He is especially well-known for his discoveries in the field of electromagnetism. He discovered the photoelectric effect in 1887. In 1888, he discovered electromagnetic waves, which he named Hertzian waves.

**Box 2.2.** *Hertz (1857–1894)*

### 2.2.3. *Einstein relation, energy function*

According to Planck's theory of quanta, each photon of light radiation has an energy $E = h\nu$. When photon energy $E$ is high enough, it is partly ($W_0$) used to remove the electron, while the remaining energy is transmitted to the electron as kinetic energy $E_c$. According to *energy conservation law*: $E = E_c + W_0$. As the ejected electron is a classical particle, its maximal kinetic energy is:

$$\frac{1}{2}mv^2 = h\nu - W_0 \qquad [2.25]$$

Energy denoted by $W_0$ is known as *work function*. Relation [2.25] is referred to as *Einstein photoelectric equation*. In equation [2.25], $m$ is expressed in kilograms (kg), $v$ in meters per second ($m \cdot s^{-1}$), $h$ in joule second ($J \cdot s$), $\nu$ in hertz (Hz) and $W_0$ in joule (J). The values of the work function for several metals are provided in Table 2.1.

| | Cesium | Lithium | Zinc | Tungsten | Chromium | Silver | Platinum |
|---|---|---|---|---|---|---|---|
| Symbol | Cs | Li | Zn | W | Cr | Ag | Pt |
| $W_0$ (eV) | 1.8 | 2.3 | 3.4 | 4.5 | 4.6 | 4.8 | 5.3 |

**Table 2.1.** *Work function for several metals*

Work function is generally expressed in eV: 1 eV ≈ $1.60 \times 10^{-19}$ J

**Albert Einstein** was a theoretical physicist of several citizenships: German, Swiss and American. He published his theory of special relativity in 1905 and his theory of gravity known as the theory of general relativity in 1915. Einstein contributed to the development of quantum mechanics and was awarded the Nobel Prize in Physics in 1921 for his interpretation of the photoelectric effect. Einstein has also become famous for his equation $E = mc^2$ expressing the mass–energy equivalence.

**Box 2.3.** *Einstein (1879–1955)*

**APPLICATION 2.4.–**

A photon of energy $5.44 \times 10^{-19}$ J is fully absorbed by a metal used for the study of photoelectric effect. The final speed of the consequently ejected electron is zero. What is the chemical nature of the metal? To answer the question, use the values $W_0$ summarized in Table 2.1.

**Solution.** Einstein equation [2.25] is used; given that electron speed is zero after photon absorption: $W_0 = 5.44 \times 10^{-19}$ J = 3.4 eV, hence the metal is zinc (Zn).

## 2.2.4. *Photoelectric threshold*

When the extracted electron is not set into motion, its speed is $v = 0$. According to equation [2.25]:

$$\begin{cases} h\nu = h\nu_0 = W_0 \\ h\dfrac{c}{\lambda} = h\dfrac{c}{\lambda_0} = W_0 \end{cases} \Rightarrow \begin{cases} \nu_0 = \dfrac{W_0}{h} \\ \lambda_0 = \dfrac{hc}{W_0} \end{cases} \qquad [2.26]$$

In [2.26], $\nu$ and $\nu_0$ are expressed in hertz (Hz), $\lambda$ and $\lambda_0$ in meters (m), $W_0$ in joule (J), $h$ is Planck constant and $c$ designates the speed of light in vacuum.

Using [2.26], Einstein equation [2.25] can be written as:

$$\frac{1}{2}mv^2 = h(\nu - \nu_0) = hc\left(\frac{1}{\lambda} - \frac{1}{\lambda_0}\right) \quad [2.27]$$

The kinetic energy of the electron being positive, photoelectric effect does not occur unless the frequency $\nu$ or the wavelength $\lambda$ of the radiation employed satisfies the inequality:

$$\nu > \nu_0 \text{ or } \lambda < \lambda_0 \quad [2.28]$$

By definition, $\nu_0$ and $\lambda_0$ are the *threshold frequency* and the *threshold wavelength* of the photoelectric effect, respectively.

**APPLICATION 2.5.–**

A photon whose wavelength is 260 nm hits a tungsten plate whose work function is 4.49 eV. Does photoelectric effect occur?

If yes, calculate the speed of the ejected electron.

*Given data.* $m = 9.109 \times 10^{-31}$ kg; $hc = 1.986 \times 10^{-25}$ SI; 1 eV = $1.602 \times 10^{-19}$ J

**Solution.**

1. According to Einstein equation, the photoelectric effect is observed provided that:

$$\frac{1}{2}mv^2 = hc\left(\frac{1}{\lambda} - \frac{1}{\lambda_0}\right) = \left(\frac{hc}{\lambda} - \frac{hc}{\lambda_0}\right) = \frac{hc}{\lambda} - W_0 > 0 \quad [2.29]$$

or:

$$E = \frac{hc}{\lambda}$$

N.A.– E = 4.77 eV > W0 = 4.49 eV: photoelectric effect is therefore observed.

2. Speed is given by the following relation:

$$v = \sqrt{\frac{2(E - W_0)}{m}} : v = 3.14 \times 10^5 \text{ m} \cdot \text{s}^{-1} \quad [2.30]$$

### 2.2.5. *Stopping potential, saturation current*

The experimental set-up for the study of the photoelectric effect is schematically represented in Figure 2.9. This shows the *photoelectric cell* constituted of a UV transparent glass envelope in which there is high vacuum.

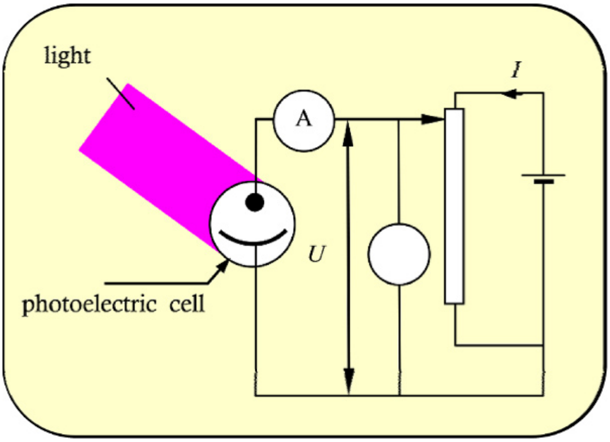

**Figure 2.9.** *Experimental setup for the study of photoelectric effect*

Voltage $U$ is applied between the light sensitive photoelectric cathode and the anode. Using a source of monochromatic light, the variations in *photocurrent* intensity $I$ due to photoelectrons are studied as a function of voltage $U$ for various increasing values of light output $P$. The observed characteristics are represented in Figure 2.10.

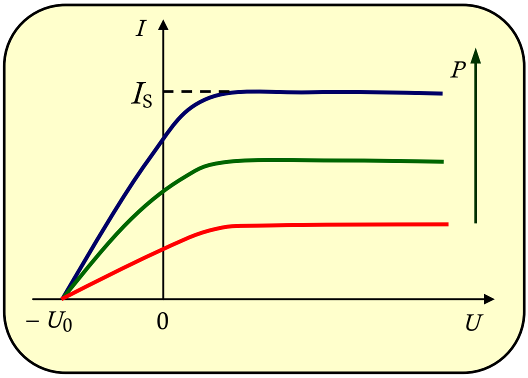

**Figure 2.10.** *Variations of photocurrent intensity I as a function of the applied voltage U, under increasing light output P*

For a given light output, the following can be noted:

– Intensity $I$ increases when voltage $U$ increases. Then it reaches a maximum $I_s$ irrespective of the value of $U$.

– For a certain voltage $U = U_0$, the *current is zero*.

By definition, the current of intensity $I_S$ is known as *saturation current*. Saturation is reached when *all the photoelectrons in the metal are ejected*. Let $n$ be their number. The intensity of saturation current per unit time is given by the following relation (*resulting from* $q = It = ne$, *where e is the elementary charge*):

$$I_s = ne \qquad [2.31]$$

To clarify the physical significance of $U_0$, let us consider the potential difference $U = V_A - V_C = -U_0$. If the origin of electric potential is chosen at photocathode level ($V_C = 0$), then: $V_A = -U_0$. When $U = -U_0$, current intensity is zero. Consequently, all photoelectrons are rejected by the anode ($V_A = -U_0$). This explains the curved trajectories shown in Figure 2.11. Voltage $U_0$ is thus known as *stopping potential*.

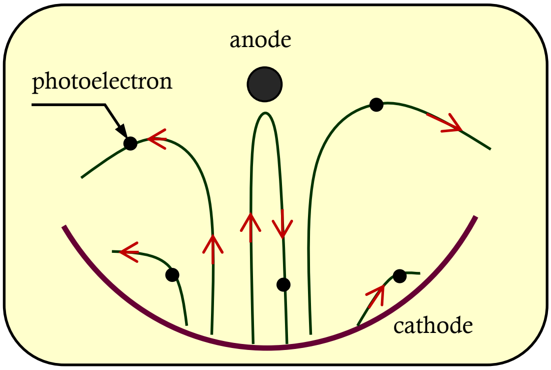

**Figure 2.11.** *Paths of photoelectrons rejected by the anode brought at electric potential $V_A = -U_0$*

Let us now fix light output $P$ and vary frequency $\nu$. It can be noted that stopping potential $U_0$ increases with frequency (Figure 2.12).

The application of work–energy theorem between cathode and anode can provide a theoretical interpretation of the observations shown in Figure 2.12. This gives:

$$E_{cA} - E_{cC} = -eU_0$$

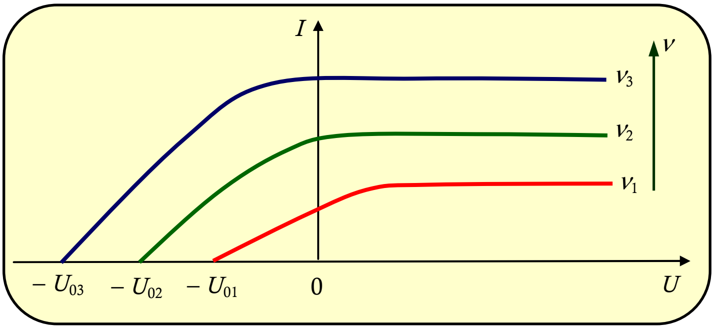

**Figure 2.12.** *Variation of stopping potential $U_0$ with frequency ν of light radiation*

Using Einstein equation [2.25] leads to (photoelectrons are rejected by the anode: therefore their speed upon arriving at the anode is 0):

$$0-\frac{1}{2}mv^2=-(E-W_0)=-eU_0$$

Hence:

$$\begin{cases} U_0=\dfrac{h}{e}\times\nu-\dfrac{W_0}{e} \\ U_0=\dfrac{hc}{e}\times\dfrac{1}{\lambda}-\dfrac{W_0}{e} \end{cases} \qquad [2.32]$$

The first equation of system [2.32] clearly shows that stopping potential $U_0$ increases when light frequency increases, according to experimental observations (Figure 2.12. Moreover, the experimental study of the curve $U_0 = f(\nu)$ or of $U_0 = f(1/\lambda)$ makes it possible to *measure* Planck constant $h$ and *identify* the photocathode by measuring the work function $W_0$ (see Exercise 2.5.6). For example, the curve $U_0 = f(1/\lambda)$ is a straight line of slope $a = hc/e$ and ordinate at the origin $b = -W_0/e$.

### APPLICATION 2.6.–

An aluminum photocathode at zero potential is bombarded by photons of energy 8.4 eV. Knowing that the work function is 4.2 eV, calculate the stopping potential.

**Solution.** It can be noted that $E = 2W_0$

According to the work–energy theorem:

$eU_0 = E - W_0 = W_0 \Rightarrow U_0 = W_0/e$. Or: $U_0 = 4.2$ V

### 2.2.6. *Quantum efficiency of a photoelectric cell*

The *quantum efficiency* $\eta$ of a photoelectric cell is equal to the ratio of the number $n$ of photoelectrons emitted by the photocathode to the number $N$ of incident photons of the light radiation, which is: $\eta = n/N$. Using [2.31] leads to $n = I_S/e$. Knowing that $N = P/h\nu$, then:

$$\eta = \frac{I_S}{e} \times \frac{h\nu}{P} \tag{2.33}$$

Quantum efficiencies of photoelectric cells range between 0.2% and 20%. These low quantum efficiencies are explained by the fact that there are very few effective photons in the set of received incident photons.

**APPLICATION 2.7.–**

> A photocathode is irradiated with a 2 mW He-Ne laser emitting monochromatic light whose wavelength is 630 nm. The measured number of effective photons per second is $9.495 \times 10^{14}$. Find the quantum efficiency of the photoelectric cell.
>
> *Given data.* $hc = 1.986 \times 10^{-25}$ SI
>
> **Solution.** The quantum efficiency of the cell is $\eta = n/N$; the number of effective photons per second is equal to the number $n$ of photoelectrons emitted per unit time. Light output $P$ is given by the following relation:
>
> $$P = Nh\nu = \frac{Nhc}{\lambda} \Rightarrow N = \frac{P\lambda}{hc}$$
>
> or:
>
> $$\eta = \frac{nhc}{P\lambda} \Rightarrow \eta \approx 15\% \tag{2.34}$$

### 2.2.7. *Sensitivity of a photoelectric cell*

By definition, the *sensitivity of a photoelectric cell* denoted $s$ is the quotient of the saturation current by the light output received by the photocathode, which is:

$$s = \frac{I_s}{P} \tag{2.35}$$

Sensitivity is expressed in ampere per watt ($A \cdot W^{-1}$).

As a function of wavelength, sensitivity is given by the relation:

$$s = \frac{I_S}{P} = \frac{n.e}{Nh\nu} = \eta\frac{e}{h\nu} = \eta\frac{e}{hc} \times \lambda$$

If the number $N$ of incident photons is assumed equal to the number $n$ of *effective photons*, then the following relation is eventually obtained ($\eta = 100\%$):

$$s = \frac{e}{hc} \times \lambda = \frac{\lambda}{hc/e} \qquad [2.36]$$

## Numerical expression:

$$\frac{hc}{e} = \frac{6.62606896 \times 10^{-34} \times 299792458}{1.602179487 \times 10^{-19}} = 1239.839 \times 10^{-9} \approx 1240 \times 10^{-9}$$

Hence sensitivity [2.36] can be written as:

$$s = \frac{\lambda(nm)}{1240} \qquad [2.37]$$

Result [2.37] shows the linear variation of *theoretical sensitivity* with wavelength. Nevertheless, the number of effective photons within the set of received incident photons being small, *actual sensitivity* is not proportional to the wavelength (Figure 2.13). Theoretical predictions are erroneous for $\lambda = \lambda_0$ (maximal sensitivity) while actual sensitivity is zero. Photoelectric effect occurs for $\lambda < \lambda_0$: sensitivity cannot be measured for $\lambda > \lambda_0$.

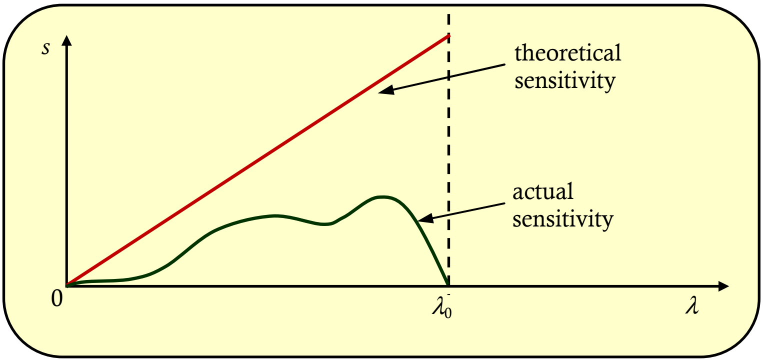

**Figure 2.13.** *Variation of theoretical and actual sensitivities of a photoelectric cell with wavelength*

## 2.3. Compton effect

### 2.3.1. *Experimental setup, definition*

The simplified experimental set-up for the observation of the *Compton effect* is schematically represented in Figure 1.19.

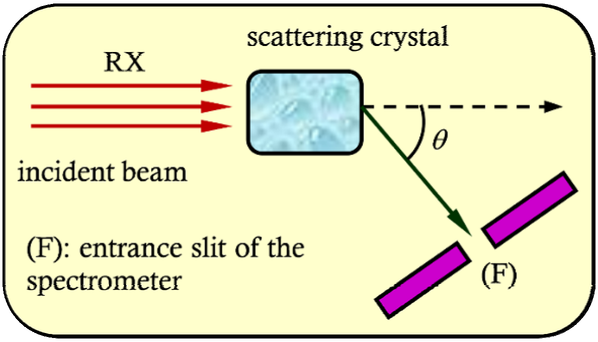

**Figure 2.14.** *Experimental set-up for the observation of Compton effect*

A monochromatic X-ray beam hits a target crystal. Scattered light waves are observed with a *crystal spectrometer* [GRO 85, SAK 12, PAR 15].

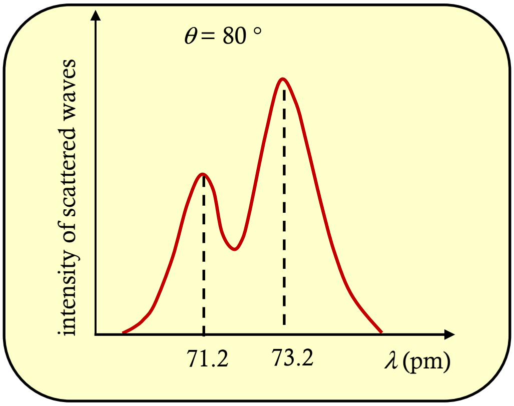

**Figure 2.15.** *Spectrum of rays due to Compton effect*

For the molybdenum ray of wavelength $\lambda$ = 71.2 pm and for a *scattering angle* $\theta$ = 80°, a spectrum of rays as shown in Figure 2.15 is observed. It can then be noted that the *spectrum of scattered waves* involves two rays: one ray of wavelength $\lambda_i$ equal to that of the incident waves and another ray of wavelength $\lambda_d > \lambda_i$: this is known as the *Compton effect*.

By definition, the Compton effect is the *scattering of a photon* by an electron at rest, accompanied by energy loss (at the expense of the incident photon). The positive difference $\Delta\lambda = (\lambda_d - \lambda_i)$ is referred to as *Compton shift in wavelength*.

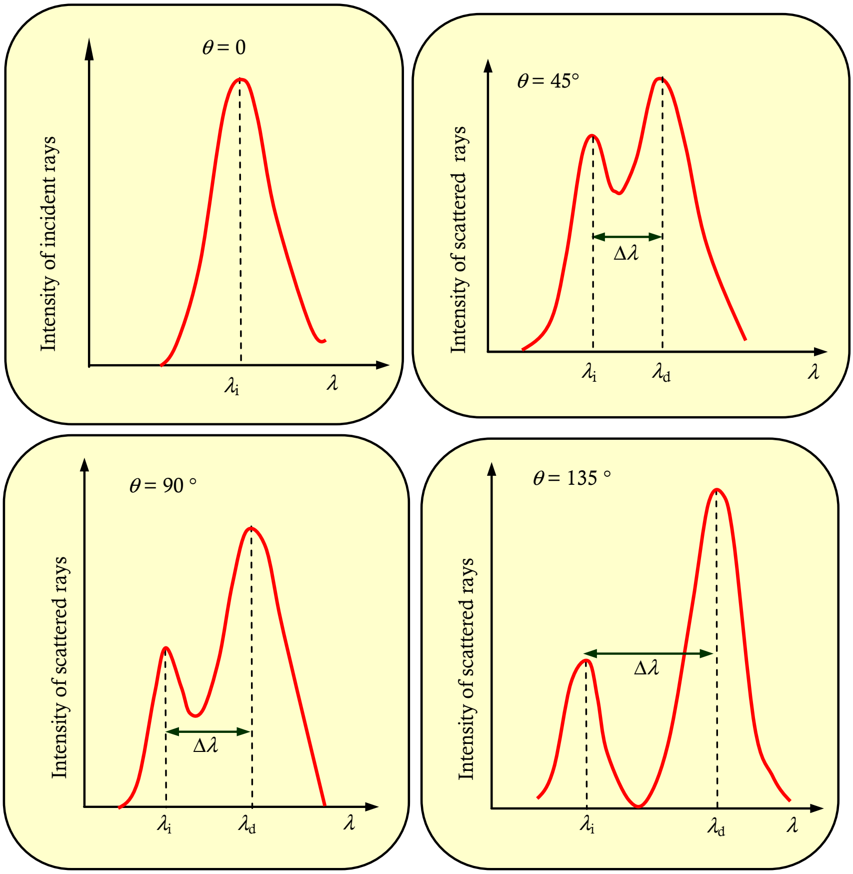

**Figure 2.16.** *Variation of Compton shift in wavelength with scattering angle $\theta$*

When the scattering angle $\theta$ varies, then Compton shift $\Delta\lambda$ increases when $\theta$ increases, as shown in Figure 2.16.

### 2.3.2. *Energy and linear momentum of a relativistic particle*

Compton effect is explained within Einstein's *theory of special relativity*. It is therefore important to first clarify the main characteristics of a *relativistic particle*, in contrast to a particle known as classical. A particle of relativistic mass $m$ and rest mass $m_0$, which is moving at speed $v$ (*with respect to a given reference frame*), has a total energy $E$ and a linear momentum $p$ given by the following expressions [GRO 85]:

$$m = \frac{m_0}{\sqrt{1-\frac{v^2}{c^2}}} \; ; \; E = mc^2 = \frac{m_0 c^2}{\sqrt{1-\frac{v^2}{c^2}}} \; ; \; p = mv = \frac{m_0 v}{\sqrt{1-\frac{v^2}{c^2}}} \qquad [2.38]$$

When the particle is at rest, $v = 0 \Rightarrow m = m_0$ and $E = E_0 = m_0 c^2$. $E_0$ is known as *rest energy* of the particle. Moreover, by definition, the kinetic energy of the relativistic particle is $E_c = E - E_0$. Relation [2.38] leads to:

$$E_c = m_0 c^2 \left\{ \frac{1}{\sqrt{1-\frac{v^2}{c^2}}} - 1 \right\} \qquad [2.39]$$

The quantity $\gamma$ is known as *Lorentz factor* defined as:

$$\gamma = \frac{1}{\sqrt{1-\frac{v^2}{c^2}}}$$

Using this factor, relations [2.38] and the first expression [2.39] are simplified as follows:

$$m = m_0\gamma \; ; \; E = m_0 c^2 \gamma \; ; p = m_0 \gamma v \; ; \; E_c = m_0 c^2 (\gamma - 1) \qquad [2.40]$$

Moreover, since $p = mv$ and $E = mc^2$, then $v = pc^2/E$. Let us replace $v$ by $pc^2/E$ in the second expression of relations [2.38]. Total relativistic energy $E$ is then written as (maintaining the positive value, since $E = mc^2 > 0$):

$$E = \sqrt{p^2 c^2 + m_0^2 c^4} \qquad [2.41]$$

The rest mass of the photon is $m_0 = 0$ (current experimental measurements indicate a mass below $10^{-54}$ kg). Using [2.41], photon energy and linear momentum verify the following relations:

$$E = pc = \frac{hc}{\lambda} \Rightarrow p = \frac{h}{\lambda} \qquad [2.42]$$

Relativistic effects can be noted from a speed $v \geq c/10 \Rightarrow \gamma \geq 1.0050$.

## 2.3.3. *Interpretation, photon linear momentum, and Compton shift*

The previous observations (Figure 2.16) can be interpreted by applying the *energy and linear momentum conservation laws* to the Compton scattering of a photon by the electron in the scattering crystal. This makes it possible to establish the theoretical expression of the Compton shift in wavelength. To be able to do this, a diagram will be used to illustrate the Compton scattering of an incident photon by an electron that is initially at rest (Figure 2.17).

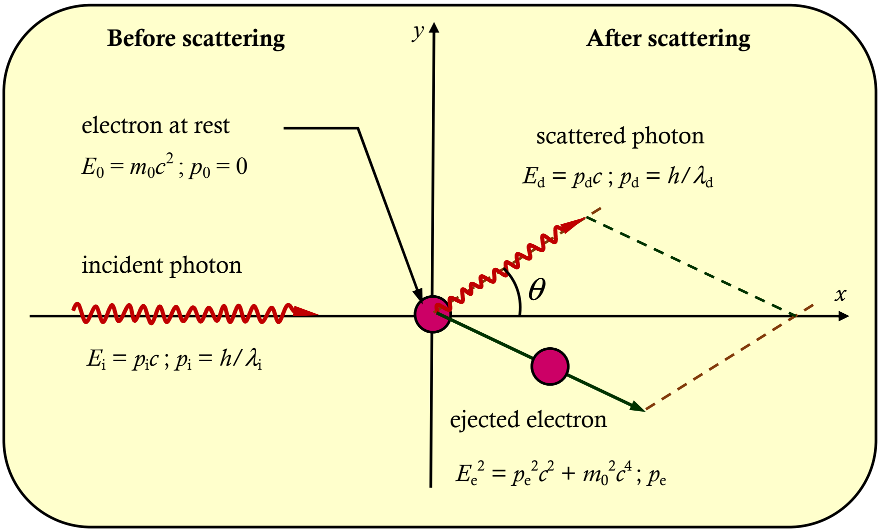

**Figure 2.17.** *Compton scattering of a photon*

Let us describe the incident photon, the scattered photon and the ejected electron by pairs of quantities ($a$, $b$), where $a$ denotes energy and $b$ denotes linear momentum. Then we have:

– incident photon: ($E_i$, $p_i$)

– scattered photon: ($E_d$, $p_d$)

– ejected electron: ($E_e$, $p_e$)

Let us then consider the diagram represented in Figure 2.18:

– *before scattering*:

- total energies:

$$E_i = \frac{hc}{\lambda_i} \quad ; \quad E_e = E_0 = m_0 c^2 \tag{2.43}$$

- linear momentum:

$$p_i = \frac{h}{\lambda_i} \quad ; \quad p_e = 0 \tag{2.44}$$

– *after scattering*:

- total energies:

$$E_d = \frac{hc}{\lambda_d} \quad ; \quad E_e = \sqrt{p_e^2 c^2 + m_0^2 c^4} \tag{2.45}$$

- linear momentum:

$$p_d = \frac{h}{\lambda_d} \quad ; \quad p_e \neq 0 \tag{2.46}$$

Applying the energy and linear momentum conservation laws we have:

$$\begin{cases} p_i c + m_0 c^2 = p_d c + \sqrt{p_e{}^2 c^2 + m_0^2 c^4} \\ \vec{p}_i = \vec{p}_e + \vec{p}_d \end{cases}$$

Hence:

$$\begin{cases} (p_i c - p_d c) + m_0 c^2 = \sqrt{p_e{}^2 c^2 + m_0^2 c^4} \\ \vec{p}_e c = \vec{p}_i c - \vec{p}_d c \end{cases}$$

Using these relations, the result is:

$$\begin{cases} \left[(p_i c - p_d c) + m_0 c^2\right] = \sqrt{p_e^2 c^2 + m_0^2 c^4} \\ p_e^2 = p_i^2 + p_d^2 - 2 p_i p_d \cos\theta \end{cases}$$

which gives:

$$\begin{cases} (p_i c - p_d c)^2 + m_0^2 c^4 + 2\, m_0 c^2 (p_i c - p_d c) = p_e^2 c^2 + m_0^2 c^4 \\ p_e^2 c^2 = p_i^2 c^2 + p_d^2 c^2 - 2 p_i p_d c^2 \cos\theta \end{cases}$$

Expanding the first equation of the latter system leads to:

$$\begin{cases} p_e^2 c^2 = (p_i c - p_d c)^2 + 2(p_i c - p_d c) m_0 c^2 \\ p_e^2 c^2 = p_i^2 c^2 + p_d^2 c^2 - 2 p_i p_d c^2 \cos\theta \end{cases} \qquad [2.47]$$

Equalizing these two equations [2.47] and expanding the first term on the right of the first equation leads after simplification and arrangement to:

$$(p_i c - p_d c) m_0 c^2 = p_i p_d (1 - \cos\theta) \qquad [2.48]$$

Knowing that $p = h/\lambda$, equation [2.48] can be written as:

$$\left(\frac{hc}{\lambda_i} - \frac{hc}{\lambda_d}\right) m_0 c^2 = \frac{hc}{\lambda_i} \times \frac{hc}{\lambda_d} (1 - \cos\theta)$$

This equation is simplified as follows:

$$\Delta\lambda = (\lambda_d - \lambda_i) = \frac{h}{m_0 c}(1 - \cos\theta) \qquad [2.49]$$

This corresponds to Compton equation. Since $(1 - \cos\theta)$ is dimensionless, the quantity $h/m_0 c$ has the dimension of a wavelength. By definition, the Compton wavelength of the electron is denoted by $\lambda_c$ and is given by the relation:

$$\lambda_c = \frac{h}{m_0 c} \qquad [2.50]$$

Knowing that $h = 6.62606896 \times 10^{-34}$ J · s; $c = 2.99792458 \times 10^{8}$ m · s$^{-1}$; $m_0 = 9.10938215 \times 10^{-31}$ kg, then: $\lambda_c = 2.43$ pm. This wavelength is within the range of γ rays. Compton shift in wavelength [2.49] is then written in a simplified form:

$$\Delta\lambda = \lambda_c(1 - \cos\theta) \qquad [2.51]$$

Quantity $\lambda_c$ is known as *Compton wavelength of an electron*. It is worth noting that the Compton effect supports the particle-like aspect of light.

**APPLICATION 2.8.–**

> An experiment of Compton scattering of a photon by an electron at rest is conducted. The wavelength of the incident photon is $\lambda = 71.2$ pm. The measured Compton shift in wavelength is 3.6 pm. Calculate the energy of the scattered *photon* in keV and the angle $\theta$.
>
> *Given data.* $\lambda_c = 2.43$ pm; $h = 6.63 \times 10^{-34}$ J · s; $c = 3.0 \times 10^{8}$ m · s$^{-1}$; 1 eV = $1.60 \times 10^{-19}$ J
>
> **Solution.**
>
> 1. *Energy of the scattered photon*: Compton shift in wavelength:
>
> $$\Delta\lambda = \lambda_d - \lambda_I \Rightarrow \lambda_d = \Delta\lambda + \lambda_i \qquad [2.52]$$
>
> hence: $\lambda_d = 74.8$ pm. The energy of the scattered photon is given by the following relation:
>
> $$E_d = \frac{hc}{\lambda_d} \Rightarrow E_d = 16.62 \text{ keV} \qquad [2.53]$$
>
> 2. *Scattering angle*: The Compton shift in wavelength is given by the relation:
>
> $$\Delta\lambda = \lambda_c\,(1 - \cos\theta) \Rightarrow \theta = \cos^{-1}(1 - \Delta\lambda_c); \quad \theta \approx 119° \qquad [2.54]$$

## 2.4. Combining the particle- and wave-like aspects of light

### 2.4.1. *Particle- and wave-like properties of the photon*

Light diffraction and interference are phenomena that support the *wave-like aspect* of light. Wave-like properties of light are characterized by the wave vector of module $k = 2\pi/\lambda$ and angular frequency $\omega = 2\pi c/\lambda$. Photoelectric effect and Compton effect support the *particle-like aspect of light*: light has a dual *wave and particle* nature. These two aspects coexist, but they never manifest simultaneously. The wave-like and particle-like combination of light properties is reflected by the following Planck–Einstein relations.

– Quantities specific to wave-like properties:

$$\omega = \frac{2\pi c}{\lambda} \quad ; \quad k = \frac{2\pi}{\lambda} \tag{2.55}$$

– Quantities specific to particle-like properties:

$$E = \frac{hc}{\lambda} \quad ; \quad p = \frac{h}{\lambda} \tag{2.56}$$

### 2.4.2. *Planck–Einstein relation*

*Planck–Einstein* relations reflect the combination of wave- and particle-like properties of light. They connect in pairs the wave- and particle-like quantities. Using [2.55] and [2.56] leads to:

$$E = \frac{hc}{\lambda} = \frac{h}{2\pi} \times \frac{2\pi c}{\lambda} = \hbar \times \omega \quad ; \quad p = \frac{h}{\lambda} = \frac{h}{2\pi} \times \frac{2\pi}{\lambda} = \hbar \times k$$

Hence the Planck–Einstein relations can be written as:

$$E = \hbar\omega; \quad \vec{p} = \hbar\vec{k} \tag{2.57}$$

**Arthur Compton** was an American physicist. He was awarded one half of the Nobel Prize for Physics in 1927 (the other half being received by Charles Wilson) for the discovery of the Compton effect proving the particle-like aspect of light (which had also been evidenced by the photoelectric effect discovered by Hertz in 1887). The Compton effect has made it possible to confirm the existence of the photon.

**Charles Thomson Rees Wilson** (1869–1959) was a British (Scottish) physicist. He was awarded half of the Nobel Prize for Physics in 1927 for building the cloud chamber that constituted the first particle detector.

**Box 2.4.** *Compton (1892–1962)*

## 2.5. Exercises

### 2.5.1. *Exercise 1 – Single-slit diffraction, interferences*

Twin sisters Amina and Fatima conduct a light interference experiment using the experimental set-up shown in Figure 2.18. They have at their disposal the following:

– a collimated laser diode emitting a monochromatic light radiation of wavelength $\lambda = 670$ nm;

– a thin rectangular slit of width $l = 100$ µm pierced on a film slide;

– pairs of thin and parallel slits on film slide and separated by distance $a$.

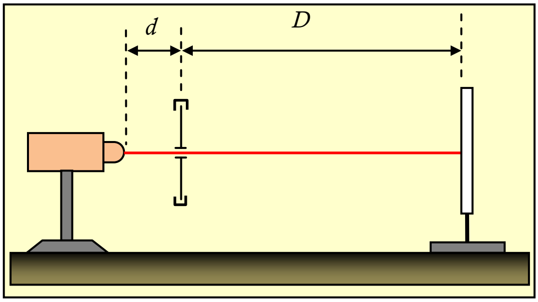

**Figure 2.18.** *Experimental setup of single-slit diffraction*

(1) Amina and Fatima light the thin slit located at approximately $d = 10.0$ cm from the laser source. For a distance $D = 2.0$ m, they note on a screen a horizontal figure constituted of bright spots regularly arranged around a larger central spot, as shown in Figure 2.19.

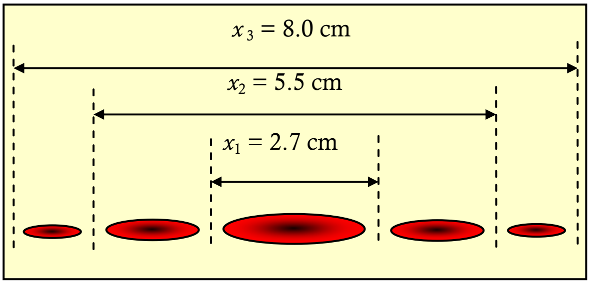

**Figure 2.19.** *Spacing $x_n$ of midpoints of various regular bright spots*

It can be theoretically proven that the spacing $x_n$ of the midpoints of various black spots that are symmetrical with respect to the central bright spot satisfy the following relation:

$$x_n = 2\frac{n\lambda}{l}D, \ n \text{ is a natural integer.}$$

Prove that the theoretical predictions are corroborated by the experiment.

(2) Amina and Fatima then replace the previous thin slit with a pair of slits separated by distance $a$.

(2.1) Is the observed phenomenon similar to the previous one (question 1)? If not, what is the observed phenomenon?

(2.2) For $D = 4$ m, they measure on the screen a length $l = 76$ mm filled by the centers of 11 bright fringes. Given this data, deduce $a$. What is the measuring accuracy knowing that the manufacturer specification is $a_0 = 350$ µm?

### 2.5.2. *Exercise 2 – Order of interference fringes*

An experimental set-up (Figure 2.20) is used to observe light interferences in air. $S_1$ and $S_2$ are two slits constituting coherent and synchronous sources. The *yy*' axis coincides with the perpendicular bisector of $S_1S_2$. The two slits are first lighted with yellow monochromatic light of wavelength $\lambda_1 = 600$ nm.

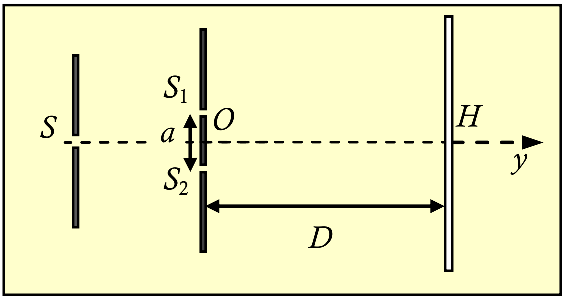

**Figure 2.20.** *Experimental setup for the study of light interference*

It can be noted that the distance between the midpoint of the zero-order central fringe and the midpoint of the bright fringe of order $k_1 = 10$ is $x_1 = 6$ mm. The two slits are then lighted with monochromatic red light of wavelength $\lambda_2$. The distance between the midpoint of the central fringe and the midpoint of the bright fringe of order $k_2 = 12$ is $x_2 = 8.64$ m.

*Given data.* $c = 3.0 \times 10^8 \text{ m} \cdot \text{s}^{-1}$

(1) Show that the wavelength is:

$$\lambda_2 = \frac{k_1 x_2}{k_2 x_1} \lambda_1$$

Calculate $\lambda_2$.

(2) Calculate the frequencies $\nu_1$ and $\nu_2$ corresponding to radiations of wavelengths $\lambda_1$ and $\lambda_2$, respectively.

(3) Slits $S_1$ and $S_2$ are exposed to two radiations of wavelengths $\lambda_1$ and $\lambda_2$; the "naked eye" perceives an "orangy" light at point $H$, where $yy'$ axis intersects the screen.

(3.1) Provide a qualitative explanation of this screen appearance (orangy shade).

(3.2) The total width of the interference field on the screen $E$ is 18 mm. How many times is the aspect observed at $H$ present?

### 2.5.3. *Exercise 3 – Experimental measurement of Planck constant and of the work function of an emissive photocathode*

An experimental study of photoelectric effect on cesium has led to the measurement of the stopping potential $U_0$ corresponding to several wavelengths. The results are summarized in Table 2.2.

| $\lambda$ (nm) | 405.0 | 436.0 | 467.0 | 515.0 | 546.0 | 577.0 | 589.0 | 615.0 |
|---|---|---|---|---|---|---|---|---|
| $U_0$ (V) | 1.190 | 0.970 | 0.780 | 0.535 | 0.400 | 0.245 | 0.230 | 0.145 |

**Table 2.2.** *Experimental values of the stopping potential corresponding to several wavelengths for a cesium photocathode*

(1) Express $U_0$ as a function of wavelength $\lambda$.

(2) Draw the curve $U_0 = f(1/\lambda)$. Choose the appropriate scale.

(3) Use the experimental curve to determine Planck constant and the work function. Determine the measuring accuracy.

(4) Use the same experimental curve to determine the work function $W_0$. Then find the measuring accuracy.

(5) Show that the wavelengths employed are well suited to the experimental study conducted.

*Given data.*

– output potentials of several metals: Pt (5.30 V); Cs (1.80 V); Cr (4.60 V)

– accepted value of Planck's constant: $h = 6.62606896 \times 10^{-34}$ J · s

– elementary charge: $e = 1.602179487 \times 10^{-19}$ C

### 2.5.4. Exercise 4 – Experimental study of the behavior of a photoelectric cell, quantum efficiency and sensitivity

An experiment is conducted for the study of a photoelectric cell irradiated by a source of monochromatic light. The threshold wavelength of the photocathode used is $\lambda_0$ = 666.7 nm. The results obtained for ($I$, $U$) pairs of values are summarized in Table 2.3.

| $I$ (μA) | 0.00 | 1.65 | 2.00 | 3.00 | 4.00 | 5.00 | 5.20 | 5.30 | 5.30 |
|---|---|---|---|---|---|---|---|---|---|
| $U$ (V) | –0.80 | 0.00 | 0.22 | 0.60 | 1.10 | 2.00 | 3.00 | 4.00 | 5.00 |

**Table 2.3.** *Experimental values of the voltage between the anode and the cathode of a photoelectric cell corresponding to several measured values of photocurrent*

(1) Draw the $I = f(U)$ characteristic of the cell.

(2) Use the curve to determine:

(2.1) The total number of emitted photoelectrons.

(2.2) The maximal speed gained by a photoelectron upon leaving the cathode.

(2.3) The frequency $\nu$ of the monochromatic light used. Is this result consistent with the photoelectric emission? Justify.

(3) Calculate the quantum efficiency $\eta$ and the sensitivity $s$ of the photoelectric cell employed if light output is $P = 10^{-4}$ W.

*Given data*. $e = 1.60 \times 10^{-19}$ C; $m = 9.10 \times 10^{-31}$ kg; $c = 3.0 \times 10^{8}$ m · s$^{-1}$; $h = 6.63 \times 10^{-34}$ J · s

### 2.5.5. *Exercise 5 – Compton backscattering*

A Compton scattering experiment is conducted. The measured Compton shift in wavelength is 4.86 pm. Moreover, the electron in the crystal lattice is ejected at a speed $v = 0.89\,c$.

(1) Prove that the experiment corresponds to Compton backscattering.

(2) Can this backscattering be studied in the context of classical mechanics? Use calculation to support your answer.

(3) Calculate the linear momentum of the ejected electron. Express this result in keV/$c$.

(4) Find the total energy of the ejected electron. Use the result to deduce its kinetic energy. Express the results in MeV.

(5) Calculate the wavelength of the incident photon, if the energy of the scattered photon is half the total energy of the ejected electron. Locate this wavelength in the spectrum range of electromagnetic radiations.

*Given data*. $m_0c^2 = 0.511$ MeV; $c = 3.0 \times 10^{8}$ m · s$^{-1}$; $h = 6.63 \times 10^{-34}$ J · s

### 2.5.6. *Exercise 6 – Energy and linear momentum of scattered photons and of the electron ejected by Compton effect*

An incident X-photon strikes an electron that is initially at rest. The direction of the Compton scattered photon makes an angle $\theta$ with the initial direction of the incident photon.

(1) Recall the expression of the Compton shift in wavelength.

(2) Express the following quantities as a function of the initial energy $E_\mathrm{i}$ of incident photons, of the rest energy $m_0c^2$ of the electron and of the angle $\theta$:

(2.1) Energy of scattered photons.

(2.2) Final kinetic energy of the electrons.

(3) Calculate the numerical values for $E_\text{i} = m_0c^2/29$ and $\theta = \pi$

*Given data*. $m_0c^2 = 0.511$ MeV; $\lambda_\text{c} = hc/m_0c^2$

### 2.5.7. *Exercise 7 – Inverse Compton effect*

On their path, photons bump into electrons in motion. The frontal collision between a photon of energy $E_\text{i}$ and an electron of total energy $E$ and linear momentum $p$ is studied within the laboratory frame of reference. After collision, the photon is scattered in a direction making an angle $\theta$ with its initial direction. Let $E_\text{d}$ be the energy of the scattered photon.

(1) Draw a schematic representation of the photon–electron interaction. This representation should include the linear momentum vectors of the incident and scattered photons and of the electron before and after collision.

(2) Using the conservation laws to be specified, express $E_\text{d}$ as a function of $E_\text{i}$, $E$, $p$ and $\theta$. Then justify the "inverse Compton effect" designation.

(3) Prove that result of (2) leads to finding the expression of the Compton shift in wavelength in case of Compton scattering.

## 2.6. Solutions

### 2.6.1. *Solution 1 – Single-slit diffraction, interferences*

(1) *Theoretical confirmation of experimental observations*

Figure 2.19 provides the experimental values of spacings $x_\text{n}$ of the midpoints of various black spots that are symmetrical with respect to the central bright spot:

$$x_{1\text{exp}} = 2.7 \text{ cm};\ x_{2\text{exp}} = 5.5 \text{ cm};\ x_{3\text{exp}} = 8.0 \text{ cm} \qquad [2.58]$$

The spacings are theoretically given by the following relation:

$$x_n = 2\frac{n\lambda}{l}D \qquad [2.59]$$

Given that $\lambda = 6.70 \times 10^{-7}$ m, $l = 1.0 \times 10^{-4}$ m and $D = 2.0$ m, then:

$$x_1 = 0.0268 \text{ m};\ x_2 = 2x_1 = 0.0536 \text{ m};\ x_3 = 3x_1 = 0.0804 \text{ m}$$

or:

$$x_{1\text{theo}} \approx 2.7 \text{ cm};\ x_{2\text{theo}} \approx 5.5 \text{ cm};\ x_{3\text{theo}} \approx 8.0 \text{ cm} \qquad [2.60]$$

Results [2.60] actually prove that the theoretical predictions are very much in agreement with experimental observations.

(2) *Replacement of previous thin slit with a pair of slits separated by distance a*

(2.1) *Observations*

When Amina and Fatima replace the thin slit with a pair of slits separated by distance $a$, each of these slits diffracts the light passing through it. The observed pattern is no longer a horizontal one constituted of bright spots regularly arranged around a central spot. The waves coming out of slits are overlapped beyond the film slide. Then interference fringes are observed on the screen.

(2.2) *Value of distance a between slits, measuring accuracy*

– *Value of distance a between slits*

For $D = 4$ m, Amina and Fatima measure on the screen a length $l = 76$ mm filled by the centers of 11 bright fringes. These results can be used to determine the spacing between fringes $i$.

Let us use an aiding diagram to find the expression of $i$. For the sake of clarity, fringes are arranged horizontally (Figure 2.21).

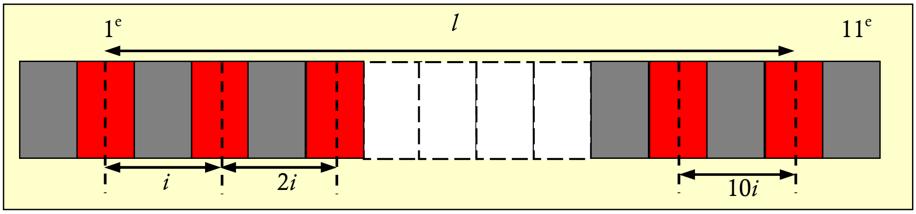

**Figure 2.21.** *Calculation principle of spacing between fringes: l = 10i*

By definition, fringe spacing $i$ is given by the expression:

$$i = \frac{\lambda}{a} D \Rightarrow a = 10\frac{\lambda}{l} D \qquad [2.61]$$

N.A.– $\lambda = 6.70 \times 10^{-6}$ m, $l = 7.6 \times 10^{-2}$ m and $D = 4.0$ m. Hence: $a = 353$ μm

– *Measuring accuracy*

$\Delta a / a_0 \approx 0.86\%$

### 2.6.2. *Solution 2 – Order of interference fringes*

(1) *Proof, calculation of $\lambda_2$*

– *Proof*

Let $x_j$ be the distance between the midpoint of zero-order central fringe and the midpoint of the bright fringe of order $k_j$. For a bright fringe, the following relations can be written as:

$$x_j = k_j i_j \quad ; \quad i_j = \lambda_j \frac{D}{a} \tag{2.62}$$

This leads to:

$$x_j = k_j \lambda_j \frac{D}{a} \tag{2.63}$$

Hence:

$$\begin{cases} x_1 = k_1 \lambda_1 \dfrac{D}{a} \\ x_2 = k_2 \lambda_2 \dfrac{D}{a} \end{cases} \Rightarrow \lambda_2 = \frac{k_1 x_2}{k_2 x_1} \lambda_1 \tag{2.64}$$

– *Value of $\lambda_2$*

$\lambda_1 = 0.6$ µm; $k_1 = 10$; $x_1 = 6$ mm; $k_2 = 12$; $x_2 = 8.64$ mm

N.A.– Using [2.65] leads to: $\lambda_2 = 720$ nm

(2) *Calculation of frequencies $\nu_1$ and $\nu_2$*

By definition:

$$\nu_j = \frac{c}{\lambda_j} \Rightarrow \nu_1 = \frac{c}{\lambda_1} ; \nu_2 = \frac{c}{\lambda_2} \tag{2.65}$$

N.A.– $\lambda_1 = 600$ nm $\lambda_2 = 720$ nm. Hence: $\nu_1 = 5.0 \times 10^{14}$ Hz; $\nu_2 = 4.2 \times 10^{14}$ Hz

(3) *Slits $S_1$ and $S_2$ are exposed*

(3.1) *Screen appearance explained*

The observed orangy shade is due to the overlapping of yellow radiations (wavelength $\lambda_1 = 600$ nm) and red radiations (wavelength $\lambda_2 = 720$ nm).

(3.2) *Number of orange fringes*

Let $l$ be the total width of the interference field on the screen (Figure 2.22).

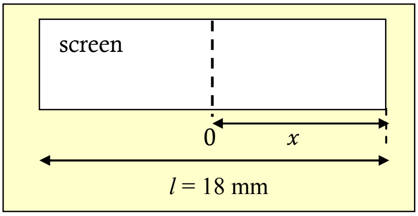

**Figure 2.22.** *Total width l of the interference field*

The same aspect observed in $H$ is due to the coincidence of bright fringes. Let $n$ be the number of times that an orangy shade is observed at $H$ and $i_j$ the fringe spacing given by [2.62]. At a point of abscissa $x$ on the screen, bright fringes coincide if:

$$x = n_1 i_1 = n_2 i_2 \Rightarrow n_1 \times \frac{\lambda_1 D}{a} = n_2 \times \frac{\lambda_2 D}{a} \quad [2.66]$$

The ratio can be calculated from [2.66] knowing that $\lambda_1 = 600$ nm $\lambda_2 = 720$ nm:

$$\frac{n_1}{n_2} = \frac{\lambda_2}{\lambda_1} \Rightarrow \frac{n_1}{n_2} = \frac{720}{600} = \frac{6\times 120}{5\times 120} = \frac{6}{5} \quad [2.67]$$

Hence $n_1 = 6n$ and $n_2 = 5n$

Furthermore, according to [2.66] and knowing that $n_1 = 6n$ and $x_1 = k_1 i_1$ [2.62], then:

$$x = n_1 i_1 = 6n i_1 = 6n \times \frac{x_1}{k_1} \quad [2.68]$$

Distance $x_1$ is considered, given that it is the smallest ($x_1 < x_2$). The objective is therefore to find the number of coincidences in $x_1$. According to Figure 2.22, and taking into account equalities [2.68], this leads to:

$$0 \le x \le \frac{l}{2} \Rightarrow 0 \le 6n \times \frac{x_1}{k_1} \le \frac{l}{2} \tag{2.69}$$

Hence:

$$0 \le 6n \times \frac{6 \times 10^{-3}}{10} \le \frac{1.8 \times 10^{-2}}{2} \Rightarrow 0 \le n \le \frac{18}{2 \times 3.6}$$

Therefore, $n \le 2.5 \Rightarrow n = 2$

Two rays are observed on both sides of the central fringe. Hence, a total of four orangy shade fringes beyond $H$. This finally gives five fringes, if the central fringe at $H$ is added.

### 2.6.3. *Solution 3 – Experimental measurement of Planck constant and of the work function of an emissive photocathode*

(1) *Stopping potential*

Let us apply the work–energy theorem between the cathode ($v_C = v$) and the anode ($v_A = 0$). This leads to:

$$eU_0 = \frac{1}{2} m v^2 \tag{2.70}$$

According to Einstein equation

$$\frac{1}{2} m v^2 = h\nu - W_0 = h\nu - \frac{hc}{\lambda_0} \tag{2.71}$$

Using [2.70] and [2.71] gives:

$$eU_0 = h.\nu - W_0 = \frac{hc}{\lambda} - W_0$$

Hence:

$$U_0 = \frac{hc}{e} \times \frac{1}{\lambda} - \frac{W_0}{e} \tag{2.72}$$

(2) *Curve plot*

Let us consider the values summarized in Table 2.4.

| $1/\lambda$ ($\times 10^5$ m$^{-1}$) | $U_0$ ($\times 10^{-1}$ V) |
|---|---|
| 24.7 | 11.90 |
| 22.9 | 9.70 |
| 21.4 | 7.80 |
| 19.4 | 5.35 |
| 18.3 | 4.00 |
| 17.3 | 2.45 |
| 17.0 | 2.30 |
| 16.3 | 1.45 |

**Table 2.4.** *Values of the stopping potential as a function of inverse wavelength*

*Appropriate scale*:

– 1 cm for $10^5$ m$^{-1}$ on the abscissa axis;

– 1 cm for $10^{-1}$ V on the ordinate axis.

The plot of $U_0 = f\,(1/\lambda)$ curve is shown in Figure 2.23 (several experimental points have been considered, as well as those that make it possible to find the slope of the resulting line).

(3) *Planck constant and work function, measuring accuracy*

The experimental curve is a line of equation:

$$U_0 = a \times \frac{1}{\lambda} + b \tag{2.73}$$

A comparison between [2.72] and [2.73] leads to finding the expressions of slope $a$ and of the ordinate at origin $b$, hence:

$$a = \frac{hc}{e}\,;\, b = -\frac{W_0}{e} \tag{2.74}$$

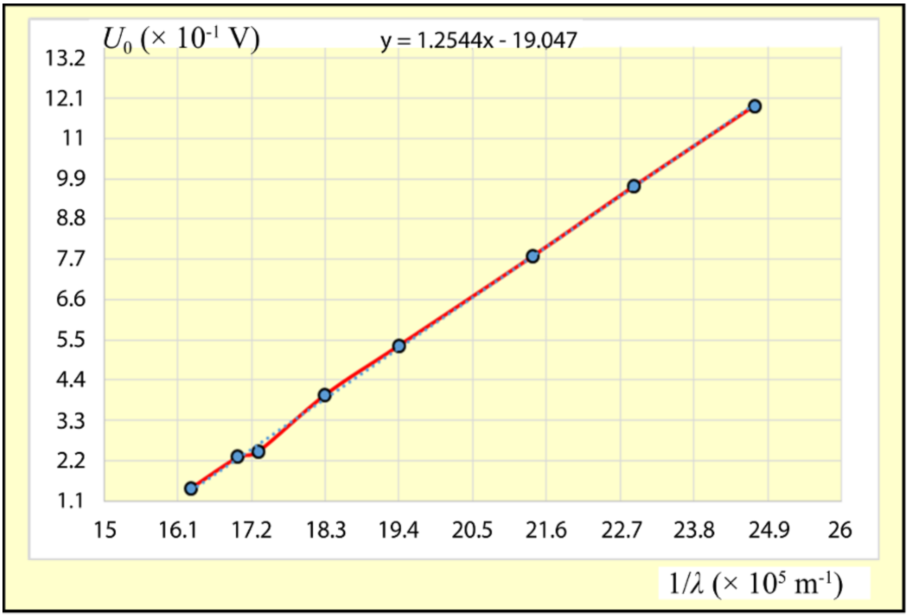

**Figure 2.23.** *Curve of the stopping potential $U_0$ as a function of 1/λ*

– *Planck constant, measuring accuracy*

The trend curve is displayed in Figure 2.23: $y = 1.2544\, x - 19.047$. Given the scale, the graphical result is:

$$U_0 = 1.25 \times 10^{-6} \times \frac{1}{\lambda} - 1.90 \ \ (\mathrm{V}) \qquad [2.75]$$

A comparison between relations [2.73] and [2.75] leads to the values of the slope $a$ and of the ordinate at the origin $b$.

Hence: $a = 1.25 \times 10^{-6}$ V · m; $b = -1.90$ V

Considering [2.74], we have:

$$a = \frac{hc}{e} \Rightarrow h = \frac{e.a}{c} \qquad [2.76]$$

N.A.– $e = 1.602179487 \times 10^{-19}$ C; $a = 1.25 \times 10^{-6}$ V · m; $c = 299792458$ m· s$^{-1}$

The use of the latter relation [2.76] leads to:

$$h_{\exp} = 6.68 \times 10^{-34}\ \mathrm{J \cdot s}$$

– *Accuracy of experimental measurements*

Let us consider $h \approx 6.63 \times 10^{-34}$ J · s. Then:

$$\Delta h/h \approx 0.75\%$$

The experimental result is acceptable.

(4) *Work function, measuring accuracy*

According to [2.74]:

$$b = -\frac{W_0}{e} \Rightarrow W_0 = -eb \qquad [2.77]$$

N.A.– $b = -1.90$ V

Using [2.78] leads to: $W_0$ = 1.90 eV. Let us consider the output potentials of metals Pt (5.30 V), Cs (1.80 V) and Cr (4.60 V). Knowing that $W_0$ = eV, it can be noted that $W_0$ = 1.90 eV # 1.80 eV: it is a cesium (Cs) photocathode.

– *Measuring accuracy*

$$\Delta W/W_0 \approx 5.5\%$$

Though quite acceptable, the experimental result can be improved.

(5) *Consistency of wavelength values*

Let us calculate the photoelectric threshold wavelength. By definition:

$$W_0 = \frac{hc}{\lambda_0} = -eb \Rightarrow \lambda_0 = -\frac{hc}{eb} \qquad [2.78]$$

N.A.– $\lambda_0$ = 652.5 nm

In practice, electromagnetic radiations that give effective photons are exclusively those of wavelengths ranging between 405.0 nm ≤ $\lambda$ ≤ 546.0 nm, for which $\lambda < \lambda_0$.

### 2.6.4. *Solution 4 – Experimental study of the behavior of a photoelectric cell, quantum efficiency and sensitivity*

(1) *Plot of the cell's $I = f(U)$ characteristic*

The $I = f(U)$ curve is represented in Figure 2.24.

(2) *Use of the curve*

(2.1) *Total number of emitted photoelectrons*

The saturation current is $I_S = n.e$. The total number of emitted photoelectrons is:

$$n = I_S/e. \qquad [2.79]$$

*The experimental value of the saturation current is* $I_S = 5.3\ \mu\text{A}$

N.A.– $n = 3.31 \times 10^{13}$ photoelectrons.

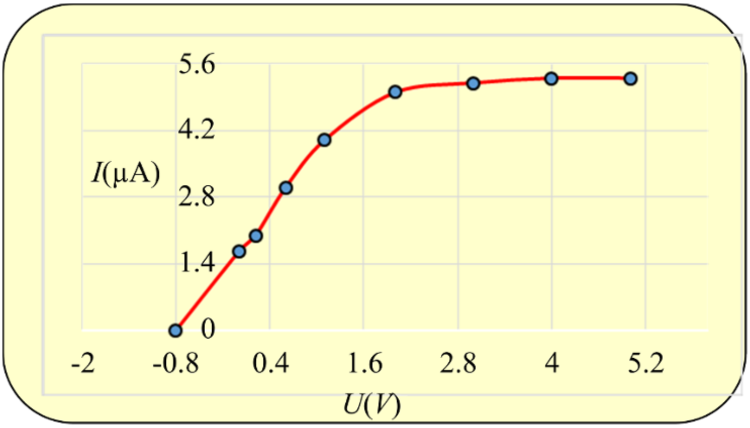

**Figure 2.24.** *I = f (U) characteristic of the studied photoelectric cell*

(2.2) *Maximal speed acquired by a photoelectron*

Let us use the work–energy theorem. Then, the maximal speed $v$ acquired by a photoelectron ejected from the cathode satisfies the following equation:

$$eU_0 = \frac{1}{2}mv^2 \Rightarrow v = \sqrt{\frac{2e.U_0}{m}} \qquad [2.80]$$

*Experimentally*, $U_0 = 0.8$ V

N.A.– $v = 5.3 \times 10^5 \text{ m} \cdot \text{s}^{-1}$

(2.3) *Frequency* $\nu$ *of the monochromatic light used and consistency*

Relation [2.71] leads to:

$$eU_0 = h\nu - W_0 = h\nu - \frac{hc}{\lambda_0} \qquad [2.81]$$

Relation [2.81] gives the light frequency expression, which is:

$$\nu = \frac{eU_0}{h} + \frac{c}{\lambda_0} \qquad [2.82]$$

N.A.– $\nu = 6.43 \times 10^{14}$ Hz

The value of the monochromatic frequency $\nu$ is consistent with the photoelectric emission if:

$$\nu > \nu_0 = c/\lambda_0 = 3.0 \times 10^8/6.667 \times 10^{-7} = 4.50 \times 10^{14} \text{ Hz}$$

which is consistent with the conducted experiment.

(3) *Quantum efficiency and sensitivity*

– *Quantum efficiency*

The quantum efficiency of a cell is equal to the ratio of the number $n$ of emitted photoelectrons to the number $N$ of effective photons, which is: $\eta = n/N$. Knowing that $n = I_S/e$ and $N = P/h\nu$, this leads to:

$$\eta = \frac{I_S}{e} \times \frac{h\nu}{P} \qquad [2.83]$$

N.A.– $\eta = 14\%$.

– *Cell sensitivity*

By definition, the sensitivity $s$ of the photoelectric cell is the quotient of the saturation current by the light intensity received by the photocathode, which is:

$$s = \frac{I_S}{P} \qquad [2.84]$$

N.A.– $s = 53 \text{ mA} \cdot \text{W}^{-1}$

### 2.6.5. *Solution 5 – Compton backscattering*

(1) *Proof*

The data provided by the exercise show that the shift in wavelength is $\Delta\lambda = 2\lambda_c$. According to Compton equation:

$$\Delta\lambda = \lambda_c(1 - \cos\theta) = 2\lambda_c \Rightarrow (1 - \cos\theta) = 2 \qquad [2.85]$$

Relation [2.85] leads to: $\theta = \pi$ . This actually corresponds to backscattering.

(2) *Scattering mechanics*

Given that the electron is ejected at very high speed $v$, within the range of relativistic particle speed values for which $v > c/10$, where $c$ is the light speed in vacuum, Compton scattering cannot be studied in the context of classical mechanics.

– *Justification*

According to the theory of special relativity, Lorentz factor is:

$$\gamma = \frac{1}{\sqrt{1 - v^2/c^2}} \qquad [2.86]$$

– For a slow particle (or for a particle at rest), $\gamma = 1.0$: the motion of the particle can be studied according to classical mechanics.

– For a rapid particle, $\gamma > 1$: the motion of the particle can be studied according to relativistic mechanics.

The speed of a particle is evaluated as low or high with respect to the speed of light. For the considered Compton effect case, $v = 0.89c$. Using relation [2.86]:

$$\gamma = 2.193 > 1$$

Compton effect results in the ejection of a relativistic electron. This is due to the very high energy of incident photons (X photons).

(3) *Calculation of linear momentum*

For a relativistic particle, linear momentum is given by the following relation:

$$p = m_0\gamma v = \frac{m_0 v}{\sqrt{1 - v^2/c^2}} \qquad [2.87]$$

Knowing that $v = 0.89c$, relation [2.87] gives:

$$p = 0.89\frac{m_0 c}{\sqrt{1 - v^2/c^2}} \qquad [2.88]$$

Let us introduce the rest energy $m_0c^2$ of the electron in [2.88]. This leads to:

$$pc = 0.89\frac{m_0 c^2}{\sqrt{1 - 0.89^2}} \qquad [2.89]$$

N.A.– $pc = 0.9974$ MeV $\Rightarrow p = 997.4$ keV/$c$

(4) *Calculation of total energy and kinetic energy*

– *Total energy of the ejected electron*

The total energy of the ejected electron is given by the relativistic expression:

$$E = m_0\gamma c^2 = \frac{m_0 c^2}{\sqrt{1 - v^2/c^2}} \qquad [2.90]$$

N.A.– $E = 1.1207$ MeV $\Rightarrow E = 1.121$ MeV

– *Kinetic energy of the ejected electron*

The total energy $E$ of a rapid particle is the sum of its kinetic energy $E_c$ and its rest energy $E_0 = m_0c^2$, hence:

$$E = E_c + E_0. \Rightarrow E_c = E - E_0 = E - m_0c^2 \qquad [2.91]$$

N.A.– $E = 0.6096$ MeV $\Rightarrow E = 0.610$ MeV

(5) *Calculation of the wavelength of the incident photon*

Let $E_i$, $E_d$ and $E$ be the total energies of the incident photon, of the scattered photon and of the ejected electron, respectively. According to the energy conservation principle: $E_i = E_d + E$. In the hypothesis that $E_d = E/2$, then:

$$E_i = (3/2)\,E \Rightarrow hc/\lambda = (3/2)E \tag{2.92}$$

This leads to:

$$\lambda = \frac{2}{3}\frac{hc}{E} \tag{2.93}$$

N.A.– $\lambda = 0.74$ pm

This wavelength is within the range of $\gamma$ rays.

### 2.6.6. *Solution 6 – Energy and linear momentum of the scattered photons and of the electron ejected by Compton effect*

(1) *Compton shift in wavelength*

The Compton shift in wavelength is given by the relation:

$$\Delta\lambda = \lambda_c\left(1 - \cos\theta\right) \tag{2.94}$$

(2) *Expressions*

(2.1) *Energy of scattered photons*

Relation [2.94] leads to:

$$\lambda_d - \lambda_i = \lambda_c(1 - \cos\theta) \Rightarrow \lambda_d = \lambda_i + \lambda_c(1 - \cos\theta) \tag{2.95}$$

Considering the latter equality [2.94], the ratio $E_d = hc/\lambda_d$ is expressed as:

$$\frac{hc}{\lambda_d} = \frac{hc}{\lambda_i + \lambda_c(1 - \cos\theta)} \Rightarrow E_d = \frac{hc}{\lambda_i + \lambda_c(1 - \cos\theta)} \tag{2.96}$$

Or $E_i = hc/\lambda_i$. Expression [2.96] gives:

$$E_d = \frac{hc}{hc + \lambda_c(1 - \cos\theta)\;E_i}\,E_i$$

The above expression is simplified by $hc$. As $\lambda_c/hc = 1/m_0c^2$, we finally obtain:

$$E_d = \frac{m_0c^2}{m_0c^2 + (1-\cos\theta)\,E_i}\,E_i \tag{2.97}$$

(2.2) *Final kinetic energy of the electrons*

Total energy conservation leads to:

$$E_i + m_0c^2 = E_e + E_d = E_c + m_0c^2 + E_d \tag{2.98}$$

The kinetic energy of electrons $E_c = E_i - E_d$. Using [2.97] leads to:

$$E_c = \left(1 - \frac{m_0c^2}{m_0c^2 + (1-\cos\theta)\,E_i}\right) E_i \tag{2.99}$$

(3) *Numerical application*

$E_i = m_0c^2/29$ and $\theta = \pi$; $m_0c^2 = 0.511$ MeV

Using [2.97] and [2.99], the results are, respectively:

N.A.– $E_d = 0.01648$ MeV = 16.48 keV; $E_c = 0.001137$ MeV = 1.14 keV

> NOTE.– Energy $E_i = m_0c^2/29$ approximately corresponds to the energy of X photons of the ray $\lambda = 71.2$ pm of molybdenum. Indeed:
>
> $E = hc/\lambda = 6.63 \times 10^{-34} \times 3 \times 10^8/(7.12 \times 10^{-11} \times 1.6 \times 10^{-19}) = 17{,}459.6$ eV
>
> $m_0c^2/17459.6 = 0.511 \times 10^6/17459.6 = 29.27 \Rightarrow E_i \approx m_0c^2/29$

## 2.6.7. *Solution 7 – Inverse Compton effect*

(1) *Schematic representation*

For schematic representation, see Figure 2.25.

(2) *Energy expression*

Given a particle, let us consider the pair of quantities $(E, p)$, with $E$ as energy and $p$ as linear momentum: incident photon $(E_i, p_i)$; scattered photon $(E_d, p_d)$, incident electron $(E_{ei}, p_{ei})$ and scattered electron $(E_{ed}, p_{ed})$. Let us write the energy and linear momentum conservation laws:

$$\begin{cases} \vec{p}_i + \vec{p}_{ei} = \vec{p}_d + \vec{p}_{ed} \\ E_i + E_{ei} = E_d + E_{ed} \end{cases} \qquad [2.100]$$

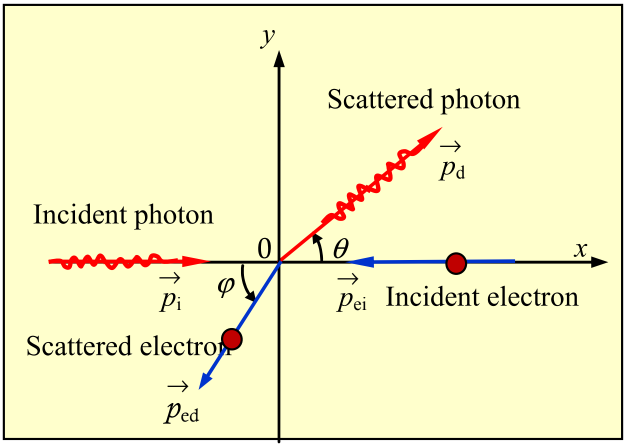

**Figure 2.25.** *Inverse Compton scattering: scattering of an incident photon by an incident electron*

The projection of vector relation [2.100] on axes *Ox* and *Oy* (Figure 2.25) leads to:

$$\begin{cases} (E_i / c) - p_{ei} = (E_d / c)\cos\theta + p_{ed}\cos\varphi \\ 0 = (E_d / c)\sin\theta - p_{ed}\sin\varphi \\ E_i + E_{ei} = E_d + E_{ed} \end{cases} \qquad [2.101]$$

Relations [2.101] give:

$$\begin{cases} p^2{}_{ed} = \left(\frac{E_i}{c} - p_{ei} - \frac{E_d}{c}\cos\theta\right)^2 + \left(\frac{E_d}{c}\sin\theta\right)^2 \\ E_{ed} = E_i - E_d + E_{ei} \end{cases} \qquad [2.102]$$

Considering the system of equations [2.102], we have:

$$E^2{}_{ed} - p^2{}_{ed}\,c^2 = (E_i - E_d + E_{ei})^2 - (E_i - p_{ei}c - E_d\cos\theta)^2 - (E_d\sin\theta)^2 \qquad [2.103]$$

Or for the electron,

$$E_{ed} = \sqrt{p_e^2 c^2 + m_0^2 c^4}$$

Relation [2.103] then gives:

$$E^2{}_{ed} = p_e^2 c^2 + m_0^2 c^4 \Rightarrow E^2{}_{ed} - p_e^2 c^2 = m_0^2 c^4$$

Hence:

$$m_0^2 c^4 = (E_i - E_d + E_{ei})^2 - (E_i - p_{ei} c - E_d \cos\theta)^2 - (E_d \sin\theta)^2 \qquad [2.104]$$

Assuming that for the incident electron $E = E_{\mathrm{ei}}$ and $p = p_{\mathrm{ei}}$, we get according to [2.104]:

$$m_0^2 c^4 = (E_i - E_d + E)^2 - (E_i - pc - E_d \cos\theta)^2 - (E_d \sin\theta)^2 \qquad [2.105]$$

After expansion and simplification, we have:

$$E_d \times (E_i + E + pc\cos\theta - E_i \cos\theta) - E_i (E + pc) = 0$$

which finally leads to:

$$E_d = \frac{E_i (E + pc)}{E_i (1 - \cos\theta) + (E + pc\cos\theta)} \qquad [2.106]$$

Result [2.106] shows that, unlike the *normal* Compton effect, where scattering involves a decrease in energy at the expense of the incident photon ($E_{\mathrm{d}} < E_{\mathrm{i}}$), in the Compton scattering of a photon by an electron in motion, there is an increase in energy at the expense of the incident electron ($E_{\mathrm{d}} > E_{\mathrm{i}}$) provided that ($E > E_{\mathrm{i}}$) and $\theta \neq 0$: this is the inverse Compton effect.

(3) *Proof*

In Compton scattering, the electron is initially at rest ($p = 0$). This gives $E = E_0 = m_0 c^2$. Expression [2.106] leads to:

$$E_d = \frac{E_i \cdot m_0 c^2}{E_i (1 - \cos\theta) + m_0 c^2} \qquad [2.107]$$

Using [2.106] leads to:

$$E_d\left[E_i(1-\cos\theta)+m_0c^2\right]=E_i\cdot m_0c^2$$

Hence:

$$E_dE_i(1-\cos\theta)=m_0c^2(E_i-E_d) \qquad [2.108]$$

Knowing that $E_\mathrm{d} = hc/\lambda_\mathrm{d}$ and $E_\mathrm{i} = hc/\lambda_\mathrm{i}$, [2.108] gives after simplification:

$$\frac{1}{\lambda_d\,\lambda_i}(1-\cos\theta)=\frac{m_0c}{h}\cdot\left(\frac{1}{\lambda_i}-\frac{1}{\lambda_d}\right) \qquad [2.109]$$

After arranging and simplifying [2.109], the final result is:

$$\lambda_d-\lambda_i=\frac{h}{m_0c}\cdot(1-\cos\theta) \qquad [2.110]$$

Result [2.110] actually corresponds to the Compton shift in wavelength given by expression [2.53].

# 3

# Quantum Numbers of the Electron

## *General objective*

Gain knowledge on the properties of the quantum numbers of the electron.

## *Specific objectives*

On completing this chapter, the reader should be able to:

- use the empirical Balmer formula;
- define the Rydberg constant for hydrogen;
- use the Ritz combination principle;
- know the main limitations of the planetary model of the atom;
- describe the shell model of electron configurations;
- state the two postulates of Bohr's theory;
- describe Planck's linear oscillator in the phase space;
- deduce Bohr's quantization principle using Planck's linear oscillator;
- know the properties of the principal quantum number;
- distinguish between absorption and emission spectra;
- establish the quantized expression of the energy of hydrogen-like systems;
- provide an interpretation of the spectral series of hydrogen-like systems;
- draw the energy level diagram for the hydrogen atom;
- know the main advantages and limitations of Bohr's model;

---

For color versions of the figures in this book, see www.iste.co.uk/sakho/quantum1.zip.

*Introduction to Quantum Mechanics 1: Thermal Radiation and Experimental Facts Regarding the Quantization of Matter,* First Edition. Ibrahima Sakho.

– define the reduced Rydberg constant;

– describe the Bohr–Sommerfeld model;

– write the electron configuration of an atom based on atomic orbitals;

– know the properties of the angular momentum quantum number;

– know the properties of the orbital magnetic quantum number;

– provide an interpretation of normal Zeeman effect;

– know the advantages and limitations of Bohr–Sommerfeld model;

– provide an interpretation of the Stern–Gerlach experiment;

– know the Uhlenbeck and Goudsmit hypothesis;

– know the properties of electron spin and magnetic spin quantum number;

– know the properties of the electron total quantum number;

– define the degree of degeneracy of the energy levels of hydrogen-like systems;

– apply the selection rules for hydrogen-like systems;

– Define the orbital magnetic moment and the spin magnetic moment;

– define the electron Landé factor and gyromagnetic ratio;

– provide an interpretation of the spin–orbit interaction;

– provide an interpretation of the Paschen–Back effect;

– know the spectroscopic notation of the quantum states of hydrogen-like systems;

– provide an interpretation of the fine structure of the energy levels of the hydrogen atom.

## *Prerequisites*

– photon properties;

– kinetic theory of gases;

– magnetic force and magnetic field;

– kinematics;

– fundamental principles and theorems of mass point dynamics;

– mechanical energy;

– characteristics (energy, linear momentum, mass) of a relativistic particle.

## 3.1. Experimental facts

### 3.1.1. *Spectrometer*

The *spectrometer* is an optical device employed for direct visual observation of light decomposition into its various components. There are *prism spectrometers* and *grating spectrometers* [BIÉ 06]. A *prism* is formed of a transparent medium limited by two plane faces. It is characterized by its *refractive index n* and by its *vertex angle A*. Figure 3.1 shows a prism representation (a) and a prism cross-section (b).

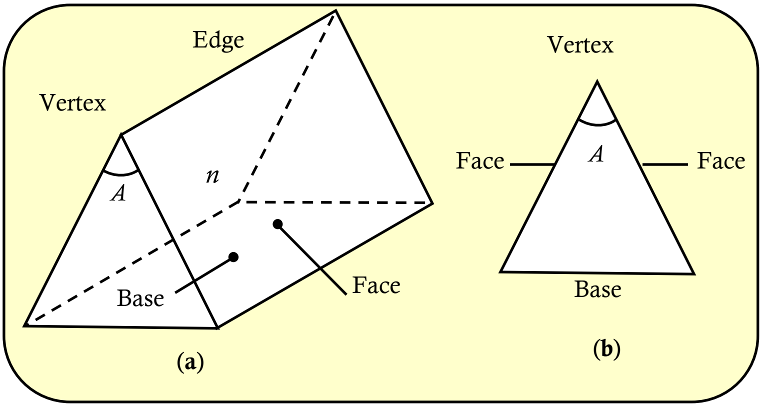

**Figure 3.1.** *Descriptive representation of a prism*

The various elements of a prism spectrometer are shown in Figure 3.2.

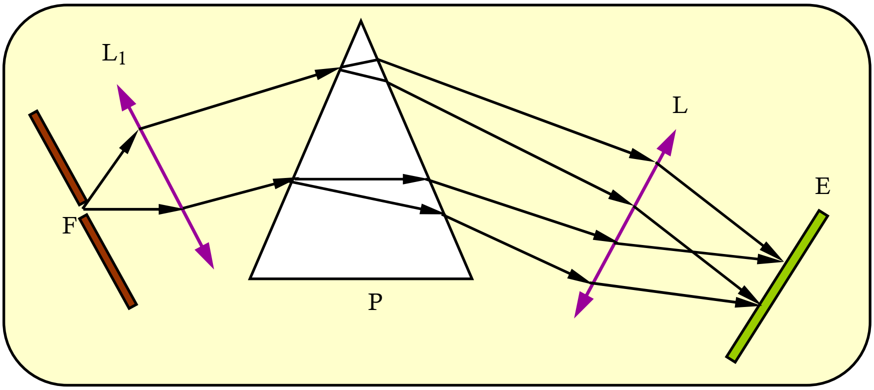

**Figure 3.2.** *Various constituent elements of a prism spectrometer*

– F designates the *entrance slit* of the spectrometer. The width of slit F varies (from several micrometers to several hundreds of micrometers) and its height depends on the prism dimensions and associated optics geometry;

– $L_1$ is a lens, known as *collimating lens*, which renders parallel the light rays exiting the slit F located at the focus of $L_1$ lens. F and $L_1$ constitute the *collimator*;

– P is the prism with edges parallel to the slit F. P is the light *dispersive element* and it is located at minimum deviation in order to reduce the astigmatism of the optical device;

– $L_2$ is the *objective* (set of lenses) constituting the *chamber lens* of the spectrometer. The spectrum provided by $L_2$ in its focal plane can be examined by means of an *ocular* (magnifier offering a clear image without accommodation of the eye);

– E is the observation screen (or photographic plate).

NOTE.– Astigmatism is an optical aberration (*defect of an optical system*) leading to image distortion.

Incident light rays are deflected by the prism. Deviation denoted by $D$ defines the angle between the (initial) incident light ray and the (final) emergent or refracted light ray. Deviation $D$ depends on the refractive index $n$ of the prism, which is itself a function of the wavelength $\lambda$ due to the dispersive character of the prism.

The variation of the refractive index of a given transparent medium as a function of wavelength is given by *Cauchy dispersion formula*:

$$n = a + \frac{b}{\lambda^2} + \frac{c}{\lambda^4} + .... \qquad [3.1]$$

In Cauchy dispersion formula [3.1], $a$, $b$ and $c$ are constants characteristic of the transparent medium and $\lambda$ is the wavelength of the light propagating through the medium. Constant $a$ is dimensionless, while constants $b$ and $c$ are expressed in $m^2$ and $m^4$, respectively. Equation [3.1] shows that the refractive index increases when the wavelength decreases, therefore when going from red to violet light. As a conclusion, red light is less deviated than violet light, according to experimental observations. Figure 3.3 illustrates white light decomposition into its various colors constituted of seven colors that can be observed due to water droplets producing the rainbow. The result is a *continuous spectrum* (Figure 3.3(a)). When light is emitted by a heated gas, for example, a *discrete spectrum* of rays constituted of spaced fine lines (Figure 3.3(b)) is obtained. Each of these rays marks the position of a clearly determined wavelength in the gas emission spectrum.

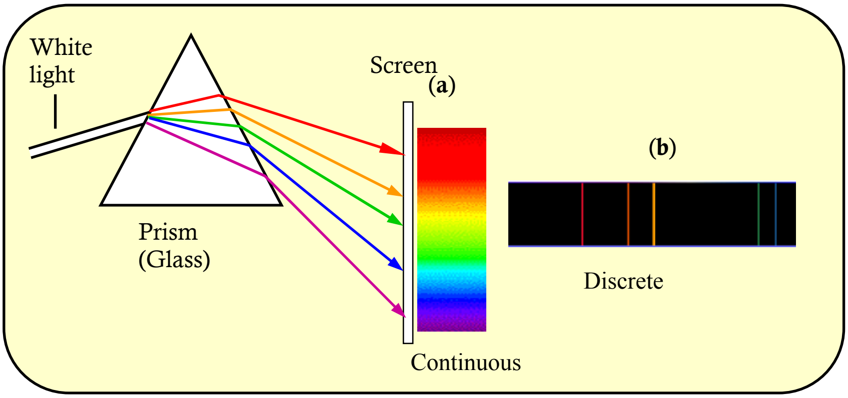

**Figure 3.3.** *White light dispersion by a glass prism*

> **Augustin Louis Cauchy** was a French mathematician. He is well-known in optics, especially for the Cauchy dispersion formula.

**Box 3.1.** *Cauchy (1789–1857)*

*Visible light* is defined in relation with the human eye. The wavelengths of electromagnetic radiations of the visible spectrum range between 400 and 800 nm. The colors composing white light vary continuously from violet to red going through indigo, blue, green, yellow and orange. Figure 3.3 shows only a few such colors.

Table 3.1 summarizes the various colors composing *white light* depending on their wavelength $\lambda_0$ in vacuum.

| Color | Violet | Indigo | Blue | Green | Yellow | Orange | Red |
|---|---|---|---|---|---|---|---|
| $\lambda_0$ (nm) | 400 | 440 | 470 | 530 | 580 | 650 | 750 |

**Table 3.1.** *The seven colors composing white light depending on their wavelength $\lambda_0$ in vacuum*

It is worth noting that similar experimental results to those above mentioned can be obtained using a grating spectrometer. Briefly, a grating is a plane or concave surface on which a large number of rectilinear, parallel and equidistant slits have been drawn.

### 3.1.2. *First lines of the hydrogen atom identified by Ångström*

In 1862, **Anders Ångström** conducted experimental studies on the *solar emission spectrum* using a combination of spectrometer and photography. **Ångström** identified four visible lines belonging to the *hydrogen atom* (Figure 3.4). The wavelengths $\lambda$ associated with these lines, which are usually denoted $H_\alpha$ (orange red), $H_\beta$ (blue green), $H_\gamma$ (indigo blue) and $H_\delta$ (violet) are 656.3, 486.1, 434.0 and 410.2 nm, respectively.

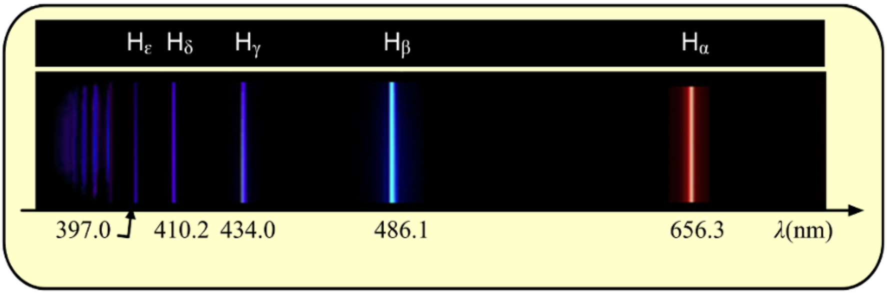

**Figure 3.4.** *The four $H_\alpha$, $H_\beta$, $H_\gamma$ and $H_\delta$ lines of the hydrogen atom identified by Ångström in the solar spectrum. All the other lines ($\lambda_\varepsilon \leq 397.0$ nm) are in the ultraviolet range*

The line denoted $H_\varepsilon$ with a wavelength $\lambda_\varepsilon = 397.0$ nm represents the fifth limiting line of the series located in the ultraviolet range of the electromagnetic spectrum. It is worth noting that *optical waves* correspond to *electromagnetic waves* in the visible range (electromagnetic waves that can be perceived by the human eye) as indicated in Figure 3.5.

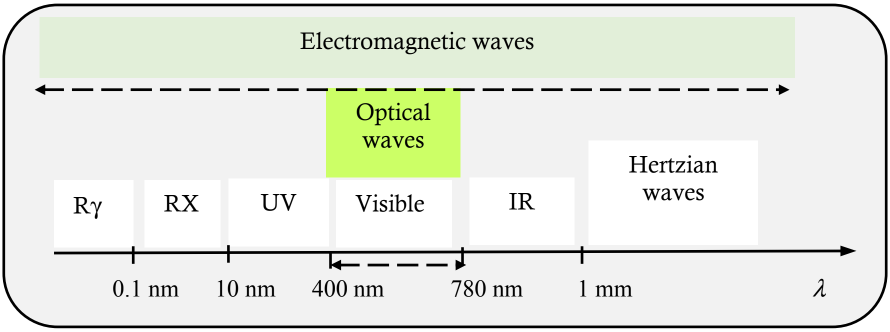

**Figure 3.5.** *Spectrum of electromagnetic radiations. Optical waves are electromagnetic waves in the visible spectrum*

> **Anders Jonas Ångström** was a Swedish physicist. He is one of the founders of spectrometry. Ångström is well-known for his experimental works on solar spectrum analysis, leading to his proof in 1862 of hydrogen presence in Sun's atmosphere. The unit of wavelength, the angström (Å), was named in his honor. 1 Å = $10^{-10}$ m.

**Box 3.2.** *Ångström (1814–1874)*

### 3.1.3. *Balmer's formula*

Through the intermediary of the Swiss physicist **Eduard Hagenbach** (1833–1910), **Johannes Balmer** had access to the wavelengths of the hydrogen atom measured by **Ångström** [CAR 79]. **Balmer** then tried to formulate a law that would make it possible to find the four lines $H_\alpha$, $H_\beta$, $H_\gamma$ and $H_\delta$. Finding out about the existence of $H_\varepsilon$ line of wavelength 397.0 nm observed by **Ångström**, **Balmer** discovered in 1885 that the wavelengths of the visible lines of the hydrogen atom follow the empirical law:

$$\lambda = \lambda_0 \frac{m^2}{m^2 - 4} \qquad [3.2]$$

In this law, $m$ is a strictly positive integer and $\lambda_0$ is the value of the limiting wavelength of the series obtained when $m = \infty$, which is $\lambda_0 = 364.56$ nm. Knowing that $m^2 - 4 > 0$, then $m \geq 3$. *Balmer's empirical law* [3.2] corresponds to the first spectral series of the hydrogen atom. With the exception of the four visible lines $H_\alpha$, $H_\beta$, $H_\gamma$ and $H_\delta$, all the other lines of the *Balmer series*, whose wavelengths range between 397.0 nm and 364.56 nm, are located in the ultraviolet range of electromagnetic radiations (Figure 3.5).

**APPLICATION 3.1.–**

> Find the wavelengths of the four visible lines as well as that of $H_\varepsilon$ line in the hydrogen atom spectrum using Balmer's empirical formula.
>
> *Given data.* $\lambda_0 = 364.56$ nm
>
> **Solution.**
>
> $m = 3$: $\lambda_3 = 656.2$ nm # 656.3 nm (line $H_\alpha$)

$m = 4$: $\lambda_4 \approx 486.0$ nm = 486.1 nm (line $H_\beta$)

$m = 5$: $\lambda_5 = 434.00$ nm = 434.0 nm (line $H_\gamma$)

$m = 6$: $\lambda_6 = 410.1$ nm # 410.2 nm (line $H_\delta$)

$m = 7$: $\lambda_7 \approx 397.0$ nm = 397.0 nm (line $H_\varepsilon$)

**Johann Jakob Balmer** was a Swiss physicist and mathematician. In 1862, Ångström identified the four lines of the hydrogen atom denoted $H_\alpha$, $H_\beta$, $H_\gamma$ and $H_\delta$, which were all within the visible spectrum range (400–780 nm). Hagenbach communicated these spectral lines to Balmer, who succeeded in 1885 to establish the first spectral series of the hydrogen atom.

**Box 3.3.** *Balmer (1825–1898)*

### 3.1.4. *Rydberg constant for hydrogen*

Having no knowledge on Balmer's empirical law, **Johannes Rydberg** tried to establish a formula for the succession of wavelengths of the hydrogen atom spectral lines measured by **Ångström**. In 1888, **Rydberg** wrote his formula as follows:

$$\lambda_{nm} = \lambda_0 \frac{m^2 n^2}{4(m^2 - n^2)} \qquad [3.3]$$

In [3.3], $m$ and $n$ are integers so that $n < m$. Moreover, $n = 2, 3, 4\ldots$ For $n = 2$, [3.3] gives:

$$\lambda = \lambda_0 \frac{m^2}{m^2 - 4}$$

which is similar to Balmer's empirical law [3.2].

Moreover, *Rydberg formula* [3.3] can be written in a convenient form using the inverse wavelength, or:

$$\frac{1}{\lambda_{nm}} = \frac{4}{\lambda_0} \frac{(m^2 - n^2)}{m^2 n^2} = \frac{4}{\lambda_0} \left\{ \frac{m^2}{m^2 n^2} - \frac{n^2}{m^2 n^2} \right\}$$

This leads to:

$$\frac{1}{\lambda_{nm}} = R_H \left\{ \frac{1}{n^2} - \frac{1}{m^2} \right\} \qquad [3.4]$$

$$R_H = 4/\lambda_0$$

By definition, $R_H$ is known as Rydberg constant for hydrogen.

### Numerical expression ($\lambda_0$ = 364.56 nm):

$$R_H = 10{,}972{,}130.79 \text{ m}^{-1} \qquad [3.5]$$

Knowing the experimental value $R_{Hexp}$ = 10,973,731.77 ± 0.83 $\text{m}^{-1}$, the relative deviation is:

$$\Delta R_H/R_H = 0.015\%$$

The theoretical value [3.5] is therefore in excellent agreement with the experimental value.

### APPLICATION 3.2.–

> Use Rydberg's formula [3.4] to find the first line of Balmer series. Consider $R_{Hexp}$ = 10,973,731.77 $\text{m}^{-1}$.
>
> **Solution.** For the Balmer series, $n = 2$. The first line corresponds to $m = 3$. This gives $\lambda_{23}$ = 656.1 nm.
>
> This is actually the wavelength of $H_\alpha$ line of the hydrogen Balmer series.

**Johannes Rydberg** was a Swedish physicist. Rydberg is especially known for having elaborated in 1888 the formula bearing his name. This formula gives the wavelengths of radiations emitted when an atom changes its energy level. Rydberg's constant, as well as the Rydberg, an energy unit, were named in his honor. Moreover, multi-electron atoms excited by increasing the number *n*, which determines the quantum state of the outer shell electron are known as Rydberg atoms. These atoms are very sensitive to the interaction with an electromagnetic field. The corresponding quantum states are known as Rydberg series, playing an important role in the study of the interaction between electromagnetic radiation and matter especially for stellar plasma diagnosis (see [SAK 18a] for further details on this subject).

**Box 3.4.** *Rydberg (1854–1919)*

### 3.1.5. *Ritz combination principle*

Before 1887, as the exact value of the speed of light was not known, spectroscopic techniques used instead of frequency $\nu = c/\lambda$, the *spectroscopic wave number* $\bar{\nu} = 1/\lambda$ ($\bar{\nu}$ in $m^{-1}$). Rydberg formula [3.4] shows that the spectroscopic wave number is the difference between two physical quantities that **Walther Ritz** called *spectral terms*.

In 1908, *Ritz* formulated the *fundamental law of spectroscopy,* known as *Ritz combination principle* [SIV 86]. According to this principle, any spectral line of a given atom can be determined by pairing up a far smaller number (than the number of lines of the spectrum) of quantities called spectral terms (or simply terms). These terms are designated by the $T$ letter. According to the Ritz combination principle, the spectroscopic wave number of each spectral line is given by the difference of two terms $T_{n1}$ and $T_{n2}$:

$$\bar{\nu} = T_{n_1} - T_{n_2} \qquad [3.6]$$

By convention, the terms are positive quantities that are numbered in such a way that the increase in the term number corresponds to a decrease of $T_n$ term. A comparison between [3.5] and [3.6] leads to $T_n$ expression:

$$T_n = \frac{R_H}{n^2} \qquad [3.7]$$

**Walther Ritz** was a Swiss physicist and mathematician. He is especially known for his works in spectroscopy for the formulation of the fundamental law of spectroscopy, known as Ritz combination principle. He is also well-known for the variational method bearing his name, which is very useful in atomic physics.

**Box 3.5.** *Ritz (1878–1909)*

## 3.2. Rutherford's planetary model of the atom

### 3.2.1. *Rutherford's scattering, atomic nucleus*

In 1911, **Ernest Rutherford** used a *radioactive radiation* of $\alpha$ *particles* emitted by a radium source to bombard thin metallic (gold) foils [SIV 86, SAK 11, PLO 16]. The simplified representation of the experimental setup is shown in Figure 3.6.

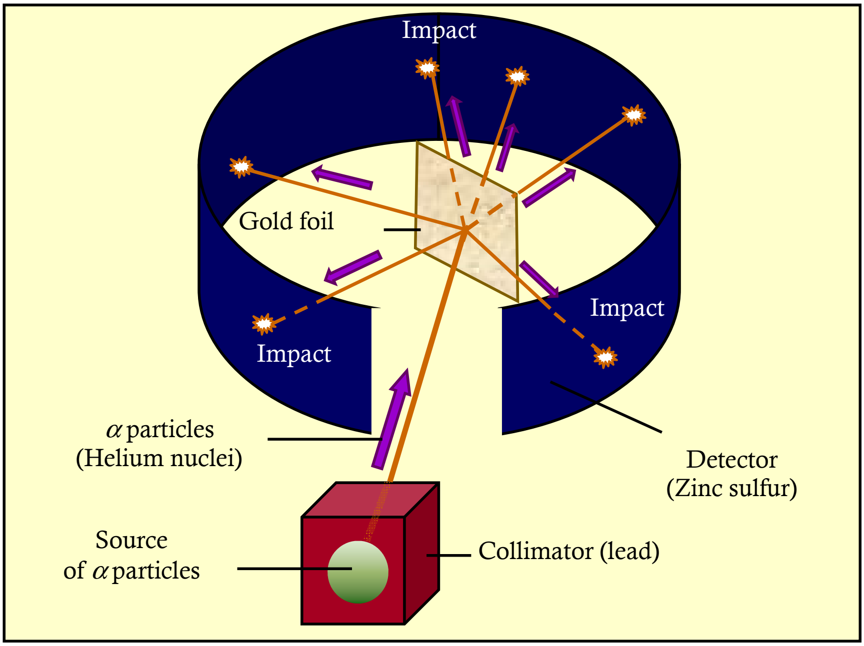

**Figure 3.6.** *Experimental setup of Rutherford scattering*

The purpose of this experiment was to verify the first model of atom presented by **Joseph John Thomson** (1856–1940) in 1902, according to which the atom was made from positive matter in which a sea of electrons was immersed [SAK 11]. Two essential observations are possible due to this experiment:

OBSERVATION 3.1.– Many particles travel through matter without being deflected (though theoretically, according to Thomson's model, several deflections should be observed).

OBSERVATION 3.2.– The path of alpha particles traveling in the proximity of the "center" suffers a large angle deflection.

The first observation leads to the conclusion that positive particles, which, according to Thomson's model were sparse, are in fact concentrated at the "center" of matter. As for the second observation, it proves that the "center" of matter repelling the alpha particles is a positively charged point particle. **Rutherford** proved that an $\alpha$ particle can be obtained by twice ionizing a helium atom: $He \rightarrow He^{2+} + 2e^{-}$. The $\alpha$ particle is a helium nucleus $He^{2+}$. The positive "center" of matter was identified as the *nucleus of an atom*. Drawing inspiration from the astronomical model of the solar system proposed by **Johannes Kepler** (1571–1630), **Rutherford** proposed the planetary model of the atom, in which electrons orbit the nucleus.

NOTE ON COLLIMATORS.– A collimator is a block of lead, tungsten or other high atomic number metal pierced by cylindrical or conical holes along a given system of axes. The partition between two neighboring holes is called *septum*. The role of the collimator is to "filter" the particles emitted by the source toward the crystal, and eliminate the scattered particles. Only those particles coming from the part of the device located on the vertical of the holes can reach the target or the detector. The rest are stopped by the *septa*.

### 3.2.2. *Limitations of the planetary model*

The planetary model has at least two limitations:

1) it does not explain the existence of spectral lines such as those of the hydrogen atom, evidenced by **Balmer** starting with 1885;

2) as charged particles, electrons are subjected to centripetal acceleration due to their orbital motion. According to classical electrodynamics predictions, any charged particle submitted to acceleration radiates energy. According to the planetary model, *electrons should radiate energy and end up falling on the nucleus*. This is not the case in reality.

**Lord Ernest Rutherford of Nelson** was a New Zealand and British physicist and chemist. Rutherford is considered the founder of nuclear physics due to his well-known discoveries in this field. He discovered $\alpha$ (helium nuclei) radiation and $\beta^-$ (electron) radiation. Rutherford also discovered that radioactivity is accompanied by disintegration of chemical elements. For this discovery, he was awarded the Nobel Prize for chemistry in 1908. Together with the British radiation chemist **Frederick Soddy** (1877–1956), Rutherford formulated in 1909 the experimental law of radioactive decay. Drawing on his experiments on the scattering of $\alpha$ particles on gold foils, Rutherford proved the existence of the atomic nucleus in 1911.

**Box 3.6.** *Rutherford (1871–1937)*

It is in this context that the first major scientific congress was organized, known as the Solvay conference (Brussels, 1911) mainly devoted to "*the theory of radiation and the quanta*". This conference was expected to eliminate some of the drawbacks of the Rutherford model [CAR 79]. However, when this international meeting ended, the participants were still not able to explain why electrons orbiting the nucleus did not radiate energy. Two years would pass until the puzzling model of Rutherford would be solved, thanks to the inventing genius of **Niels Bohr**, who had not attended the conference in 1911.

## 3.3. Bohr's quantized model of the atom

### 3.3.1. *Shell model of electron configurations*

*Electron shells* have been historically designated by letters K, L, M, etc., used in X-ray spectroscopy. The *electron configuration* of an atom can be described as $K^a$ $L^b$ $M^c$, etc. Shells K, L, M, etc., are associated with numbers 1, 2, 3, 4, etc., respectively. According to the planetary model, electrons are orderly distributed in shells, starting with the first one, K. For a given configuration described as $K^a$ $L^b$ $M^c$, etc., the atomic number $Z$ verifies the following relation:

$$Z = a + b + c + \ldots \qquad [3.8]$$

Depending on the number $Z$ of electrons in the atom, shells K, L, M, etc., are saturated at 2, 8, 18, etc., electrons, respectively.

As an example, let us write the electron configurations of hydrogen H, helium He and argon Ar. These are:

$$\text{H } (Z = 1)\text{: } K^1\text{; He } (Z = 2)\text{: } K^2\text{; Ar } (Z = 18)\text{: } K^2\ L^8 M^8 \qquad [3.9]$$

### 3.3.2. *Bohr's postulates, principal quantum number*

As already mentioned above, the first Solvay conference in 1911 had ended without explaining the origin of spectral lines, and particularly those of the hydrogen atom. Moreover, the fact that electrons orbiting the nucleus, according to the planetary model, did not radiate energy remained to be explained by the participants to the conference. In an attempt to shed light on these two enigmas raised by the planetary model of Rutherford, **Niels Bohr** formulated in 1913 two fundamental *postulates* as the basis for his semiclassical theory on the hydrogen atom [SIV 86, HLA 00, GUY 03, BIÉ 06, PÉR 86, SAK 08, MOI 16, PLO 16].

FIRST POSTULATE.–

*Though according to classical mechanics, electrons in an atom are allowed an infinity of circular orbits, in fact they orbit the nucleus only on certain orbits known as stationary states, in which they emit no radiation. These allowed orbits are* *determined by a quantization condition imposed on the angular momentum L of the electron:*

$$L = mvr = n\frac{h}{2\pi} \qquad [3.10]$$

*where*

– *m: mass of the electron;*

– *v: linear velocity of the electron on its orbit;*

– *r: radius of the electron orbit;*

– *n: principal quantum number,* $n \in \{1\ ;\ 2\ ;\ 3\ ;\ \ldots\infty\}$;

– *h: Planck constant.*

SECOND POSTULATE.–

*Each allowed orbit corresponds to a discrete level of energy. Transitions of the electron from one orbit to another involve quantum jumps and are accompanied by the emission or absorption of a quantum of energy such that:*

$$\Delta E = |E_f - E_i| = h\nu \qquad [3.11]$$

*where*

– $E_i$: *energy corresponding to the initial orbit;*

– $E_f$: *energy corresponding to the final orbit;*

– $\nu$: *frequency of the emitted or absorbed radiation.*

Relation [3.11] expresses *Bohr frequency condition*.

The *first postulate* introduces the notion of *stationary state* characterized by a discrete value of energy $E_n$. The *energy of the hydrogen atom* is therefore quantized. This postulate introduces the first quantum number of the electron: the *principal quantum number n*.

The *second postulate* introduces the notion of *electron transition* between stationary states corresponding to photon absorption and emission (Figure 3.7). Figure 3.8 illustrates two *processes of absorption* and *emission* of a photon between two energy levels $E_p$ and $E_n$. The discrete character of the energy levels shows that the hydrogen atom can absorb energy, and it consequently passes from a lower level of energy $E_p$ to a higher level of energy $E_n$ absorbing a photon $h\nu$.

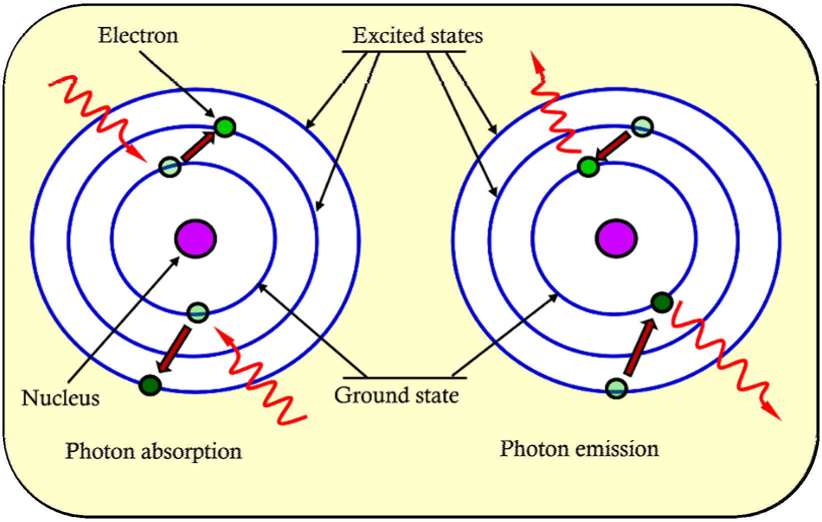

**Figure 3.7.** *Bohr's model of quantized atom*

This absorption process is not possible unless the photon has precisely the required energy $\Delta E = E_p - E_n$ equal to the energy difference between the final and the initial transition level, according to Bohr frequency condition [3.11]. Bohr's theory presents the model of quantized atom (Figure 3.7).

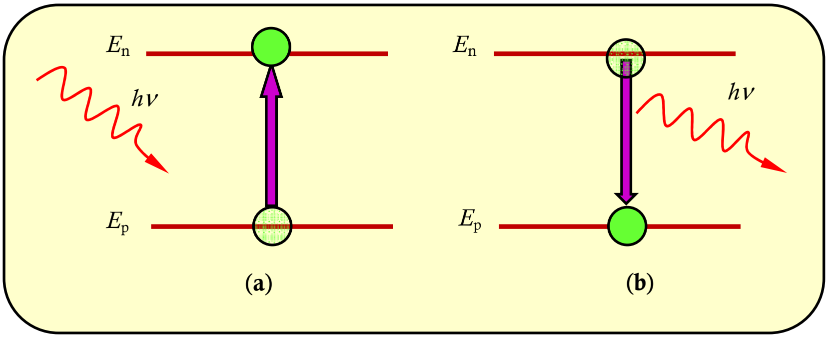

**Figure 3.8.** *Absorption (a) and emission (b) of a photon of energy* $h\nu$

Likewise, the hydrogen atom can emit a photon if its energy is equal to the energy difference between the two levels $E_n$ and $E_p$. As a consequence of Bohr's theory, the energy of the absorbed photon (Figure 3.8(a)) is similar to that of the emitted photon (Figure 3.8(b)).

### 3.3.3. *Absorption spectrum, emission spectrum*

As previously noted, according to Bohr's theory, the frequency of the absorbed radiation is equal to that of the emitted radiation. In other terms, when a hydrogen sample is exposed to a *polychromatic beam* constituted of a flow of photons of various wavelengths, only the photons having precisely the energy required to trigger the allowed transitions between $n$ and $p$ levels can be absorbed. A *continuous spectrum* is observed under these conditions, and it corresponds to the photons that have traveled through the sample without interaction. The resulting continuous spectrum is scattered with a set of *absorption lines* corresponding to the *absorption spectrum* of the hydrogen atom. For an atom, absorption corresponds to selectively absorbed photons, which consequently disappear from the polychromatic light beam for certain wavelengths characteristic to the studied atom. Moreover, during the *de-excitation process* corresponding to electron transitions from higher energy levels to lower energy levels, the hydrogen atom can release several photons of various wavelengths. The set of emitted wavelengths constitutes the *emission spectrum*.

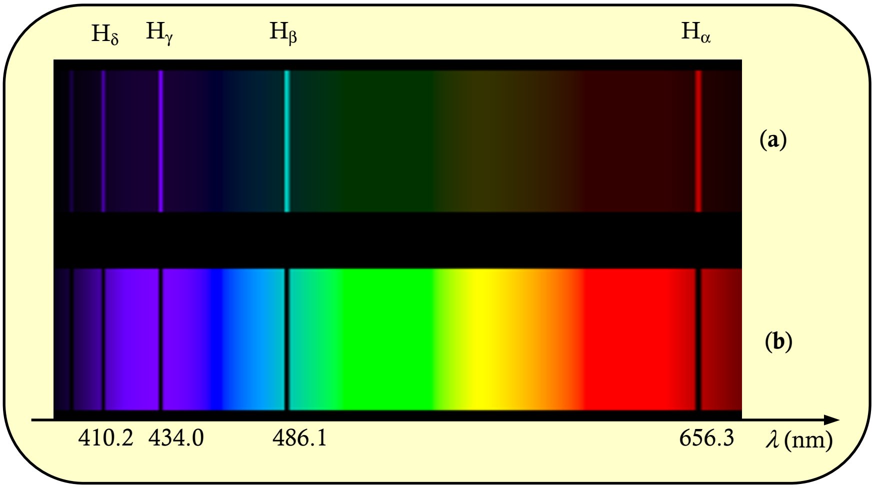

**Figure 3.9.** *Emission (a) and absorption (b) spectra of the hydrogen atom in the visible range. It can be noted that the emission lines and the absorption lines overlap*

Knowing that the emitted and absorbed photons have the same wavelengths, the position of the black lines on a continuous colored background of the absorption spectrum (Figure 3.9(a)) is exactly the same as that of the colored lines of the emission spectrum (Figure 3.9(b)). Atomic absorption and emission spectra generally *overlap*.

### 3.3.4. *Principle of angular momentum quantization*

Let us consider a particle of mass $m$ executing a circular motion at velocity $\vec{v}$ around a point $O$ in space. By definition, the angular momentum $\vec{L}$ of the particle with respect to point $O$ is the cross-product of its position vector and its linear momentum $\vec{p}$ :

$$\vec{L} = \overrightarrow{OM} \wedge \vec{p} = \vec{r} \wedge \vec{p} \qquad [3.12]$$

The angular momentum vector $\vec{L}$ is perpendicular to the plane formed by the directions of the position vector $\vec{r}$ and linear momentum vector $\vec{p}$ . Its direction is such that ( $\vec{r}$ , $\vec{p}$ , $\vec{L}$ ) is a right-handed trihedron (Figure 3.10).

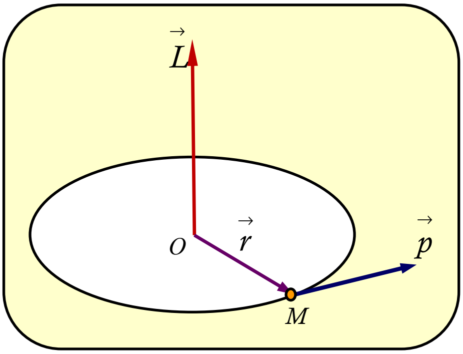

**Figure 3.10**. *Angular momentum $\vec{L}$ of a particle in circular motion*

As $\vec{r}$ and $\vec{p} = m\vec{v}$ are orthogonal vectors, the norm of the angular momentum is:

$$L = rp = mvr \qquad [3.13]$$

In the context of Bohr's theory, the first postulate is supported by a principle of angular momentum quantization, which intuitively justifies the stationary character of the quantum states or of the electron circular orbits of the hydrogen atom. The principle of quantization of the electron angular momentum in the hydrogen atom is expressed by relation [3.10] according to Bohr. These are rewritten here using the *reduced Planck constant* or *Dirac constant* $\hbar = h/2\pi$ :

$$L = n\frac{h}{2\pi} = n\hbar \qquad [3.14]$$

For the proof of relation [3.14], please see Exercise 3.7.21.

### 3.3.5. *Quantized expression of the energy of the hydrogen atom*

In the elaboration of his theory, **Bohr** assumed that the electron in the hydrogen atom is a classical particle. To determine the quantized expression of the energy of the hydrogen atom, **Bohr** applied the laws of classical mechanics. We should, nevertheless, keep in mind that the properties of atomic systems are correctly studied in the context of quantum mechanics, which was elaborated 13 years after Bohr's theory, in 1926. Bohr had at his disposal only the laws of classical mechanics, in which he integrated purely quantum concepts, such as the stationary states, the discrete character of the atom energy, etc. This is why Bohr's theory is referred to as semiclassical. In what follows, the rest mass $m_0$ of the electron is denoted by $m$ ("0" index is useless here; it is however very important in relativistic mechanics, see [2.38]).

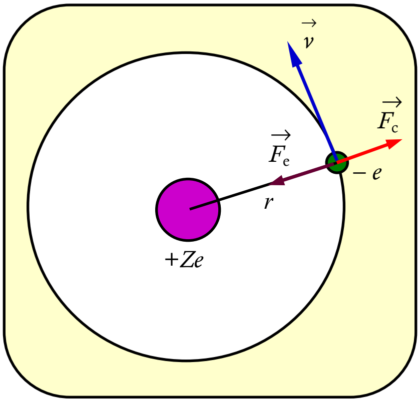

**Figure 3.11.** *Hydrogen-like {nucleus–electron} system*

In order to determine the quantized expression of the energy of the hydrogen atom within Bohr's theory, let us consider the general case of a *hydrogen-like system* defined as an atomic system constituted of a nucleus of $+Ze$ charge orbited by only one electron (Figure 3.11). It is the case of the hydrogen atom and its *isoelectronic ions*: $He^+$, $Li^{2+}$, $Be^{3+}$, etc.

In order to express the *mechanical energy of hydrogen-like systems* as a function of the radius $r$ of the electron orbit, let us use the *principle of inertia* and the *theorem of the center of inertia* to express the *centrifugal force*. Since the electron is in uniform circular motion on an orbit of radius $r$ (Figure 3.11), the vector sum of external forces acting on the electron is zero, hence:

$$\sum \vec{F}_{ext} = \vec{F}_e + \vec{F}_c = \vec{0} \Rightarrow -k\frac{Ze^2}{r^2}\vec{u} + m\frac{v^2}{r}\vec{u} = \vec{0} \quad [3.15]$$

The last equality of the above relations leads to the expression of the kinetic energy $E_c$ of the electron as a function of radius $r$:

$$mv^2 = k\frac{Ze^2}{r} \Rightarrow E_c(r) = k\frac{Ze^2}{2r} \quad [3.16]$$

By definition, the *total mechanical energy E* (*r*) of a hydrogen-like system is given by the following relation:

$$E(r) = E_c(r) + U(r) = E_c(r) - k\frac{Ze^2}{r} \quad [3.17]$$

The last equality [3.16] leads to:

$$E = -k\frac{Ze^2}{2r} \quad [3.18]$$

In the international system, the *electric constant is* $k = 1/4\pi\varepsilon_0 = 9 \times 10^9$ SI.

Equalizing relations [3.13] and [3.14] leads to:

$$mvr = n\hbar \quad [3.19]$$

Relation [3.19] implicitly shows that the velocity $v$ of the electron as well as the radius $r$ of the electron orbit (mass $m$ is constant) are quantized quantities. Therefore, the quantized energy $E_n$ of hydrogen-like systems is related to the quantized radius $r_n$ of the electron orbit by the relation [3.18]:

$$E_n = -k\frac{Ze^2}{2r_n} \quad [3.20]$$

The quantized expression of $r_n$ can be used to deduce the expression of energy $E_n$ from relation [3.20]. Squaring relation [3.19] leads to:

$$(mvr)^2 = n^2\hbar^2 \Rightarrow v^2 = \frac{n^2\hbar^2}{m^2r^2} \quad [3.21]$$

Inserting the expression of $v^2$ given by the second equality in [3.21] in the second equality [3.20] leads to:

$$m\frac{n^2\hbar^2}{m^2r^2} = k\frac{Ze^2}{r} \Rightarrow \frac{n^2\hbar^2}{mr_n} = kZe^2$$

From this last relation the quantized expression of radius $r_n$ can be deduced:

$$r_n = \frac{n^2\hbar^2}{mkZe^2} = n^2 \times \frac{a_0}{Z} \qquad [3.22]$$

For $n = 1$ and for the hydrogen atom ($Z = 1$), the *radius of the first orbit is*: $r_1 = a_0$. By definition, the radius $a_0$ is referred to as *Bohr radius*, which is given by the expression:

$$a_0 = \frac{\hbar^2}{mke^2} \qquad [3.23]$$

## Numerical expression:

$$a_0 = 0.5280375987 \times 10^{-10}\,\text{m} \approx 0.53\ \text{Å}$$

**APPLICATION 3.3.–**

> Calculate the radius of the first orbit of the electron of $He^+$ ion and the radius of the third orbit of $C^{5+}$ ion. Consider $a_0$= 0.529 Å.
>
> **Solution.** Using [3.22]:
>
> – *radius of the first orbit of the electron of* $He^+$ ion: $n = 1$; $Z = 2$. Hence: $r_1 = 0.265$ Å;
>
> – *radius of the third orbit of the electron of* $C^{5+}$ ion: $n = 3$; $Z = 6$. Hence: $r_3 = 0.794$ Å.

Let us now express the energy $E_n$ using [3.20] and [3.22]. We have:

$$E_n = -\frac{Z^2k^2me^4}{2\hbar^2n^2} \qquad [3.24]$$

In atomic physics, it is very convenient to express the quantized energy of a hydrogen-like system as a function of the rest energy of the electron $m_0c^2$ and of the *fine structure constant* $\alpha$ defined by:

$$\alpha = \frac{e^2}{\hbar c} \qquad [3.25]$$

In relation [3.24], $\alpha$ is a dimensionless quantity and the other quantities are expressed in electromagnetic unit centimeter gram second (emu cgs).

### Numerical expression:

$$\alpha = 7.297379866 \times 10^{-3} \approx 1/137.0354865$$

Moreover, in emucgs, the electric constant $k = 1$. Inserting the fine structure constant $\alpha$ and the rest energy of the electron $mc^2$, expression [3.24] can be written as:

$$E_n = -\frac{Z^2\alpha^2 mc^2}{2n^2} \qquad [3.26]$$

In relation [3.25], $\alpha^2 = 5.325135412 \times 10^{-5}$; $mc^2 = 0.510999910$ MeV. For the hydrogen atom, $Z = 1$. According to [3.26]:

$$E_n = -\frac{\alpha^2 mc^2}{2n^2} \qquad [3.27]$$

Expression [3.27] makes it possible to introduce an energy unit that is commonly used in atomic physics: the *Rydberg* abbreviated as Ryd (values of energies expressed in joule are significant at microscopic scale, see Application 3.4). Using [3.27], the Rydberg can be expressed as a function of $\alpha$ and $mc^2$. Hence:

$$\text{Ryd} = \frac{\alpha^2 mc^2}{2} \qquad [3.28]$$

### Numerical expression:

$$\text{Ryd} = 13.60571858 \text{ eV}$$

Moreover, another energy unit that is very convenient to use in atomic physics can be introduced: *atomic unit* (a.u.), where 1 a.u. = 2 Ryd. Hence, the quantized energy of hydrogen-like systems expressed in Ryd and in a.u. can be written as:

$$E_n = -\frac{Z^2}{n^2} \text{ (Ryd)}; E_n = -\frac{Z^2}{2n^2} \text{ (a.u.)} \qquad [3.29]$$

**APPLICATION 3.4.–**

> Calculate the energy of the ground state of the hydrogen atom, as well as the energy of the second excited state of the hydrogen-like $He^+$ ion. Express the results in joule, emu cgs, electronvolt, Rydberg and atomic units. Draw a conclusion.
>
> *Given data.* 1 Ryd = 13.60580 eV; 1 eV = $1.602179487 \times 10^{-19}$ J; 1 erg = $1.0 \times 10^{-7}$ J
>
> **Solution.** Use [3.29].
>
> The ground state of the hydrogen atom H ($Z = 1$) corresponds to $n = 1$ and the second excited state of $He^+$ ion ($Z = 2$) corresponds to $n = 3$. Hence:
>
> – in joule: $E_1$ (H) = $-2.17989 \times 10^{-18}$ J; $E_3$ ($He^+$) = $-9.68841 \times 10^{-18}$ J
>
> – in uemcgs: $E_1$(H) = $-2.17989 \times 10^{-11}$ erg; $E_2$ ($He^+$) = $-9.68841 \times 10^{-11}$ erg
>
> – in eV: $E_1$(H) = $-13.60580$ eV; $E_2$ ($He^+$) = $-6.04702$ eV
>
> – in Rydberg: $E_1$(H) = $-1$ Ryd; $E_2$ ($He^+$) = $-0.444$ Ryd
>
> – in atomic units: $E_1$ (H) = $-2$ a.u.; $E_2$ ($He^+$) = $-0.889$ Ryd

CONCLUSION.– The joule and the erg are not fit as units for atomic physics. Energy values are more relevant when expressed in electronvolt.

### 3.3.6. *Interpretation of spectral series*

Let us consider the $p \rightarrow n$ electron transition (Figure 3.8). Using Bohr frequency condition [3.11] and expression [3.25], we have:

$$h\nu = \frac{hc}{\lambda} = E_n - E_p = -\frac{Z^2\alpha^2 mc^2}{2n^2} + \frac{Z^2\alpha^2 mc^2}{2p^2}$$

which gives:

$$h\nu = Z^2 \frac{\alpha^2 mc^2}{2}\left(\frac{1}{p^2} - \frac{1}{n^2}\right)$$

Hence:

$$\frac{1}{\lambda} = Z^2 \frac{\alpha^2 mc^2}{2hc}\left(\frac{1}{p^2} - \frac{1}{n^2}\right) \qquad [3.30]$$

For the hydrogen atom ($Z = 1$), [3.30] leads to:

$$\frac{1}{\lambda} = \frac{\alpha^2 mc^2}{2hc}\left(\frac{1}{p^2} - \frac{1}{n^2}\right) \qquad [3.31]$$

Let us compare expression [3.31] to Rydberg formula [3.4], reminded below:

$$\frac{1}{\lambda_{nm}} = R_{\mathrm{H}}\left\{\frac{1}{n^2} - \frac{1}{m^2}\right\}$$

This leads to the expression of Rydberg constant $R_{\mathrm{H}}$ for hydrogen:

$$R_{\mathrm{H}} = \frac{\alpha^2 mc^2}{2hc} \qquad [3.32]$$

*Spectral series* [3.30] *of hydrogen-like systems* are then written as a function of Rydberg constant for hydrogen:

$$\frac{1}{\lambda} = Z^2 R_{\mathrm{H}}\left(\frac{1}{p^2} - \frac{1}{n^2}\right) \qquad [3.33]$$

For the hydrogen atom, [3.33] leads to:

$$\frac{1}{\lambda} = R_{\mathrm{H}}\left(\frac{1}{p^2} - \frac{1}{n^2}\right) \qquad [3.34]$$

Let us calculate $R_{\mathrm{H}}$ considering:

$\alpha^2 = 5.325135412 \times 10^{-5}$; $mc^2 = 0.51099991$ MeV; 1 eV = $1.602179487 \times 10^{-19}$ J; $c = 2.99792458 \times 10^{8}$ m · s$^{-1}$; $h = 6.62606896 \times 10^{-34}$ J · s

## Numerical expression:

$R_{\mathrm{H}} = 10{,}973{,}773.3$ m$^{-1}$

Moreover, a comparison between [3.34] and [3.4.bis] series reveals the physical significance of numbers $p$ and $m$ in Rydberg formula [3.4]: these are principal quantum numbers according to Bohr's theory.

Furthermore, [3.34] makes it possible to express all the observed spectral series of the hydrogen atom. They are presented here in their chronological order.

### 3.3.6.1. *Balmer series (1885): p = 2*

$$\frac{1}{\lambda} = R_{\mathrm{H}}\left(\frac{1}{4} - \frac{1}{n^2}\right), n \geq 3 \quad [3.35]$$

– *First line*: $n = 3$: $1/\lambda = 10{,}973{,}731.77 \times (1/4 - 1/9) \Rightarrow \lambda = 656.1$ nm;

– *Limiting line*: $n = \infty$. $1/\lambda = 10{,}973{,}731.77/4 \Rightarrow \lambda_\infty = 364.5$ nm.

Hence: 364.0 nm < $\lambda$ < 657.0 nm. The Balmer series is in the visible range (the first four lines $H_\alpha$ (orangy red), $H_\beta$ (blue green), $H_\gamma$ (indigo blue) and $H_\delta$ (violet)) and in the ultraviolet range (see Figure 3.4).

### 3.3.6.2. *Lyman series (1906): p = 1*

$$\frac{1}{\lambda} = R_{\mathrm{H}}\left(1 - \frac{1}{n^2}\right), n \geq 2 \quad [3.36]$$

– *First line*: $n = 2$ : $1/\lambda = 10{,}973{,}731.77 \times (1 - 1/4) \Rightarrow \lambda = 121.5$ nm;

– *Limiting line*: $n = \infty$. $1/\lambda = 10{,}973{,}731.77 \Rightarrow \lambda_\infty = 91.1$ nm.

Hence: 90.0 nm < $\lambda$ < 122.0 nm. Lyman series is in the ultraviolet range.

### 3.3.6.3. *Paschen series (1908): p = 3*

$$\frac{1}{\lambda} = R_{\mathrm{H}}\left(\frac{1}{9} - \frac{1}{n^2}\right), n \geq 4 \quad [3.37]$$

– *First line*: $n = 4$. $1/\lambda = 10{,}973{,}731.77 \times (1/9 - 1/16) \Rightarrow \lambda = 1{,}874.6$ nm;

– *Limiting line*: $n = \infty$. $1/\lambda = 10{,}973{,}731.77/9 \Rightarrow \lambda_\infty = 820.1$ nm.

Hence: 820.0 nm < $\lambda$ < 1,875.0 nm. *Paschen series* is in the infrared range.

### 3.3.6.4. *Brackett series (1922): p = 4*

$$\frac{1}{\lambda} = R_{\mathrm{H}}\left(\frac{1}{16} - \frac{1}{n^2}\right),\ n \geq 5 \qquad [3.38]$$

– *First line*: $n = 5$. $1/\lambda = 10{,}973{,}731.77 \times (1/16 - 1/25) \Rightarrow \lambda = 4{,}050.1$ nm;

– *Limiting line*: $n = \infty$. $1/\lambda = 10{,}973{,}731.77/16 \Rightarrow \lambda_\infty = 1{,}458.0$ nm.

Hence: 1,457.0 nm < $\lambda$ < 4,051.0 nm. *Brackett series* is in the far infrared range.

### 3.3.6.5. *Pfund series (1924): p = 5*

$$\frac{1}{\lambda} = R_{\mathrm{H}}\left(\frac{1}{25} - \frac{1}{n^2}\right),\ n \geq 6 \qquad [3.39]$$

– *First line*: $n = 6$. $1/\lambda = 10{,}973{,}731.77 \times (1/25 - 1/36) \Rightarrow \lambda = 7{,}455.8$ nm;

– *Limiting line*: $n = \infty$. $1/\lambda = 10{,}973{,}731.77/25 \Rightarrow \lambda_\infty = 4{,}556.3$ nm.

Hence: 4,556.0 nm < $\lambda$ < 7,456.0 nm. *Pfund series* is in the far infrared range.

## 3.3.7. *Energy diagram of the hydrogen atom, ionization energy*

Considering the approximation 1 Ryd = 13.60 eV, let us use [3.29] to calculate in eV the hydrogen atom energies for the first five levels. The results are:

$E_1 = -13.60$ eV; $E_2 = -3.40$ eV; $E_3 = -1.51$ eV; $E_4 = -0.86$ eV

$E_5 = -0.54$ eV

Moreover, for $n = \infty$, $E_\infty = 0$ eV: the hydrogen atom is *ionized*, the proton and the electron are separated, and the $H^+$ ion (proton) is obtained. Electron energy is no longer quantized. The corresponding states are *unbound states* forming a *continuum*. By definition, the *ionization energy* $E_\mathrm{i}$ of the hydrogen atom is the energy it must receive while in its ground state, in order to move the electron to infinity where its final velocity is zero. Hence: $E_\mathrm{i} = E_\infty - E_1 = 13.6$ eV.

Figure 3.12 shows the *energy diagram of the hydrogen atom*. Several electron transitions corresponding to emission lines belonging to Lyman, Balmer and Paschen series are represented in this diagram.

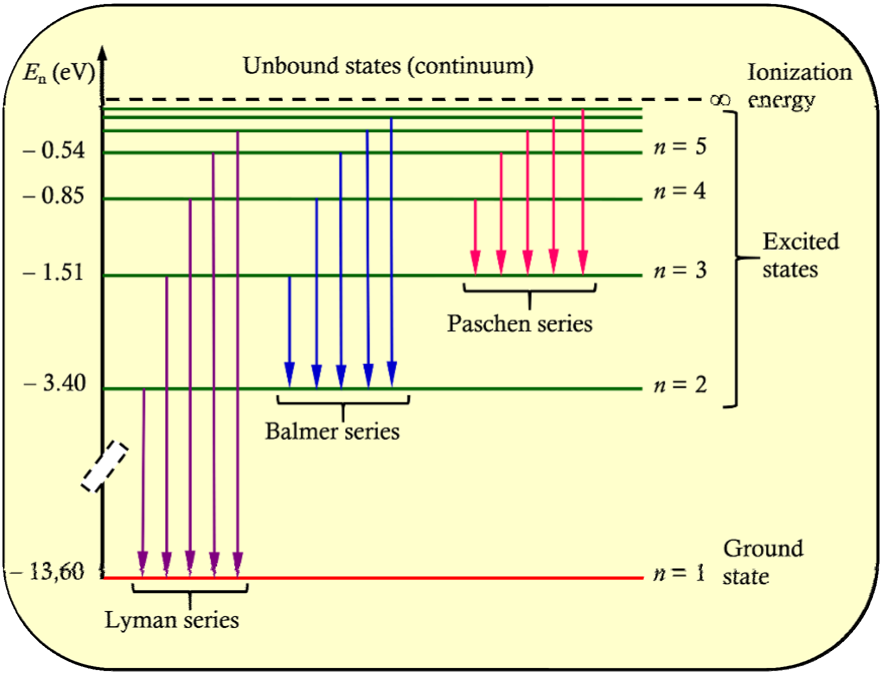

**Figure 3.12.** *Energy diagram of the hydrogen atom*

**Theodore Lyman** was an American physicist. Lyman is known for his works in spectroscopy. In 1906, he established the second spectral series of the hydrogen atom situated in the ultraviolet range of electromagnetic radiations.

**Friedrich Louis Carl Heinrich Paschen** was a German physicist. Paschen is known for his works on electric discharges and mainly related to spectroscopy. In 1889, he established the Paschen curve used in plasma physics. Then in 1908 he established the third spectral series of the hydrogen atom situated in the infrared range of electromagnetic radiations.

**Frederik Sumner Brackett** and **August Herman Pfund** were American physicists. Their names are especially related to the spectral series of the hydrogen atom discovered in 1922 and 1924, respectively. These two series are both in the far infrared range.

**Box 3.7**. *Lyman (1874–1954); Paschen (1865–1947); Brackett (1896–1988); Pfund (1879–1949)*

**APPLICATION 3.5.–**

Using the energy diagram of the hydrogen atom, calculate the minimal frequency of the transition line in the Lyman series.

*Given data.* $h = 6.63 \times 10^{-34}$ J · s; 1 eV = $1.60 \times 10^{-19}$ J

**Solution.** According to Bohr frequency condition, $\Delta E = h\nu$. The minimal frequency $\nu$ of a transition line corresponds to the smallest energy gap $\Delta E$. For the Lyman series, it corresponds to 2 → 1 transition. Hence:

$\Delta E$= 10.2 eV

The value of the minimal frequency is then: $\nu = \Delta E/h$

Hence: $\nu = 2.46 \times 10^{15}$ Hz

### 3.3.8. *Advantages and limitations of Bohr's model*

Bohr's model is an important stage in understanding the quantum theory of the atom. This model introduces the principal quantum number and consistently explains the emission and absorption spectra of hydrogen-like systems. It is however a simplified model for describing the electron behavior in hydrogen-like systems.

The following limitations of Bohr's theory are worth retaining:

1) Bohr's theory ignores relativistic effects such as electron mass variation with velocity formulated by **Albert Einstein** (1879–1955) in 1905 while elaborating the theory of special relativity;

2) Bohr's theory cannot explain why some spectral lines are brighter than others. In this model, frequencies of the emitted lines can be calculated without determining their brightness;

3) Bohr's model is not applicable to multielectron atoms;

4) Bohr's theory cannot explain the polarization (and splitting) of spectral lines, as energy does not depend on the angular momentum quantum number (and on electron spin);

5) The major limitation of Bohr's theory is that it treats the electron of the hydrogen atom as a classical particle, while introducing the notion of stationary states, which is alien to classical mechanics. This limitation of Bohr's model has been noted with a touch of irony by the English physicist **William Henry Bragg**

(1862–1942) according to whom "*Bohr's theory uses the laws of classical mechanics on Mondays, Wednesdays and Fridays and quantum mechanics on Tuesdays, Thursdays and Saturdays*" [SIV 86].

**Niels Henrik David Bohr** was a Danish physicist. His renown is especially due to his contribution to the elaboration of quantum mechanics, for which he received many honors. He was awarded the Nobel Prize for physics in 1922 for his contributions to the research on the structure of atoms (quantization of the levels of energy) and on the radiation they emit (spectral lines).

**Box 3.8.** *Bohr (1885–1962)*

### 3.3.9. *Reduced Rydberg constant*

Bohr's model of quantized atom relies on the *approximation of a fixed nucleus of infinitely large mass*. If $M$ designates the nucleus mass, then the ratio $m/M \to 0$ according to the approximation adopted by Bohr. But nucleus mass is actually finite. One of the first corrections to be brought to Bohr's theory is to consider the *reduced mass* of the {nucleus – electron} system, denoted $\mu$ and defined by the relation:

$$\frac{1}{\mu}=\frac{1}{m}+\frac{1}{M}\Rightarrow \mu=\frac{mM}{m+M}=\frac{m}{1+m/M} \quad [3.40]$$

If the mass $m$ of the electron is replaced by the reduced mass $\mu$ given by [3.40] in the expression of the spectral series [3.30], then:

$$\frac{1}{\lambda}=Z^2\frac{\alpha^2\mu c^2}{2hc}\left(\frac{1}{p^2}-\frac{1}{n^2}\right)=Z^2\times\frac{1}{(1+m/M)}\times\frac{\alpha^2 mc^2}{2hc}\left(\frac{1}{p^2}-\frac{1}{n^2}\right) \quad [3.41]$$

Taking into account the expression of $R_H$ given by [3.34], relation [3.41] is written as:

$$\frac{1}{\lambda}=Z^2\times\frac{R_H}{(1+m/M)}\left(\frac{1}{p^2}-\frac{1}{n^2}\right)=Z^2\times\frac{R_\infty}{(1+m/M)}\left(\frac{1}{p^2}-\frac{1}{n^2}\right) \quad [3.42]$$

The Rydberg constant for hydrogen $R_H$ is very often noted $R_\infty$ to reflect the fact that the mass of the nucleus is assumed infinite. This explains the writing of the last term of relation [3.42]. By definition, the *reduced Rydberg constant* denoted $R_\mu$ is given by the relation:

$$R_\mu=\frac{R_\infty}{(1+m/M)} \quad [3.43]$$

The expression of $R_\infty$ is given by [3.34] since $R_\infty = R_H$.

Taking into account the reduced mass $\mu$, the spectral series of hydrogen-like systems is written according to [3.42]:

$$\frac{1}{\lambda} = Z^2 R_\mu \left( \frac{1}{p^2} - \frac{1}{n^2} \right) \qquad [3.44]$$

**APPLICATION 3.6.–**

> In order to put into evidence the difference between Rydberg constants $R_H$ and $R_{He}$, calculate the wavelength of the Lyman-$\alpha$ line of the $He^+$ ion using [3.33] and [3.44]. Then justify the *isotope displacement effect* of spectral lines.
>
> *Given data*. $R_H = 10{,}973{,}731.77\ m^{-1}$; $R_{He} = 10{,}978{,}231.0\ m^{-1}$
>
> **Solution.** The wavelength of the Lyman-$\alpha$ line results from the 2 →1 transition.
>
> According to [3.33], for $R_{He} = R_H$: $\lambda = 30.376$ nm
>
> According to [3.44], for $R_{He}$ # $R_H$: $\lambda = 30.363$ nm [3.45]

Because $R_{He}$ is slightly above $R_H$, the results [3.45] actually show that the spectral lines of $He^+$ ion are slightly shifted toward short wavelengths: it is the *isotope displacement effect* of spectral lines.

## 3.4. Sommerfeld's atomic model

### 3.4.1. *Experimental facts: normal Zeeman effect*

Bohr's model provides the possibility to correctly interpret the lines of the hydrogen atom and of its isoelectronic ions.

According to experimental observations, when an atomic vapor gas is exposed to a strong magnetic field, and an *electric discharge* is generated in the gas, the spectral lines multiply, and this cannot be explained using only the principal quantum number *n*. This phenomenon resulting from the splitting up of spectral lines under the action of a magnetic field was discovered in 1896 by **Pieter Zeeman** and is referred to as *Zeeman effect* in his honor. The main elements of the experimental set-up for the study of the Zeeman effect are indicated in Figure 3.13.

For a strong magnetic field, the *normal Zeeman effect* can be observed (Figure 3.14(a)). For a weak magnetic field $B << 37$ T, the *anomalous* or *complex Zeeman effect* can be observed (Figure 3.14(b)).

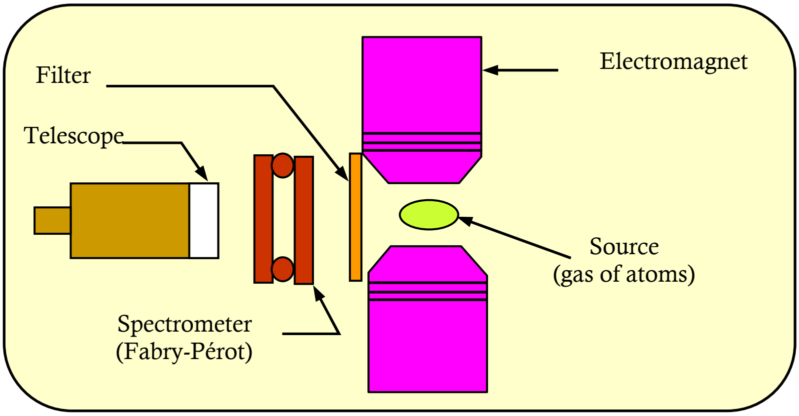

**Figure 3.13.** *Experimental set-up for the study of Zeeman effect*

The Zeeman effect cannot be explained within Bohr's theory, which takes into consideration only the principal quantum number *n*. For sodium vapor, Bohr's model predicts only one *yellow line* denoted D, resulting from the 3p → 3s electron transition.

When a strong magnetic field is applied, the simple Zeeman–Lorentz triplet is observed (Figure 3.14(a)). Using a high-resolving power device (by definition, resolving power is the ability of a device to produce separate images of two very close points), the experiment shows that the yellow sodium D-line is constituted of two very close lines denoted $D_1$ (589.0 nm) and $D_2$ (589.6 nm). Under the effect of a weak magnetic field, these two lines split into four and six components, respectively (Figure 3.14(b)). A theoretical explanation of the normal and anomalous Zeeman effect is provided in sections 3.4.4 and 3.5.5, respectively.

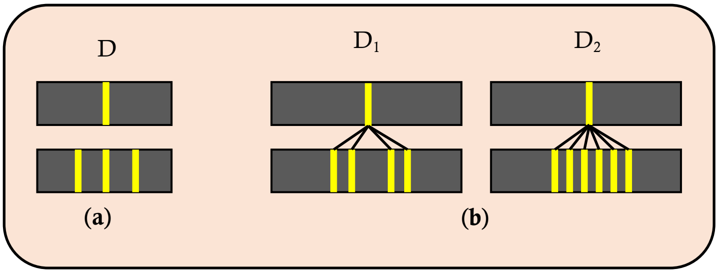

**Figure 3.14.** *Normal Zeeman effect (a) and anomalous Zeeman effect (b) on the yellow sodium D-line*

**Pieter Zeeman** was a Dutch physicist. In spectroscopy, he is especially well-known for his works related to the effect of magnetic fields on the emission spectra of atoms. In 1886, Zeeman discovered that the spectral lines of a light source subjected to a magnetic field split into several components, each of which has a certain polarization. This phenomenon is known as Zeeman effect in his honor. For this discovery, in 1902 he was awarded the Nobel Prize for physics, which he shared with the Dutch physicist **Antony Hendrix Lorentz** for his significant contributions to electromagnetism. Lorentz has also become famous for formulating the electromagnetic force acting on a charged particle moving in an electromagnetic field (known as Lorentz force) as well as for formulating the linear transformations of symmetry of electrodynamics laws. Known as Lorentz transformations, they opened the way to special relativity.

**Box 3.9**. *Zeeman (1865–1943); Lorentz (1853–1928)*

**APPLICATION 3.7.–**

Let us designate by $E_1$ the energy of the ground state (1) of the sodium atom. Let $E_2$ and $E_3$ be the energies corresponding, respectively, to the excited levels (2) and (3), state (3) being the higher energy state. (2) → (1) and (3) → (2) transitions are associated with wavelengths $\lambda_1 = 568.8$ nm and $\lambda_2 = 589.0$ nm, respectively. When the sodium atom, which is in the initial state (1), is lighted by a monochromatic beam of wavelength $\lambda$, it can go directly from level (1) to level (3). Express $\lambda$ as a function of $\lambda_1$ and $\lambda_2$. Calculate the numerical value.

**Solution.** $\lambda = \dfrac{\lambda_1 \times \lambda_2}{\lambda_1 + \lambda_2} = 289.5 \text{ nm}$

### 3.4.2. *Bohr–Sommerfeld model, angular momentum quantum number*

The normal Zeeman effect can be interpreted within Sommerfeld atom model of *elliptical orbits of electrons*. Bohr's model relies, among others, on the approximation of *circular orbits of the electrons*.

In 1916, **Arnold Sommerfeld** proposed that electron orbits are rather elliptical; circular orbits adopted by **Bohr** were particular cases. According to *Bohr–Sommerfeld model* [PAR 01, MOI 16], the nucleus is located in one of the foci (here *F*) of the *elliptical orbit* (Figure 3.15).

In *Sommerfeld's atomic model*, the position of the electron in the orbital plane is defined by the radius *r* and the *azimuthal angle* $\varphi$.

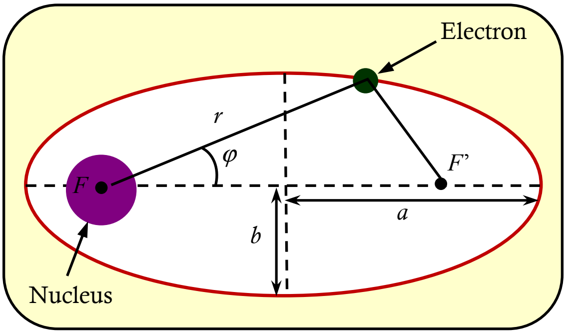

**Figure 3.15.** *Bohr–Sommerfeld atomic model of elliptical orbit*

If $a$ is the *semi-major axis* of the ellipse and $b$ is the *semi-minor axis*, then Sommerfeld established that:

$$\frac{a}{b} = \frac{n}{\ell + 1} \qquad [3.46]$$

In relation [3.46], $n$ is the principal quantum number and $\ell$ designates a new quantum number referred to as *azimuthal quantum number* or *secondary quantum number* or, finally, *angular momentum quantum number*. For the circular orbit, $a = b$. Hence, according to [3.46]:

$$n = \ell + 1 \Rightarrow \ell = n - 1 \qquad [3.47]$$

The above equality [3.47] makes it possible to determine all the values taken by the angular momentum quantum number:

$$n \geq 1;\ \ell = 0, 1, \ldots.\ n - 1 \qquad [3.48]$$

### 3.4.3. *Atomic orbital, electron configuration*

Well before Sommerfeld's theory, the electron configuration of an atom was written according to the *shell model*. While the quantum number $n$ reflects the number of a given shell, there are also *subshells*, denoted in spectroscopy by s, p, d, f, etc.; the number of a subshell is reflected by the angular momentum quantum number $\ell$. Several equivalences between shells and subshells are summarized below.

| | | | | | | |
|---|---|---|---|---|---|---|
| Shells | K | L | M | N | | |
| Numbers | $n$ | 1 | 2 | 3 | 4 | |
| Subshells | | s | p | d | f. | [3.49] |
| Numbers | $\ell$ | 0 | 1 | 2 | 3 | |

Hence, starting with 1916, the electron configurations of atoms could be described according to the *model of atomic orbitals*. As an example, the electron configurations of hydrogen H, helium He and argon Ar according to the shell model can be written using the atomic orbitals denoted *nl*. Using [3.48] leads to:

$$\mathrm{H}\ (Z=1)\text{: } \mathrm{K}^1\,(1\mathrm{s}^1)\text{; He } (Z=2)\text{: } \mathrm{K}^2\,(1\mathrm{s}^2)$$

$$\mathrm{Ar}\ (Z=18)\text{: } \mathrm{K}^2\,\mathrm{L}^8\mathrm{M}^8\,(1\mathrm{s}^2 2\mathrm{s}^2 2\mathrm{p}^6 3\mathrm{s}^2 3\mathrm{p}^6) \qquad [3.50]$$

$$\mathrm{Ni}\ (Z=28)\text{: } \mathrm{K}^2\,\mathrm{L}^8\,\mathrm{M}^{18}\,(1\mathrm{s}^2 2\mathrm{s}^2 2\mathrm{p}^6 3\mathrm{s}^2 3\mathrm{p}^6 3\mathrm{d}^8 4\mathrm{s}^2)$$

The electron configurations between parentheses show that *n*s orbitals are each saturated with two electrons, while *n*p orbitals are each saturated with six electrons. The d orbital is saturated with 10 electrons. Nevertheless, starting with $3\mathrm{p}^6$, the *order of filling* of atomic orbitals changes: *n*s orbital ($n > 3$) is first saturated before *n*d orbital ($n \geq 3$) according to *Klechkowski's rule.* This rule is an empirical method that makes it possible to quite accurately predict the order in which orbitals (s, p, d, f, etc.) fill with electrons in neutral atoms that are in ground state.

Considering the possible values of the sum $(n+\ell)$ defined by [3.48], the principle that underlies Klechkowski's rule is to fill the orbitals in ascending order of atomic number $Z$ and in ascending order [WIK 17] of:

1) values $(n+\ell)$ defining the atomic orbitals;
2) values of $n$ when several orbitals have equal values of $(n+\ell)$.

Therefore, the order for filling of subshells of electrically neutral atoms in ground state, ranked in ascending order of atomic number is:

$$1\mathrm{s} \rightarrow 2\mathrm{s} \rightarrow 2\mathrm{p} \rightarrow 3\mathrm{s} \rightarrow 3\mathrm{p} \rightarrow 4\mathrm{s} \rightarrow 3\mathrm{d} \rightarrow 4\mathrm{p} \rightarrow 5\mathrm{s} \rightarrow 4\mathrm{d} \rightarrow 5\mathrm{p}$$

$$\rightarrow 6\mathrm{s} \rightarrow 4\mathrm{f} \rightarrow 5\mathrm{d} \rightarrow 6\mathrm{p} \rightarrow 7\mathrm{s} \rightarrow 5\mathrm{f} \rightarrow 6\mathrm{d} \rightarrow 7\mathrm{p} \qquad [3.51]$$

Klechkowski's rule is very often applied as a schematic representation called *Klechkowski's diagram*, that can be used to easily find the sequence [3.51] according to the following principle (Figure 3.16):

– all the subshells are diagonally arranged;

– subshells p, d, f,…, etc. are added one after the other on the same line;

– the diagram is read column by column.

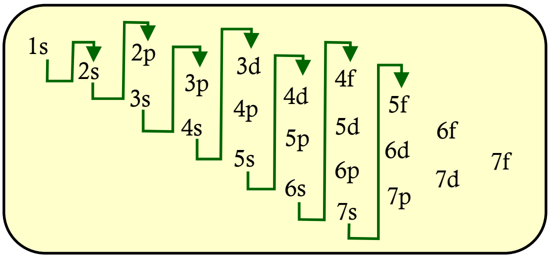

**Figure 3.16.** *Klechkowski's diagram. Atomic orbitals are filled in the direction indicated by the arrow. Each column corresponds to a value of (n + ℓ)*

**Vsevolod Mavrikievich Klechkowski** was a Russian chemist. His renown in chemistry is especially due to his works on radioisotopes and on their use in agriculture. In 1962, he proposed a justification of Madelung's rule, making it possible to quite accurately predict the order in which orbitals (s, p, d, f, etc.) are filled with electrons in neutral atoms at ground state.

**Erwin Madelung** (1881–1972) was a German physicist. He specialized in atomic physics and quantum mechanics. In 1936, Madelung clarified the rules of filling the electron subshells, on the empirical basis of ground states determined by analysis of atomic spectra. This rule stipulates that atomic orbitals are filled in ascending order of the sum of quantum numbers $(n+\ell)$. In 1962, Klechkowski presents the first theoretical justification of Madelung's rule. This explains why the Anglo-Saxon literature mentions Madelung's rule, unlike the French literature, which has retained Klechkowski's rule. A consensus has been reached by some authors, who mention the Madelung-Klechkowski rule. This does justice to both scientists.

**Box 3.10.** *Klechkowski (1900–1972); Madelung (1881–1972)*

A more common alternative representation of Klechkowski's diagram places $n$s orbitals in the first column, $n$p orbitals in the second column, $n$d orbitals in the third column and so on (Figure 3.17).

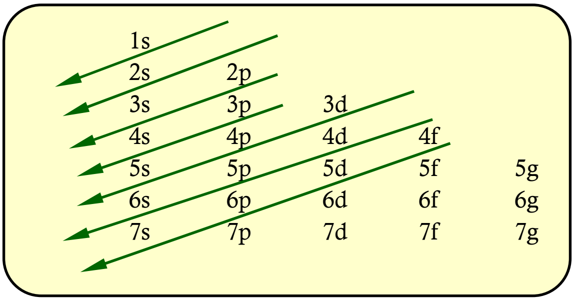

**Figure 3.17.** *More common representation of Klechkowski's diagram, in which each diagonal arrow corresponds to a value of (n +$\ell$)*

It is worth noting that, though quite accurate, Klechkowski's rule does not provide information on the order of filling of atomic orbitals. This rule provides no indication on the number of electrons that each orbital can contain. Moreover, this rule is not applicable to the filling of electron configurations of ions and of the excited states of atomic systems. For example, the electron configuration of $Fe^{4+}$ ion is written as $1s^22s^22p^63s^23p^63d^4$, abbreviated as $[Ar]3d^4$, instead of $1s^22s^22p^63s^23p^6$ $4s^23d^2$ ($[Ar]4s^23d^2$) according to Klechkowski's rule.

The use of orbitals or electron subshells in writing electron configurations justifies the importance of the principal quantum number $n$ and of the angular momentum quantum number $\ell$, which facilitate the understanding of many physical and chemical properties of the atomic systems starting with 1916.

### 3.4.4. *Interpretation of normal Zeeman effect, angular momentum quantum number*

Let us consider an electron orbit in the horizontal plane of center $O$ and radius $r$. In the absence of magnetic field, the orbital angular momentum $\vec{l}$ of the electron is perpendicular to the orbit plane (discontinuous line in Figure 3.18).

For an interpretation of the normal Zeeman effect, let us consider the electron on its path as a *circular current loop* equivalent to a small magnet. Under the action of a magnetic field of direction $Oz$, the small magnet is subjected to a torque that directs the orbital angular momentum of the electron with respect to the direction of the magnetic field (Figure 3.18). The angle between the direction of the magnetic field $\vec{B}$ and that of the angular momentum is designated by $\theta$ [SAK 08].

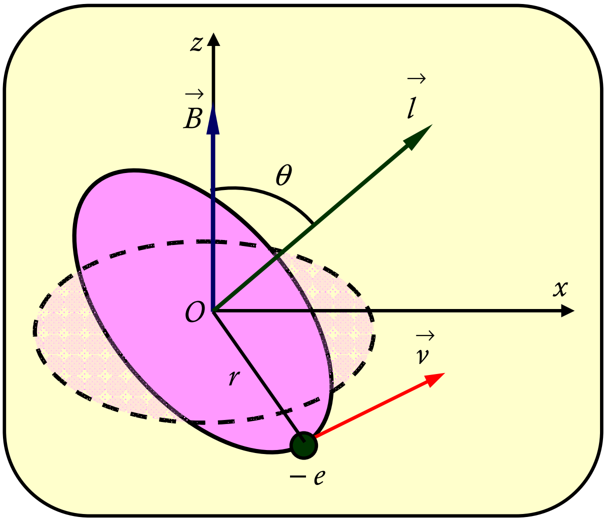

**Figure 3.18.** *Orientation of the angular momentum under the action of a magnetic field*

Projecting the angular momentum vector on the direction of the magnetic field vector, we have:

$$l_z = l\cos\theta \tag{3.52}$$

By analogy with Bohr's principle for angular momentum quantization ($L = n\hbar$), the orbital angular momentum in Sommerfeld's approach is also considered quantized. Hence:

$$l = \ell\hbar \tag{3.53}$$

Inserting [3.53] in [3.52], we obtain:

$$l_z = \ell\hbar\cos\theta \tag{3.54}$$

This equation shows that the projection of the angular momentum on the $Oz$ axis takes the maximal value $+\ell\hbar$ for $\theta = 0$ and the minimal value $-\ell\hbar$ for $\theta = \pi$. This shows that the $l_z$ component of the angular momentum is quantized. Therefore relation [3.54] can be written in a form of type [3.53] considering:

$$l_z = m_\ell\hbar \tag{3.55}$$

The integer in relation [3.55] is a third quantum number of the electron, known as *magnetic quantum number* and it satisfies the double inequality:

$$-\ell \leq m_\ell \leq +\ell \qquad [3.56]$$

Given [3.56], it can be readily noted that the magnetic quantum number $m_\ell$ takes all the integer values ranging from $-\ell$ to $+\ell$, hence a total of $(2\ell+1)$ values.

When the magnetic quantum number $m_\ell$ is considered, the normal Zeeman effect (*this terminology will be clarified in section 3.5.5*) can be consistently explained. For this purpose, let us consider as an example the yellow sodium D-line generated by the 3p → 3s transition. Line splitting under the action of magnetic field is due to the properties of the magnetic quantum number $m_\ell$:

– for the 3s state, $\ell = 0 \Rightarrow m_\ell = 0$: 3s level does not split;

– for the 3p state, $\ell = 1 \Rightarrow m_\ell = -1, 0, +1$: 3p level splits in three sublevels.

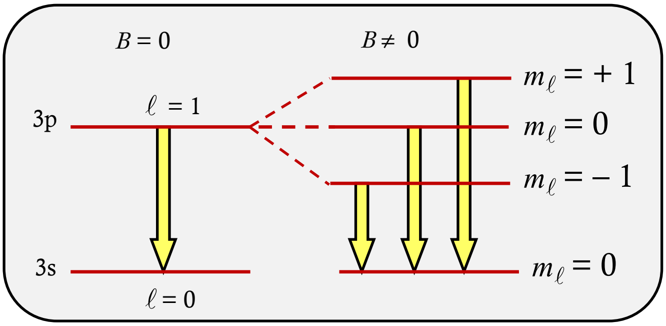

**Figure 3.19.** *The normal Zeeman effect on the yellow sodium D-line*

Thanks to the properties of quantum numbers $\ell$ and $m_\ell$, Sommerfeld's model can be used to establish the first *selection rules* defining the allowed transitions between quantized atomic systems. Hence, a transition between two quantized levels is only allowed if:

$$\begin{cases} \Delta\ell = \pm 1 \\ \Delta m_\ell = 0\,;\pm 1 \end{cases} \qquad [3.57]$$

When taking into account the selection rules [3.57], the splitting of the yellow sodium line into three components (Figure 3.19) according to experimental observations (Figure 3.14(a)) can be consistently explained. The three transition lines obtained by the Zeeman effect (Figure 3.19) constitute what is referred to as the *Zeeman-Lorentz* triplet (see Exercise 3.7.12).

### 3.4.5. *Advantages and limitations of the Bohr–Sommerfeld model*

At least three advantages of the Bohr–Sommerfeld model are worth being retained. It makes it possible to:

1) interpret the normal Zeeman effect based on the properties of the angular momentum quantum number and of the magnetic quantum number;

2) write the electron configuration of atoms using s, p, d, f, etc. values (possible values of the angular momentum quantum number) [3.50];

3) establish the first selection rules that determine the allowed transitions between quantized energy levels of the atomic systems [3.57].

As any model, the Bohr–Sommerfeld approach has its limitations, which are at least four. This model does not offer the possibility of:

1) interpreting the anomalous Zeeman effect (due to spin, see section 3.5);

2) setting the maximum number of electrons per energy level (spin contribution);

3) establishing the general selection rules.

**Arnold Sommerfeld** was a German physicist. One of his major contributions to spectroscopy is related to the generalization of Bohr's model of circular orbits to elliptical orbits (1916). This has offered the possibility to introduce the angular momentum quantum number and to consistently interpret the normal Zeeman effect. Moreover, Sommerfeld explained the fine structure of the lines of hydrogen atom and thus introduced the fine structure constant $\alpha$, which is one of the fundamental physical constants.

**Box 3.11.** *Sommerfeld (1868–1951)*

## 3.5. Electron spin

### 3.5.1. *The Stern–Gerlach experiment*

In 1922, **Otto Stern** and **Walther Gerlach** conducted an experiment in which they vaporized a beam of silver atoms in an oven ($E$) at temperature $T$ = 1,000 K.

This experiment proved that atoms have a new quantum property [SIV 86, GRI 95, SAK 08]. A brief description of the experimental setup used by Stern and Gerlach is shown in Figure 3.20.

A beam of neutral atoms focused by a diaphragm *F* that selects the atoms whose velocity is directed along *Oy* ($v = 500 \text{ m} \cdot \text{s}^{-1}$) is sent through high vacuum. This beam crosses the air-gap of an electromagnet before condensing on a plate *P*. The applied magnetic field is strongly inhomogeneous and perpendicular to the direction *Oy* of the atomic beam, each atom being at ground state.

The experiment shows that the beam splits into two components that hit the screen and form two spots $T^+$ and $T^-$ that are symmetrical with respect to the initial direction *Oy* of the beam and have the same intensity (Figure 3.20).

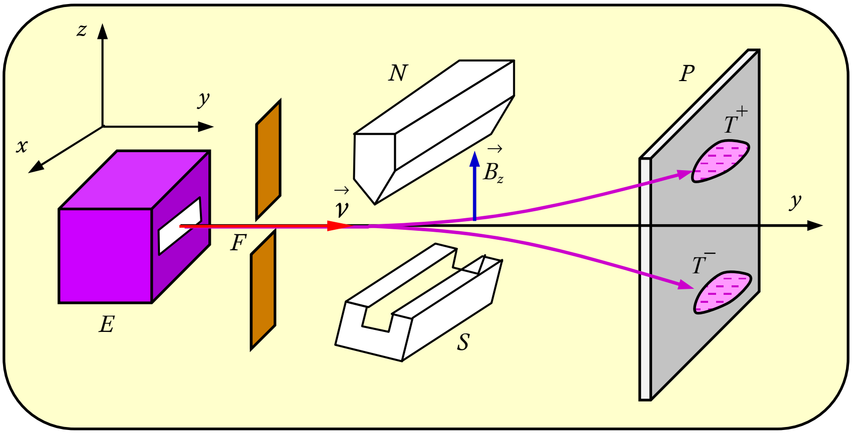

**Figure 3.20.** *Stern–Gerlach experimental setup*

Nevertheless, **Stern** and **Gerlach** advanced no theoretical explanation of the splitting of the beam of silver atoms into two components under the action of component $B_z$ of the magnetic field.

### 3.5.2. *The Uhlenbeck and Goudsmit hypothesis, electron spin*

Using the order of filling of electron subshells [3.50], the electron configuration of the ground state of the silver atom with $Z = 47$ electrons is obtained. Hence:

$$1s^2\, 2s^2\, 2p^6\, 3s^2\, 3p^6\, 4s^2 3d^{10}\, 4p^6\, 5s^1\, 4d^{10} \qquad [3.58]$$

Let us note that configuration [3.58] of the silver atom does not correspond exactly to sequence [3.51] (since the 5s orbital is not saturated). Indeed, Klechkowski’s rule has its limitations, even for certain neutral atoms such as Ag. The electron configuration [3.58] can be formally written as [Kr] $4d^{10}$ $5s^1$. This shows that at ground state the silver atom behaves as a particle with only one electron (the inner shells are all completed). In other terms, the physical and chemical properties of the silver atom at ground state are determined by the outer electron occupying the 5s orbital. For this orbital, the angular momentum quantum number is $\ell = 0$. Consequently, the magnetic quantum number is $m_\ell = 0$. It follows that the splitting of the beam of silver atoms is not due to the properties of quantum numbers $\ell$ and $m_\ell$.

Besides its orbiting the nucleus, the electron spins about its own axis as a *classical spinning top*. Knowing that the orbital motion of the electron around the nucleus is characterized by the angular momentum quantum number $\ell$, by analogy, the spin of the electron is characterized by another intrinsic quantum number.

This is how, in 1925, **Georges Uhlenbeck** and **Samuel Goudsmit** formulated the *hypothesis of the electron spin*, denoted *s*. It is worth noting that the term “*spinning*” designates the rotation on its own axis. The symbol “*s*” denotes the electron spin.

By analogy with the magnetic quantum number $m_\ell$ taking $(2\ell + 1)$ values, the spin *s* is also assumed to have a corresponding *magnetic spin quantum number*, denoted $m_s$ and taking $(2s + 1)$ possible values. In order to determine the spin value, a fundamental hypothesis is adopted, namely that the two components observed in Stern–Gerlach experiments correspond to the two possible values of the magnetic spin quantum number $m_s$. Hence:

$$(2s+1) = 2 \Rightarrow s = 1/2 \qquad [3.59]$$

Result [3.59] shows that $m_s$ takes two possible values: $m_s = +1/2$ (spin up) and $m_s = -1/2$ (spin down). Hence, for $m_s = +1/2$, a number $N^+$ of silver atoms are deviated upwards and form the spot $T^+$. For $m_s = -1/2$, a number $N^-$ of silver atoms are deviated downwards and form the spot $T^-$. On the other hand, Stern–Gerlach experiments showed that the two spots $T^+$ and $T^-$ are symmetrical with respect to the initial direction *Oy* of the silver atom beam and have the same intensity. Hence: $N^+ = N^-$ (see Exercise 3.7.14).

Taking electron spin into account, the electron configuration of an atom can be written according to the quantum cells model that involves the *spin up* and *spin* *down* concepts, symbolized by ascending and descending arrows respectively. A quantum cell can only contain a maximum of two electrons of opposite spins.

Starting with 1925, there were three models for writing the electron configurations of atoms: the *shell model*, the *atomic orbital model* and the *quantum cell model*. Figure 3.21 compares the electron structures of hydrogen H ($Z$ = 1), helium He ($Z$ = 2) and sodium Na ($Z$ = 11) atoms.

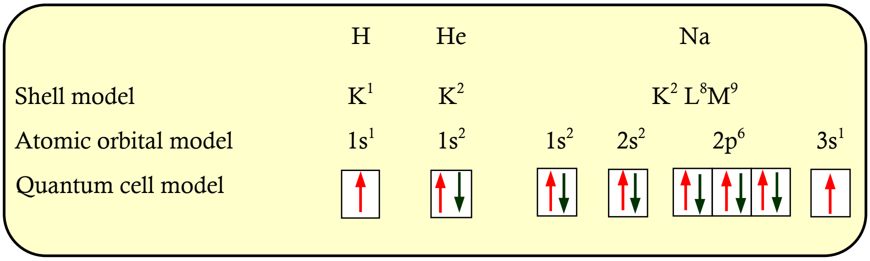

**Figure 3.21.** *Comparison of various models of electron configurations*

This illustration shows that a quantum cell is saturated with two electrons whose principal quantum number $n$, angular momentum quantum number $\ell$ and magnetic angular momentum $m_\ell$ can be equal, while the values of their magnetic spin quantum number $m_s$ must differ: one of the two electrons has a spin up ($m_s = +1/2$) and the other has a spin down ($m_s = -1/2$). Taking into account the electron spin contributes to consistently explain the anomalous Zeeman effect (see Exercises 3.7.16 and 3.7.17).

NOTE.– Lorentz's objection to spin hypothesis: in 1925, physicists had different perceptions on the Uhlenbeck and Goudsmit hypothesis. While Bohr was very enthusiastic, scientists such as **Lorentz**, who presided at the Solvay conference in 1911, raised serious objections related to the electron spin idea advanced by Uhlenbeck and Goudsmit. Relying on Einstein's theory of special relativity, **Lorentz** explained that by modeling the electron as a sphere of radius $r$, and assuming that the *Coulomb energy* $e^2/r$ of the sphere is equal to the rest energy $mc^2$, the resulting radius of the electron is $r = e^2/mc^2$ (*classical radius of the electron*). A value of the angular momentum $L = mvr = |m_s| = \hbar/2$ requires an equatorial velocity of the electron $v_e = \hbar c^2/2e^2 = c/2\alpha$, where $\alpha$ is the fine structure constant. Knowing that $\alpha \approx 1/137$, then $v_e \approx 68\ c > c$: an unacceptable result, since $c$ designates the upper limit speed. However, this objection has at least two weaknesses: the electron is not a point mass; therefore it is not possible to define an electron radius.

Furthermore, there is no classical equivalent of the intrinsic angular momentum of the electron of the *mvr* type: spin is a purely quantum property of particles.

### 3.5.3. *Degree of degeneracy of energy levels*

Taking into account the angular momentum quantum number and the spin quantum number makes it possible to determine the total number of quantum states that can be achieved from a state of given $n$. This number of states is known as *degree of degeneracy* or *multiplicity* of the energy levels often denoted by $g_n$.

As explained above, for a state of given $\ell$, the magnetic quantum number takes a total of $(2\ell + 1)$ values. Knowing that $\ell$ varies between 0 and $(n - 1)$, the total number of quantum states corresponding to a given value of $n$ is equal to $\sum_{\ell=0}^{n-1}(2\ell+1)$. Similarly, for a state of given $n$, the magnetic spin quantum number $m_s$ takes $(2s + 1)$ values. Knowing that $s = 1/2$, the degree of degeneracy of the energy levels of hydrogen-like systems is equal to:

$$g_n = (2s+1)\sum_{\ell=0}^{n-1}(2\ell+1) = 2n^2 \qquad [3.60]$$

Result [3.60] shows that a level of energy of a hydrogen-like system is $2n^2$ times degenerate. This means that for a given $n$, there are $2n^2$ quantum states characterized by the same energy. It is notably the case of the energy levels of the hydrogen atom as described within Bohr's theory. Let us illustrate this degeneracy in the particular cases of the ground state ($n = 1$) and the first excited state ($n = 2$).

– For $n = 1$, $\ell = 0$, we obtain $g_1 = 2$. Therefore, there are two different quantum states due to the projection of electron spin. In the first state, $m_s = +1/2$ and in the second state, $m_s = -1/2$. The global state corresponds to the ground state 1*s*, which is therefore 2 times degenerate.

– For $n = 2$ ($\ell = 0$ or 1), we obtain $g_2 = 8$. There are, therefore, eight quantum states that are determined at the same time by the values of the magnetic quantum number $m_\ell$ and by the values of the magnetic spin quantum number $m_s$. For $\ell = 0$, a 2s state is obtained. For this state, $m_\ell = 0$ and $m_s = \pm 1/2$. The 2s state is then two times degenerate (*which amounts to two states*). For $\ell = 1$, we obtain a 2p excited state for which $m_\ell = -1, 0, +1$; each state characterized by a value of $m_\ell$ is 2 times degenerate due to spin ($m_s = \pm 1/2$). For the 2p state this gives a total: $2 \times 3 = 6$

quantum states. Overall, the first excited level $n = 2$ is then $2 + 6 = 8$ times degenerate.

**Otto Stern** was a German physicist. He was an outstanding experimenter whose work contributed to the development of molecular beam epitaxy (a technique used in the fabrication of quantum wells of semiconductor materials) at the measurement of magnetic moment of atoms. His famous experiment conducted in cooperation with Gerlach in 1922 evidenced the quantization of the electron spin. The hypothesis explaining this phenomenon was formulated much later, in 1925, by Uhlenbeck and Goudsmit. Stern was awarded the Nobel Prize for physics in 1943, as recognition of his important contributions to the development of molecular beam epitaxy.

**Walther Gerlach** was also a German physicist. He is well-known in physics, especially for having experimentally evidenced the spin magnetic moment (Stern–Gerlach experiment).

**Georges Uhlenbeck** and **Samuel Goudsmit** were both American physicists of Dutch origin. They are known especially for having proposed the hypothesis of the electron spin in 1925.

**Box 3.12.** *Stern (1888–1969); Gerlach (1889–1979); Uhlenbeck (1900–1988); Goudsmit (1902–1978)*

### 3.5.4. *Total quantum number, selection rules*

For a hydrogen-like system, the *total angular momentum* $\vec{j}$ is defined by the relation:

$$\vec{j} = \vec{l} + \vec{s} \qquad [3.61]$$

When the quantum numbers $\ell$ and $s$ have determined values, the possible values of the total quantum number $j$ are ($s$ =1/2):

$$j = \ell \pm \frac{1}{2} \qquad [3.62]$$

If $\ell$ is an integer number, $j$ is always a half-integer.

Moreover, the squared angular momenta $\vec{j}$, $\vec{l}$ and $\vec{s}$ have determined values:

$$\vec{j}^{\,2} = \hbar^2 j(j+1)\,;\ \vec{l}^{\,2} = \hbar^2 \ell(\ell+1)\,;\ \vec{s}^{\,2} = \hbar^2 s(s+1)\,. \qquad [3.63]$$

Moreover, quantum numbers $\ell$, $s$ and $j$ have corresponding magnetic quantum numbers $m_\ell$, $m_s$ and $m_j$ that determine the projections of $\vec{l}$, $\vec{s}$ and $\vec{j}$ vectors, respectively, along a preferential direction (for example *Oz*). Hence:

$$l_z = m_\ell \hbar\,;\ s_z = m_s \hbar\,;\ j_z = m_j \hbar \qquad [3.64]$$

When quantum numbers $\ell$, $s$ and $j$ are given, quantum numbers $m_\ell$, $m_s$ and $m_j$ have the following values:

- $m_\ell = -\ell, -(\ell - 1), \ldots\ldots, +(\ell + 1), +\ell$
- $m_s = -s, -(s - 1), \ldots\ldots, +(s + 1), +s$ [3.65]
- $m_j = -j, -(j - 1), \ldots\ldots, +(j + 1), +j$

**Wolfgang Pauli** was an Austrian physicist. In 1925, Pauli proposed a physical principle known as the Pauli exclusion principle, according to which electrons cannot simultaneously occupy the same quantum state. Pauli was awarded the Nobel Prize for physics in 1945 for the formulation of the exclusion principle. The matrices used in quantum mechanics for spin representation (see Exercise 6.8.5) are known as Pauli matrices in his honor.

**Box 3.13.** *Pauli (1900–1958)*

Moreover, during the quantum jumps through which an electron passes from one state to another, only certain *electric dipole transitions* are allowed, namely those following the *selection rules* defined by relations [3.66] (that complete the partial selection rules [3.57]):

$$\begin{cases} \Delta\ell = \pm 1 \quad ; \quad \Delta m_\ell = 0, \pm 1 \\ \Delta j = 0, \pm 1 \quad ; \quad \Delta m_j = 0, \pm 1 \\ \Delta m_s = 0 \end{cases} \qquad [3.66]$$

## 3.6. Electron magnetic moments

### 3.6.1. *Orbital and spin magnetic moments*

In what follows, the angular momentum of the electron is denoted by a small letter $\vec{l}$ to avoid confusion with the angular momentum $\vec{L}$ defined within Bohr's theory. The orbital angular momentum $\vec{l}$ is defined by the same expression [3.12] that can be rewritten as follows:

$$\vec{l} = \vec{r} \wedge \vec{p} \qquad [3.67]$$

The hydrogen-like system is subjected to a uniform magnetic field $\vec{B}$ along ($Oz$). The angle between the directions of the angular momentum and of the magnetic field is $\theta$.

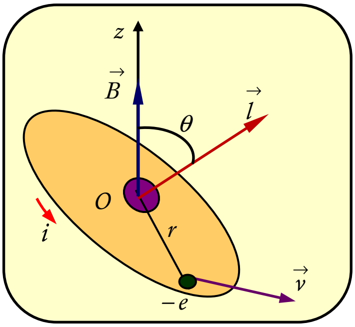

**Figure 3.22.** *Hydrogen-like system subjected to a magnetic field*

The electron motion on the assumed circular orbit generates a current of constant intensity $i$ (Figure 3.22) such that:

$$i = -\frac{e}{T} \qquad [3.68]$$

In relation [3.68], $T$ is the period of the motion of angular frequency $\omega$. As the motion is circular:

$$T = \frac{2\pi}{\omega}\,;\ v = r\omega \qquad [3.69]$$

Using relations [3.69], expression [3.67] can be written as:

$$i = -\frac{ev}{2\pi r} \tag{3.70}$$

Moreover, according to *classical electrodynamics*, a *circular loop* through which a current of intensity $i$ flows has a *magnetic moment* defined by:

$$\overrightarrow{\mathcal{M}_\ell} = i\vec{S} \tag{3.71}$$

In this definition, $\vec{S}$ is the *surface vector* perpendicular to the plane of the loop. Introducing expression [3.69] of intensity $i$ in [3.71], we obtain:

$$\overrightarrow{\mathcal{M}_\ell} = -\frac{ev}{2\pi r}\vec{S} \tag{3.72}$$

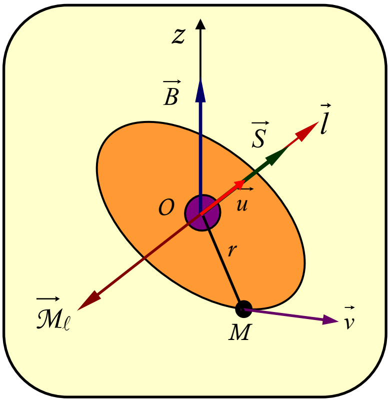

**Figure 3.23.** *Orbital magnetic moment*

Let us designate by $\vec{u}$ the unit vector along the direction that is common to the surface vector and orbital angular momentum vector (Figure 3.23). Knowing that $S = \pi r^2$, the magnetic moment [3.72] is written as:

$$\overrightarrow{\mathcal{M}_\ell} = -\frac{erv}{2}\vec{u} \tag{3.73}$$

Multiplying the numerator and the denominator of the expression on the right of equation [3.73] by the mass $m$ of the electron, we get:

$$\overrightarrow{\mathcal{M}_\ell} = -\frac{e}{2m} mvr\vec{u} \quad [3.74]$$

Figure 3.22 shows that:

$$\vec{l} = \vec{r} \wedge \vec{p} = mvr\vec{u} \quad [3.75]$$

Taking into account [3.75], expression [3.74] of the orbital magnetic moment can be written as:

$$\overrightarrow{\mathcal{M}_\ell} = \gamma\vec{l} \quad [3.76]$$

In relation [3.76], the physical quantity $\gamma$ is referred to as *gyromagnetic ratio of electron* defined by:

$$\gamma = -\frac{e}{2m} \quad [3.77]$$

As the constant $\gamma$ is negative, relation [3.76] indicates that the orbital magnetic moment of the electron is always opposite to the angular momentum; this explains its direction, as shown in Figure 3.23. Moreover, relation [3.77] indicates that an orbital magnetic moment is associated with electron orbiting. It can thus be thought that a *spin magnetic moment*, though it has no classical equivalent, can be associated with electron *spinning*. By analogy to the orbital magnetic moment given by [3.76], the spin magnetic moment is defined by:

$$\overrightarrow{\mathcal{M}_S} = g\gamma\vec{s} \quad [3.78]$$

In relation [3.78], $g$ is a constant known as *Landé factor* of the electron, which is given by:

$$g = 2\left(1 + \frac{\alpha}{2\pi}\right) \quad [3.79]$$

In this relation, $\alpha$ is the fine structure constant defined above [3.24].

### Numerical value:

$\alpha = 1/137.036$

A calculation of the Landé factor according to [3.79] gives: $g$ = 2.00232. This value is generally approximated as 2.00 and leads to:

$$\overrightarrow{\mathcal{M}_S} = 2\gamma \vec{s} \qquad [3.80]$$

Referring to equation [3.79], it is worth noting that the second-order corrections $\alpha^2$ and higher order corrections are considered negligible, though they can be calculated in quantum electrodynamics.

### 3.6.2. *Magnetic potential energy*

In a magnetic field of preferred direction (*Oz*), each of the orbital magnetic moments [3.76] and spin magnetic moments [3.78] of the electron has a determined value:

$$\mathcal{M}_{\ell z} = \gamma l_z \,;\, \mathcal{M}_{sz} = g\gamma s_z \qquad [3.81]$$

In quantum mechanics, projections $l_z$ and $s_z$, of the orbital angular momentum $\vec{l}$ and spin angular momentum $\vec{s}$ respectively, are quantized according to relations [3.64]. Taking into account these results, relations [3.80] become:

$$\mathcal{M}_{\ell z} = \gamma m_\ell \hbar \,;\, \mathcal{M}_{sz} = g\gamma m_s \hbar \qquad [3.82]$$

In [3.82], the magnetic quantum numbers $m_\ell$ and $m_s$ satisfy the relations: $-\ell \leq m_\ell \leq +\ell$ and $m_s = \pm$ ½ respectively. When the hydrogen-like system is immersed in a magnetic field $\vec{B}$, the orbital and spin magnetic moments [3.82] interact with the magnetic field $\vec{B}$. This generates an additional *magnetic potential energy given by*:

$$W = -\overrightarrow{\mathcal{M}} \cdot \vec{B} \qquad [3.83]$$

In this relation, $\overrightarrow{\mathcal{M}}$ is the sum of the orbital and spin magnetic moments of the electron. Using relations [3.76] and [3.78], this can be expressed as follows:

$$W = -\gamma(\vec{l} + g\,\vec{s}) \cdot \vec{B} \qquad [3.84]$$

Using [3.84] makes it possible to correctly interpret the anomalous Zeeman effect (see Exercises 3.7.17 and 3.7.20).

**Alfred Landé** was a German physicist. His renown is especially due to having determined the $g$ factor, known as the Landé factor in his honor. This factor has contributed to a major advance in quantum mechanics, particularly in the interpretation of the anomalous Zeeman effect. Between 1925 and 1926, he studied the quantum theory of radiation, light coherence, spontaneous emission and stimulated emission, the latter two processes being involved in the theory of laser emission. In 1925, together with Back (see Box 3.15), Landé published the work entitled "*Zeeman effect and the multiplet structure of spectral lines*" (Springer, Berlin).

**Box 3.14.** *Landé (1888–1976)*

### 3.6.3. *Spin–orbit interaction, spectroscopic notation of states*

In the case of hydrogen-like systems, the main interaction is the *Coulomb interaction* between electron and nucleus. However, because of the electron orbital motion, an additional interaction due to electron spin and the nuclear charge is observed. This is referred to as *spin–orbit interaction* or *spin–orbit coupling,* denoted by *LS* coupling. Let us further illustrate this notion in the particular case of the hydrogen atom.

For this purpose, let us consider a reference frame attached to the electron moving around the proton. With respect to this reference frame, in which the electron is at rest, the proton is moving and generates a magnetic field $\vec{B}_0$ acting on at the location of the electron. This field acts on the spin magnetic moment $\vec{\mathcal{M}}_S$ of the electron.

As the absolute values of proton and electron charges are equal, the magnetic field generated by the proton is similar to the one that the electron orbiting the proton would create in a fixed reference frame. This is why the spin–orbit interaction is formally assimilated to an interaction between the orbital magnetic moment and the spin magnetic moment of the electron. Knowing that the direction of the magnetic moment $\vec{\mathcal{M}}_S$ can be parallel or antiparallel to the direction of the magnetic field $\vec{B}_0$, in the first case, the potential energy of interaction of the {electron–nucleus} system increases, and in the second case, it decreases. This is why each energy level of the atom splits into two sublevels under the effect of the spin–orbit interaction. This splitting does not occur when the atom is in $n^2\mathrm{s}_{1/2}$ states, for which there is no spin–orbit interaction, as the orbital magnetic moment is zero. Moreover, the notation used for a quantum state is:

$$n^{2s+1}L_j \qquad [3.85]$$

In this notation, the number (2*s* +1) designates what is known as *multiplicity of the energy level* under consideration, and *L* denotes the quantum state being considered, which is determined by the value of the orbital quantum number $\ell$.

For example, for $\ell = 0$, L ≡ s; for $\ell = 1$, L ≡ p; for $\ell = 2$, L ≡ d; etc. When spin–orbit interaction is taken into account, the physical significance of $(2s+1)$ level multiplicity in notation [3.85] can be clarified. For a hydrogen-like system, $s = 1/2$ and $(2s+1) = 2$. Consequently, level multiplicity indicates the various possible directions of spin $\vec{s}$ (or of the spin magnetic moment $\vec{\mathcal{M}}_s = g\gamma\vec{s}$) with respect to the direction of the orbital angular momentum $\vec{l}$ (or of the orbital magnetic moment $\vec{\mathcal{M}}_\ell = \gamma\vec{l}$). Hence, given the spin–orbit interaction, all the energy levels of the hydrogen-like systems whose orbital angular momentum is non-zero split into two sublevels and form what are referred to as *doublets* of $n^2L_j$ type, which reads "*n, doublet* $L_j$".

Let us illustrate this reading mode by several examples of specific cases of ground state $n = 1$ and excited levels $n = 2$ and $n = 3$.

– for $n = 1$, $\ell = 0$ ($L \equiv$ s); this corresponds to s state (it is worth noting that the same letter is used to designate the s subshell of the s orbital and the spin $s$ of the electron) or $s = 1/2$. Therefore the multiplicity is $(2s+1) = 2$ and the total quantum number $j = 1/2$ ($j = \ell + 1/2 = 1/2$; the value $j = \ell - 1/2 = -1/2$ is not allowed, because $j > 0$). The resulting state is denoted $1^2\mathrm{s}_{1/2}$ (one, doublet s one-half);

– for $n = 2$, $\ell = 0$ or 1 (L ≡ s or p).

- for $\ell = 0$, $j = 1/2$: the spin magnetic moment is therefore parallel to the orbital magnetic moment. We obtain the state denoted by $2\ {}^2\mathrm{s}_{1/2}$ (two, doublet $\mathrm{p}_{1/2}$);

- for $\ell = 1$, $j = \ell - 1/2 = 1/2$: the spin magnetic moment is antiparallel to the orbital magnetic moment. We obtain the state denoted by $2\ {}^2\mathrm{p}_{1/2}$ (two, doublet $\mathrm{p}_{1/2}$);

- for $\ell = 1$, $j = \ell + 1/2 = 3/2$: the spin magnetic moment is parallel to the orbital magnetic moment. We obtain the state denoted by $2\ {}^2\mathrm{p}_{3/2}$ (two, doublet $\mathrm{p}_{3/2}$);

– for $n = 3$, a similar reasoning leads to obtaining five quantum states: $3\ {}^2\mathrm{s}_{1/2}$, $3\ {}^2\mathrm{p}_{1/2}$, $3\ {}^2\mathrm{p}_{3/2}$, $3\ {}^2\mathrm{d}_{3/2}$ and $3\ {}^2\mathrm{d}_{5/2}$.

The same doublets are noted for all the states defined by a value $\ell \geq 1$. The quantum states $n\ {}^2\mathrm{s}_{1/2}$, though read "*n*, *doublets*$_{1/2}$", are an exception to the rule, as there is no spin–orbit interaction for these states. They are therefore formally referred to as "*doublets*".

### 3.6.4. *Fine structure of the levels of energy of the hydrogen atom*

As explained above, due to the spin–orbit interaction, the levels of energy characterized by a non-zero angular momentum quantum number split into several components. This *LS* coupling effect on the energy levels of the atoms determines what is referred to as the *fine structure of spectral terms* or *fine structure of the energy levels* [SIV 86, COH 77, GRI 95, SAK 08]. The splitting of a spectral line into several components is known as the *fine structure of the spectral lines*, determined by the allowed electronic transitions between the sublevels formed as result of the spin–orbit interaction. As an example, let us examine the fine structure of the lines for the specific cases of the Lyman alpha ($L_\alpha$) and Balmer alpha ($H_\alpha$) line of the hydrogen atom.

– The wavelength of the $L_\alpha$ line is $\lambda = 121.6$ nm. It corresponds to the transition from the first excited level $n = 2$ to the ground state $n = 1$. Let us recall for these two levels the corresponding spectral terms. For $n = 1$ level, we obtain only one term: $1s_{1/2}$. For $n = 2$, we obtain the three terms: $2s_{1/2}$, $2p_{1/2}$ and $2p_{3/2}$. The structure of the Lyman alpha line of the hydrogen atom is illustrated in Figure 3.24.

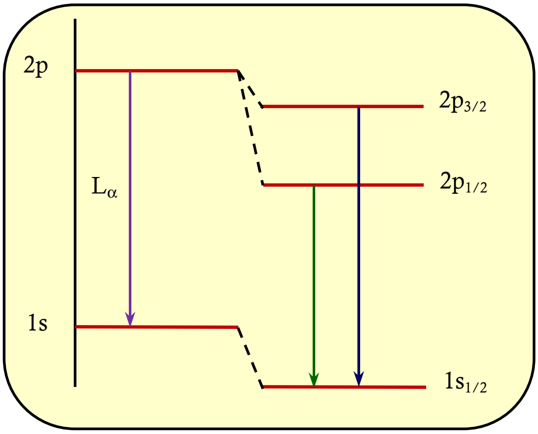

**Figure 3.24.** *Fine structure of the Lα line of the hydrogen atom*

In Figure 3.24, the 2p → 1 s transition has been added to the Lyman series as an illustration. This transition has not been observed. Only the two lines resulting from $2p_{3/2} \rightarrow 1s_{1/2}$ and $2p_{1/2} \rightarrow 1s_{1/2}$ transitions actually exist, and they satisfy the selection rules [3.66] reminded below:

$$\begin{cases} \Delta\ell = \pm 1 \quad ; \quad \Delta m_\ell = 0, \pm 1 \\ \Delta j = 0, \pm 1 \quad ; \quad \Delta m_j = 0, \pm 1 \\ \Delta m_s = 0 \end{cases}$$

Given the [3.66] rules, 2s → 1s transition is not allowed, as it corresponds to $\Delta\ell = 0$. For this reason, the 2s level is not represented in Figure 3.24. Let us recall that the selection rules [3.66] are rigorously verified only in the absence of any field of external forces that may induce *forbidden transitions*. Hence, as a result of spin–orbit coupling, the fine structure of level $n = 2$ gives a doublet formed of two very close lines separated by a distance $\Delta\lambda = 5.3\times10^{-4}$ nm (see Exercise 3.7.18). Each of the other lines $L_\alpha$, $L_\gamma$, $L_\delta$, etc. in the Lyman series has a doublet fine structure.

– The wavelength of $H_\alpha$ line is $\lambda = 656.3$ nm and corresponds to the transition from the second excited level $n = 3$ to the first excited level $n = 2$. For these two levels, we obtain the spectral terms: $2\,^2s_{1/2}$, $2\,^2p_{1/2}$, $2\,^2p_{3/2}$ and $3\,^2s_{1/2}$, $3\,^2p_{1/2}$, $3\,^2p_{3/2}$, $3\,^2d_{3/2}$ and $3\,^2d_{5/2}$, respectively. $H_\alpha$ line splits into seven components (Figure 3.25) resulting from the transitions allowed by the selection rules [3.66].

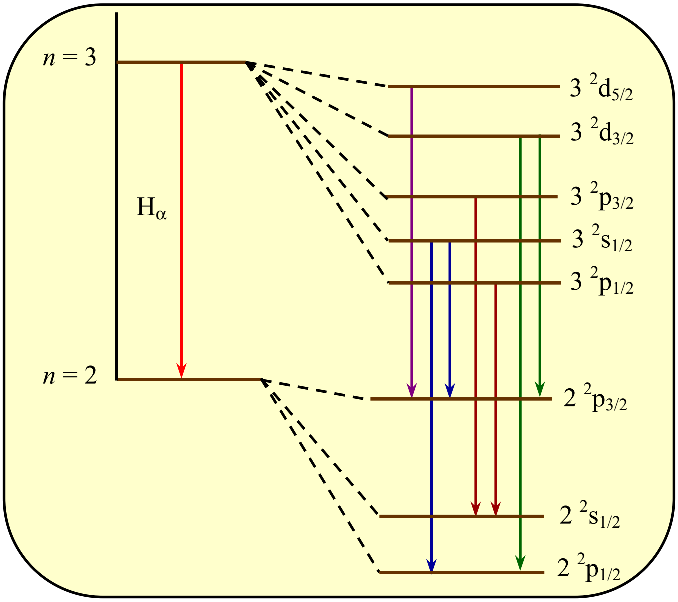

**Figure 3.25.** *Fine structure of the $H_\alpha$ line of the hydrogen atom*

It is worth noting there are no spectral lines due to $3s_{1/2}$, → $2s_{1/2}$ and $3p_{1/2}$, → $2p_{1/2}$ transitions, which are forbidden, as they correspond to $\Delta\ell = 0$. The same is applicable to the lines corresponding to $3d_{5/2} \rightarrow 2s_{1/2}$, $2p_{1/2}$ transitions for which $\Delta j = 2$ are forbidden by the selection rule $\Delta j = 0, \pm 1$. Similar to $H_\alpha$ line, $H_\beta$, $H_\gamma$, $H_\delta$, etc., lines in the Balmer series have each a fine structure. It can be noted that the levels of energy of hydrogen-like systems characterized by a non-zero value of the angular momentum quantum number, naturally split due to spin–orbit interaction and not because of the Zeeman effect. It follows that when a hydrogen-like system (in a state with $\ell \neq 0$), is subjected to a magnetic field, the splitting due to spin–orbit interaction and the Zeeman effect are competing. This competition is worth being studied in further detail.

When an atom is subjected to a weak magnetic field, the spin–orbit interaction is such that the behavior of orbital angular momentum $\vec{l}$ and spin angular momentum $\vec{s}$ cannot be studied separately. Only the total angular momentum $\vec{j} = \vec{l} + \vec{s}$ is conserved and becomes a constant of the motion. For a quite high intensity of the magnetic field, the width of splitting of the energy levels due to the magnetic field-orbital magnetic moment becomes predominant compared to the splitting of energy levels due to spin-orbit interaction. In this case, the spin–orbit interaction can be ignored and the *complex Zeeman spectrum* becomes the *simple Zeeman–Lorentz triplet*: this is the *Paschen–Back effect* (experimentally observed in 1912 by **Paschen** and **Back**). Let us note that the set of sublevels resulting from the spin–orbit interaction are referred to as *multiplets*.

**Ernst Back** was a German physicist. He is known for his works on the influence of magnetic fields on the line spectrum of atoms. In 1912, he observed with Paschen (see Box 3.7), that when an atom is subjected to a strong magnetic field, the complex Zeeman spectrum is reduced to the simple Zeeman–Lorentz triplet, the phenomenon referred to as the Paschen–Back effect. Moreover, in 1925, Back, together with Landé, published the book entitled "*Zeeman effect and the multiplet structure of spectral lines*". In 1976, a lunar crater was named Back in his honor.

**Box 3.15.** *Back (1881–1959)*

## 3.7. Exercises

Numerical data for the exercises:

– *Planck constant*: $h = 6.626 \times 10^{-34}$ J · s

– *speed of light in a vacuum*: $c = 2.998 \times 10^{8}$ m · s$^{-1}$

– *elementary charge*: $e = 1.602 \times 10^{-19}$ C

– *rest mass* of the electron: $m = 9.109 \times 10^{-31}$ kg

– *electric constant*: $k = 1/(4\pi\varepsilon_0) = 9.0 \times 10^{9}$ SI

– 1 eV = $1.602 \times 10^{-19}$ J

### 3.7.1. *Exercise 1 – Spectrum of hydrogen-like ions*

(1) The focus is on the spectral series of the hydrogen atom.

(1.1) Express the spectroscopic wave number for the $n \rightarrow p$ transition based on the Ritz combination principle and Balmer's expression of spectral terms. Then prove that the wavelengths $\lambda_{\mathrm{np}}$ of the radiations emitted by the hydrogen atom during the $n \rightarrow p$ transition can be calculated using the formula:

$$\frac{1}{\lambda_{np}} = R_1 \times \left( \frac{1}{p^2} - \frac{1}{n^2} \right) \tag{1}$$

In this relation, $R_1$ is a constant to be defined.

(1.2) Express $R_1$ as a function of the ionization energy $E_{\mathrm{I}}$ of the hydrogen atom, Planck's constant $h$ and the speed of light in a vacuum $c$. Calculate $R_1$ in $\mathrm{m}^{-1}$. Explain why this unit is appropriate.

(2) In the spectrum of the hydrogen-like $\mathrm{He}^+$ ion let us consider four lines numbered (1), (2), (3) and (4) and whose spectroscopic wave numbers in the Lyman series are respectively equal to:

$$3.292 \times 10^7\ \mathrm{m}^{-1};\ 3.901 \times 10^7\ \mathrm{m}^{-1};\ 4.115 \times 10^7\ \mathrm{m}^{-1};\ 4.213 \times 10^7\ \mathrm{m}^{-1}$$

(2.1) Verify numerically that these values are compatible with the relation:

$$\frac{1}{\lambda_{np}} = R_2 \times \left( \frac{1}{p^2} - \frac{1}{n^2} \right) \tag{2}$$

In this relation, $n = 2, 3, 4$ and $5$ for the lines (1), (2), (3) and (4) respectively, and $R_2$ is a constant to be calculated in $\mathrm{m}^{-1}$.

(2.2) Express $R_2$ as a function of $R_1$ based on an approximation to be specified. Then deduce the atomic number of the helium ion $\mathrm{He}^+$.

(2.3) Find relation (2) using Bohr's model applied to hydrogen-like systems.

*Given data*. $E_{\mathrm{I}} = 13.605680$ eV; *Rydberg expression*: $\mathrm{Ryd} = \alpha^2 mc^2/2$.

### 3.7.2. *Exercise 2 – Using the energy diagram of the lithium atom*

Figure 3.26 shows the simplified diagram of the energy levels of the Li atom.

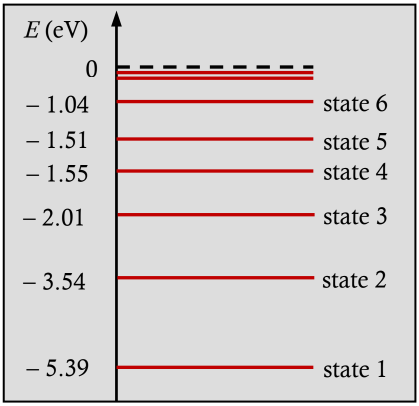

**Figure 3.26.** *Simplified diagram of the energy levels of the lithium atom*

(1) Calculate the wavelength $\lambda$ of the radiation emitted when the lithium atom passes from excited state 3 to ground state 1.

(2) A sample of lithium atoms that are all in ground state is lighted. The polychromatic light used is constituted of photons of wavelengths $\lambda_1 = 528.0$ nm, $\lambda_2 = 323.0$ nm and $\lambda_3 = 205.0$ nm.

(2.1) Which of these three photons can be absorbed by a lithium atom in the sample? What is the excited state of the lithium atom after absorption?

(2.2) What happens in the case of the photon of wavelength $\lambda_3 = 205.0$ nm? Deduce the kinetic energy of the resulting electron.

(3) A lithium atom in ground state is hit by an electron of mass $m$ and kinetic energy $E_c = 5.00$ eV. It consequently passes to state 4. Find the speed of the electron after its collision with the lithium atom (*the motion of the lithium atom is assumed beyond the influence of this event*).

The numerical data provided at Exercise 3.7.1 shall be used.

*Given data*. $m = 9.19 \times 10^{-31}$ kg.

### 3.7.3. *Exercise 3 – Spectra of the hydrogen atom, application to astrophysics*

The *Orion Nebula* (Figure 3.27) comprises four hot stars immersed in a wide "cloud" of interstellar gas largely composed of hydrogen atoms.

**Figure 3.27.** *Orion Nebula*

The wavelength of the light radiated by the stars is below 91.2 nm, in the range of ultraviolet waves.

(1) The light emitted by certain nebulae rich in hot but low-pressure gaseous hydrogen is due to the electron transition between energy levels $n = 2$ and $n = 3$.

(1.1) Calculate the wavelength resulting from the $3 \rightarrow 2$ electron transition.

(1.2) Explain the color of such a nebula, as perceived by a terrestrial observer.

(2) A terrestrial observer photographs the spectrum of light received from the star. They use the same film under the same experimental conditions to capture the emission spectrum of argon, a chemical element that is used as reference. The spectral lines of the star are numbered from 1 to 27 (Figure 3.28). The reference argon wavelengths are given in nm (433–668 nm).

(2.1) Besides a continuous and colored light spectrum, the film capturing the light coming from the observed star also shows dark lines. What phenomenon explains the presence of these dark lines?

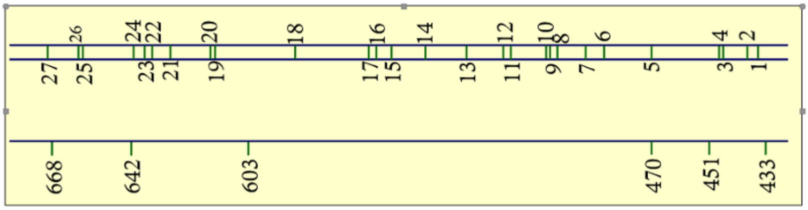

**Figure 3.28.** *Film showing the line spectrum of the studied star*

(2.2) When a grating spectrometer is used, the wavelength differences between the lines are proportional to the distances between them. Use Figure 3.28 to accurately determine the scale of correspondence $e$ between the wavelength difference (in nm) and the distance $d$ (in cm) between them.

(2.3) The argon line whose wavelength is 603 nm serves as a reference for the measurements to be conducted. Using the previously determined scale, identify, based on its number in the spectrum of the star, the absorption line $H_\beta$ of the hydrogen atom of wavelength $\lambda_\beta = 486$ nm.

(2.4) The line number 5 belongs to the spectrum of one of the elements presented in the data. Identify this element simply by reading Figure 3.28.

*Given data.*

– Energy of the ground state of the hydrogen atom: $E_1 = -13.60568$ eV.

– Colors of several radiations:

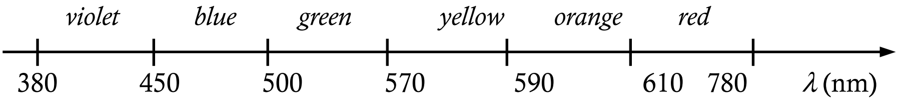

*To identify the lines, the following wavelengths expressed in nanometer (nm) can be used:*

– *Balmer series of H atom*: $H_\beta$: 486; $H_\gamma$: 434; $H_\delta$: 410; $H_\varepsilon$: 397;

– *He atom*: 389; 405; 447; 471; 493; 502; 505; 588; 668; 707; 728.

### 3.7.4. *Exercise 4 – Atomic resonance*

Let us consider a sodium lamp emitting practically monochromatic orangy-yellow light. This lamp is used to intensely light a glass bowl filled with sodium vapor. An attenuation of the emerging beam is observed (Figure 3.29).

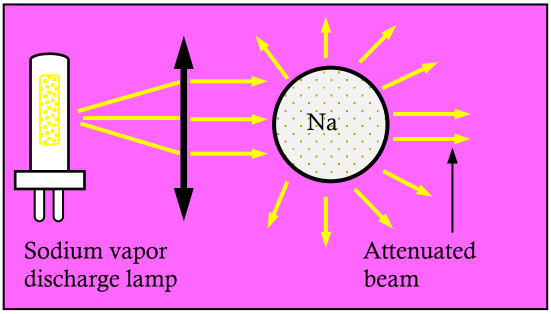

**Figure 3.29.** *Atomic resonance for sodium*

Consequently, the lighted sodium vapor emits photons in all directions (Figure 3.29). This phenomenon is known as *atomic resonance*: the frequency of the exciting wave (*exciter*) is equal to that of the irradiated vapor (*resonator*).

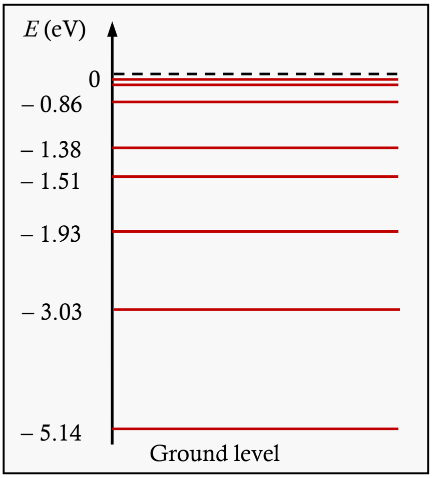

**Figure 3.30.** *Simplified diagram of sodium energy levels*

(1) The analysis of the emission spectrum of a sodium lamp reveals the presence of lines of well-defined wavelengths. Figure 3.30 shows a simplified diagram of sodium energy levels (not a scale representation). This spectrum is due to the electron transitions from the outer shell of the sodium atom at its ground state.

(1.1) Provide an interpretation of the experimental observations (attenuation of the incident beam and emission of photons by the sodium vapor).

(1.2) Use a postulate to justify the discontinuity of the sodium atom spectrum, which is schematically represented above (Figure 3.30).

(1.3) Write the electron configuration of sodium ($Z = 11$). Which one of the electrons generates the observed sodium emission spectrum?

(1.4) Is it possible to find the ground state energy of the sodium atom using Bohr's theory? Provide a theoretical justification for the answer.

*Given data*. 1 Ryd ≈ 13.60 eV.

(2) The sodium atom is considered in its ground state.

(2.1) Specify the levels of energy that are involved in the emission of the yellow sodium D-line. How does this atom behave when it absorbs a photon whose wavelength is $\lambda = 589.0$ nm?

(2.2) What happens if the energy of the photon is 3.00 eV? Can the sodium atom be then excited? Justify the answer.

(3) The sodium atom, considered in its ground state, is hit by an electron whose kinetic energy is 3.00 eV. The sodium atom is practically fixed during the interaction, and it thus passes to an excited state $n$ that has to be determined.

(3.1) After the interaction, the residual kinetic energy of the electron is 0.89 eV. Determine the excited level of the sodium atom after collision.

(3.2) The sodium atom, still in its ground state, is lighted with radiation whose wave number is $4.82946 \times 10^6$ m$^{-1}$. What phenomenon occurs? Write the balance equation for this phenomenon. Find the speed of the ejected electron.

*Consider the mass of the electron*: $m = 9.109 \times 10^{-31}$ kg.

### 3.7.5. *Exercise 5 – X-ray spectrum*

X-rays are generated in *X-ray tubes*, also known as *Coolidge tubes* or *hot cathode tubes* (Figure 3.31). The X-ray production principle is described below.

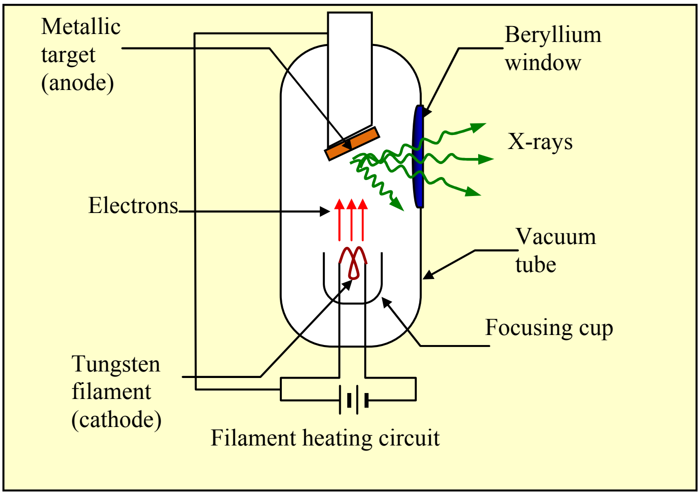

**Figure 3.31.** *X-ray production in a Coolidge tube*

Electrons emitted by a cathode (*a filament most commonly made from tungsten, heated by an electric current flow*) are accelerated by a high potential difference (from 10 to 150 kV) toward a target constituted from a metallic (also tungsten) anode. X-rays are emitted by the target by two mechanisms:

– deceleration of the electrons by the target atoms produces a *continuous radiation* (*braking radiation* or *Bremsstrahlung*), which is partly in the X-ray range;

– accelerated electrons have enough energy to excite certain atoms of the target, perturbing their inner electron shells. These excited atoms emit X-rays when they return to their ground state.

(1) A *monokinetic beam* of electrons emitted by the heated filament is accelerated by a 40,000 V voltage. Electrons emitted with zero initial velocity hit a copper plate target.

(1.1) Determine in keV the kinetic energy of emitted electrons.

(1.2) Can the emitted electrons be dealt with as relativistic particles? Provide a theoretical justification for the answer.

*Given data*. $m_0c^2 = 0.511$ MeV.

(2) Figure 3.32 shows a relative arrangement of several levels of energy of the electrons in *K*, *L* and *M* shells of copper atoms. The diagram is not a scale representation.

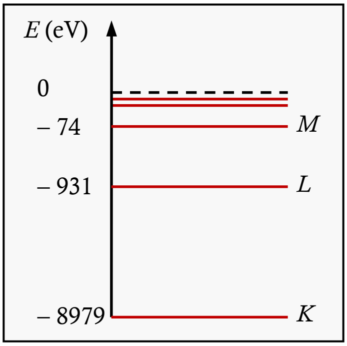

**Figure 3.32.** *Relative arrangement of K, L and M shells of copper atoms*

(2.1) Is the kinetic energy acquired by one of the electrons in the above mentioned monokinetic beam sufficient to extract a K electron from the copper atom?

(2.2) Assuming that the entire kinetic energy of an incident electron in the monokinetic beam is transmitted to the electrons in the $K$ shell, what is the kinetic energy of a K-electron ejected from the copper atom? Express the result in keV.

(3) Once the K-electron is ejected, another electron coming from the $L$ shell or from the $M$ shell can pass in the $K$ shell.

(3.1) Draw a schematic representation of the two expected recombination processes (*electron–hole recombination*). Represent in this figure the two emitted X photons by undulating arrows.

(3.2) Deduce the wavelengths of the two emitted radiations, characteristic to the spectrum emitted by the X-ray tube ($K_\alpha$ and $K_\beta$ lines of the spectrum).

**William David Coolidge** was an American physicist. He is known for his work leading to the use of tungsten as a filament in light bulbs. In 1913, he invented the X-ray tube, known as the Coolidge tube in his honor. This tube, which also used tungsten as a filament, was a major progress in medical physics, especially in the beginning of radiology.

**Box 3.16.** *Coolidge (1873–1975)*

### 3.7.6. *Exercise 6 – Lifetime of the hydrogen atom according to the planetary model*

The objective is to explain the instability of the planetary model of the atom by calculating the *lifetime of the hydrogen atom*. The electron in the hydrogen atom is assumed in motion around the proton, as described by Rutherford's planetary model.

(1) Prove that the electron is subjected to a centripetal acceleration.

(2) According to classical electrodynamics, any charged particle in accelerated motion emits electromagnetic waves. The *loss of energy per unit time* (radiated power) is expressed by the relation:

$$-\frac{dE}{dt}=\frac{2}{3}\times\frac{e^2}{4\pi\varepsilon_0 c^3}a^2$$

In this expression, $a$ designates the acceleration.

Moreover, the total energy of the {nucleus–electron} system is given by the relation:

$$E(r) = -k\frac{e^2}{2r}$$

(2.1) Is the Rutherford atomic model stable according to the theory of classical electrodynamics? Justify the answer.

(2.2) Prove that the radius $r$ of the electron orbit verifies the equation:

$$\frac{d}{dt}\left(\frac{1}{r}\right) = \frac{A}{r^4}$$

where $A$ is a constant to be clarified.

(2.3) Considering the fall of the electron from its initial position $r = a_0$, express the duration $\Delta t$ of the fall of the electron on the proton. Deduce from it the lifetime of the hydrogen atom.

(2.4) Using a postulate, explain why the hydrogen atom is stable, contrary to the predictions of classical electrodynamics.

*Given data* (Bohr radius). $a_0 = 5.29$ nm.

### 3.7.7. *Exercise 7 – Correspondence principle, quantization of the angular momentum*

The objective is to find Bohr's principle of quantization of the angular momentum of the electron from the *correspondence principle*.

Let $L$ be the module of the angular momentum of the electron with respect to the center $O$ of the electron orbit assumed to be circular and of radius $r$.

(1) Let us consider the $n \to p$ electron transition, with $n > p$.

(1.1) Using the Ritz combination principle, express as a function of wavelength, the spectroscopic wave number corresponding to the $n \to p$ electron transition.

(1.2) Find the expression of the spectroscopic term $T_n$ according to Balmer. Deduce from it the expression of the spectroscopic wave number.

(1.3) Let $E_n$ be the quantized energy of the hydrogen-like systems. Using the Bohr frequency condition, prove that:

$$E_n \times n = C \tag{1}$$

where $C$ is a constant.

(2) Let us now study the motion of the electron of hydrogen-like systems, according to the approximation of circular orbits. Let $Z$ be the atomic number.

(2.1) Using the principle of inertia, express the angular frequency $\omega_{\text{rot}}$ of the rotational motion of the electron as a function of $L$, $e$, $r$ and $Z$.

(2.2) Express the total mechanical energy $E$ of a hydrogen-like system. Deduce from it the expression of $\omega_{\text{rot}}$ as a function of $E$ and $L$.

(2.3) Assuming that for high values of $n$ and small variations $\Delta n$ relation 1 is satisfied, prove that the angular frequency of the emitted line can be written as:

$$\omega_e = -\frac{2E_n}{\hbar n}\Delta n \qquad \text{(relation 2)}$$

(2.4) Explain why it is possible to approximate $E_n \approx E$ for high values of the quantum number $n$.

(2.5) According to the correspondence principle, the ground state angular frequency of the emitted line for which $\Delta n = 1$ coincides with the angular frequency of the electron orbiting the nucleus. Use the correspondence principle to deduce the rule for the quantization of the angular momentum $L$ of the electron according to Bohr's theory.

### 3.7.8. *Exercise 8 – Franck–Hertz experiment: experimental confirmation of Bohr's atomic model*

In 1914, **James Franck** and **Gustave Hertz** (see Box 3.17) performed an experiment on the measurement of the ionization potential of atoms. This experiment validated Bohr's model of quantized atom [SIV 86, RAP 06, SAK 08, SAK 12]. In their experiment, Franck and Hertz sent a beam of adequately accelerated electrons through the gas to be studied (mercury vapor in this case). After collision, the electrons excite the atoms whose excited states have each a well determined energy.

In their study, Franck and Hertz varied the density of the mercury vapor by placing several drops of mercury in a tube, which was then put in an oven whose adjustable temperature was maintained constant throughout the experiment. Franck and Hertz's experimental setup is schematically presented in Figure 3.33.

To make sure that the current that heats the cathode has a constant value, an ammeter A is used. A potential difference $U_{\text{AB}} = U$ is applied between the hot cathode $K$ and the grid $S$ in order to accelerate the electrons. If their kinetic energies are sufficient, the electrons pass through the grid $S$ after having penetrated the *deceleration potential barrier* $V_1$ (whose value is around 0.5 V). They reach the *collector* $P$, which leads to the detection of an electric current through the galvanometer G inserted in the circuit.

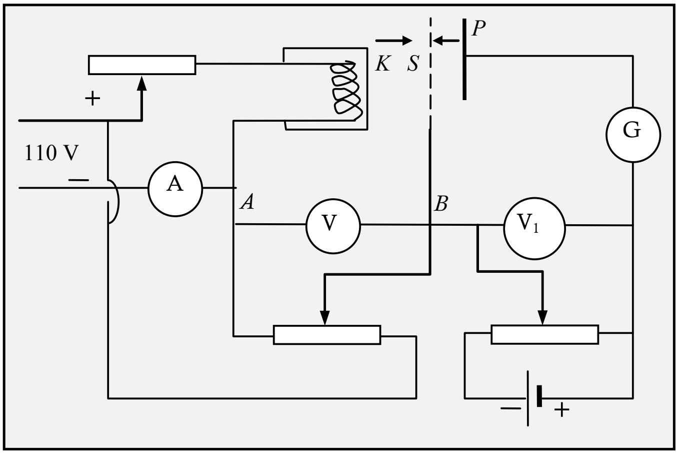

**Figure 3.33.** *Simplified representation of Franck–Hertz experimental setup*

For the mercury vapor used, the Franck–Hertz experiment has shown that the intensity $I$ of the electron current varies with voltage $U$ according to the curve represented in Figure 3.34.

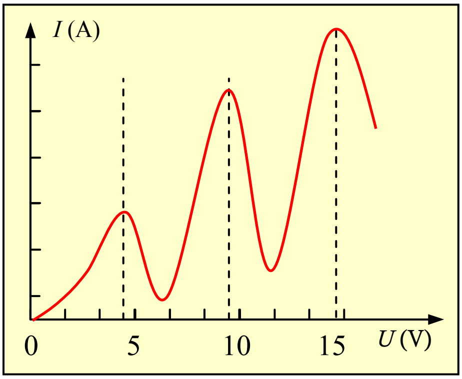

**Figure 3.34.** *Variation of current intensity I with voltage U*

It is worth noting that the $I = f(U)$ curve has maxima and minima. The gap between two maxima or two minima is approximately 4.9 V.

(1) In their experiment, Franck and Hertz used relatively dense mercury vapor.

(1.1) Explain why Franck and Hertz did not use a rarefied gas.

(1.2) Explain why a successful experiment requires the kinetic energy of the electrons to be equal to or above a certain minimal value. Use one of Bohr's postulates as specified.

(1.3) How can the existence of maxima and minima of the experimental curve representing the variation of current intensity $I$ with voltage $U$ be explained?

(2) For the mercury atom, the wavelength of the line of transition between the ground level and the first excited level is 2,536.52 Å.

(2.1) Deduce the energy $E_1$ of the first excited level of the mercury atom with respect to the ground level.

(2.2) Is the previous result (value of $E_1$) confirmed by the Franck–Hertz experiment? Justify the answer. Which Bohr postulate(s) is (are) thus confirmed?

(2.3) What is the nature (elastic or plastic) of the collision between an electron and a mercury atom when the kinetic energy $E_c$ of the electron is below $E_1$? Should we take into account the transfer of electron kinetic energy to the mercury atoms when $E_c < E_1$? Provide a theoretical justification for the answer.

(2.4) Justify the increase in current intensity $I$ with voltage $U$.

(2.5) What happens when the kinetic energy of an electron is above or equal to $E_1$? What is the nature of the collisions between electrons and atoms? How does the current $I$ vary with voltage $U$ in case of plastic collisions? Is this variation confirmed by the Franck–Hertz experiment? Justify.

(2.6) Explain why the intensity $I$ of the electrical current is not equal to zero when the kinetic energy of an electron is equal to $E_1$?

(2.7) Similarly, explain why the maxima of the curve $I = f(U)$ are located around the atom excitation energy equal to $E_1$.

(2.8) Justify the occurrence of successive maxima, according to experimental observations.

(2.9) Draw a general conclusion from the results of the Franck–Hertz experiment.

*Given data.*

– Mass of the mercury atom: m(Hg) = 202.0 u;

– Mass of the electron: $m = 5.486 \times 10^{-4}$ u;

– u: atomic mass unit.

**James Franck** and **Gustav Ludwig Hertz** (nephew of Heinrich Rudolf Hertz, see Box 2.2) were German physicists. Their renown in quantum physics is especially due to their experiment (the Franck–Hertz experiment) which proved the quantization of the energy levels of atoms, thus confirming Bohr's model of the quantized atom. Conducted in 1914, this is one of the fundamental experiments in quantum physics and brought Franck and Hertz the Nobel Prize for physics in 1925.

**Box 3.17.** *Franck (1882–1964); Hertz (1887–1975)*

### 3.7.9. *Exercise 9 – Identification of a hydrogen-like system*

Depending on the fine structure constant $\alpha$ and on the rest energy $mc^2$ of the electron, the energy of the hydrogen atom and of its isoelectronic ions (hydrogen-like ions) can be written in the form (in eV):

$$E_n = -\frac{Z^2\alpha^2 mc^2}{2n^2}$$

Figure 3.35 shows a representation of several levels of the energy diagram of a hydrogen-like ion that needs to be identified.

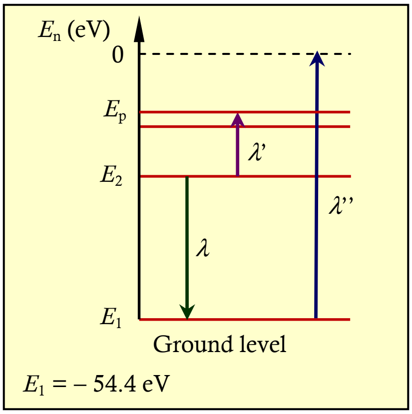

**Figure 3.35.** *Energy diagram of the hydrogen-like ion under study*

(1) Without making the calculation, compare $\lambda$, $\lambda'$ and $\lambda''$ wavelengths ranking them in ascending order of their values.

(2) Based on its chemical formula, identify the *hydrogen-like ion*.

(3) Calculate $\lambda$ and the highest frequency in the emission spectrum of the identified hydrogen-like ion.

(4) Determine the value of the quantum number $p$ of the energy level $E_p$ corresponding to the absorption of a photon of wavelength $\lambda'$ = 108.8 nm.

(5) While in ground state, the hydrogen-like ion absorbs a photon of energy 48.353eV. What will be its state after the absorption?

(6) The hydrogen-like ion absorbs a photon of energy 48.353 while on $p$-level. Show that an $\alpha$ particle is emitted after absorption.

*Given data*. 1 Ryd = 13.606 eV.

### 3.7.10. *Exercise 10 – Nucleus drag effect: discovery of deuteron*

Bohr's theory relies on the approximation of an infinitely heavy nucleus. Hence, in the laboratory frame of reference, the electron of mass $m$ orbits the proton assumed to be fixed. However, the mass $M$ of the proton is finite. To account for the *nucleus drag effect*, the reduced mass {electron–nucleus} system is considered in the center of the mass frame of reference.

In 1932, **Harold Urey** discovered in the emission spectrum of hydrogen a specific line of wavelength $\lambda$ = 485.9975 nm, very close to the $H_\beta$ line in the Balmer series of wavelength $\lambda_\beta$ = 486.132 0 nm. The line of wavelength $\lambda$ is emitted by an ${}^{a}X$ atom whose nucleus mass is denoted by $M'$. Our objective is to identify the ${}^{a}X$ atom. We consider $M' = aM$.

(1) Express the reduced mass $\mu$ of the {electron–nucleus} system.

(2) Using the Bohr frequency condition, prove that $\lambda\mu = A$, where $A$ is a constant to be clarified.

(3) Express the $a$ constant as a function of $M/m$ and $\lambda/\lambda_\beta$ ratios.

(4) Determine the value of the constant $a$ and then identify the ${}^{a}X$ atom based on its formula and name. Is this atom a hydrogen-like system?

*Given data*. Proton mass to electron mass ratio: M/m = 1,836.

**Harold Clayton Urey** was an American chemist. He discovered the $^2$H hydrogen isotope, for which he proposed the name of deuterium and notation by letter D. In 1931, he proved, together with his collaborators, the existence of heavy water (deuterium oxide, $D_2O$). This discovery brought him the Nobel Prize for chemistry in 1934.

**Box 3.18.** *Urey (1893–1981)*

### 3.7.11. *Exercise 11 – Normal Zeeman effect on the Lyman alpha line of the hydrogen atom*

The objective is to illustrate the normal Zeeman effect on the *resonance line of the hydrogen atom* corresponding to the Lyman alpha line ($L_\alpha$ line) resulting from the $2p \to 1s$ transition.

(1) Using atomic orbitals, prove that there is a theoretical possibility for the $L_\alpha$ line to result from two transitions. Specify which one of these transitions is allowed.

(2) Prove that under the effect of a uniform magnetic field, the 2p subshell splits into three sublevels. What happens to the ground state?

(3) Draw a diagram to illustrate the fine structure of the $L_\alpha$ line of the hydrogen atom. Use this diagram to represent the line in the absence of the magnetic field and the observable lines in the presence of the magnetic field.

### 3.7.12. *Exercise 12 – Zeeman–Lorentz triplet, Larmor precession*

The normal Zeeman effect makes it possible to observe that the resonance line $H_\alpha$ (656.3 nm) of the hydrogen atom in the Balmer series splits into three components corresponding to the Zeeman–Lorentz triplet. One of the three lines has a frequency $\omega_0$ equal to the frequency of the transition line in the absence of the magnetic field and the other two lines of frequencies $\omega_1$ and $\omega_2$ are shifted with respect to frequency $\omega_0$ by an amount $\pm \Delta E / \hbar$ (Figure 3.36), which will be calculated in this exercise.

Let us consider a hydrogen-like system submitted to a uniform magnetic field of intensity $B$. Let $E$ be the energy of the atom in the field $\vec{B}$ of direction $Oz$. $E_0$ is the energy of the hydrogen-like system when $B = 0$. Electron spin is not taken into account.

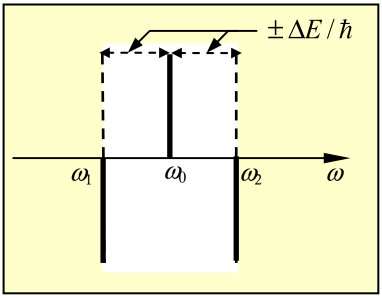

**Figure 3.36.** *Zeeman–Lorentz triplets $\omega_1$ and $\omega_2$ are shifted relative to frequency $\omega_0$*

(1) Express $E$ as a function of $E_0$, $\vec{B}$ and $\vec{l}$ (electron angular momentum).

(2) Using Bohr frequency condition, express the Zeeman–Lorentz triplet according to experimental observations (Figure 3.36).

(3) Using the selection rules, indicate the value(s) of the variation $m_\ell$ corresponding to vibrations that are parallel or transversal to the direction of the magnetic field.

(4) Verify that the module of the magnetic moment does not depend on time.

(5) Does the angle $\theta$ between the directions of the orbital magnetic moment and the magnetic field vary in time? Provide a theoretical justification of the answer.

(6) Prove that the magnetic moment executes a precession motion (*Larmor precession*) with an angular speed denoted $\Omega$ to be defined and calculated. Use a schematic representation to illustrate this precession.

NOTE.– *Nuclear magnetic resonance* (NMR) and *electron paramagnetic resonance* (EPR) are experimental methods for the study of quantum spin systems [HAM 90, BLI 15, DUT 16]. As a general case, a material of magnetic moment $\vec{\mu}$ placed in an isotropic medium is considered. When a static magnetic field $\vec{H}$ is applied, the direction of moment $\vec{\mu}$ follows that of $\vec{H}$ and starts to execute a precession motion around it at Larmor frequency $\omega_0 = \gamma H$ ($\gamma$ is the gyromagnetic ratio). If the material is subsequently applied a microwave field of frequency $\omega_0$ (generated by an electromagnetic wave), perpendicular to the direction of the static magnetic field $\vec{H}$, then the material reaches resonance by absorbing electromagnetic energy: it is the *magnetic resonance phenomenon*. If the magnetic moment is generated by the electron spin, the phenomenon is referred to as EPR. When the magnetic moment is generated by the nuclear spin, the phenomenon is referred as NMR. NMR and EPR have concrete applications in organic chemical analysis and in the medical field (biomedical applications, medical imaging, etc.). For further details on this subject, the reader is referred to the doctoral thesis of **Rémi Blinder** [BLI 15] on NMR and to that of **Charles-Emmanuel Dutoit** [DUT 16] on EPR.

**Joseph Larmor** was an Irish physicist, mathematician and politician. In physics, he published, in 1897, 2 years before Lorentz (see Box 3.9), a form of the spatial transformation laws that are currently known as Lorentz transformations. Larmor also proved that the angular momentum of an atom subjected to a magnetic field undergoes a rotational motion about the direction of the external magnetic field. This rotational motion is called Larmor precession in his honor and the angular speed of the motion is also known as Larmor frequency. Let us note that Larmor precession plays a very important role in nuclear magnetic resonance and in electron paramagnetic resonance (see the previous note).

**Box 3.19.** *Larmor (1857–1942)*

### 3.7.13. *Exercise 13 – The Stern–Gerlach experiment, magnetic force*

The *Stern–Gerlach experiment* conducted in 1922 proved that the atoms have quantized magnetic moments. Silver atoms are vaporized in an oven and a neutral atom beam is obtained in a high vacuum. This beam is focused using a diaphragm that selects the atoms whose speed is aligned along the *Oy* axis. The beam travels through the air gap of an electromagnet and then deposits on a collector plate *P*. The magnetic field applied is strongly inhomogeneous and perpendicular to the *Oy* direction of the atomic beam, each atom being in ground state.

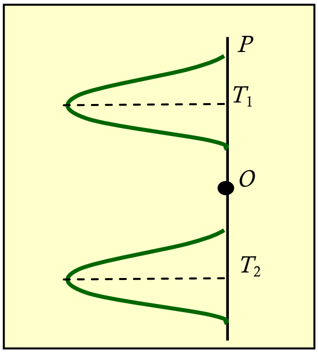

**Figure 3.37.** *Spots $T_1$ and $T_2$ observed in the Stern–Gerlach experiment*

(1) The beam of silver atoms is considered a beam of particles with non-zero magnetic moment.

(1.1) Express the potential energy $W$ of an atom in the magnetic field.

(1.2) Express the magnetic force $\overrightarrow{F}$ exerted on a silver atom. Then deduce the component $F_z$ of the force $\overrightarrow{F}$, the $Oz$ axis being vertical. Explain why it is important to apply an inhomogeneous magnetic field.

(1.3) Draw a schematic representation of the Stern–Gerlach experimental setup. Represent the $Oy$ and $Oz$ axes, as well as the trajectory of an atom both in the absence and in the presence of a magnetic field.

(1.4) Does the theory predict the observation of a point where the atoms impact the screen $P$? If not, what should be observed?

(2) Nevertheless, the experiment shows the presence of two spots centered in two points $T_1$ and $T_2$ that are symmetrical with respect to $O$ (Figure 3.37) and have equal intensities.

(2.1) Provide a classical interpretation and then a quantum interpretation of the observations resulting from the Stern–Gerlach experiment.

(2.2) Prove that the silver atom in ground state behaves as a single electron atom. The atomic number of the silver atom is $Z = 47$.

(2.3) Is the split observed on the screen $P$ due to the orbital magnetic moment? Justify the answer. What does the split of the atomic beam suggest?

### 3.7.14. *Exercise 14 – Intensities of the spots in the Stern–Gerlach experiment*

The objective of this exercise is to determine the intensity of the spots in the Stern–Gerlach experiment. The numerical data to be used are given at the end of the exercise. Let us consider:

– $L$ is the distance between the center of the air gap and the collector plate $P$;

– $l$ is the length of the path of atoms in the air gap;

– $d$ is the distance between the spots on the plate.

(1) The magnetic force is assumed to have a constant intensity $f$ in the magnetic field space.

(1.1) Draw a simplified diagram of the Stern–Gerlach experiment that should include the air gap, the velocity vector of a silver atom along $Oy$, the direction of the component of the magnetic field along $Oz$ and the $d$, $l$ and $L$.

(1.2) Show that the trajectory of the center of inertia of a silver atom of mass $m$ in the air gap is a parabolic curve.

(1.3) Determine the expression of the force $f$ acting on a silver atom of the beam as a function of $m$, $u$ (*root mean square velocity*), $d$, $l$ and $L$.

(1.4) Express the magnetic moment $M$ of a silver atom. Make the numerical application. Then deduce $f$.

(1.5) According to the predictions of classical electrodynamics, the *intrinsic magnetic moment of the electron* (*spin magnetic moment*) $\mu_e$ is:

$$\mu_e = (1.0011596522091 \pm 31)\ \mu_B$$

where $\mu_B$ is the *Bohr magneton*.

Is this theoretical value corroborated by the experimental result obtained in question 14.1.4?

(2) If $N$ designates the total number of atoms in the beam, the number of atoms $N_i$ making a spot at point $T_i$ follows Boltzmann statistical distribution. Hence:

$$N_i = \alpha e^{-W_i / kT}$$

In this expression, $\alpha$ is a constant and $W_i$ is the potential energy of interaction between the magnetic field and the spin magnetic moment of the atom for a given level $i$.

(2.1) Express $W_1$ and $W_2$ as a function of the Bohr magneton and intensity $B$ of the magnetic field.

(2.2) Prove the following relations:

$$N_1 = N \times \frac{e^{+\varepsilon}}{e^{+\varepsilon} + e^{-\varepsilon}} \ ; \ N_2 = N \times \frac{e^{-\varepsilon}}{e^{+\varepsilon} + e^{-\varepsilon}}$$

In these expressions, $\varepsilon$ is a quantity to be expressed.

(2.3) The temperature $T$ at which the atoms leave the oven is deduced from the kinetic theory of gases. The average kinetic energy of an atom due to thermal agitation is proportional to $T$. Express and then calculate $T$.

(2.4) Calculate $\varepsilon$. Prove that the spots observed in Stern–Gerlach experiment have the same intensity within experimental errors.

*Given data.*

– intensity of the magnetic field: $B = 5$ T;

– gradient of the magnetic field: $dB/dz = 15 \text{ T} \cdot \text{m}^{-1}$;

– root mean square velocity: $u = 350 \text{ m} \cdot \text{s}^{-1}$;

– distance between air-gap center and collector plate: $L = 1.0$ m;

– length of the path of atoms in the air gap: $l = 10$ cm;

– distance between the spots on the plate: $d = 1.3$ mm;

– molar mass of a silver atom: $M = 107.9 \text{ g} \cdot \text{mol}^{-1}$;

– Avogadro constant: $N_A = 6.02 \times 10^{23} \text{ mol}^{-1}$

– Planck constant: $h = 6.63 \times 10^{-34} \text{ J} \cdot \text{s}$;

– Bohr magneton: $\mu_B = 9.27 \times 10^{-24} \text{ Am}^2$.

### 3.7.15. *Exercise 15 – Normal Zeeman effect on the 2p level of hydrogen-like systems*

A hydrogen-like system is subjected to a magnetic field $\vec{B}$ assumed uniform in direction $Oz$. The electron spin is not taken into account and the potential energy of interaction between the magnetic moment of the atom and the magnetic field is designated by $W$.

(1) Express $W$ as a function of the magnitude $B$ of the magnetic field.

(2) Find the degree of degeneracy of the 2p level.

(3) Express the energy gap between the 2p sublevels appearing under the effect of the magnetic field. This gap should be expressed as a function of the Bohr magneton $\mu_B$ and of the intensity of the magnetic field $B$.

(4) Use a diagram to illustrate the normal Zeeman effect on the 2p level of hydrogen-like systems. Represent on this diagram the 2p level when $B = 0$, the values of the orbital magnetic quantum number $m_\ell$ corresponding to various sublevels formed when $B \neq 0$ as well as the energy gaps between the sublevels resulting from the splitting of the 2p level.

### 3.7.16. *Exercise 16 – Anomalous Zeeman effect on the ground state of hydrogen-like systems*

The objective is to study the effect of a uniform magnetic field $\vec{B}$ of direction $Oz$ acting on a hydrogen-like system in ground state. The potential energy of interaction between the magnetic moment of the hydrogen-like system and the magnetic field is denoted by $W$.

(1) What is the electron property that explains the anomalous Zeeman effect?

(2) Express $W$ as a function of the magnitude $B$ of the magnetic field.

(3) Determine the degree of degeneracy of the ground level.

(4) Express the energy gap between the sublevels generated as a result of the magnetic field. Express this gap as a function of the Bohr magneton $\mu_B$ and of the intensity of the magnetic field $B$.

(5) Use a diagram to illustrate the anomalous Zeeman effect on the ground level of hydrogen-like systems. Represent on this diagram the ground level when $B = 0$, the values of $m_s$ corresponding to various sublevels formed when $B \neq 0$ as well as the previously determined energy gap.

### 3.7.17. *Exercise 17 – Anomalous Zeeman effect on the 2p level of hydrogen-like systems*

A hydrogen-like system is subjected to a uniform magnetic field of direction $Oz$. Let us study the effect of this field on the 2p excited level.

(1) Express the total magnetic moment of a hydrogen-like system. Deduce from it the expression of the potential energy $W$ of interaction between the total magnetic moment of the atom and the magnetic field $\vec{B}$ .

(2) Find the degree of degeneracy of 2p level.

(3) Use a diagram to illustrate the anomalous Zeeman effect on the 2p level of hydrogen-like systems. Represent on this diagram the 2p level when $B = 0$, the values of $m_s$ and $m_\ell$ corresponding to the various sublevels formed when $B \neq 0$.

### 3.7.18. *Exercise 18 – Fine structure of the resonance line of the hydrogen atom*

The objective is to study the fine structure of the resonance line (Lyman alpha line) of the hydrogen atom. According to Dirac relativistic theory, the energy of hydrogen-like systems in the weakly relativistic domain is given by the following formula:

$$E_{nj} = -\frac{Z^2\alpha^2 mc^2}{2n^2} - \frac{Z^4\alpha^4 mc^2}{2n^3}\left(\frac{1}{j+1/2} - \frac{3}{4n}\right)$$

In this expression, $j$ is the total quantum number, $\alpha$ is the fine structure constant and $mc^2$ designates the rest energy of the electron.

(1) Find the value of the wavelength of the resonance line $L_\alpha$ of the hydrogen atom. Express this result in nanometers.

(2) Prove that the $L_\alpha$ line has a fine structure whose physical origin will be clarified. Use a diagram to illustrate this fine structure (the spectroscopic notations related to the states involved in the concerned transitions will be represented).

(3) Using the Dirac formula, find the wavelengths $\lambda_1$ and $\lambda_2$ of the two lines into which the $L_\alpha$ line is split. Then deduce the gap $\Delta\lambda$ between them.

*Given data*. Ryd/$hc = R_H$; $R_H = 10{,}967{,}758\ \mathrm{m}^{-1}$.

NOTE.– For Dirac's biography, please see Chapter 2 Volume 2.

### 3.7.19. *Exercise 19 – Fine structure of n = 2 level of the hydrogen atom*

The objective of this exercise is to study the effect of the spin–orbit interaction on the excited $n = 2$ level of hydrogen-like systems.

As a result of Lamb and Retherford experiments, it is known that the $2s_{1/2}$ and $2p_{1/2}$ levels of the hydrogen atom do not coincide (Figure 3.38). The energy gaps indicated in Figure 3.38 have been measured by **Willis Lamb** and his student **Robert Retherford** in 1949 (and published in several articles between 1950 and 1952).

According to Dirac relativistic theory, the total energy of a hydrogen-like system is given in Exercise 3.7.18.

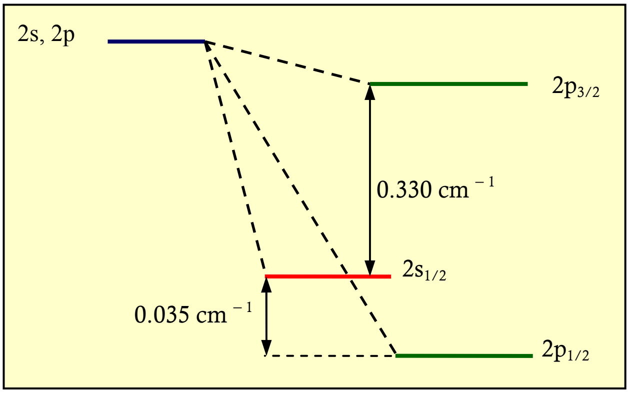

**Figure 3.38.** *Relative positions of $2s_{1/2}$, $2p_{1/2}$ and $2p_{3/2}$ levels of the hydrogen atom; the energy gaps measured by Lamb and Retherford have been represented*

(1) Is there a theoretical explanation for the relative positions of $2s_{1/2}$ and $2p_{1/2}$ levels using Dirac theory? Justify the answer.

(2) Express the energy gap between $2s_{1/2}$ and $2p_{3/2}$ sublevels. Calculate in cm$^{-1}$ the previous gap and then compare the result with the experimental data obtained by Lamb and Retherford.

(3) Is it possible to detect in the spectrum of the hydrogen atom a spectral line due to the $2s_{1/2} \rightarrow 2p_{1/2}$ transition? Justify the answer.

(4) Answer the same question (3) considering the $2p_{1/2} \rightarrow 2p_{3/2}$ transition. Justify the answer.

*Numerical data*: 1 eV/$hc$ = 8,066 cm$^{-1}$; $\alpha^2 = 5.325 \times 10^{-5}$; $mc^2 = 0.511$ MeV.

NOTE.– For Lamb's biography, see Appendix A4.

### 3.7.20. *Exercise 20 – Illustration of complex Zeeman effect on the yellow sodium line, selection rules*

Let us consider the 3p → 3s transition in the sodium atom corresponding to the yellow D-line. Experiments show that this line is constituted of two very close lines denoted $D_1$ (589.0 nm) and $D_2$ (589.6 nm).

(1) Use a diagram to illustrate the complex Zeeman effect. Indicate the electron transitions corresponding to the yellow sodium $D_1$ and $D_2$ lines.

(2) Explain why the transition between the sublevels of the fine structure of the 3p level is forbidden.

### 3.7.21. *Exercise 21 – Linear oscillator in the phase space, Bohr's principle for angular momentum quantization*

Bohr's principle for angular momentum quantization, as stated in the first postulate, follows logically from a generalization of the Planck postulate related to the quantum states of the linear oscillator. This generalization relies on the conservation of the mechanical energy of the oscillator. In this perspective, canonical coordinates $q$ (*generalized coordinate*) and $p$ (*generalized momentum*) in a non-Cartesian space called phase space are introduced.

Spring constant $k$ is related to the opposing spring force by the relation $f = -kq$. Moreover, according to the Planck hypothesis, the quantized energy of the harmonic oscillator is given by the relation $E_n = nh\nu$, where $n$ is a positive integer, $h$ is the Planck constant and $\nu$ represents the frequency of the oscillator.

*Given data*. Equation (1) and area (2) of an ellipse of semimajor axis $a$ along Oy and semiminor axis $b$ along Oz in the Cartesian space:

$$\frac{y^2}{a^2} + \frac{z^2}{b^2} = 1 \tag{1}$$

$$\oint z\,dy = \pi ab \tag{2}$$

(1) The objective is to express first the quantization condition for the Planck linear oscillator.

(1.1) Draw a schematic representation of the oscillator trajectory in the phase space.

(1.2) Find the expression of the mechanical energy of a classical linear oscillator of elongation $y$. Deduce from it the differential equation of the classical harmonic oscillator considered as a conservative system. Find the expression of the frequency $\nu$ of the oscillator.

(1.3) Deduce from (1.2) the expression of the mechanical energy of the linear oscillator in the phase space.

(1.4) Prove that the trajectory of the oscillator is an ellipse.

(1.5) Express the area of the ellipse in the phase space as a function of energy $E$ and frequency $\nu$ of the linear oscillator.

(1.6) Deduce the quantization condition of Planck linear oscillator.

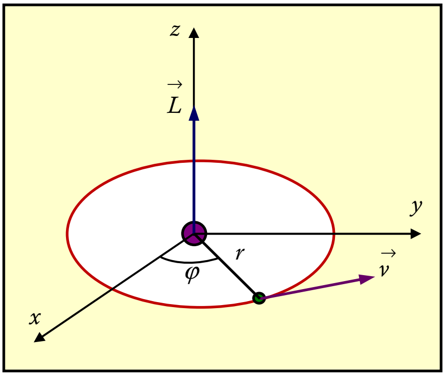

**Figure 3.39.** *Circular orbit of an electron located by the azimuthal angle $\varphi$*

(2) Let us now determine Bohr's condition for the quantization of the angular momentum. It is worth recalling that according to Bohr's model, the electron executes a uniform circular motion around the nucleus. Let $r$ be the radius of the circle and $v$ the orbital speed of the electron. A single variable can be used for the characterization of the circular orbit, namely the azimuthal angle $\varphi$ (Figure 3.39).

(2.1) Prove the following relations:

$$q = r\varphi\,;\ \ p = mr\frac{d\varphi}{dt}$$

(2.2) Prove that within Bohr's model, the angular momentum $L$ is constant.

(2.3) Determine Bohr's quantization principle of the angular momentum.

## 3.8. Solutions

### 3.8.1. *Solution 1 – Spectrum of hydrogen-like ions*

(1) *Spectral series of the hydrogen atom*

(1.1) *Proof*

Let us consider two terms $T_p$ and $T_n$. According to Ritz combination principle, the spectroscopic wave number $\bar{\nu}_{np} = 1/\lambda_{np}$ corresponding to the $n \to p$ transition is given by relation:

$$\bar{\nu}_{np} = \frac{1}{\lambda_{np}} = T_p - T_n \qquad [3.86]$$

On the other hand, for a hydrogen-like system spectral terms can be written according to Balmer:

$$T_p = \frac{Z^2}{p^2}R \quad ; \quad T_n = \frac{Z^2}{n^2}R \qquad [3.87]$$

In relation [3.87], $R$ is the Rydberg constant for the hydrogen-like system under consideration. Using [3.87], relation [3.86] becomes for the hydrogen atom:

$$\frac{1}{\lambda_{np}} = R_H \times \left(\frac{1}{p^2} - \frac{1}{n^2}\right) \qquad [3.88]$$

Comparing [3.88] to relation (1), which is:

$$\frac{1}{\lambda_{np}} = R_1 \times \left(\frac{1}{p^2} - \frac{1}{n^2}\right)$$

It can be noted that $R_1 = R_H$: the Rydberg constant for hydrogen.

(1.2) *Expression of* $R_1$, *numerical application*

By definition, the ionization energy of the hydrogen atom corresponds to the energy provided to the hydrogen atom in its ground state in order to move the electron to infinity, where its final speed is zero. This corresponds to 1 → ∞ transition. The corresponding variation of energy is written as:

$$E_{\mathrm{I}} = \Delta E = -E_1 = \frac{hc}{\lambda_{1\infty}} \qquad [3.89]$$

or, according to [3.88]:

$$\frac{1}{\lambda_{1\infty}} = R_H \cdot \qquad [3.90]$$

The combination of relations [3.90] and [3.89] leads to the expression of the Rydberg constant $R_1$. Hence:

$$E_{\mathrm{I}} = hcR_1 \Rightarrow R_1 = \frac{E_{\mathrm{I}}}{hc} \qquad [3.91]$$

N.A.– $R_1 = 10{,}973{,}739.1\ \mathrm{m}^{-1}$

It is very convenient to use the Rydberg constant expressed in $\mathrm{m}^{-1}$, as it offers the possibility of directly calculating the wavelength in meters from relation [3.88].

(2) *Hydrogen-like* $\mathrm{He}^+$ *ion*

Let us recall the four lines (1), (2), (3) and (4), whose spectroscopic wave numbers in the Lyman series are, respectively, equal to:

$$3.292\times 10^7\ \mathrm{m}^{-1};\ 3.901\times 10^7\ \mathrm{m}^{-1};\ 4.115\times 10^7\ \mathrm{m}^{-1};\ 4.213\times 10^7\ \mathrm{m}^{-1}.$$

(2.1) *Numerical verification*

The objective is to verify that the values of the above wave numbers are compatible with the law expressed by relation (2) of the formula that can be rewritten as follows:

$$\bar{\nu}_{np} = R_2 \times \left( \frac{1}{p^2} - \frac{1}{n^2} \right) \qquad [3.92]$$

In this relation, $n$ = 2, 3, 4, and 5 for lines (1), (2), (3) and (4), respectively. As the spectroscopic wave numbers are in the Lyman series, then $p$ =1. We then express the constant $R_2$ using [3.92]:

$$\bar{\nu}_{n1} = R_2 \times \left(1 - \frac{1}{n^2}\right) \Rightarrow R_2 = \bar{\nu}_{n1} \times \frac{n^2}{n^2 - 1} \qquad [3.93]$$

The use of [3.93] leads to the results summarized in Table 3.2.

| $n$ | 2 | 3 | 4 | 5 |
|---|---|---|---|---|
| $\nu_{n1}$ ($\times 10^7$ m$^{-1}$) | 3.292 | 3.901 | 4.115 | 4.213 |
| $R_2$ ($\times 10^7$ m$^{-1}$) | 4.389333 | 4.388625 | 4.389333 | 4.388542 |

**Table 3.2.** *Values of the Rydberg constant $R_2$ of the hydrogen-like ion*

Using the results listed in the last line of the table, the average value of $R_2$ can be found, which is: $\overline{R}_2 = 4.389 \times 10^7$ m$^{-1}$.

(2.2) *Expression of $R_2$, atomic number of the helium ion*

According to Bohr's approximation of the infinitely heavy nucleus, the spectral series of the hydrogen-like systems can be written according to [3.86] and [3.87]:

$$\bar{\nu}_{np} = Z^2 R_H \times \left(\frac{1}{p^2} - \frac{1}{n^2}\right) = Z^2 R_1 \times \left(\frac{1}{p^2} - \frac{1}{n^2}\right) \qquad [3.94]$$

A comparison between [3.92] and [3.94] reveals that:

$$R_2 = Z^2 R_1 \Rightarrow Z = \sqrt{\frac{R_2}{R_1}} \qquad [3.95]$$

N.A.– $R_1 = 1.097 \times 10^7$ m$^{-1}$ m$^{-1}$; $R_2 = 4.389 \times 10^7$ m$^{-1}$. Hence: $Z = 2$

This is actually the atomic number of helium.

(2.3) *Proof*

According to Bohr's theory, the quantized energy (in Rydberg) of the hydrogen-like systems is given by the relation:

$$E_n = -\frac{Z^2}{n^2}\ \text{Ryd} \tag{3.96}$$

But, given the data, Ryd = $\alpha^2 mc^2/2$. Therefore, expression [3.96] is written as:

$$E_n = -\frac{Z^2\alpha^2 mc^2}{2n^2} \tag{3.97}$$

Moreover, given the Bohr frequency condition (second Bohr postulate), the wavelength of the $n \to p$ transition is given by the relation:

$$\Delta E = E_n - E_p = \frac{hc}{\lambda_{np}} \tag{3.98}$$

Using expression [3.97], relation [3.98] can be written as:

$$\frac{1}{\lambda_{np}} = \frac{Z^2\alpha^2 mc^2}{2hc} \times \left(\frac{1}{p^2} - \frac{1}{n^2}\right) \tag{3.99}$$

Using [3.99], the ionization energy of the hydrogen atom can be written according to [3.90] and [3.91] as:

$$E_{\text{I}} = \frac{\alpha^2 mc^2}{2} = hcR_1 \tag{3.100}$$

Using [3.100], the spectral series [3.99] can be written in the following form:

$$\frac{1}{\lambda_{np}} = Z^2 R_1 \times \left(\frac{1}{p^2} - \frac{1}{n^2}\right) \tag{3.101}$$

This is actually relation (2) if $R_2 = Z^2 R_1$ according to [3.95].

### 3.8.2. *Solution 2 – Using the energy diagram of the lithium atom*

(1) *Wavelength calculation*

The wavelength $\lambda$ of the radiation emitted when the lithium atom passes from excited state 3 to ground state can be deduced from the Bohr frequency condition using [3.98]. Hence:

$$\Delta E = E_1 - E_3 = \frac{hc}{\lambda} \Rightarrow \lambda = \frac{hc}{E_1 - E_3}\,. \quad [3.102]$$

N.A.– According to Figure 3.26: $E_3$ = –2.01 eV; $E_1$ = –5.39 eV. Hence: $\lambda$ = 366.82 nm.

(2) *Polychromatic light constituted of photons of the following wavelengths*:

$\lambda_1$= 528.0 nm, $\lambda_2$= 323.0 nm and $\lambda_3$= 205.0 nm.

(2.1) *Absorbed photon(s), excited level*

A photon of wavelength $\lambda_i$ cannot be absorbed by the lithium atom unless the corresponding radiation is generated by a transition between quantized levels of the lithium atom. For a 1 → *n* transition, relation [3.102] leads to:

$$\lambda_i = \frac{hc}{E_1 - E_i} \Rightarrow E_i = E_1 + \frac{hc}{\lambda_i} \quad [3.103]$$

To ease the calculations, let us express the numerator *hc* of [3.103] so that the wavelength $\lambda_i$ is expressed in nm and the energies in eV. This leads to:

$$E_i = E_1 + \frac{1239.8}{\lambda_i} \quad [3.104]$$

Let us calculate the energy $E_i$ of the excited (*i*) level for various wavelengths $\lambda_1$, $\lambda_2$ and $\lambda_3$. Using [3.104] and $E_1$ = –5.39 eV, we obtain the following results:

– For $\lambda_1$ = 528.0 nm: $E_1$ = –3.04 eV.

– For $\lambda_2$ = 323.0 nm: $E_2$ = –1.55 eV. [3.105]

– For $\lambda_3$ = 205.0 nm: $E_3$ = +0.66 eV.

The diagram in Figure 3.26 shows that only the photon of wavelength $\lambda_2$ = 323.0 nm can be absorbed (atomic resonance takes place). After absorption, the lithium atom reaches excited state 4.

(2.2) *Observed phenomenon*

The photon of wavelength $\lambda_3$ = 205.0 nm triggers the ionization of the lithium atom. The electron reaches the continuum with a kinetic energy of 0.66 eV.

(3) *Speed of the electron*

When the lithium atom in ground state is hit by an electron of initial kinetic energy $E_c = 5.00$ eV, it passes to excited state 4. The energy in excess $\Delta E = E_c + E_4$ is then transmitted to the electron as kinetic energy. Hence:

$$\Delta E = \frac{1}{2}mv^2 \Rightarrow v = \sqrt{\frac{2\Delta E}{m}} \qquad [3.106]$$

N.A.– $\Delta E = 3.45$ eV $\Rightarrow v = 1.1 \times 10^6 \text{ m} \cdot \text{s}^{-1}$

### 3.8.3. Solution 3 – Spectra of the hydrogen atom, application to astrophysics

(1) *Electron transition*

(1.1) *Calculation of the wavelength*

The relation between the energy $E_n$ of the hydrogen atom and the energy $E_1$ of the ground state is:

$$E_n = \frac{E_1}{n^2} \qquad [3.107]$$

According to the second Bohr postulate, the wavelength corresponding to the 3 → 2 transition is given by the relation:

$$\frac{1}{\lambda} = \frac{E_3 - E_2}{hc} \Rightarrow \lambda = -\frac{36hc}{5E_1}. \qquad [3.108]$$

N.A.– $\lambda = 656.19$ nm.

(1.2) *Justification*

The wavelength $\lambda = 656.19$ nm corresponds to the red–orange line $H_\alpha$ in the Balmer series. This explains the red color on a part of the nebula.

(2) *Spectrum of light*

(2.1) *Phenomenon due to dark lines*

Absorption of photons is shown.

(2.2) *Scale of correspondence, distance*

Let $d$ be the distance between two wavelengths of argon coinciding with numbers 5 and 27 (see Figure 3.40).

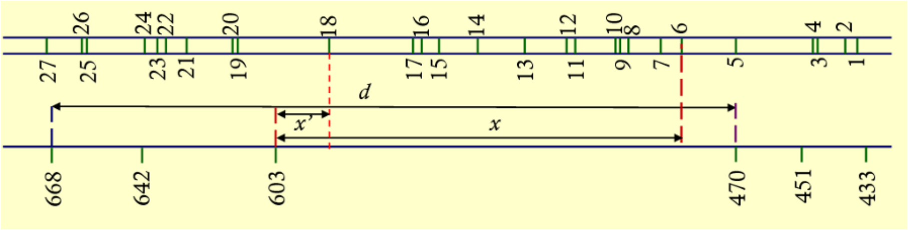

**Figure 3.40.** *Distance d between the two wavelengths of argon coinciding with numbers 5 and 27*

ATTENTION.– Figure 3.28 may be reduced as result of the book layout. Distances between wavelengths may be modified. Nevertheless, this modification has no impact on the results to be obtained.

The scale of correspondence $e$ is then given by the following relation:

$$e = \frac{\Delta\lambda}{d} = \frac{(668 - 470)}{d} \ \text{(nm/cm)} \qquad [3.109]$$

N.A.– The distance measured on the film (Figure 3.40) is $d \approx 11.3$ cm $\Rightarrow e \approx 17.5$ nm/cm.

(2.3) *Number of the absorption line*

The argon line whose wavelength is 603 nm is chosen as a reference. Let $x$ be the distance between the wavelength $\lambda_r$ of the reference line of argon and the wavelength $\lambda_\beta$ of the absorption line $H_\beta$ of the hydrogen atom. According to [3.109], we have:

$$e = \frac{\Delta\lambda}{x} \Rightarrow x = \frac{(603 - 486)}{e} \ \text{(nm/cm)} \qquad [3.110]$$

N.A.– $e = 17.5$ nm/cm $\Rightarrow x = 6.686$ cm; hence $x \approx 6.7$ cm

Locating this value on the film (Figure 3.40), it can be seen that the absorption line $H_\beta$ of the hydrogen atom corresponds to number 6 on the star spectrum.

(2.4) *Identification*

Line number 5 corresponds to argon wavelength $\lambda = 470$ nm. This line coincides with the line of wavelength 471 nm of the helium atom. Therefore, the element is helium.

NOTE.– Hydrogen and helium are the most abundant elements in the universe. Lines no. 18 (587.6 nm ≈ 588 nm: verify this result by measuring $x'$ and using [3.109]) and no. 27 (668 nm) give evidence of the presence of helium in the star cloud.

### 3.8.4. *Solution 4 – Atomic resonance phenomenon*

(1) *Emission spectrum of a sodium vapor lamp*

(1.1) *Interpretation of the experimental observations*

– *Attenuation of the incident beam*: absorption of a part of the incident photons by the sodium vapor.

– *Emission of photons by the sodium* vapor: the absorbed photons excite the sodium atoms, which start emitting photons in all directions.

(1.2) *Justification of the spectrum discontinuity*

The energy levels of the sodium atom are quantized according to Bohr's first postulate.

(1.3) *Electron configuration of sodium, electron responsible for the emission spectrum*

Using Klechkowski's rule, sodium ($Z = 11$) configuration at ground state is: $1s^2\ 2s^2\ 2p^6\ 3s^1$. Therefore, the electron of the 3s orbital is responsible for sodium emission spectrum.

(1.4) *Deduction of the energy of the ground state of the sodium atom*

According to Bohr's theory, the quantized energy is given by the relation:

$$E_n = -\frac{1}{n^2}\,\text{Ryd} \qquad [3.111]$$

Bohr's theory is applicable to hydrogen-like systems containing a single electron in 1s orbital. The sodium atom contains 11 electrons. Though erroneous, the result of the application of Bohr's theory is justified. Ignoring the electrons in the inner shells of the sodium atom leads to the following result for the 3s electron:

$$E_3 = -13.6/9 = -1.51 \text{ eV} \neq -5.14 \text{ eV as indicated in Figure 3.30}$$

The 10 "core" electrons have an important role in the calculation of the energy of the ground state of the sodium atom.

(2) *The sodium atom is in its ground state*

(2.1) *Energy levels involved in the emission of the yellow line, behavior*

– *Energy levels*: 3p and 3s levels (3p → 3s transition);

– *Behavior*: by absorbing a photon of wavelength $\lambda$ = 589.0 nm, the sodium atom passes from the 3s state to the 3p excited state (3s→ 3p transition).

(2.2) *Behavior of the sodium atom*

For a photon of 3.00 eV, the energy gap is $\Delta E$ = (3.00 – 5.14) eV = –2.14 eV. This energy does not correspond to any of the discrete levels of the sodium atom (see Figure 3.30): the photon is not absorbed and the sodium atom remains in its ground state.

(3) *Sodium atom still in its ground state*

(3.1) *Excited level n*

The sodium atom in its ground state of energy $E1$ is hit by an electron of kinetic energy $E_c$ = 3.00 eV. After interaction, the residual kinetic energy of the electron is $E_{cr}$ = 0.89 eV. The sodium atom being fixed, according to the energy conservation we have:

$$E_n - E_1 = E_c - E_{cr} \Rightarrow E_n = E_1 + (E_c - E_{cr}) \qquad [3.112]$$

N.A.– $E_n = -5.14 + (3.00 - 0.89)$ eV = –3.03 eV: first excited level $n = 2$

(3.2) *Observed phenomenon, speed of the electron*

– *Observed phenomenon*

The sodium atom in its ground state is lighted with a radiation whose wave number is $4.82946 \times 10^6$ m$^{-1}$. The corresponding energy is given by the relation:

$$E = hc\frac{1}{\lambda} = hc\bar{\nu} \qquad [3.113]$$

N.A.– $\bar{\nu} = 4.82946 \times 10^6 \text{ m}^{-1} \Rightarrow E = 5.987 \text{ eV}$

It can be noted that $E = 5.987$ eV ≈ 5.99 eV > $|E_1| = 5.14$ eV: the sodium atom is ionized. The ionization phenomenon generating the $\mathrm{Na}^+$ ion can then be observed, and the following balance equation can be written:

$$h\nu + \mathrm{Na} \rightarrow \mathrm{Na}^+ + \mathrm{e}^- \qquad [3.114]$$

– *Speed of the ejected electron*

The excess energy $\Delta E = E_c + E_1$ is transmitted to the electron in the form of kinetic energy. Hence:

$$\Delta E = \frac{1}{2}mv^2 \Rightarrow v = \sqrt{\frac{2\Delta E}{m}} \qquad [3.115]$$

N.A.– $\Delta E = 0.85$ eV $\Rightarrow v = 5.47 \times 10^{5}\ \mathrm{m \cdot s^{-1}}$

## 3.8.5. *Solution 5 – X-ray spectrum*

(1) *Homokinetic beam of electrons* accelerated under a voltage $U$, emitted electrons have no initial speed

(1.1) *Kinetic energy of the electrons*

Applying the work–energy theorem ($E_{ci} = 0$, $E_{cf} = E_c$), we have:

$$E_c = eU \qquad [3.116]$$

N.A.– $U = 40$ kV $\Rightarrow E_c = 40$ keV

(1.2) *Relativistic nature of the electrons*

The relativistic kinetic energy of a particle is given by the relation:

$$E_c = m_0c^2\,(\gamma - 1) \qquad [3.117]$$

It should be recalled that the relativistic factor $\gamma$ in [3.117] has the expression:

$$\gamma = \frac{1}{\sqrt{1 - v^2/c^2}} \qquad [3.118]$$

Let us calculate the relativistic factor using [3.117]. We obtain:

$$(\gamma - 1) = \frac{E_c}{m_0c^2} \qquad [3.119]$$

N.A.– $m_0c^2 = 511$ MeV $\Rightarrow (\gamma - 1) = 0.07828$. Hence: $\gamma = 1.07828$

Electrons are actually relativistic particles. The value of the $v/c$ ratio can be found using [3.118]: $v/c \approx 0.374 > 1/10$ (for a classical particle moving at speed $v$, $v/c < 1/10$).

NOTE.– A 1% error is generally accepted for the limit between classical and relativistic mechanics. The limit between classical and relativistic speed amounts to one-tenth (10%) of the speed of light, hence 0.1 $c$. Ultra-relativistic speeds are reached by particles in extreme cases. They can reach speeds above 99% of the speed of light (0.99 $c$).

(2) *Energy levels of the copper atom* (Figure 3.31)

(2.1) *Value of the acquired kinetic energy*

The minimal energy needed to extract an electron from the K shell is 8.979 keV. But the kinetic energy of an electron in the constant velocity beam is 40 keV. It is therefore sufficient to extract a K electron from the copper atom.

(2.2) *Kinetic energy of the electron*

Let $E_{ci}$ be the kinetic energy of an electron in the beam and $E_K = -8.979$ keV, the ionization energy from the K shell. According to the energy conservation:

$$E_c = E_{ci} - |E_K| \qquad [3.120]$$

N.A.– $E_{ci} = 40$ keV; $E_K = 8.979$ keV $\Rightarrow E_c = 31.021$ keV

(3) X-ray emission

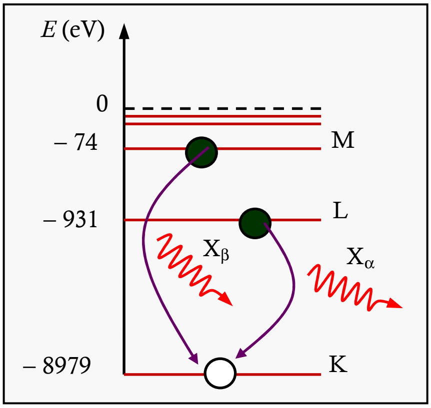

**Figure 3.41.** *Electron-hole recombination process*

(3.1) *Diagram, recombination process*

The hole (vacant orbital) in the K shell can be occupied by an electron of the M shell with emission of an $X_1$ photon or by an electron of the L shell with emission of an $X_2$ photon (see Figure 3.41).

(3.2) *Wavelengths of two emitted radiations*

Let us consider two arbitrary levels of energy, Q and N. According to the Bohr frequency condition, we have:

$$\Delta E = E_Q - E_N = \frac{hc}{\lambda_i} \qquad [3.121]$$

The wavelengths associated with the $K_\alpha$ and $K_\beta$ lines of the X-ray spectrum are deduced from [3.121]. We obtain:

$$\lambda_\alpha = \frac{hc}{E_L - E_K}\ ;\ \lambda_\beta = \frac{hc}{E_M - E_K} \qquad [3.122]$$

N.A.– $\lambda_\alpha = 154.075$ pm; $\lambda_\alpha = 139.247$ pm.

### 3.8.6. *Solution 6 – Lifetime of the hydrogen atom according to the planetary model*

(1) *Centripedal acceleration*

Let us consider Figure 3.42. The velocity of the electron with respect to the Frenet basis $(M, \vec{n}, \vec{\tau})$ is given by the relation:

$$\vec{v} = v\vec{\tau} \qquad [3.123]$$

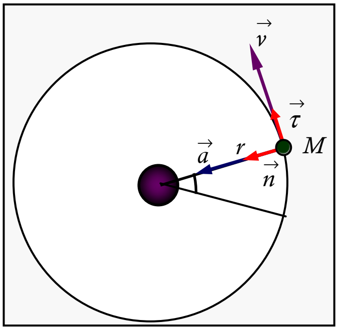

**Figure 3.42.** *Frenet basis (M, n, τ)*

Using relation [3.123], acceleration can be written as:

$$\vec{a}=\frac{d\vec{v}}{dt}=\frac{dv}{dt}\vec{\tau}+v\frac{d\vec{\tau}}{dt} \qquad [3.124]$$

Knowing that $v = r\omega = rd\theta/dt$, we obtain:

$$\vec{a}=\frac{dv}{dt}\vec{\tau}+v\frac{d\vec{\tau}}{d\theta}\frac{d\theta}{dt}\Rightarrow\vec{a}=\frac{dv}{dt}\vec{\tau}+\frac{v^2}{r}\vec{n} \qquad [3.125]$$

According to the planetary model, the motion of the electron is uniform circular. Hence, $v$ = cst. Then relation [3.125] gives:

$$\vec{a}=\vec{a}_n=\frac{v^2}{r}\vec{n} \qquad [3.126]$$

(2) *Power radiated by the electron*

The total mechanical energy of the {nucleus–electron} system and the power radiated by the electron orbiting the nucleus are, respectively, given by the following relations:

$$E(r)=-\frac{ke^2}{2r} \qquad [3.127]$$

$$-\frac{dE}{dt}=\frac{2}{3}\times\frac{e^2}{4\pi\varepsilon_0 c^3}\dot{v}^2 \qquad [3.128]$$

(2.1) *Stability of Rutherford's atomic model*

During its orbiting motion, the electron is subjected to a centripetal acceleration [3.126]. It should therefore radiate energy and end up by falling on the nucleus. Rutherford's atomic model is therefore unstable according to classical electrodynamics theory.

(2.2) *Proof*

Knowing that $\dot{v}=a_n=v^2/r$ according to [3.126], the loss of energy per time unit [3.128] can be written as:

$$-\frac{dE}{dt}=\frac{2}{3}\times\frac{ke^2}{c^3}\frac{v^4}{r^2} \qquad [3.129]$$

Moreover, for a system governed by a central force proportional to $1/r^2$, such as the {nucleus–electron} system, the kinetic energy $E_c$ ($r$) is equal to the opposite of the total energy $E$ ($r$) [3.127] of the system, hence:

$$E_c(r) = \frac{1}{2}mv^2 = k\frac{e^2}{2r} \qquad [3.130]$$

From relation [3.130], we obtain:

$$v^4 = k^2\frac{e^4}{m^2r^2} \qquad [3.131]$$

Taking [3.131] into account, equation [3.129] can be written as:

$$-\frac{dE}{dt} = \frac{2}{3}\times\frac{k^3e^6}{m^2c^3}\cdot\frac{1}{r^4} \qquad [3.132]$$

The differentiation of [3.127] with respect to time leads to:

$$\frac{dE(r)}{dt} = -\frac{ke^2}{2}\frac{d}{dt}\left(\frac{1}{r}\right) \qquad [3.133]$$

Equalizing [3.132] and [3.133], we obtain:

$$\frac{d}{dt}\left(\frac{1}{r}\right) = \frac{4}{3}\times\frac{k^2e^4}{m^2c^3}\cdot\frac{1}{r^4}$$

Hence:

$$\frac{d}{dt}\left(\frac{1}{r}\right) = \frac{A}{r^4} \qquad [3.134]$$

where:

$$A = \frac{4}{3}\frac{k^2e^4}{m^2c^3} \qquad [3.135]$$

(2.3) *Duration of the electron fall*

Using [3.134], we obtain:

$$-\frac{dr}{r^2}=\frac{A}{r^4}dt \Rightarrow -r^2\,dr = Adt \qquad [3.136]$$

At $t = 0$, the electron is on its orbit at a distance $r = a_0$ from the nucleus. Falling on the nucleus at $t_c$, $r = 0$. The integration of equation [3.136] yields:

$$-\int_{a_0}^{0} r^2 dr = A\int_{t_0}^{t_c} dt$$

Hence:

$$\Delta t = A(t_c - t_0) = a_0^3/3 \qquad [3.137]$$

Replacing $A$ by its expression [3.135], we finally obtain:

$$\Delta t = \frac{m^2c^3a_0^3}{4k^2e^4} \qquad [3.138]$$

N.A.– $\Delta t = 1.6 \times 10^{-11}$ s

(2.4) *Postulate, explanation*

According to Bohr's first postulate, the electron on the ground level is in a stationary state and does not radiate energy, which contradicts the predictions of classical electrodynamics. This justifies the stability of the hydrogen atom.

### 3.8.7. *Solution 7 – Correspondence principle, angular momentum quantization principle*

(1) Let us consider the $n \to p$ electron transition, where $n > p$.

(1.1) *Expression of the spectroscopic wave number*

According to the Ritz combination principle, the spectroscopic wave number of the line corresponding to the $n \to p$ electron transition is given by the difference between the two terms $T_n$ and $T_p$:

$$\bar{\nu} = \frac{1}{\lambda} = T_p - T_n \qquad [3.139]$$

### (1.2) *Expressions of $T_n$ and of the spectroscopic wave number*

By convention, $T_\mathrm{n}$ terms are of the Balmer type, hence:

$$T_n = \frac{Z^2}{n^2}R \qquad [3.140]$$

In [3.140], $R$ is the Rydberg constant and $n$ is the principal quantum number.

Using [3.140], expression [3.141] can be written as:

$$\frac{1}{\lambda} = \frac{Z^2R}{p^2} - \frac{Z^2R}{n^2} \qquad [3.141]$$

### (1.3) *Proof*

According to Bohr's second postulate, we have:

$$h\frac{c}{\lambda} = E_n - E_p$$

Hence:

$$\frac{1}{\lambda} = \frac{E_n}{hc} - \frac{E_p}{hc} \qquad [3.142]$$

From [3.141] and [3.142], we obtain the expression of $E_\mathrm{n}$:

$$E_n = -Z^2chR \times \frac{1}{n^2} \qquad [3.143]$$

hence:

$$E_n \times n^2 = C \qquad [3.144]$$

where $C = -Z^2chR$ = constant.

### (2) *Hydrogen-like systems*

#### (2.1) *Expression of the angular frequency of the rotational motion*

By definition, the angular momentum $\vec{L}$ of the electron is given by:

$$\vec{L} = \vec{r} \wedge \vec{p}$$

The norm of this vector is:

$$L = mvr \qquad [3.145]$$

According to [3.130], for the hydrogen-like systems of atomic number $Z$ we have:

$$m\frac{v^2}{r} = kZ\frac{e^2}{r^2} \qquad [3.146]$$

Hence:

$$(mvr)v = kZe^2$$

Knowing that $v = r.\omega$, we get:

$$(mvr)r\omega = kZe^2 \qquad [3.147]$$

Considering relations [3.145] and [3.147], we get:

$$Lr\omega = kZe^2 \qquad [3.148]$$

From the above, we obtain the rotational frequency $\omega_{\text{rot}}$ of the electron ($\omega = \omega_{\text{rot}}$)

$$\omega_{rot} = \frac{kZe^2}{Lr} \qquad [3.149]$$

#### (2.2) *Expression of the total mechanical energy*

The total mechanical energy $E$ of a system can be obtained by a generalization of [3.127]:

$$E = -kZ\frac{e^2}{2r} \qquad [3.150]$$

Comparing [3.149] and [3.150], we get:

$$\omega_{rot} = -2\frac{E}{L} \tag{3.151}$$

(2.3) *Proof*

Applying the natural logarithm to equation [3.144], we get:

$$\ln E_n + 2\ln n = \ln C$$

Hence:

$$\frac{dE_n}{E_n} + 2\frac{dn}{n} = 0 \Rightarrow \frac{\Delta E_n}{E_n} + 2\frac{\Delta n}{n} = 0 \tag{3.152}$$

or:

$$\Delta E = -2\frac{E_n}{n}\Delta n \tag{3.153}$$

According to Bohr's frequency condition, we have:

$$\Delta E = \hbar\omega = E_n - E_p$$

or according to [3.153]:

$$\omega_e = -2\frac{E_n}{n\hbar}\Delta n \tag{3.154}$$

(2.4) *Explanation*

For large values of *n,* the hydrogen-like system behaves like a classical system (*the discrete structure of the energy levels becomes blurred*). Consequently, we can approximate $E_n \approx E$. Based on this approximation, expression [3.154] becomes:

$$\omega_e = -2\frac{E}{n\hbar}\Delta n \tag{3.155}$$

(2.5) *Deduction of the correspondence principle*

According to the correspondence principle, the ground state frequency of the emitted line [3.155] for which $\Delta n = 1$ coincides with the rotational frequency of the electron [3.151]. This leads to:

$$2\frac{E}{L} = 2\frac{E}{\hbar n} \Rightarrow L = n\hbar \tag{3.156}$$

Result [3.156] is actually the expression of Bohr's rule for the quantization of the angular momentum of the atom.

### 3.8.8. *Solution 8 – Experimental confirmation of Bohr's model: Franck–Hertz experiment*

Figure 3.43 shows the graphical representation of $I$ = f ($U$). The voltage gaps $\Delta U \approx 4.9$ V between two maxima or two minima of $I = f(U)$ curve are marked in the figure, as they have been observed in Franck–Hertz experiment.

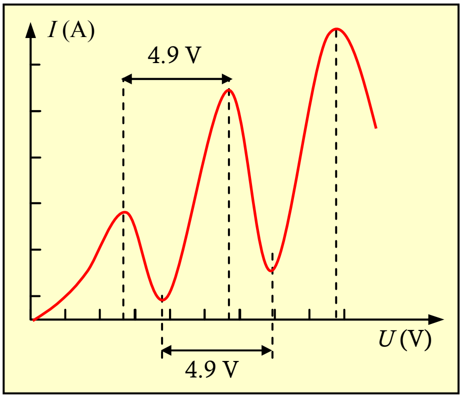

**Figure 3.43.** *Voltage gaps between two maxima or two minima of the I = f (U) experimental curve*

(1) *Gas employed: relatively dense mercury vapor*

(1.1) *Use of relatively dense gas*

Franck and Hertz have used relatively dense mercury vapor in their experiment to increase the frequency of electron–mercury atom collisions. A rarefied gas (low pressure) does not facilitate such collisions.

(1.2) *Excitation threshold*

Given that the energy levels are discrete, in accordance with Bohr's first postulate, the kinetic energy of the electrons must be equal to or higher than a certain minimal value to be able to excite the mercury atoms.

(1.3) *Origin of extremes*

The existence of maxima and minima of the experimental curve $I = f(U)$ is related to the discrete character of the energy levels of the (mercury) atoms. This confirms Bohr's first postulate.

(2) *Transition line of wavelength 2,536.52 Å*

(2.1) *First excitation energy of mercury*

Let $E_0$ be the energy of the ground state of the mercury atom. $E_1$ is the energy of the first excited level. According to the Bohr frequency condition [3.11], we have:

$$\Delta E = E_1 - E_0 = \frac{hc}{\lambda} \qquad [3.157]$$

If the energies of the excited levels are considered with respect to the ground level of energy $E_0 = 0$, according to [3.157] we obtain:

$$E_1 = \frac{hc}{\lambda} \qquad [3.158]$$

N.A.– $E_1 = 4.88857 \text{ eV} \approx 4.9 \text{ eV}$ [3.159]

(2.2) *Experimental confirmation, postulate(s)*

– *Confirmation*

The experimental curve (Figure 3.34) shows that the voltage gap between two maxima or two minima is: $\Delta U \approx 4.9$ V. This corresponds to mercury excitation energy $E_{\text{exct}} = e\Delta U = 4.9$ eV. This is in very good agreement with the theoretical result [3.159].

– *Confirmed Bohr postulate(s): both postulates*

- first postulate: *discrete character* of the energy levels;
- second postulate: validity of Bohr *frequency condition*.

(2.3) *Nature of collisions, energy transfer process*

– *Nature of the electron–mercury atom collision*

For $E_c < E_1$, the kinetic energy $E_c$ of the electron is not sufficient for the excitation of a mercury atom: therefore the collision between the electron and the mercury atom is elastic.

– *Kinetic energy transfers are taken into account*

If $E_c < E_1$, the electron rebounds off the atom after collision. The energy $E_c$ can be transferred to a mercury atom that would in this way increase its kinetic energy.

This energy transfer process must, nevertheless, be taken into account, given that the ratio of the mass of the mercury atom ($m_{\mathrm{Hg}}$) to the mass of the electron ($m_{\mathrm{e}}$) is equal to: $m_{\mathrm{Hg}}/m_{\mathrm{e}} = (202/5.486 \times 10^{-4}) = 368{,}209.989 \approx 400{,}000$.

Let us provide a theoretical justification for this assertion and calculate the kinetic energy of a mercury atom after the energy transfer process. For the sake of simplicity, let us designate by $m$ and $M$ the masses of the electron and mercury atom, respectively. Without limiting the scope of the proof, a specific case will be considered. The linear momenta of the interacting electron and mercury atom are directed horizontally before and after collision. The linear momenta of the electron before and after collision are designated by $p$ and $p'$, respectively. Let $P$ be the linear momentum of a mercury atom after collision (the mercury atom is assumed to be initially fixed).

According to the laws of conservation of energy and linear momentum:

$$\begin{cases} \dfrac{p^2}{2m} = \dfrac{P^2}{2M} + \dfrac{p'^2}{2m} \\ p = P - p' \end{cases} \Rightarrow \begin{cases} (p + p')(p - p') = \dfrac{m}{M} P^2 \\ P = p + p' \end{cases}$$

Hence:

$$\begin{cases} (p - p') = \dfrac{m}{M} P \\ p + p' = P \end{cases} \Rightarrow \begin{cases} 2p = P\left(1 + \dfrac{m}{M}\right) \\ 2p' = P\left(1 - \dfrac{m}{M}\right) \end{cases}$$

This leads to:

$$\begin{cases} \dfrac{p}{p'} = \dfrac{1 + (m/M)}{1 - (m/M)} \\ P = \dfrac{2p'}{1 - (m/M)} \end{cases} \Rightarrow \begin{cases} p' = \dfrac{M - m}{M + m} p \\ P = \dfrac{2M}{M + m} p \end{cases} \qquad [3.160]$$

Let us now express the ratio of the kinetic energies $E_{\mathrm{cM}}$ and $E_{\mathrm{ce}}$ of the interacting mercury atom and electron, respectively, taking into account [3.160]. We obtain:

$$\frac{E_{cM}}{E_{ce}} = \frac{P^2}{2M} \times \frac{2m}{p^2} = \frac{m}{M} \times \left(\frac{P}{p}\right)^2 \Rightarrow \frac{E_{cM}}{E_{ce}} = \frac{m}{M} \times \left(\frac{2M}{M + m}\right)^2$$

Hence:

$$\frac{E_{cM}}{E_{ce}}=\frac{4Mm}{(M+m)^2}=\frac{4m}{M(1+m/M)^2} \qquad [3.161]$$

But $m/M = 5.486 \times 10^{-4}/202 \approx 3 \times 10^{-6} \Rightarrow m/M \approx 1$

Therefore, [3.161] leads in the end to:

$$\frac{E_{cM}}{E_{ce}}\approx\frac{4m}{M}\Rightarrow E_{cM}\approx 0.00001086E_{ce} \qquad [3.162]$$

Result [3.162] actually shows that the mercury atoms are practically immobile after the elastic collisions between electrons and atoms. We can therefore consider $E_{\mathrm{cHg}} = 0$.

(2.4) *Justification of the increase in current intensity*

Because of the accelerating voltage, electrons acquire kinetic energies that allow them to penetrate the decelerating potential barrier $U_0$ = 0.5 V (minimal energy is around 0.5 eV). Thus, they reach the collector and consequently intensity $I$ increases, as long as collisions are elastic.

(2.5) *Behavior, current variation*

– *Behavior, nature of collisions*

When the kinetic energy of an electron is higher than or equal to E1, an electron of the beam can spend all or part of its energy to excite a mercury atom. Under these conditions, the collisions between electrons and mercury atoms become plastic.

– *Current variation with voltage, experimental confirmation*

When the collisions are plastic, after having transferred their energy to excite the mercury atoms, the electrons may be left with insufficient residual energy to penetrate the decelerating potential barrier. In this case, they are not able to reach the collector. This leads to a decrease in the intensity $I$ of the electric current, a consequence that is corroborated by the experimental curve obtained by Franck and Hertz.

(2.6) *Current intensity is zero*

Not all the electrons that leave the hot cathode K have the same ejection velocity (*velocities are dispersed due to the width of the electron exit slit*). After the plastic collisions, some of the electrons that excite the mercury atoms have enough energy to penetrate the decelerating potential barrier and reach the collector. Moreover, some electrons have no collision and are able to penetrate the decelerating potential barrier and reach the collector. This explains why the current does not suddenly drop to zero when $E_c = E_1$.

### (2.7) *Justification of the curve maxima*

After a plastic collision, the velocity of an electron can have any direction. But only the longitudinal component (*parallel to the direction of the electric field*) plays a role during the penetration of the potential barrier. The direction of this component changes after each collision leading to a smoothing of the $I = f(U)$ curve. This is why the observed maxima are located around the excitation energy, which is $E_1 = 4.9$ eV.

### (2.8) *Justification of successive maxima*

When the accelerating voltage increases, an electron can acquire sufficient energy to bring a mercury atom to the first excited level $E_1$. Consequently, after a plastic collision, it can remain in the accelerating field and acquire again the energy required for bringing a mercury atom to the energy level $E_1$, and so on and so forth. These multiple excitations of the first level for energies equal to $E_1$, $2E_1$, $3E_1$, etc., justify the successive maxima observed in Franck–Hertz experiment.

### (2.9) *Conclusion*

The experimental results obtained by Franck and Hertz have brought a resounding confirmation of the Bohr postulates.

NOTES.–

(1) The existence of a contact potential difference between cathode K and grid S falsifies the indications of the voltmeter measuring the UAB voltage. This shifts the curve entirely to the left or to the right. This is why successive maxima do not correspond to points of abscissa $V_1 = 4.9$ V; 2 $V_1 = 9.8$ V; 3 $V_1 = 14.7$ V, etc. Hence, for an accurate measurement of the value of $E_1$, the gap between two successive maxima or minima is considered, as this gap does not depend on the contact potential difference.

(2) An electron having energy $E_1$ cannot excite a mercury atom and continue acquiring energy. Therefore, it can have enough energy to excite the second level of energy $E_2$ or the third level of energy $E_3$ of a mercury atom. This makes it possible to measure various excitation potentials of these atoms. It may be that other maxima emerge on the experimental curve $I = f(U)$ at various points of abscissa 4.9 V; 9.8 V; 14.7 V, etc. In quite dense gases, these maxima cannot be observed. Indeed, an electron can have enough energy to excite an energy level above $E_2$, for example, it must travel, without undergoing collisions, a large distance in the accelerating field

compared to the length of the mean free path between two successive plastic collisions. This condition is not achievable in gases of quite high density. This was the case of Franck–Hertz experiment, the pressure of the mercury vapor being 24 mm Hg at a temperature of 210 °C. The cathode must be heated at low temperatures enabling pressures of 0.5 mm Hg in order to excite the higher levels of mercury atoms.

### 3.8.9. *Solution 9 – Identification of a hydrogen-like system*

Let us recall the quantized energy of hydrogen-like systems (in eV):

$$E_n = -\frac{Z^2\alpha^2 mc^2}{2n^2} \qquad [3.163]$$

(1) *Comparison*

According to Bohr's second postulate, the energy gap between two levels is:

$$\Delta E = \frac{hc}{\lambda} \Rightarrow \lambda = \frac{hc}{\Delta E} \qquad [3.164]$$

The last equality in [3.164] shows that the wavelength is all the shorter as the energy gap $\Delta E$ is larger. Hence: $\lambda' > \lambda > \lambda''$.

(2) *Identification of a hydrogen-like ion*

The ionization energy of the hydrogen atom H is equal to the opposite of its ground state energy $E_1$. Using [3.163], we obtain ($Z = 1$ for the hydrogen atom):

$$E_{\mathrm{I}} = \frac{\alpha^2 mc^2}{2} \qquad [3.165]$$

Using [3.165], the energy [3.163] of hydrogen-like systems can be written as:

$$E_n = -Z^2 \frac{E_{\mathrm{I}}}{n^2} \qquad [3.166]$$

$E_1 = -54.4$ eV. Knowing that $E_{\mathrm{I}} = 13.6$ eV, relation [3.166] gives $Z = 2$: the hydrogen-like ion is a helium ion $\mathrm{He}^+$.

(3) *Wavelength, frequency*

– *Calculation of the wavelength* $\lambda$

Using [3.164] and considering Figure 3.35, we get:

$$\lambda = \frac{hc}{E_2 - E_1} \qquad [3.167]$$

N.A.– $\lambda = 30.392$ nm

– *Calculation of the highest frequency*

The highest frequency in the emission spectrum of the $He^+$ ion corresponds to the largest energy gap, according to [3.164]. Therefore, it corresponds to the frequency at which the $He^+$ ion can be ionized in its ground state. Hence:

$$\Delta E = E_\infty - E_1 = h\nu \Rightarrow \nu = \frac{E_I}{h} \qquad [3.168]$$

N.A.– $\nu = 3.289 \times 10^{15}$ Hz

(4) *Determination of p*

Using [3.168] leads to:

$$\lambda' = \frac{hc}{E_p - E_2} \Rightarrow E_p = \frac{hc}{\lambda'} + E_2 \qquad [3.169]$$

N.A.– $\lambda' = 108.8$ nm; $E_p = -2.2$ eV

Using [3.166], we get for the $He^+$ ion:

$$E_p = -4 \times \frac{13.606}{p^2} \Rightarrow p = 5 \qquad [3.170]$$

(5) *Identification of the excited state*

The hydrogen-like ion absorbs a photon of energy $E = 48.353$ eV on the ground level. Let $E_n$ be the energy of the $He^+$ ion after photon absorption. Applying the energy conservation principle and replacing *p* by *n* in relation [3.170], we get:

$$E = E_n - E_1 \Rightarrow E_n = -6.0 \text{ eV} \Rightarrow n = 3 \text{ (second excited state)}$$

(6) *Behavior of the He$^+$ ion*

The He$^+$ ion absorbs a photon of energy 48.353 eV from the excited level $p = 5$. The energy of this level is $E_5 = -2.2$ eV: therefore, the He$^+$ ion is ionized according to the following balance equation:

$$h\nu + \mathrm{He}^+ \rightarrow \mathrm{He}^{2+} + e- \qquad [3.171]$$

In [3.171], He$^{2+}$ is the $\alpha$ particle (helium nucleus).

## 3.8.10. *Solution 10 – Nucleus drag effect: discovery of the deuton*

(1) *Expression of reduced mass*

By definition, the reduced mass $\mu$ of the {electron–nucleus} system is such that:

$$\frac{1}{\mu} = \frac{1}{M} + \frac{1}{m}; \mu = \frac{Mm}{M+m} \qquad [3.172]$$

(2) *Proof*

According to the infinitely heavy nucleus approximation, the wavelength of the radiation emitted by the hydrogen atom during a $p \rightarrow n$ transition is given by the following relation ([3.163] has been used):

$$\frac{1}{\lambda} = \frac{\alpha^2 mc^2}{2hcn^2}\left(\frac{p^2 - n^2}{p^2}\right) \qquad [3.173]$$

In this expression, the mass $m$ of the electron should be replaced by the reduced mass $\mu$ of the {electron–nucleus} system. This leads to:

$$\frac{1}{\lambda} = \frac{\alpha^2 \mu c^2}{2hcn^2}\left(\frac{p^2 - n^2}{p^2}\right)$$

hence:

$$\lambda\mu = \frac{2hcn^2}{\alpha^2 c^2}\left(\frac{p^2}{p^2 - n^2}\right) \qquad [3.174]$$

For a given $p \to n$ transition, the quantity:

$$\frac{2hcn^2}{\alpha^2 c^2}\left(\frac{p^2}{p^2 - n^2}\right) = A$$

Hence:

$$\lambda\mu = A \qquad [3.175]$$

(3) *Expression*

The mass of the nucleus of atom ${}^{a}X$ is denoted by $M_X$ and we have $M_X = aM$, where $M$ is the mass of the nucleus of atom H. According to [3.175], we have:

$$\lambda_\beta \mu_\beta = \lambda\mu \qquad [3.176]$$

Moreover, according to [3.172]:

$$\mu_\beta = \frac{Mm}{M+m} ; \mu = \frac{M_X m}{M_X + m} \qquad [3.177]$$

Using [3.177], relation [3.176] gives:

$$\lambda_\beta \times \frac{Mm}{M+m} = \lambda \times \frac{M_X m}{M_X + m}$$

Hence:

$$\frac{\lambda_\beta}{\lambda} = \frac{(M/m)+1}{(M_X/m)+1} \times \frac{M_X}{M}$$

This leads to:

$$\frac{\lambda_\beta}{\lambda} = \frac{(M/m)+1}{(M_X/M)\times(M/m)+1} \times \frac{M_X}{M} \qquad [3.178]$$

Knowing that $a = M_X/M$, relation [3.178] gives:

$$\frac{\lambda_\beta}{\lambda} = \frac{(M/m)+1}{a\times(M/m)+1} \times a$$

Hence:

$$a = \frac{\lambda_\beta / \lambda}{1 + (M/m)\left(1 - \lambda_\beta / \lambda\right)} \qquad [3.179]$$

(4) *Numerical application, identification of the atom*

N.A.– $\lambda_\beta/\lambda = 486.1320/485.9975$; $M/m = 1{,}836 \Rightarrow a = 2.03 \approx 2$

Therefore, the atom is deuterium $^2$H, a hydrogen isotope.

NOTE.– 1 m$^3$ of water contains 35 mg of deuterium in the form of $^2H_2O$.

### 3.8.11. *Solution 11 – Normal Zeeman effect on the Lyman alpha line of the hydrogen atom*

(1) *Justification*

The $L_\alpha$ line is generated by the transition from the first excited state $n = 2$ corresponding to 2s and 2p orbitals toward the ground level $n = 1$ (1s orbital). In the absence of any external field, 2s → 1s transition is forbidden by the selection rule $\Delta\ell = \pm 1$. The only allowed electron transition is 2p →1s.

(2) *Explanation*

The atom in the 2p state has a magnetic moment, which interacts with the magnetic field. Consequently, the energy depends on the magnetic quantum number $m_\ell$. For the 2p level, $\ell = 1$. The magnetic field induces the split of the 2p level into three components determined by three possible values of $m_\ell$, namely −1, 0, +1. On the other hand, for the ground level $m_\ell = 0$, there is no effect of the magnetic field. Therefore, the ground level remains a single level.

(3) *Fine structure illustration*

The splitting of spectral lines into several lines is known as fine structure of lines. The 2p level splits into three components according to the *normal Zeeman effect*, as shown in Figure 3.44.

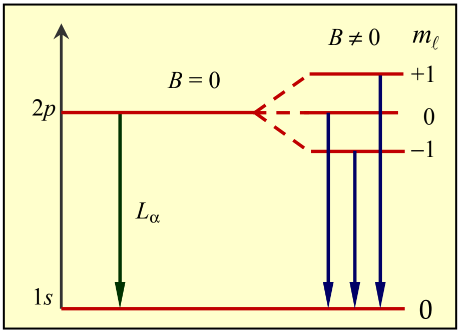

**Figure 3.44.** *Fine structure of the $L\alpha$ line of the hydrogen atom due to the normal Zeeman effect*

### 3.8.12. *Solution 12 – Zeeman–Lorentz triplet, Larmor precession*

(1) *Energy expression*

Let $E_0$ be the energy of the hydrogen-like system of magnetic moment $\overrightarrow{M}$. When subjected to a magnetic field $\vec{B}$, the atom's total energy is equal to the sum of energy $E_0$ and potential energy of interaction between moment $\overrightarrow{M}$ and magnetic field: $W = -\overrightarrow{M} \cdot \vec{B}$. Hence:

$$E = E_0 - \overrightarrow{M} \cdot \vec{B} \qquad [3.180]$$

The spin being ignored, the magnetic moment of the atom is reduced to its orbital magnetic moment so that:

$$\overrightarrow{M} = \gamma \vec{l} \qquad [3.181]$$

In this relation, $\gamma$ is the gyromagnetic ratio of the electron ($\gamma = -e/2m$). Inserting [3.181] in [3.182] we obtain:

$$E = E_0 - \gamma \vec{l} . \vec{B} \qquad [3.182]$$

(2) *Expression of Zeeman–Lorentz triplet*

Knowing that the magnetic field is directed along $Oz$, equation [3.182] gives:

$$E = E_0 - \gamma l_z B$$

Knowing that $l_z$ is quantized:

$$E = E_0 - \gamma B m_\ell \hbar \qquad [3.183]$$

According to Bohr frequency condition, $\Delta E = \hbar\omega$. Hence, according to [3.183]:

$$\Delta E = \Delta E_0 - \gamma B \hbar \Delta m_\ell$$

Hence:

$$\omega = \omega_0 - \gamma B \Delta m_\ell \qquad [3.184]$$

Knowing that $\Delta m_\ell$ is a number, the positive quantity $-\gamma B$ has the dimension of an angular frequency known as *Larmor frequency* denoted by Ω expressed as:

$$\Omega = -\gamma B \qquad [3.185]$$

Using [3.185], angular frequency [3.184] is written as:

$$\omega = \omega_0 + \Omega \Delta m_\ell \qquad [3.186]$$

Taking into account the selection rules verified by $\Delta m_\ell$, we can determine the Zeeman–Lorentz triplet. Hence:

$$\begin{cases} \omega'_1 = \omega_1 = \omega_0 - \Omega & ; \quad \Delta m_\ell = -1 \\ \omega'_2 = \omega_0 & ; \quad \Delta m_\ell = 0 \\ \omega'_3 = \omega_2 = \omega_0 + \Omega & ; \quad \Delta m_\ell = +1 \end{cases} \qquad [3.187]$$

Results [3.187] properly corroborate experimental observations (Figure 3.45).

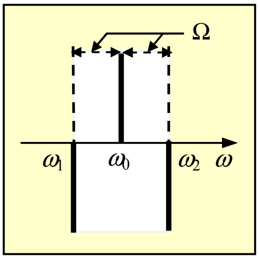

**Figure 3.45.** *Experimentally observed Zeeman–Lorentz triplet*

NOTE.– The Zeeman effect has been observed by Zeeman, but its theoretical interpretation has been given by Lorentz. This explains why the three angular frequencies are known as the Zeeman–Lorentz triplet [3.187].

(3) *Parallel and transverse vibrations*

Electron transitions are governed by the values of the *electric dipole moment* of the atom. When transitions are allowed, the mean value of the electric dipole moment is an oscillating function of time. Such a dipole radiates energy. In the specific case of the Zeeman effect:

– for $\Delta m_\ell = -1$, the angular frequency of the emitted line is $\omega_1 = \omega_0 - \Omega$. According to the classical theory, *dipole radiation* is emitted along the *Oz* direction of the magnetic field vector and it is *left-circularly polarized* ($\sigma_-$ component);

– for $\Delta m_\ell = 0$: the dipole linearly oscillates along *Oz*. *Polarization is rectilinear* or linear (component $\pi$);

– for $\Delta m_\ell = +1$, the angular frequency of the emitted line is $\omega_2 = \omega_0 + \Omega$. The line is *right-circularly polarized* (component $\sigma_+$). The dipole's rotation direction is opposite to that of the left-circularly polarized with $\Delta m_\ell = -1$.

Figure 3.46 illustrates the linear polarization and left- and right-circular polarizations of Zeeman–Lorentz lines, which have been observed from a direction that is perpendicular to that of the magnetic field.

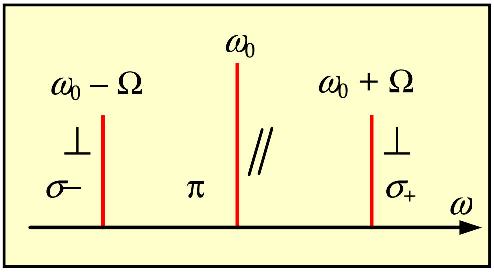

**Figure 3.46.** *Illustration of linear, left- and right-circular polarizations of Zeeman–Lorentz lines*

NOTE.– Let us consider an *electrostatic dipole* constituted of two opposite charges $-q$ and $+q$ located in two arbitrary points *A* and *B* in space. By definition, the dipole moment denoted by $\vec{p}$ is equal to:

$$\vec{p} = q\overrightarrow{AB} = qa\vec{u} \qquad [3.188]$$

The direction of the dipole moment goes from the negative charge toward the positive charge since $q > 0$. The unit of the dipole moment is the coulomb meter (C · m). However, at atomic or molecular scale, the convenient unit of the dipole moment is *debye* (Dy), whose definition is: 1 Dy = (1/3) × $10^{-29}$C · m. For further details on the electric dipole moment, see [SAK 18].

(4) *Verification*

In the magnetic field, the magnetic moment of the atom is subjected to a *magnetic torque*:

$$\vec{\Gamma} = \overrightarrow{M} \wedge \vec{B} \tag{3.189}$$

Given the *angular momentum theorem*:

$$\frac{d\vec{l}}{dt} = \vec{\Gamma} \tag{3.190}$$

Inserting [3.190] in [3.189], we get:

$$\frac{d\vec{l}}{dt} = \overrightarrow{M} \wedge \vec{B} \tag{3.191}$$

Knowing that the orbital magnetic moment is $\overrightarrow{M} = \gamma \vec{l}$, equation [3.191] leads to:

$$\frac{d\overrightarrow{M}}{dt} = \gamma \overrightarrow{M} \wedge \vec{B} \tag{3.192}$$

Let us make the scalar multiplication of this equation by $\overrightarrow{M}$. Given the properties of the vector product, we have:

$$\overrightarrow{M} \cdot \frac{d\overrightarrow{M}}{dt} = \gamma \overrightarrow{M} \cdot \left(\overrightarrow{M} \wedge \vec{B}\right) = 0 \tag{3.193}$$

But the term on the left of equation [3.193] verifies the following relation:

$$\overrightarrow{M} \cdot \frac{d\overrightarrow{M}}{dt} = \frac{1}{2} \frac{d\left(\overrightarrow{M}^2\right)}{dt}$$

Taking this result into account, [3.193] leads to:

$$\frac{d\left(\overrightarrow{M}^2\right)}{dt}=0 \tag{3.194}$$

The angular momentum module is therefore constant (time independent).

(5) *Time-invariance of $\theta$ angle*

Let us make the scalar multiplication of [3.192] by $\overrightarrow{B}$ . We obtain:

$$\overrightarrow{B}\cdot\frac{d\overrightarrow{M}}{dt}=\gamma\overrightarrow{B}\cdot\left(\overrightarrow{M}\wedge\overrightarrow{B}\right)=0$$

Hence:

$$\frac{d\left(\overrightarrow{B}\cdot\overrightarrow{M}\right)}{dt}=0 \tag{3.195}$$

Knowing that $\overrightarrow{B}\cdot\overrightarrow{M}=BM\cos\theta$ and that $B$ and $M$ are constant, then according to [3.195]:

$$BM\frac{d\theta}{dt}=0\Rightarrow\theta=\text{Cst} \tag{3.196}$$

(6) *Precession motion, calculation of angular speed, illustration: Larmor precession*

Let us consider Figure 3.47 knowing that $\theta$ is constant. Let $P$ be the point such that $\overrightarrow{OP}=\overrightarrow{M}$. This point can move on a circle of radius $r$ at speed:

$$\vec{v}=\frac{d\overrightarrow{OP}}{dt}=\frac{d\overrightarrow{M}}{dt} \tag{3.197}$$

Taking [3.192] into account, relation [3.197] can be written as:

$$\vec{v}=\frac{d\overrightarrow{M}}{dt}=\gamma\overrightarrow{OP}\wedge\overrightarrow{B} \tag{3.198}$$

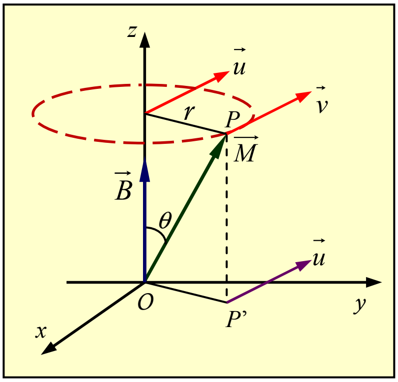

**Figure 3.47.** *Precession of the magnetic moment about the direction of the magnetic field*

According to Figure 3.47 and using [3.198], we get:

$$\overrightarrow{OP} = \overrightarrow{OP'} + \overrightarrow{P'P} \Rightarrow \vec{v} = \gamma\left(\overrightarrow{OP'} + \overrightarrow{P'P}\right) \wedge \vec{B} \qquad [3.199]$$

Taking into account that $\overrightarrow{P'P} \wedge \vec{B} = \vec{0}$, the last equality [3.199] gives

$$\vec{v} = \gamma \overrightarrow{OP'} \wedge \vec{B} \qquad [3.200]$$

Moreover, as indicated in Figure 3.47, the vector product is:

$$\overrightarrow{OP'} \wedge \vec{B} = -OP'B\vec{u} = -rB\vec{u}$$

Equation [3.200] leads to the following relation:

$$\vec{v} = -\gamma rB\vec{u} \qquad [3.201]$$

Relation [3.201] shows that the velocity has the direction of the unit vector $\vec{u}$, since $\gamma < 0$. For a circular motion, $v = r\omega$. The rotational angular velocity can be written according to [3.201] as:

$$\omega = \Omega = -\gamma B \qquad [3.202]$$

Therefore, the head $P$ of the magnetic moment executes a uniform circular motion. Consequently, the magnetic moment executes a rotational motion known as *Larmor precession* at *Larmor frequency* Ω [3.202].

N.A.– $\gamma = -e/2m = -8.79 \times 10^{10}\ \mathrm{C \cdot kg^{-1}}$; $\Omega = 8.79 \times 10^{9}\ \mathrm{rad \cdot s^{-1}}$

## 3.8.13. Solution 13 – Theoretical interpretation of the Stern–Gerlach experiment, magnetic force

(1) *The silver atom beam has a non-zero magnetic moment*

(1.1) *Expression of the potential energy*

If the magnetic moment $\overrightarrow{M}$ is non-zero, the potential energy $W$ of an atom in the magnetic field can be written as:

$$W = -\overrightarrow{M} \cdot \vec{B} \qquad [3.203]$$

(1.2) *Expression of the magnetic force, justification*

– *Expression of $F_z$ component*

Given that the magnetic moment of a silver atom in the beam is not zero in ground state, each atom is subjected to the force:

$$\vec{F} = -\vec{\nabla} W \qquad [3.204]$$

Inserting [3.203] in [3.204], we get:

$$\vec{F} = -\vec{\nabla}(\overrightarrow{M} \cdot \vec{B}) \qquad [3.205]$$

The $F_z$ component of the magnetic force [3.205] along the $Oz$ direction of the magnetic field is given by the expression:

$$F_z = \frac{\partial}{\partial z}(M_z B) = M_z \frac{\partial B}{\partial z} \qquad [3.206]$$

– *Justification*

Expression [3.206] clearly shows why it is important to apply an inhomogeneous magnetic field: this force would be zero if the field was uniform (*which is the case in the Zeeman experiment*). This justifies the use of a highly inhomogeneous field in the Stern–Gerlach experiment.

(1.3) *Schematic representation*

Figure 3.48 shows the simplified diagram of Stern–Gerlach experiment. The trajectory of the atomic beam is rectilinear when the magnetic field is zero.

Therefore the beam is deflected within the air gap by the gradient [3.206] of the magnetic field and in the end it condenses at point $P$ on the plate.

(1.4) *Theoretical predictions*

Given the finite width of the slit and the velocity dispersion, no impact point can be observed in $P$. The atoms in the beam should therefore condense in various points on the plate and form *a spot* centered in $P$. Moreover, from a classical point of view, the measurement of the $M_z$ component of the magnetic moment should yield all the values between $-|M_z|$ and $+|M_z|$. This would also result in a single spot in $P$.

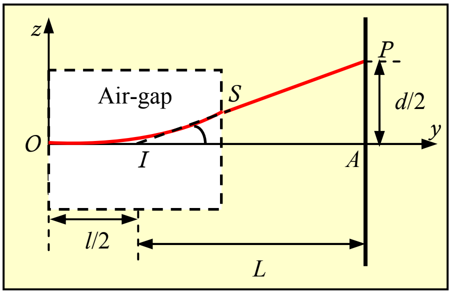

**Figure 3.48.** *Simplified diagram of Stern–Gerlach experimental setup*

(2) *Experimental observations*

(2.1) *Interpretation*

Contrary to the theoretical predictions, the experiment proves the existence of two spots centered in two points $T_1$ and $T_2$ that are symmetrical with respect to $O$ (Figure 3.49).

Experimental observations (Figure 3.49) prove that the measure of $M_z$ can only have two possible results. In other terms, the measure of $M_z$ is *quantized* (*quantization of the measure*) contrary to the theory predicting all the values of $M_z$ between $-|M_z|$ and $+|M_z|$.

(2.2) *Proof*

Let us use Klechkowski's rule. The following electron configuration is obtained for the silver atom ($Z = 47$) (reminder of [3.58]):

$$1s^2\,2s^2\,2p^6\,3s^2\,3p^6\,4s^2\,3d^{10}\,4p^6\,5s^1\,4d^{10} \text{ or } [\mathrm{Kr}]\,4d^{10}5s^1$$

The physical and chemical properties of the silver atom in ground state are determined by the electron of 5s orbital: therefore, it behaves similarly to a single electron system.

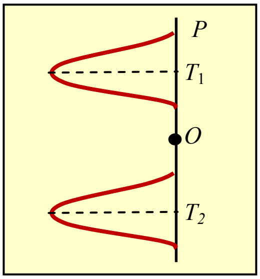

**Figure 3.49.** *Spots centered in two points $T_1$ and $T_2$ observed in the Stern–Gerlach experiment*

(2.3) *Justification*

In ground state, the orbital quantum number is zero. The magnetic moment evidenced by the Stern–Gerlach experiment is therefore not due to the orbital magnetic moment. Consequently, the observed splitting suggests the existence of an *intrinsic magnetic moment* of the 5s electron. The spin magnetic moment of the electron is given by the following expression:

$$\overrightarrow{M} = -2\gamma \vec{s} \qquad [3.207]$$

Relation [3.207] takes into account the approximation $g_s \approx 2$ ($g_s = 2.00232$). The direction of the magnetic field being along $Oz$, we have:

$$M_z = -2\gamma\, s_z \Rightarrow M_z = -2\gamma\, m_s\hbar \qquad [3.208]$$

Using the *Bohr magneton* $\mu_B = -\gamma\hbar$, we obtain:

$$M_z = 2m_s\mu_B \qquad [3.209]$$

Knowing that $m_s = \pm 1/2$, expression [3.209] theoretically justifies the quantization of the measure of $M_z$ component of the spin angular momentum according to the Stern–Gerlach experimental observations. Inserting [3.209] in [3.206], the component $F_z$ of the magnetic force acting on a silver atom is expressed as a function of the magnetic spin quantum number $m_s$. Hence:

$$F_z = -2m_s\mu_B \frac{\partial B_z}{\partial z} \qquad [3.210]$$

Taking [3.210] into account, the splitting of the silver atom beam into two components that are symmetrical with respect to the initial direction, as shown in Figure 3.50, can be easily explained.

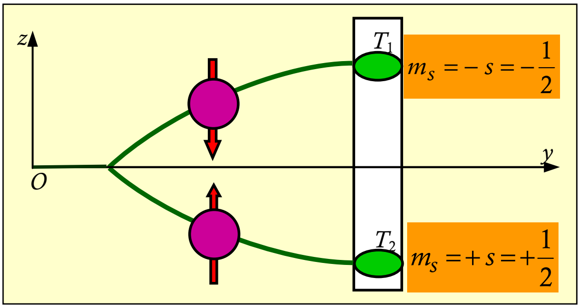

**Figure 3.50.** *Splitting of the silver atom beam into two components under the action of the magnetic force*

### 3.8.14. *Solution 14 – Intensities of the spots in the Stern–Gerlach experiment*

(1) *The magnetic force has a constant intensity f in the region governed by the magnetic field*

(1.1) *Schematic representation*

For more details, see Figure 3.48.

(1.2) *Proof*

The position vector of the center of inertia of a silver atom that is moving in a magnetic field can be written as:

$$\overrightarrow{OG} = \frac{1}{2}\vec{a}\,t^2 + \vec{v}\,t + \overrightarrow{OG}_0 \qquad [3.211]$$

According to *Newton's second law* (*theorem of the center of inertia*):

$$F_z = f = ma \qquad [3.212]$$

As the motion takes place in the *yOz* plane, and the position $G_0$ of the center of inertia at $t$ = 0 coincides with the origin of coordinates, the projection of equation [3.211] taking into account [3.212] leads to:

$$z(t) = \frac{1}{2}\frac{f}{m}t^2 \quad ; \quad y(t) = vt \qquad [3.213]$$

Eliminating the time variable in [3.213], the Cartesian equation of the trajectory of the center of inertia of a silver atom in the magnetic field is:

$$z = \frac{1}{2}\frac{f}{mv^2}y^2 \qquad [3.214]$$

Equation [3.214] is actually a parabolic curve.

(1.3) *Expression of intensity f*

Let us reconsider Figure 3.48. The point *S* where the beam exits the air gap has the coordinates ($y_s = l/2$, $z_s$). Moreover, the tangent of angle $\hat{I}$ satisfies the relations:

$$\tan \hat{I} = \frac{2z_S}{l} = \frac{d}{2L} \; ; \; z_S = \frac{d}{4L}l \qquad [3.215]$$

The point *S* belongs to trajectory [3.214], hence:

$$z_S = \frac{1}{2}\frac{f}{mv^2}l^2 \qquad [3.216]$$

After equalization of relations [3.215] and [3.216] and rearrangement we have:

$$f = \frac{m\,v^2 d}{2\,lL} \qquad [3.217]$$

(1.4) *Expression of the magnetic moment, deduction*

According to [3.206], the magnitude of the magnetic force is:

$$f = M_z \frac{dB}{dz} \qquad [3.218]$$

Taking [3.217] into account, the projection of the magnetic moment of a silver atom along *Oz* is expressed by the relation:

$$M_z = \frac{m v^2 d}{2 l L \dfrac{dB}{dz}} \qquad [3.219]$$

N.A.– $M_z = 9.5 \times 10^{-24}$ A · m$^2$

The magnitude of $f$ results from [3.218].

Hence: $f = 1.4 \times 10^{-22}$ N

This force is weak but very significant at the atomic scale if compared to the weight of the electron $P = mg$, as evidenced by the value of $f/P$ ratio:

N.A.– $f/mg = 1.4 \times 10^{-22}/(9.1 \times 10^{-31} \times 10) = 15{,}680{,}000$ [3.220]

The result [3.220] shows that the magnitude $f$ of the magnetic force due to the *magnetic field gradient* is therefore around 16 million times higher than the electron weight.

(1.5) *Experimental confirmation*

According to the predictions of quantum electrodynamics, the *intrinsic magnetic moment of the electron* is equal to:

$$M_z = (1.0011596522091 \pm 31)\, \mu_B \qquad [3.221]$$

Given the *Bohr magneton* $\mu_B = 9.27 \times 10^{-24}$ A · m$^2$ and using the result [3.221], we obtain:

$$M_z/\mu_B = 9.5/9.27 = 1.0248 \Rightarrow M_z = 1.024\,8\, \mu_B \qquad [3.222]$$

The experimental result [3.222] is slightly above the predictions [3.221] of quantum electrodynamics. The gap is due to the classical approach of the calculation of the intrinsic angular momentum of the electron. Nevertheless, the classical result [3.222] has the advantage of showing that the electron magnetic moment due to spin is slightly higher than the Bohr magneton, according to the predictions of quantum electrodynamics [3.221].

(2) *Number of atoms $N_i$ generating a spot at point $T_i$*

$$N_i = \alpha e^{-W_i/kT} \qquad [3.223]$$

(2.1) *Expressions*

According to [3.203], we have:

$$W = -\vec{M}.\vec{B} = -M_z B \qquad [3.224]$$

But the $M_z$ component of the spin magnetic moment is quantized according to [3.209]. As a result, energy $W$ is also quantized. Hence:

$$\begin{cases} W_1 = -\mu_B B \quad ; \; m_s = -\dfrac{1}{2} \\ W_2 = +\mu_B B \quad ; \; m_s = +\dfrac{1}{2} \end{cases} \qquad [3.225]$$

(2.2) *Proof*

According to [3.223], and taking into account [3.225], the populations $N_1$ and $N_2$ of levels (1) and (2), respectively, are given by the relations:

$$\begin{cases} N_1 = \alpha\, e^{-W_1/kT} \\ N_2 = \alpha\, e^{-W2/kT} \end{cases} \Rightarrow \begin{cases} N_1 = \alpha\, e^{+\mu_B B/kT} \\ N_2 = \alpha\, e^{-\mu_B B/kT} \end{cases} \qquad [3.226]$$

Let us note $\varepsilon = \mu_B B/kT$. Knowing that $N = N_1 + N_2$, we have:

$$\begin{cases} N_1 = \alpha e^{+\varepsilon} \\ N_2 = \alpha e^{-\varepsilon} \end{cases} \Rightarrow \alpha\, e^{+\varepsilon} + \alpha\, e^{-\varepsilon} = N$$

The last equality in the above system leads to:

$$\alpha = \frac{N}{e^{+\varepsilon} + e^{-\varepsilon}} \qquad [3.227]$$

Using [3.227], we can write the populations $N_1$ and $N_2$ according to [3.226]:

$$N_1 = N \frac{e^{+\varepsilon}}{e^{+\varepsilon} + e^{-\varepsilon}} \quad ; \quad N_2 = N \frac{e^{-\varepsilon}}{e^{+\varepsilon} + e^{-\varepsilon}} \qquad [3.228]$$

In these expressions, $\varepsilon = \mu_B B/kT$.

(2.3) *Expression of temperature, numerical application*

Let us express the *root mean square velocity u* according to the *kinetic theory of gases*. The average kinetic energy due to thermal agitation is equal to:

$$E_c = \frac{1}{2} m \langle v^2 \rangle = \frac{3}{2} kT \qquad [3.229]$$

Using [3.229], we have:

$$T = \frac{m\langle v^2 \rangle}{3k} = \frac{m u^2}{3k} \;;\; u = \sqrt{\langle v^2 \rangle} \qquad [3.230]$$

N.A.– $T = 530$ K

(2.4) *Value of ε, spot intensity*

The quantity $\varepsilon = \varepsilon = \mu_B B/kT$.

N.A.– $\mu_B = 9.27\times 10^{-24}$ A · m$^2$: $\varepsilon \approx 0.006$

Expressions [3.228] can be written in the form:

$$\begin{cases} N_1 = N \times \dfrac{1}{1 + e^{-2\varepsilon}} \\ N_2 = N \times \dfrac{1}{1 + e^{+2\varepsilon}} \end{cases} \qquad [3.231]$$

Inserting the value of $\varepsilon$ in [3.231], we have:

$$\begin{cases} N_1 = N \times \dfrac{1}{1 + e^{-2\times 0.006}} \\ N_2 = N \times \dfrac{1}{1 + e^{+2\times 0.006}} \end{cases} \Rightarrow \begin{cases} N_1 = N \times \dfrac{1}{1 + 0.98807} \approx \dfrac{N}{2} \\ N_2 = N \times \dfrac{1}{1 + 1.01207} \approx \dfrac{N}{2} \end{cases} \qquad [3.232]$$

Results [3.232] indicate that the total number $N$ of atoms in the beam exiting the oven is nearly equally divided in two components: the two spots observed in the Stern–Gerlach experiment are practically equally intense.

### 3.8.15. *Solution 15 – Normal Zeeman effect on the 2p level of hydrogen-like systems*

The hydrogen-like system under consideration is subjected to a uniform magnetic field $\vec{B}$ of direction $Oz$. The electron spin is not taken into consideration.

(1) *Potential energy due to magnetic interaction*

The potential energy $W$ is given by [3.203]. If the electron spin is ignored, the potential energy $W$ due to the interaction between the magnetic moment of the atom and the magnetic field is given by the following expression (knowing that $l_z$ is quantized):

$$W = -\gamma \vec{l} \cdot \vec{B} = -\gamma m_\ell \hbar B \qquad [3.233]$$

(2) *Degree of degeneracy*

The degree of degeneracy $g$ of an energy level (spin is ignored) is given by the possible values of the magnetic quantum number $m_\ell$. Hence:

$g = (2\ell + 1)$; for the 2$p$ level, $\ell = 1$. Hence: $g = 3$

(3) *Expression of the gap between two successive sublevels*

The 2p sublevels appearing due to the magnetic field are determined by the various values of $m_\ell$. Knowing that the Bohr magneton is $\mu_B = -\gamma\hbar$, expression [3.233] can be written as:

$$W = \mu_B m_\ell B \qquad [3.234]$$

The potential energy relative to the three 2p sublevels is then:

$$W = \begin{cases} +\mu_B B & ;\ m_\ell = +1 \\ 0 & ;\ m_\ell = 0 \\ -\mu_B B & ;\ m_\ell = -1 \end{cases} \Rightarrow |\Delta W| = \mu_B B \qquad [3.235]$$

(4) *Schematic illustration of the normal Zeeman effect*

Figure 3.51 illustrates the normal Zeeman effect on the 2p level of hydrogen-like systems. This diagram indicates the 2p level when $B$ = 0, the values of $m_\ell$ corresponding to various sublevels formed when $B \neq 0$, as well as the energy gaps [3.235] (the spin–orbit interaction is not taken into account).

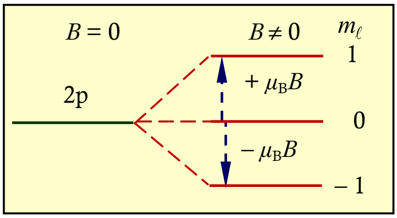

**Figure 3.51.** *Schematic illustration of the normal Zeeman effect on the 2p level of hydrogen-like systems*

### 3.8.16. *Solution 16 – Anomalous Zeeman effect on the ground level of hydrogen-like systems*

The hydrogen-like system under consideration is in the ground state and is submitted to a uniform magnetic field $\vec{B}$ of direction *Oz*.

(1) *Quantum number clarification*

The *anomalous* or *complex Zeeman effect* is due to the properties of the electron spin *s*.

(2) *Expression of the potential energy*

The potential energy *W* is given by [3.203]. For the ground level, $\ell = 0$. The magnetic moment of the hydrogen-like system is therefore due to the spin. The energy *W* is given by the following expression (knowing that $s_z$ is quantized):

$$W = -g\gamma\vec{s}\cdot\vec{B} = -2\gamma m_s\hbar B \qquad [3.236]$$

(3) *Finding the degree of degeneracy*

The degree of degeneracy *g* of an $ns^2$ level is given by the possible values of the magnetic spin quantum number $m_s$. Hence: $g = 2s + 1$; $s = 1/2$. Therefore, $g = 2$.

(4) *Expression of the gap between two successive sublevels*

The 1s sublevels appearing due to the magnetic field are determined by the various values of $m_s$. Expression [3.236] can be written as a function of Bohr magneton:

$$W = 2\mu_B B m_s \qquad [3.237]$$

The potential energy related to the two sublevels 1s is then:

$$W = \begin{cases} +\mu_B B\,;\, m_s = +\dfrac{1}{2} \\ -\mu_B B;\, m_s = -\dfrac{1}{2} \end{cases}. \qquad [3.238]$$

Hence:

$$|\Delta W| = 2\mu_B B \qquad [3.239]$$

(5) *Schematic illustration of the anomalous Zeeman effect*

Figure 3.52 illustrates the anomalous Zeeman effect on the ground level of hydrogen-like systems. The figure also indicates the ground level when $B = 0$, the values of $m_s$ corresponding to the two sublevels formed when $B \neq 0$, as well as the energy gap [3.239].

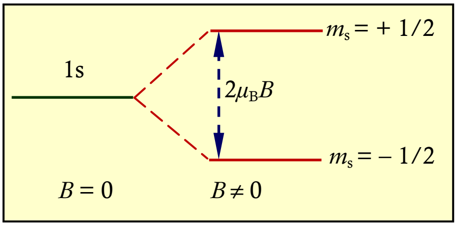

**Figure 3.52.** *Illustration of the anomalous Zeeman effect on the ground level of hydrogen-like systems*

### 3.8.17. *Solution 17 – Anomalous Zeeman effect on the 2p level of hydrogen-like systems*

The hydrogen-like system under study is subjected to a uniform magnetic field $\vec{B}$ of direction $Oz$. Spin contribution is taken into account.

(1) *Expressions of the total magnetic moment and potential energy*

If the spin is considered, the magnetic moment of a hydrogen-like system is given by the relation:

$$\vec{M}_j = -g_j \gamma \vec{j} \; ; \vec{j} = \vec{l} + \vec{s} \qquad [3.240]$$

Knowing that $j_z$ is quantized, the p*otential energy* $W$ of interaction between the total magnetic moment of the atom and the magnetic field is given by the expression:

$$W = -g_j \gamma \vec{j} \cdot \vec{B} \Rightarrow W = -g_j \gamma m_j \hbar B \qquad [3.241]$$

(2) *Degree of degeneracy*

The degree of degeneracy $g$ is given by the possible values of the magnetic quantum number $m_j$. Hence: $g_j = 2j + 1$. The sum of this number is also equal to

$g = (2s+1)\times(2\ell+1)$. For the 2p level, $\ell = 1$ and $s$ = 1/2. Hence, $g$ = 6. This number can be found from the formula $g_j = 2j + 1$, where $j = \ell \pm s = \ell \pm 1/2$. Knowing that $\ell = 1$, then $j = 1/2$ or 3/2. For $j$ =1/2, $g$ = 2; for $j$ =3/2, $g$ = 4. Summing up, the result is actually $g$ = 6.

(3) *Schematic illustration of the anomalous Zeeman effect*

The anomalous Zeeman effect on the 2p level is illustrated in Figure 3.53. The 2p level when $B = 0$ has been indicated, the values of the magnetic quantum number $m_j$ taking values from $-j$ to $+j$, hence $(2j + 1)$. This leads to four sublevels for the 2 $^2p_{3/2}$ state and two sublevels for the 2 $^2p_{1/2}$ and 1 $^2s_{1/2}$ states. Transition (a) reflects the theoretical Lyman alpha line generated by the 2p → 1s transition. Transitions (b) reflect the fine structure of the 2p level due to spin–orbit interaction. Transitions (c) reflect the anomalous Zeeman effect due to the fact that the intensity of the spin–orbit interaction outweighs the action of the magnetic field applied. A total of 10 transitions are allowed.

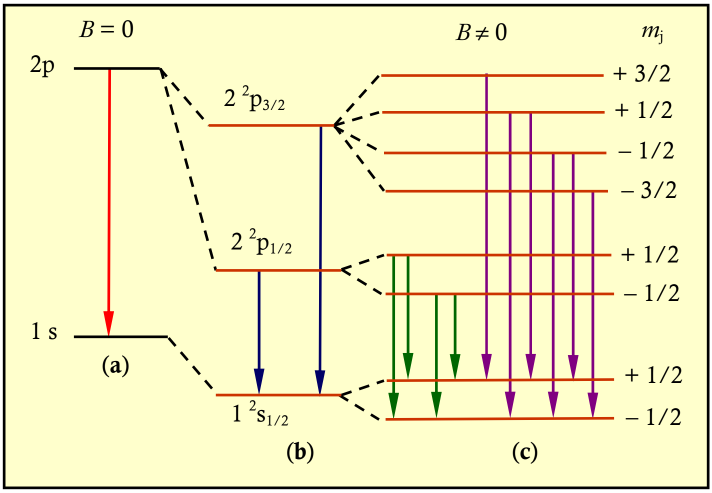

**Figure 3.53.** *Illustration of the anomalous Zeeman effect on the 2p level of hydrogen-like systems*

## 3.8.18. *Solution 18 – Fine structure of the resonance line of the hydrogen atom*

The quantized energy of weakly relativistic hydrogen-like systems is given by the following Dirac formula:

$$E_{nj} = -\frac{Z^2\alpha^2 mc^2}{2n^2} - \frac{Z^4\alpha^4 mc^2}{2n^3}\left(\frac{1}{j+1/2} - \frac{3}{4n}\right) \qquad [3.242]$$

(1) *Wavelength of the resonance line*

The spectral series corresponding to $n \to p$ electron transitions are given by the formula:

$$\frac{1}{\lambda} = R_H\left(\frac{1}{n^2} - \frac{1}{p^2}\right) \qquad [3.243]$$

The wavelength of the resonance line of the hydrogen atom corresponds to the first line in the Lyman series (1 ↔ 2 transition), or according to [3.243]:

$$\lambda_\alpha = \frac{4}{3R_H} \qquad [3.244a]$$

N.A.– $R_H = 10{,}967{,}758\ \text{m}^{-1} \Rightarrow \lambda_\alpha = 121.6\ \text{nm}$

(2) *Fine structure of Lyman alpha line, schematic illustration*

According to the Bohr–Sommerfeld theory, the Lyman alpha transition involves the quantum states: 1s ($n = 1$, $\ell = 0$) and 2s ($n = 2$, $\ell = 0$), 2p ($n = 2$, $\ell = 1$). Using the spectroscopic notation, the 1*s* state corresponds to $1^2s_{1/2}$ level and the 2p state to $2^2p_{1/2}$ and $2^2p_{3/2}$ levels.

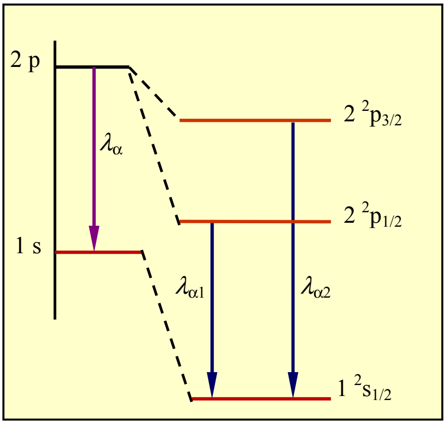

**Figure 3.54.** *Fine structure of the Lyman alpha line of the hydrogen atom*

The splitting of the 2p level due to the spin–orbit coupling determines the splitting of the Lyman alpha line into three components. This reflects the fine structure of this line, as indicated in Figure 3.54.

(3) *Determination of wavelengths* $\lambda_1$ *and* $\lambda_2$, $\Delta\lambda$ *gap*

The two wavelengths $\lambda_{\alpha 1}$ and $\lambda_{\alpha 2}$ involved in the fine structure of the resonance line of the hydrogen atom result from the transitions:

- $\lambda_{\alpha 1}$: $2^2p_{1/2} \to 1^2s_{1/2}$ transition;
- $\lambda_{\alpha 2}$: $2^2p_{3/2} \to 1^2s_{1/2}$ transition.

Moreover, according to the Bohr frequency condition, we obtain:

$$\frac{hc}{\lambda_{\alpha_1}} = E_{2,1/2} - E_{1,1/2} \quad ; \quad \frac{hc}{\lambda_{\alpha_2}} = E_{2,3/2} - E_{1,1/2} \qquad [3.244b]$$

Using [3.242], for the hydrogen atom ($Z=1$) we obtain:

$$\begin{cases} E_{1,1/2} = -\dfrac{\alpha^2 mc^2}{2}\left(1 + \dfrac{\alpha^2}{4}\right) \\ E_{2,3/2} = -\dfrac{\alpha^2 mc^2}{2}\left(\dfrac{1}{4} + \dfrac{\alpha^2}{64}\right) \\ E_{2,1/2} = -\dfrac{\alpha^2 mc^2}{2}\left(\dfrac{1}{4} + \dfrac{5\alpha^2}{64}\right) \end{cases}$$

Hence:

$$\begin{cases} E_{2,3/2} - E_{1,1/2} = \dfrac{\alpha^2 mc^2}{2}\left(\dfrac{3}{4} + \dfrac{15\alpha^2}{64}\right) \\ E_{2,1/2} - E_{1,1/2} = \dfrac{\alpha^2 mc^2}{2}\left(\dfrac{3}{4} + \dfrac{11\alpha^2}{64}\right) \end{cases} \qquad [3.244c]$$

Knowing that $Ryd/hc = R_H = 10{,}967{,}770\ \text{m}^{-1}$, we obtain:

$$\begin{cases} \dfrac{1}{\lambda_{\alpha_1}} = \dfrac{Ryd}{hc}\left(\dfrac{3}{4} + \dfrac{11\alpha^2}{64}\right) \\ \dfrac{1}{\lambda_{\alpha_2}} = \dfrac{Ryd}{hc}\left(\dfrac{3}{4} + \dfrac{15\alpha^2}{64}\right) \end{cases}$$

Hence:

$$\begin{cases} \dfrac{1}{\lambda_{\alpha_1}} = 10967770\left(\dfrac{3}{4} + \dfrac{11\alpha^2}{64}\right) \\ \dfrac{1}{\lambda_{\alpha_2}} = 10967770\left(\dfrac{3}{4} + \dfrac{15\alpha^2}{64}\right) \end{cases} \qquad [3.245]$$

N.A.– $\alpha^2 = 5.325 \times 10^{-5} \Rightarrow \lambda_{\alpha 1} = 121.5668329$ nm; $\lambda_{\alpha 2} = 121.5662934$ nm. The wavelength gap is then: $\Delta\lambda = \lambda_{\alpha 1} - \lambda_{\alpha 2} = 5.395 \times 10^{-4}$ nm.

## 3.8.19. *Solution 19 – Fine structure of n = 2 level of the hydrogen atom*

Figure 3.55 indicates the energy gaps measured by Lamb and Retherford.

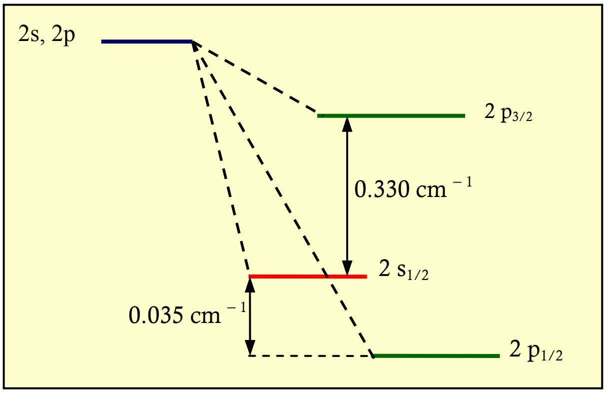

**Figure 3.55.** *Energy gaps between $2p_{3/2}$ and $2s_{1/2}$ levels and between $2p_{1/2}$ and $2s_{1/2}$ sublevels*

(1) *Theoretical explanation*

The $2s_{1/2}$ and $2p_{1/2}$ levels have the same energy as indicated by the formula [3.242]. The relative arrangement of these levels cannot be theoretically explained using Dirac theory.

(2) *Expression, comparison*

Using [3.242], the energy gap $\Delta E$ between the $2s_{1/2}$ and $2p_{3/2}$ levels is equal to:

$$\Delta E = -\frac{\alpha^2 mc^2}{2}\left[\frac{1}{4} + \frac{\alpha^2}{8}\left(\frac{1}{2} - \frac{3}{8}\right)\right] + \frac{\alpha^2 mc^2}{2}\left[\frac{1}{4} + \frac{\alpha^2}{8}\left(1 - \frac{3}{8}\right)\right] \qquad [3.246]$$

After arrangement:

$$\Delta E = \frac{\alpha^4 mc^2}{32} \qquad [3.247]$$

Inserting the spectroscopic number $\bar{\nu} = \frac{1}{\lambda}$, we have:

$$\Delta E = \frac{hc}{\lambda} = hc\bar{\nu} = \frac{\alpha^4 mc^2}{32}$$

Hence:

$$\bar{\nu} = \frac{\alpha^4 mc^2}{32} \times \left(\frac{eV}{hc}\right) \qquad [3.248]$$

N.A.– $\bar{\nu} = 0.365\ \text{cm}^{-1}$; $\Delta E = 4.528 \times 10^{-5}$ eV.

The theoretical result $\bar{\nu} = 0.365\ \text{cm}^{-1}$ is in good agreement with the measures resulting from Lamb and Retherford experiments giving the value 0.330 $\text{cm}^{-1}$. The accuracy of the calculations is however average, since |0.365 – 0.330|/0.330 = 10.6%. This is mainly due to the fact that Dirac theory does not integrate the properties due to photon vacuum and that are responsible for the Lamb shift (see section A5.1) between $2s_{1/2}$ and $2p_{1/2}$ levels. For example, Dirac theory predicts a zero gap between $2s_{1/2}$ and $2p_{1/2}$ levels, while experiments indicate a value of 0.035 $\text{cm}^{-1}$ (see Figure 3.55).

(3) *Spectral line due to* $2s_{1/2} \rightarrow 2p_{1/2}$ *transition*

The spectrum of the hydrogen atom contains a spectral line due to the $2s_{1/2} \rightarrow 2p_{1/2}$ transition. This line is allowed by the selection rule $\Delta\ell = \pm 1$.

(4) *Spectral line due to* $2p_{1/2} \rightarrow 2p_{3/2}$ *transition*

The $2p_{1/2} \rightarrow 2p_{3/2}$ electronic transition is forbidden, as it breaks the selection rule $\Delta\ell = \pm 1$.

### 3.8.20. *Solution 20 – Illustration of complex Zeeman effect on the yellow line of sodium, selection rules*

The yellow sodium *D*-line resulting from the 3p → 3s transition is constituted by two very close lines denoted $D_1$ (589.0 nm) and $D_2$ (589.6 nm).

(1) *Schematic illustration*

The electron configuration of sodium $^{23}$Na is: $1s^2 2s^2 2p^6 3s^1$.

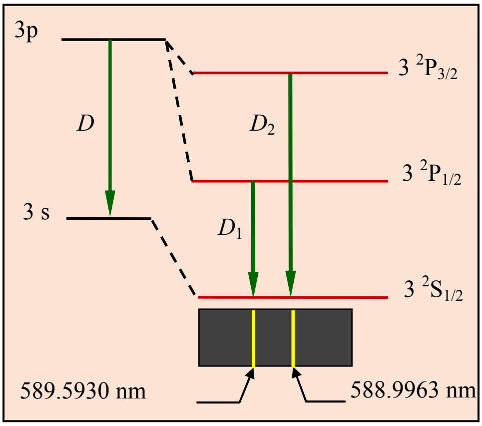

**Figure 3.56.** *Illustration of the fine structure of the yellow sodium D-line*

Knowing that the valence electron occupies the $3s^1$ state ($n = 3$, $\ell = 0$, 1 or 2), according to the spectroscopic notation $^{2S+1}L_J$, we obtain the following states: $S = ½$. Level multiplicity is $2S + 1 = 2$.

– For $\ell = 0, J = 1/2$: we obtain the $3\ ^2S_{1/2}$ level;

– For $\ell = 1$, $J = 1/2$ or $3/2$: we obtain the two terms $3\ ^2P_{1/2}$ and $3\ ^2P_{3/2}$. The yellow D-line due to radiative 3s → 3p transition is therefore double.

We obtain the two $D_1$ and $D_2$ lines whose respective wavelengths are:

$$\lambda_1 = 589.5930 \text{ nm } (3^2P_{1/2} \to 3\ ^2S_{1/2}) \text{ and } \lambda_2 = 588.9963 \text{ nm } (3^2P_{3/2} \to 3^2S_{1/2})$$

This corresponds to a wavelength gap $\Delta\lambda = 0.5967$ nm $\approx 0.6$ nm. These transitions are illustrated in Figure 3.56.

(2) *Explanation*

The 3 $^2P_{3/2} \rightarrow 3\ ^2P_{1/2}$ transition is forbidden by the selection rule $\Delta\ell = \pm 1$.

## 3.8.21. *Solution 21 – Linear oscillator in the phase space, Bohr's angular momentum quantization principle*

Expressions [3.249] correspond respectively to the equation and to the area of an ellipse whose semimajor axis along *Oy* is *a* and semiminor axis along *Oz* is *b* in the Cartesian space:

$$\frac{y^2}{a^2} + \frac{z^2}{b^2} = 1\,;\ \oint z\,dy = \pi ab \qquad [3.249]$$

(1) *Linear oscillator quantization condition*

(1.1) *Schematic representation*

For more details, see Figure 3.57.

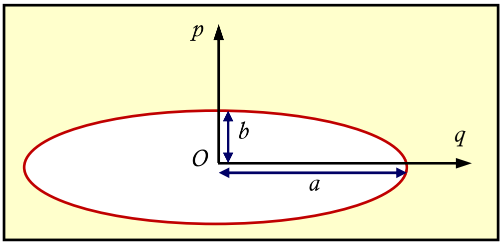

**Figure 3.57.** *Trajectory of the linear oscillator in the phase space*

(1.2) *Expression of the mechanical energy, differential equation*

– *Mechanical energy*

The mechanical energy of a classical linear oscillator of elongation $y$ is given by the relation:

$$E = E_c + V(y) = \frac{1}{2}mv^2 + V(y) \qquad [3.250]$$

The opposing spring force (verify that the curl of the opposing spring force is zero: therefore, it results from the gradient of a scalar function denoted by V):

$$f = -ky = -\frac{dV(y)}{dy} \tag{3.251}$$

Using [3.251], we obtain:

$$V(y) = \frac{1}{2}ky^2 + V(0) \tag{3.252}$$

Choosing the origin of coordinates so that $V(0) = 0$, the mechanical energy [3.250] can then be written knowing that $v = p/m$ as follows:

$$E = \frac{1}{2}mv^2 + \frac{1}{2}ky^2 \tag{3.253}$$

– *Differential equation*

The classical harmonic oscillator is a conservative system. Mechanical energy [3.253] is therefore constant. Hence:

$$\frac{dE}{dt} = mv\,\frac{dv}{dt} + ky\,\frac{dy}{dt} = 0$$

This leads to:

$$v\left(\frac{dv}{dt} + \frac{k}{m}y\right) = 0$$

Knowing that $v \neq 0$, the differential equation of the harmonic oscillator can be written as:

$$\frac{dv}{dt} + \frac{k}{m}y = 0 \Rightarrow \frac{d^2y}{dt^2} + \omega^2 y = 0 \tag{3.254}$$

Angular frequency $\omega$ and frequency $\nu$ of the oscillator are given by the relations:

$$\omega = \sqrt{\frac{k}{m}}\,;\, \nu = \frac{\omega}{2\pi} = \frac{1}{2\pi}\sqrt{\frac{k}{m}} \tag{3.255}$$

(1.3) *Expression of the mechanical energy in the phase space*

The mechanical energy of a linear oscillator in the phase space is deduced from [3.253] by substituting $y$ by the generalized coordinate $q$ and replacing $v$ by $p/m$. Hence:

$$E = \frac{p^2}{2m} + \frac{1}{2}kq^2 \cdot \qquad [3.256]$$

(1.4) *Proof*

If divided by $E$, equation [3.256] has the form of the equation of an ellipse:

$$1 = \frac{p^2}{2mE} + \frac{1}{2E}kq^2$$

$$\frac{p^2}{2mE} + \frac{q^2}{2E/k} = 1 \qquad [3.257]$$

The last equation [3.257] is actually an ellipse, provided that we make the following notations:

$$a = \sqrt{2E/k} \quad ; \quad b = \sqrt{2mE} \qquad [3.258]$$

Expressions [3.258] show that in the phase space, the semiminor axis $b$ and the semimajor axis $a$ are determined by the energy $E$ of the linear oscillator.

(1.5) *Expression*

The area of an ellipse in the phase space is deduced from the second equation [3.249] if $y$ and $z$ are substituted by $q$ and $p$, respectively, and [3.258] is taken into account. Hence:

$$\oint p\,dq = \pi ab$$

The following is obtained:

$$\oint p\,dq = 2\pi E\sqrt{\frac{m}{k}} = \frac{E}{\nu} \qquad [3.259]$$

Considering the last expression [3.255], we finally get:

$$\oint p\,dq = \frac{E}{\nu} \qquad [3.260]$$

The result [3.260] proves that the area of the ellipse in the phase space is determined by the ratio of energy $E$ to frequency $\nu$ of the linear oscillator.

(1.6) *Planck's quantization condition*

According to the theory of quanta, the energy of the quantum oscillator is $E = nh\nu$. This yields $E/\nu = nh$. Planck's quantization condition of the linear oscillator according to [3.260] can be written as:

$$\oint p\, dq = nh \qquad [3.261]$$

NOTE.– It should be kept in mind that the energy of the one-dimensional quantum oscillator is not equal to $nh\nu$. In fact, the precise expression of this energy is the following:

$$E_n = \hbar\omega\left(n + \frac{1}{2}\right) = h\nu\left(n + \frac{1}{2}\right) \qquad [3.262]$$

According to [3.262], the oscillation energy of the photon vacuum ($n = 0$) in the black body cavitation is $E_0 = h\nu/2$. The energy of Planck oscillator is therefore equal to:

$$E = E_\mathrm{n} - E_0 = nh\nu \qquad [3.263]$$

(2) *Bohr's condition for the quantization of the angular momentum*

(2.1) *Proof*

The speed of the electron is given by the relation:

$$v = r\omega = \frac{dq}{dt}\ ;\ \omega = \frac{d\varphi}{dt} \qquad [3.264]$$

This leads to:

$$\frac{dq}{dt} = \frac{d(r\varphi)}{dt} \Rightarrow q = r\varphi\ ;\ p = mv = rm\omega.$$

Hence:

$$p = rm\frac{d\varphi}{dt} \qquad [3.265]$$

(2.2) *Proof*

Bohr's model relies on the approximation of the uniform circular motion. Therefore, the speed $v$ and the radius $r$ of the electron orbit are constant. The angular momentum $L = mrv$ is consequently constant.

(2.3) *Bohr's quantization condition*

Considering Planck's linear oscillator quantization condition [3.261] and relations [3.265], we obtain:

$$\oint mvr\,d\varphi = nh \Rightarrow \oint L\,d\varphi = nh \qquad [3.266]$$

Let us consider Figure 3.58.

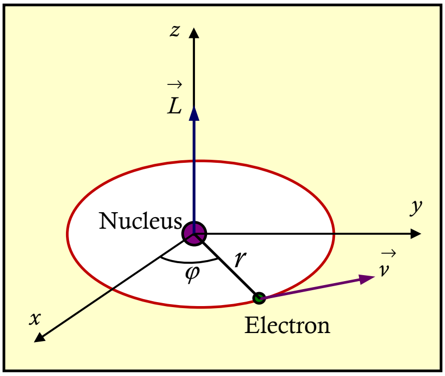

**Figure 3.58.** *Circular orbit characterized by the azimuthal angle $\varphi$*

Angle $\varphi$ varies between 0 and 2π, the orbit orientation being given by the motion direction, which is determined by the direction of the electron velocity (Figure 3.58). Hence [BEL 03, MOI 16]:

$$L\int_0^{2\pi} d\varphi = nh \Rightarrow L = n\frac{h}{2\pi} = n\hbar \cdot \qquad [3.267]$$

The above result is actually the angular momentum quantization condition, according to Bohr's first postulate [3.10].

# 4

# Matter Waves – Uncertainty Relations

### *General objective*

Gain knowledge on the properties of de Broglie's plane waves and on the physical contents of Heisenberg's uncertainty relations.

### *Specific objectives*

On completing this chapter, the reader should be able to:

– make the connection between light wave–particle duality and matter wave–particle duality;

– distinguish between light wave dispersion relation and matter wave dispersion relation;

– define de Broglie's plane wave;

– know the limits of de Broglie's plane wave;

– define the phase velocity and the group velocity of a matter wave;

– provide an interpretation of the phase velocity and group velocity of a matter wave;

– use de Broglie's relation;

– deduce Bohr's quantization principle from de Broglie's relation;

– provide an interpretation of the experiments of Davisson and Germer;

– know the physical contents of Heisenberg's uncertainty relations;

– provide evidence for the uncertainty principle by means of Heisenberg's microscope.

---

For color versions of the figures in this book, see www.iste.co.uk/sakho/quantum1.zip.

*Introduction to Quantum Mechanics 1: Thermal Radiation and Experimental Facts Regarding the Quantization of Matter,* First Edition. Ibrahima Sakho.

### *Prerequisites*

- particle and wave aspect of light;
- Planck–Einstein relations;
- structure of an electromagnetic plane wave;
- quantization of energy levels;
- energy and linear momentum of a relativistic particle;
- integration by parts.

## 4.1. De Broglie's matter waves

### 4.1.1. *From light wave to matter wave*

Until 1923, particles in the microcosm (electron, proton, nucleus, atom, etc.) were treated as such, being exclusively characterized by their particle-specific properties. A particular case is that of light constituted of photons, as light interference phenomena, photoelectric effect and Compton scattering indicate that light has both a wave- and a particle-like nature.

Toward 1923, **Louis de Broglie** proposed that matter particles have both wave- and particle-like properties, by analogy with the photon [BRO 25, SIV 86, PHI 03, SAK 08, SAK 11]. In his doctoral thesis (1924), he advanced the revolutionary hypothesis according to which any free matter particle of velocity $v$ is associated with a *matter wave* or *pilot wave*. Here is an excerpt of his writing:

> "The fundamental idea of [my 1924 thesis] was the following: 'The fact that, following Einstein's introduction of photons in light waves, one knew that light contains particles which are concentrations of energy incorporated into the wave, suggests that all particles, like the electron, must be transported by a wave into which it is incorporated. […] My essential idea was to extend to all particles the coexistence of waves and particles discovered by Einstein in 1905 in the case of light and photons'. 'Every particle of matter of mass m and velocity v must be 'associated' with a real wave' linked to the linear momentum by the relation λ = h/p […]".

The de Broglie wave is a plane wave given by the expression:

$$\Psi(\vec{r},t) = \Psi_0 e^{i(\vec{k}\vec{r}-\omega t)} \qquad [4.1]$$

In this expression, $\vec{k}$ is the *wave vector*, $\vec{r}$ designates the position vector of the particle with respect to an origin $O$ of the reference frame in which the particle is in uniform translational motion with velocity $v$, $\omega$ is the angular frequency of the wave and $\Psi_0$ is a constant.

Matter waves were experimentally proven to exist in 1927 by the *experiments of Davisson and Germer* on the *diffraction of electrons* by crystals (see section 4.1.4). It should however be kept in mind that *de Broglie's plane wave* [4.1] cannot represent the physical state of a particle. Indeed, from the point of view of quantum mechanics, which was elaborated two years later (1926), the quantity denoted by $\left|\Psi(\vec{r},t)\right|^2$ designates the *density of probability of finding* (see section 4.2.2) the particle at point $\vec{r}$ within element volume $dr^3$ at instant $t$.

Using de Broglie plane wave [4.1], we obtain:

$$\left|\Psi(\vec{r},t)\right|^2 = \Psi(\vec{r},t)\Psi(\vec{r},t)^* = \left|\Psi_0\right|^2 \qquad [4.2]$$

From a physical point of view, [4.2] reflects the fact that the *probability of finding* the particle at any point of space and at any instant is the same. This is quite obviously impossible, since the particle is necessarily located somewhere in space. *De Broglie's wave theory* was nevertheless the starting point in the elaboration of quantum mechanics, in which the wave function describing the physical state of a particle is a superposition of monochromatic plane waves of type [4.1] (see Chapter 1, Volume 2).

### 4.1.2. *De Broglie's relation*

The combination of wave- and particle-like properties of light is reflected by the following Planck–Einstein relations:

$$E = \hbar\omega \ ; \vec{p} = \hbar\vec{k} \qquad [4.3]$$

In the formulation of his wave theory, de Broglie sought to unify the wave–particle duality into a universal characteristic common to both photon and matter particles. Consequently, Planck–Einstein relations [4.3] established for the photon are also valid for any particle of matter driven by a wave of type [4.1]. Knowing that $k = 2\pi/\lambda$, we obtain:

$$p = \frac{h}{2\pi}k = \frac{h}{\lambda}$$

In the end, the wavelength of a particle of matter moving with linear momentum $p = mv$ is given by *de Broglie's relation*:

$$\lambda = \frac{h}{p} \qquad [4.4]$$

Let us note that de Broglie's relation [4.4] is valid for any free classical or relativistic particle in motion. $\lambda$ is known as the de Broglie wavelength.

**Louis Victor de Broglie** was a French mathematician and physicist. In physics, he is well-known for having postulated in 1924 the existence of waves associated with the particles of matter, which was confirmed by the experiments of Davisson and Germer in 1927. This postulate laid the foundation for wave mechanics and opened the way for the elaboration in 1926 of quantum mechanics formalism, which relies on the fundamental concept of a "wave". De Broglie was awarded the Nobel Prize for physics in 1929, at a very young age, 37, for his discovery of the wave nature of the particles of matter in motion.

**Box 4.1.** *De Broglie (1892–1987)*

**APPLICATION 4.1.–**

A particle of mass $m$, charge $q$ and virtually zero initial velocity is accelerated under constant voltage $U = 20$ kV. Calculate the de Broglie wavelength for:

– electron ($m = 9.1 \times 10^{-31}$ kg)

– proton ($m = 1.67 \times 10^{-27}$ kg)

– $\alpha$ particle ($m_2 = 6.64 \times 10^{-27}$ kg)

*Given data.* $e = 1.6 \times 10^{-19}$ C; $h = 6.63 \times 10^{-34}$ J · s

**Solution.** According to the work–energy theorem:

$$|q|U = \frac{1}{2}mv^2 \Rightarrow v = \sqrt{\frac{2|q|U}{m}} \qquad [4.5]$$

Using [4.5], the de Broglie wavelength [4.4] can be written as follows:

$$\lambda = \frac{h}{\sqrt{2|q|mU}} \qquad [4.6]$$

N.A.–

- electron: $\lambda_1 = 8.7 \times 10^{-12}$ m = 8.7 pm
- proton: $\lambda_2 = 2.0 \times 10^{-13}$ m = 0.2 pm
- $\alpha$ particle ($He^{2+}$): $\lambda_3 = 7.2 \times 10^{-14}$ m = 0.07 pm

The calculated wavelengths are very short compared to atomic sizes of the order of 1 Å = $10^{-10}$ m (the interplanar spacing of the crystal lattice used in the experiments of Davisson and Germer is $d = 2.150 \times 10^{-10}$ m). This is due to the high accelerating voltage of 20 kV. Nevertheless, these results suggest that electrons should be used to provide evidence of the existence of waves associated with particles of matter using lower accelerating voltages. This was the approach adopted by Davisson and Germer during their experiments of electron diffraction by nickel crystals with a voltage ranging between 32.0 and 42.5 V (see section 4.1.6).

### 4.1.3. *Law of dispersion of matter waves*

The following relations are verified for the photon:

$$\omega = \frac{2\pi c}{\lambda} \; ; \; k = \frac{2\pi}{\lambda} \tag{4.7}$$

The *dispersion relation* for a monochromatic plane light wave propagating through a vacuum can be deduced from [4.4]:

$$\omega(k) = ck \tag{4.8}$$

For relativistic particles whose rest mass $m_0$ is non-zero, the total energy $E$ and linear momentum $p$ are related by [2.41]. Hence:

$$E^2 = p^2c^2 + m_0^2c^4$$

This leads to:

$$\left(\frac{E}{c}\right)^2 - p^2 = (m_0c)^2 \tag{4.9}$$

Using relations [4.3], we obtain:

$$\left(\frac{\hbar\omega}{c}\right)^2 - (\hbar k)^2 = (m_0c)^2 \tag{4.10}$$

Equation [4.10] expresses the law of dispersion of de Broglie matter waves. It can be noted that it is a generalization of the relation of dispersion of a monochromatic plane wave [4.8] resulting from [4.10] if $m_0 = 0$ for the photon. Hence, the de Broglie plane wave undergoes dispersion during propagation. This dispersion further supports the fact that the plane wave [4.1] cannot represent the physical state of a particle.

**APPLICATION 4.2.–**

Prove that for a free classical particle, the law of dispersion of matter waves has the form $\omega(k) = f(k)$, where $f(k)$ is a function of $k$ to be specified.

**Solution.** A free particle is not subjected to any force field. Therefore, the potential energy of the {particle-field} system is zero. The total energy $E$ of the classical particle is therefore equal to its kinetic energy. If $v$ is substituted by $p/m$ and relations [4.3] are taken into account, we have:

$$E = \frac{\hbar^2 k^2}{2m}$$

Hence:

$$\omega(k) = \frac{\hbar k^2}{2m} \tag{4.11}$$

Dispersion relation [4.11], which is valid for a free classical particle, is very different from dispersion relation [4.8] of a plane light wave.

### 4.1.4. *Phase velocity and group velocity*

Let us consider a one-dimensional plane wave that is propagating in the ascending direction of $x$, for example. Using [4.1], we obtain:

$$\Psi(x,t) = \Psi_0 \, e^{i(kx-\omega t)} \tag{4.12}$$

The phase velocity of the de Broglie wave can be evaluated if a constant value of the wave phase is chosen: $\varphi(t) = kx - \omega t$ = constant. Hence:

$$\frac{d\varphi}{dt} = k\frac{dx}{dt} - \omega\frac{dt}{dt} = 0 \tag{4.13}$$

If $v_\varphi$ designates the *phase velocity* ($v_\varphi = dx/dt$), we have according to [4.13]:

$$\frac{d\varphi}{dt} = kv_\varphi - \omega = 0$$

Hence:

$$v_\varphi = \frac{\omega}{k} \qquad [4.14]$$

According to relations [4.3] postulated by de Broglie for the free particle, we have: $\omega/k = E/p$. Hence, the phase velocity can be written according to [4.14]:

$$v_\varphi = \frac{E}{p} \qquad [4.15]$$

Moreover, for a relativistic particle, the total energy is $E = mc^2$ and the linear momentum $p = mv$. Therefore, expression [4.15] can be written as:

$$v_\varphi = \frac{c^2}{v} \qquad [4.16]$$

Knowing that $c$ designates the limit velocity, then $v < c$. Relation [4.16] then shows that phase velocity is above the limit velocity: $v_{ph} > c$. This obviously has no physical meaning. This result is a further confirmation of the lack of validity of de Broglie waves for the description of a physical state of the particle. Let us note that a plane light wave propagates in vacuum with $v = c$. Consequently, according to [4.16], $v_\varphi = c$. This is a satisfactory result, since no constraint is imposed to the phase velocity. The phase velocity of plane light waves that are propagating in vacuum is $v_\varphi = c$ irrespective of the wave frequency: there is no dispersion in vacuum.

Such waves undergo dispersion only in a medium of refractive index $n$ since in this case, $v_\varphi = c/n$. It is the case of the prism (see Figure 3.2) whose law of dispersion is given by Cauchy formula [3.1].

Moreover, within de Broglie's wave model, the particle of matter moves at velocity $v$. We should then be able to use the pilot wave [4.1] to find this velocity. This requires the use of a *wave packet* constituted of [4.1] type of plane waves.

For the sake of simplicity, let us consider a wave packet or a *wave group* constituted of two monochromatic plane waves $\Psi_1$ ($x$, $t$) and $\Psi_2$ ($x$, $t$) of the same amplitude $A$ that propagate in the ascending direction of $x$. Using [4.12], we have:

$$\Psi_1(x,t) = Ae^{i(k_1x-\omega_1t)};\ \Psi_2(x,t) = Ae^{i(k_2x-\omega_2t)} \qquad [4.17]$$

The global wave function corresponding to the wave packet is:

$$\Psi(x,t) = \Psi_1(x,t) + \Psi_2(x,t) = Ae^{i(k_1x-\omega_1t)} + Ae^{i(k_2x-\omega_2t)} \qquad [4.18]$$

Let us give [4.18] the form of [4.12]. For this purpose, we write:

$$k_1x - \omega_1t = (k_1x - \omega_1t) - (k_2x - \omega_2t) + (k_2x - \omega_2t)$$

$$k_2x - \omega_2t = (k_2x - \omega_2t) - (k_1x - \omega_1t) + (k_1x - \omega_1t)$$

Hence:

$$k_1x - \omega_1t = (k_1 - k_2)x - (\omega_1 - \omega_2)t + (k_2x - \omega_2t) \qquad [4.19]$$

$$k_2x - \omega_2t = -(k_1 - k_2)x + (\omega_1 - \omega_2)t + (k_1x - \omega_1t)$$

Let us insert the following variations and mean values:

$$\Delta k = (k_1 - k_2)/2;\ \Delta\omega = (\omega_1 - \omega_2)/2;\ k_0 = (k_1 + k_2)/2\ ;\ \omega_0 = (\omega_1 + \omega_2)/2$$

Using these relations, we have:

$$k_1 = k_0 + \Delta k\ ;\ k_2 = k_0 - \Delta k\ ;\ \omega_1 = \omega_0 + \Delta\omega\ ;\omega_2 = \omega_0 - \Delta\omega \qquad [4.20]$$

Using [4.20], relations [4.19] become:

$$k_1x - \omega_1t = 2\Delta k\, x - 2\Delta\omega\, t + (k_2x - \omega_2t) \qquad [4.21]$$

$$k_2x - \omega_2t = -2\Delta k\, x + 2\Delta\omega\, t + (k_1x - \omega_1t)$$

Relations [4.21] are real irrespective of the frequencies of the two waves [4.17]. In particular, for waves of very close frequencies, the approximation $k_1 \approx k_2 \approx k_0$ and $\omega_1 \approx \omega_2 \approx \omega_0$ can be adopted. Relations [4.21] can therefore be written as follows:

$$k_1x - \omega_1t = 2\Delta k\, x - 2\Delta\omega\, t + (k_0x - \omega_0t) \qquad [4.22]$$

$$k_2x - \omega_2t = -2\Delta k\, x + 2\Delta\omega\, t + (k_0x - \omega_0t)$$

Using [4.22], the global wave function [4.18] can be written in the form:

$$\Psi(x,t) = Ae^{2i(\Delta k\, x - \Delta\omega t)} \times e^{i(k_0x-\omega_0t)} + e^{-2i(\Delta k\, x - \Delta\omega t)} \times e^{i(k_0x-\omega_0t)}$$

Hence:

$$\Psi(x,t) = A\left[e^{2i(\Delta k\, x - \Delta\omega t)} + e^{-2i(\Delta k\, x - \Delta\omega t)}\right] \times e^{i(k_0 x - \omega_0 t)} \qquad [4.23]$$

Expanding the factor between square brackets, we have:

$$\Psi(x,t) = 2\cos 2(\Delta k\, x - \Delta\omega t) \times e^{i(k_0 x - \omega_0 t)} \qquad [4.24]$$

Let us consider:

$$A_0\,(x,\,t) = 2A\,\cos 2(\Delta k\, x - \Delta\omega\, t) \qquad [4.25]$$

The wave function [4.24] is written as:

$$\Psi(x,t) = A_0(x,t)\; e^{i(k_0 x - \omega_0 t)} \qquad [4.26]$$

The global wave function [4.26] would be a de Broglie plane wave [4.12] if its amplitude [4.25] was constant. But amplitude $A_0\,(x,\,t)$ is constant if:

$$\Phi = \Delta kx - \Delta\omega\, t = \text{Cte} \qquad [4.27]$$

Let us then consider an observer that travels with velocity $v_g = dx/dt$ along $Ox$ axis. For such an observer, amplitude [4.25] verifies condition [4.27]. Hence [PÉR 86]:

$$\frac{d\Phi}{dt} = \Delta k\, dx - \Delta\omega\, d\,t = 0 \Rightarrow v_g = \frac{dx}{dt} = \frac{\Delta\omega}{\Delta k} \qquad [4.28]$$

By definition, velocity $v_g$ is referred to as *group velocity*, a characteristic of the group or wave packet [4.18]. By extension, for an arbitrary packet of plane waves of variable amplitude, group velocity is equal to the derivative of the angular frequency $\omega$ with respect to the wave number $k$, hence:

$$v_g = \frac{d\omega}{dk} \qquad [4.29]$$

Knowing that $E = \hbar\omega$ and $p = \hbar k$, we have:

$$v_g = \frac{dE}{dp} \qquad [4.30]$$

**APPLICATION 4.3.–**

> Prove that the group velocity of matter waves is equal to the velocity $v$ of the free particle. Draw a conclusion.
>
> **Solution.** According to the special theory of relativity, the total energy $E$ and the linear momentum $p$ of a particle are linked by relation [2.41]:
>
> $$E^2 = p^2c^2 + m_0^2c^4 \Rightarrow EdE = pc^2dp \quad [4.31]$$
>
> Using [4.31], we obtain according to [4.30]:
>
> $$v_{gr} = \frac{dE}{dp} = \frac{pc^2}{E} = \frac{mvc^2}{mc^2} = v \quad [4.32]$$
>
> Result [4.32] shows that the group velocity of de Broglie matter waves is equal to the velocity of the free particle.

CONCLUSION.– Unlike phase velocity, group velocity is an observable (measurable) quantity.

### 4.1.5. *Bohr's quantization principle and de Broglie hypothesis*

According to de Broglie's theory of matter waves applied to hydrogen-like systems, for example, the pilot wave associated with the electron oscillates along the Bohr circular orbit, as shown in Figure 4.1. As it can be noted in the same figure, the pilot wave associated with the electron is stationary. The wave amplitude is the same at any point, the energy carried by the wave being confined in the electron. Therefore, no energy is lost by radiation.

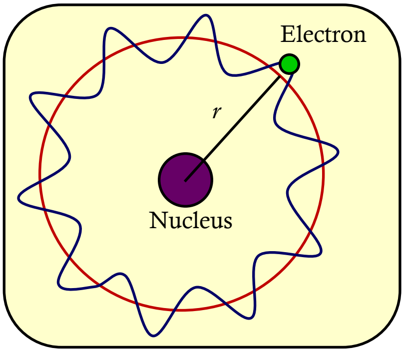

**Figure 4.1.** *De Broglie wave orbit*

The *condition for wave orbit stability* requires the circumference of the electron circular orbit to be a multiple of the de Broglie wavelength. Hence:

$$2\pi r = n\lambda \qquad [4.33]$$

Using the de Broglie relation [4.4] and [4.33], we obtain [SIV 86, MOI 16]:

$$mvr = n\frac{h}{2\pi}$$

The above can finally be written as:

$$L = n\hbar \qquad [4.34]$$

This corresponds to Bohr's principle for angular momentum quantization.

### APPLICATION 4.4.–

Is the de Broglie wave a standing wave if the number of nodes is odd?

As a first step, define the notions of *nodes* and *antinodes of a wave function* and then use a diagram to answer the question. Consider 10 nodes and then 5 nodes.

**Solution.** By definition, the number of *nodes* of a wave function is equal to the number of points in space where the wave function is zero. In other terms, it is the set of points where the wave function does not oscillate (the amplitude of the wave function is zero in a considered node). The points of maximal amplitude where the wave function oscillates are known as *antinodes*. For a de Broglie plane wave, nodes and antinodes alternate. It is worth noting that the distance between two successive nodes is $\lambda/2$ (Figure 4.2).

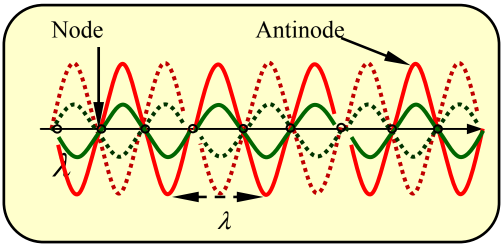

**Figure 4.2.** *Antinodes and nodes of a de Broglie plane wave*

Figure 4.2 shows a total number of nodes $N = 10$. The corresponding number of wavelengths is:

$$n = N\frac{\lambda}{2} = 5\lambda \tag{4.35}$$

Result [4.35] signifies that the number of nodes is a multiple of the wavelength (*an equivalent statement is that the circumference of the electron circular orbit is a multiple of the wavelength*): the wave function is therefore stationary and the electron orbit is stable. Let us now consider the case of an odd number of nodes; for example, $N = 5$. Then the number of wavelengths is:

$$n = N\frac{\lambda}{2} = \frac{5}{2}\lambda \tag{4.36}$$

Result [4.36] reflects the fact that the circumference of the electron circular orbit is a half-integer multiple of the wavelength: the wave function is no longer stationary and the electron orbit is unstable.

### 4.1.6. *Experimental confirmation, experiment of Davisson and Germer*

The experiment involving electron diffraction by crystals conducted in 1927 by **Clinton Davisson** and **Lester Germer** made it possible to confirm de Broglie's wave hypothesis. Indeed, if matter waves were associated with electrons, as de Broglie proposed, then these waves should be diffracted by the atoms in a crystal lattice. For certain values of the diffusion angle $\theta$, the diffracted waves should add up (constructive interferences) in the interference field [DAV 27, GUY 03, PÉR 86, SIV 86, THO 10]. For other values of $\theta$, these waves should cancel out (destructive interferences).

According to *Bragg's condition*, interferences are constructive if:

$$2\,d\sin\theta = n\lambda \tag{4.37}$$

In *Bragg's law* expressed by [4.37]:

– $d$ is the interplanar spacing (i.e. the perpendicular distance between two crystal planes);

– $\theta$ (Bragg's angle) is the deviation half-angle: (half of the angle between the direction of the initial beam and the direction of the detector);

– $n$ is the order of diffraction (strictly positive integer);

– $\lambda$ designates the wavelength of X-rays.

In the international system, $d$ and $\lambda$ are expressed in meters (m) and $\theta$ in radians (rad).

**William Lawrence Bragg** was an Australian physicist. He is especially known for his analysis of crystal structures using X-rays. In 1912, together with his father, Sir William Henry Bragg (1862–1942), he discovered the empirical law of X-rays diffraction by crystals. Known as Bragg's law in their honor, this law makes it possible to calculate the position of atoms in a crystal by using how the crystal lattice diffracts the X-rays. Henry Bragg taught at the University of Adelaide in Australia during 1886–1908, which explains the Australian nationality of his son. Lawrence Bragg and his father were the recipients of the Nobel Prize for physics in 1915 for their work on X-ray diffraction by crystal structures.

**Box 4.2.** *Bragg (1890–1971)*

Figure 4.3 illustrates the diffraction of a beam of X photons by a crystal. The Bragg angle, as well as the interplanar spacing, is indicated in this figure.

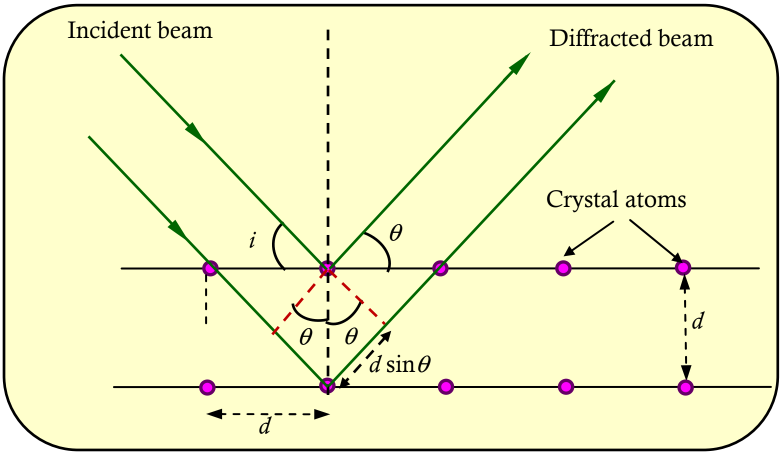

**Figure 4.3.** *Elastic scattering of electrons by a crystal: the incident beam encounters a regular alignment of crystal atoms and scattered under an angle $\theta$*

Between 1925 and 1927, **Davisson** and **Germer** conducted electron diffraction with nickel crystals. The simplified experimental setup used by these authors is schematically represented in Figure 4.4. An electron gun emits electrons that are accelerated under an accelerating voltage $U = V_1 - V_2$. They hit a nickel Ni monocrystal and are then scattered under an angle $\theta$ with respect to their incident direction. When the electron beam hits the crystal lattice, the matter waves associated with the electrons are diffracted by the nickel atoms. A mobile detector is used to study the dependence of the angle on the intensity of the diffracted beam. A galvanometer that is not shown in the figure measures the intensity *i* due to electrons whose associated waves are diffracted.

Intensity is then maximal for scattering angles $\theta$ for which the diffracted waves are in phase. Figure 4.5 shows an extract of the intensity *i* variation with accelerating voltage *U*. The current is maximal for $\theta = 80°$ and $U = 33$ V [PÉR 86].

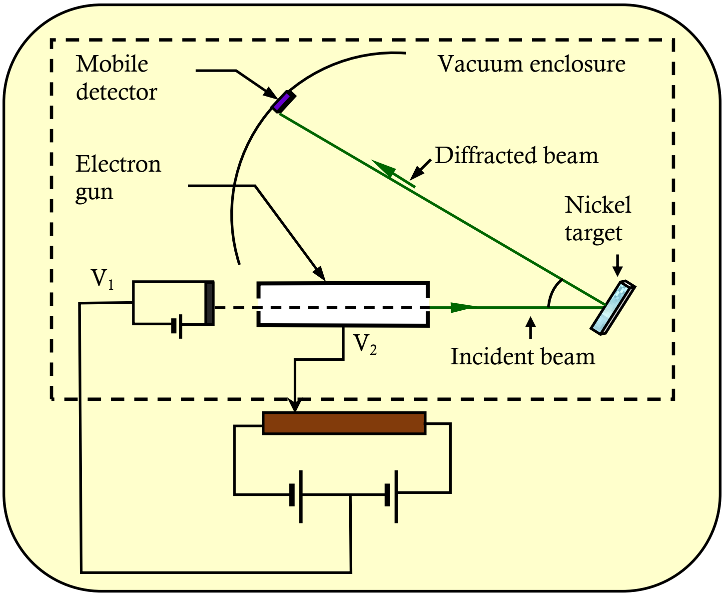

**Figure 4.4.** *Simplified diagram of the Davisson and Germer experimental setup*

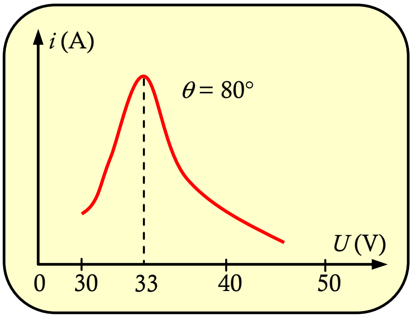

**Figure 4.5.** *Variation of electronic current intensity i with accelerating voltage U*

Table 4.1 summarizes several experimental results obtained by Davisson and Germer corresponding to maximal values of the electric current intensity $i$ measured by the galvanometer $G$. The measurements are conducted in two lattice planes {100} and {111} (see Note (1) of this chapter).

| | Lattice plane {100} | | | | |
|---|---|---|---|---|---|
| $\theta$(°) | 60 | 65 | 70 | 75 | 80 |
| $U$(V) | 42.5 | 38.5 | 36.0 | 35.0 | 33.0 |
| | Lattice plane {111} | | | | |
| $\theta$(°) | 60 | 65 | 70 | 75 | 80 |
| $U$(V) | – | 35.0 | 36.5 | 35.0 | 34.0 |

**Table 4.1.** *Excerpt of the experimental results of Davisson and Germer [DAV 27]*

According to experiments, diffracted electrons have a preferred direction. Diffracted waves meet de Bragg's condition [4.37]. Figure 4.6 reproduces an excerpt of the diffraction curves, indicating a maximum of intensity for a scattering angle of 50° corresponding to a voltage of 54 V [DAV 27].

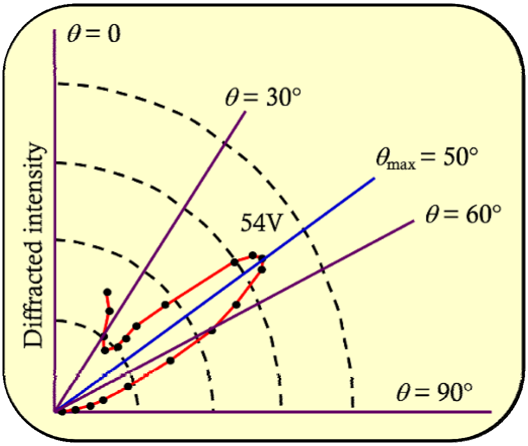

**Figure 4.6.** *Diffraction curve indicating a maximum of intensity for a diffraction angle of 50° corresponding to an accelerating voltage of 54 V*

The next step is the theoretical interpretation of the experimental observations (Figure 4.6) using de Broglie's model of matter waves. Relation [4.4] will be used for this purpose, as it involves the only experimentally verifiable quantity in the wave model.

According to the work–energy theorem applied between anode $A$ and cathode $C$ (*output velocity at the cathode can be considered negligible compared to velocity v of the electrons flowing through a hole in the anode*), we obtain:

$$E_c = eU \Rightarrow \frac{p^2}{2m} = eU \qquad [4.38]$$

Or according to de Broglie's relation [4.4], $\lambda = h/p$. Using [4.38], we have:

$$\lambda = \frac{h}{\sqrt{2emU}} \qquad [4.39]$$

Considering Bragg's condition [4.37], we can deduce the expression of the wavelength $\lambda$. Equalizing the resulting relation with [4.39], we have:

$$\sqrt{U}\sin\theta = \frac{n}{2d}\frac{h}{\sqrt{2em}} \qquad [4.40]$$

Formula [4.40] provides evidences for the order of interferences of the waves associated with electrons. Assuming that one of the peaks observed in the experiments of Davisson and Germer corresponds to $n = 2$, we have:

$$\sqrt{U}\sin\theta = A \qquad [4.41]$$

with:

$$A = \frac{h}{d\sqrt{2em}} \qquad [4.42]$$

Let us calculate constant $A$.

*Given data.* $h = 6.626 \times 10^{-34}$ J · s; $d = 2.150 \times 10^{-10}$ m; $m = 9.109 \times 10^{-31}$ kg; $e = 1.602 \times 10^{-19}$ C $\Rightarrow A = 5.71$

Using the $A$ value, [4.41] can be theoretically written as follows:

$$\sqrt{U}\sin\theta = 5.71 \qquad [4.43]$$

| $\theta$(°) | 60 | 65 | 70 | 75 | 80 |
|---|---|---|---|---|---|
| $U$ (V) | 42.5 | 38.5 | 36.0 | 35.0 | 33.0 |
| | 5.646 | 5.623 | 5.638 | 5.714 | 5.657 |

**Table 4.2.** *Experimental values of the product $\sqrt{U}\sin\theta = A$. The values are deduced from the experiment of Davisson and Germer*

If the waves associated with electrons exist, the experiments of Davisson and Germer must corroborate the theoretical result [4.43]. For this purpose, let us determine the values of the product $\sqrt{U}\sin\theta$ using the experimental results summarized in Table 4.1. Results are grouped in Table 4.2.

Let us determine the mean of the product $\sqrt{U}\sin\theta$ using the data in Table 4.2. We obtain:

$$\overline{\sqrt{U}\times\sin\theta} = 5.652 \approx 5.71 = A \qquad [4.44]$$

CONCLUSION.– The experiments of Davisson and Germer conducted in 1927 have brightly confirmed the existence of plane waves associated with matter particles, as stated by de Broglie's hypothesis in 1924.

Let us note that result [4.43] is valid for a single maximal value of the diffraction angle $\theta$ corresponding to a well-determined value of the accelerating voltage $U$. Strictly speaking, the order of interference $n = 2$ would correspond to $\theta = 75°$ and $U = 35.0$ V, as indicated by the results grouped in the fifth column of Table 4.2.

It is interesting to take advantage of the experimental results presented in Figure 4.6 using the *lattice formula*. Let us express the path difference $\delta$ between two waves issued by two neighboring slits separated by a distance $a = d$. As shown in Figure 4.3, we have: $\delta = d\,(\sin i + \sin\theta)$. Waves diffracted in different directions interfere for angles $\theta$ such that [BIE 06]:

$$\delta = d\,(\sin i + \sin\theta) = n\lambda \qquad [4.45]$$

Relation [4.45] expresses what is known as the lattice formula, which gives the deviation $\theta$ of the order $n$. Let us use relation [4.45] considering the experimental peak of Davisson and Germer, for which $\theta_{\max} = 50°$ and $U = 54.0$ V (Figure 4.6). Supposing that this peak has been obtained for an incidence angle $i = 0$ and that it corresponds to $n = 1$ [THO 10], we have:

$$\lambda = d\sin\theta_{\max} = 2.150\times10^{-10}\sin 50 \approx 1.65\ \text{Å} \qquad [4.46]$$

Let us now calculate the de Broglie wavelength using relation [4.39]. We consider the peak obtained by Davisson and Germer for which $U = 54.0$ V. Using the above numerical data, we find:

$$\lambda = 1.67\times10^{-10}\ \text{m} = 1.67\ \text{Å}$$

The de Broglie wavelength $\lambda$ = 1.67Å associated with diffracted electrons is in very good agreement with the experimental result $\lambda_{\text{exp}}$ = 1.65 Å [4.46]. The relative deviation is approximately 1.3%.

### APPLICATION 4.5.–

Diffractions of *slow neutrons* (or *thermal neutrons*) were observed in 1946 in nuclear reactors. Provide a theoretical justification for these observations.

*Given data.*

– *Temperature of thermal agitation of neutrons*: $T = 300$ K

– *Mass of the neutron*: $m = 1.675 \times 10^{-27}$ kg

– *Boltzmann constant*: $k = 1.381 \times 10^{-23}$ J · K$^{-1}$

**Solution.** A thermal or slow neutron is a neutron whose kinetic energy is equal to the energy of thermal agitation, hence:

$$E_c = \frac{1}{2}mv^2 = \frac{3}{2}kT \Rightarrow v = \sqrt{\frac{3kT}{m}} \qquad [4.47]$$

Using the de Broglie relation [4.4], we have according to [4.47]:

$$\lambda = \frac{h}{\sqrt{3kTm}}$$

N.A.– $\lambda = 1.452 \times 10^{-10}$ m ≈ 1.45 Å [4.48]

Result [4.46] shows that the wavelength of thermal neutrons has the same order of magnitude as the distances between atoms. This justifies the occurrence of neutron diffraction phenomena on crystals.

NOTES.–

(1) Table 4.1 indicates the experimental results obtained by Davisson and Germer for two lattice planes denoted by {100} and {111}. In the French literature, the notation of these planes features square brackets: [100] and [111]. Let us briefly explain this notation. By convention, a *family of lattice rows* is designated by three integers denoted by u, v and w. These integers are known as *indices of the family of lattice rows* and are written between square brackets. Indices u, v and w are the coordinates of the first node from the origin located on the lattice row of the family passing through the origin of $\vec{a}, \vec{b}, \vec{c}$ frame of reference. This is known as a [u, v, w] family

of lattice rows. The set of three relative integers h, k, l thus defined fully characterizes the family of planes considered. These three relative integers, arranged between brackets, are known as *Miller indices* of the family of planes. The family of lattice planes is denoted by (hkl), where h, k and l (except for the signs) are the numbers of equal segments cut by the family of planes (hkl), respectively, on the three base vectors $\vec{a}, \vec{b}, \vec{c}$ [MIL 14]. Figure 4.7 indicates the lattice rows [100], [010] and [001] as well as the lattice rows [110] and [111] corresponding to the directions indicated by vectors $\vec{a}, \vec{b}, \vec{c}$.

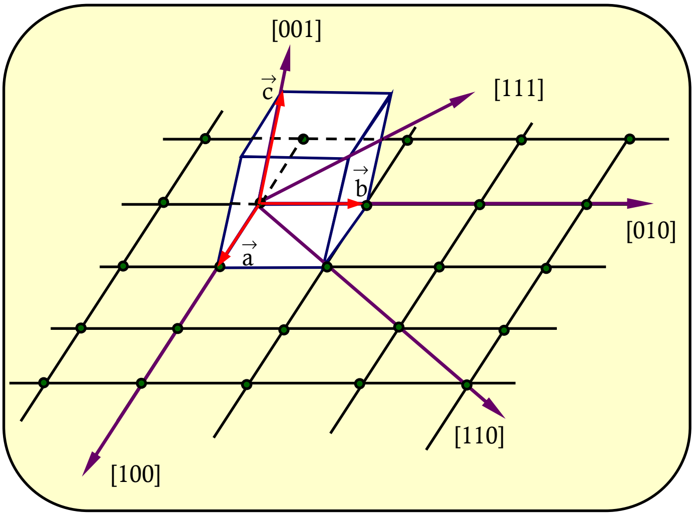

**Figure 4.7.** *Examples of indices of the main families of lattice rows*

(2) The first neutron diffraction experiment was conducted in 1945 by the American physicist **Ernest Omar Wollan** (1902–1984) at the Oak Ridge National Laboratory in the United States. In 1946, together with the American physicist **Clifford Glenwood Shull** (1915–2001), he established the basic principles of the *neutron diffraction* technique, which was successfully applied to several different materials. Neutrons are nucleons in the nucleus. Due to their relatively short lifetime (around 15 min), free neutrons in nature cannot be used for *neutron scattering* experiments. This is why free neutrons generated through *nuclear fission* in reactors are used. A monochromator makes it possible to obtain a monokinetic neutron beam. *Fissile sources* are mainly uranium 235 ($^{235}$U) or plutonium 239 ($^{239}$Pu) nuclei. Neutrons thus generated are slowed down by *heavy water* $D_2O$ (see Box 3.18, Chapter 3, Volume 1) in order to reach a wavelength of the order of angström ($10^{-10}$ m), which is the same order of magnitude of the distances between atoms in crystals. This makes it possible to use them in diffraction experiments, similarly to electrons (Davisson

and Germer experiments, Figure 4.4) or X-rays (Compton scattering experiments, Figure 2.14).

**Clinton Joseph Davisson** and **Lester Halbert Germer** were American physicists. In 1927, they conducted the landmark experiment (known as Davisson and Germer's experiment) that confirmed the existence of the matter waves postulated by de Broglie in 1924. Davisson shared with the British physicist **George Pager Thomson** (1892–1975) the Nobel Prize for physics in 1935 for their discovery of electron diffraction by crystals. Let us note in passing that George Pager Thomson is the son of the British physicist **Joseph John Thomson** (1856–1940), who received the Nobel Prize for physics in 1906 for his theoretical and experimental works on the electrical conductivity of gases, which provided concrete proof of electron existence.

**Box 4.3.** *Davisson (1881–1958); Germer (1896–1971)*

## 4.2. Heisenberg's uncertainty relations

### 4.2.1. *Uncertainty principle*

In classical mechanics, the dynamics of a particle is fully determined if its position $q$ and linear momentum $p$ in a one-dimensional context are known at each instant. The values of these two real and continuous *dynamic quantities* range between $-\infty$ and $+\infty$.

In the *phase space* of the particle defined by the $(q, p)$ pair, any physical quantity can be represented by a real function $f(q, p)$. If the position and velocity of a particle at instant $t_0$ are known, one can *simultaneously and precisely* determine the position and velocity of the particle at instant $t_0 + \Delta t$.

Things are completely different in quantum mechanics. The precise value of a physical quantity, such as position or velocity, can only be determined by measurement. In fact, the particles in the microcosm have wave-like properties. The measurement of a physical quantity defined for an arbitrary system involves the wave function describing the state of the system. This state is known as *state vector* (see Chapter 2). But during the measurement of one of the physical quantities of a system, the state vector undergoes an unpredictable leap, which in quantum mechanics is known as *fundamental perturbation* [COH 77]: *any measurement process perturbs the physical system under study*.

Hence, contrary to classical mechanics predictions, if the position of a particle is precisely known, its linear momentum is completely undetermined and vice versa. This *indeterminism* is rooted in a purely quantum principle referred to as the *indeterminacy principle* stating that the precision with which two *complementary* *physical quantities* of the same particle can be simultaneously known is fundamentally limited. This principle was proposed in 1927 by Heisenberg. It is therefore referred to as *Heisenberg's uncertainty principle*.

### 4.2.2. *Probabilistic interpretation of the wave function*

As mentioned above, the de Broglie monochromatic plane waves do not actually exist. A plane wave undergoes dispersion during its propagation: therefore it fills all the space. The particle associated with the plane wave is, so to speak, present throughout the space, at any point and at any instant. But a *physical wave* is always located at a point in space at a given instant *t*. This explains why the fundamental notion of the *wave function* has been introduced in quantum mechanics. The wave function corresponds to the representation of the *physical state of a system* (electron, nucleons, atom, molecule, etc.). The wave function describing the physical state of an arbitrary particle is a complex function denoted by $\Psi(\vec{r},t)$.

In 1926, **Max Born** proposed a *probabilistic interpretation* of the wave function. For bound states, the *density of the probability* $\rho(\vec{r}, t)$ of finding a particle at point $\vec{r}$ in space at an instant *t* is given by the relation:

$$\rho(\vec{r},t) = \left|\Psi(\vec{r},t)\right|^2 \tag{4.49}$$

In the definition [4.49], $\Psi(\vec{r},t)$ designates the *amplitude of the probability of presence* of the particle. This definition implies that the probability of finding the particle at point $\vec{r}$ in space at a given instant *t*, within the elementary volume $d^3r$, is given by the following relation:

$$dP(r) = \left|\Psi(\vec{r},t)\right|^2 d^3r \tag{4.50}$$

But the probability of a given event varies between 0 and 1. Knowing that the particle is present somewhere in the space, the integral of probability [4.50] is convergent, hence:

$$\int_{-\infty}^{+\infty} dP(r) = \int_{-\infty}^{+\infty} \left|\Psi(\vec{r},t)\right|^2 d^3r = 1 \tag{4.51}$$

$\Psi(\vec{r},t)$ functions are particular cases of *square-summable wave functions* for which the integral [4.51] is finite. The general properties of square-summable wave functions are presented in Chapter 5.

NOTE.– Copenhagen interpretation. The *Copenhagen school* or the *Copenhagen interpretation* is a school of thought providing a consistent interpretation of quantum mechanics. The probabilistic interpretation of the wave function advanced by **Max Born** was developed by the physicists of the Copenhagen school grouped around **Niels Bohr**. The Copenhagen interpretation considers that Heisenberg's uncertainty relations are due to the inevitable interaction between the measurement apparatus and the system subjected to measurement. Moreover, according to the Copenhagen interpretation, it makes no sense to speak about objects independently of any measurement; furthermore, it is impossible to know the evolution of a system between two measurements. This interpretation was proposed by **Niels Bohr**, **Werner Heisenberg**, **Pascual Jordan** and **Max Born**.

### 4.2.3. *Root mean square deviation*

According to the uncertainty principle, only a *statistical distribution* of the values of measured physical quantities is perfectly determined at any instant. Due to the randomness of detection, any measurement, no matter how precise, is always accompanied by a statistical uncertainty. To better understand this assertion, let us consider the measurement of a particle position $x$. This involves conducting the same measurement $N$ times on $N$ particles that are in the same state $\Psi(x, t)$. Position $x$ no longer has a single well-defined value. From a quantum point of view, the particle can be found in various regions in space with certain probabilities. The measurement of position $x$ yields a set of results characterized by a *mean value* $\langle x\rangle$ and a *root mean square deviation* or *spatial extension* $\Delta x$. The mean value $\langle x\rangle$ is defined by [COH 77, PHI 03]:

$$\langle x\rangle = \int_{-\infty}^{+\infty} x\left|\Psi(x,t)\right|^2 dx \qquad [4.52]$$

From a statistical perspective, the dispersion of measurements around the mean value $\langle x\rangle$ is measured by the *root mean square deviation* defined by:

$$(\Delta x)^2 = \left\langle \left(x-\langle x\rangle\right)^2 \right\rangle = \left\langle x^2 - 2x\langle x\rangle + \langle x\rangle^2 \right\rangle$$

Hence:

$$(\Delta x)^2 = \left\langle x^2 \right\rangle - \left\langle x \right\rangle^2 \qquad [4.53]$$

A similar result is obtained for the linear momentum $p_x = p$. Hence:

$$(\Delta p)^2 = \left\langle p^2 \right\rangle - \left\langle p \right\rangle^2 \qquad [4.54]$$

Using relations [4.48] and [4.49], we obtain the *root mean square deviations* (or *standard deviations*):

$$\Delta x = \sqrt{\left\langle x^2 \right\rangle - \left\langle x \right\rangle^2}\,;\Delta p = \sqrt{\left\langle p^2 \right\rangle - \left\langle p \right\rangle^2} \qquad [4.55]$$

If the precision $\delta x$ of the measurement apparatus is below $\Delta x$, we have a proper representation of a localized particle. However, if $\delta x$ is above $\Delta x$, the result of a measurement of the position $x$ cannot be stated with certainty. This is why $\Delta x$ is called uncertainty of $x$.

We should nevertheless keep in mind that quadratic deviations $\Delta x$ and $\Delta p$ have no relation with the resolution of the measurement apparatus. These quadratic deviations are intrinsically related to the interaction between the measurement apparatus (considered at *macroscopic scale*) and the quantum system (at *microscopic scale*).

### 4.2.4. *Spatial uncertainty relations, complementary variables*

*Heisenberg's spatial uncertainty relations* express the inequalities, indicating the higher precision limit attainable during simultaneous measurements of position and momentum variables. The variables satisfying Heisenberg's uncertainty relations are known as *complementary variables*. For spatial coordinates, we have the complementary variables grouped in $(x, p_x)$, $(y, p_y)$ and $(z, p_z)$ pairs.

Let us specify the order of magnitude of the product $\Delta q \Delta p_q$, $q = x, y$ or $z$. For this purpose, let us consider an experiment of diffraction of particles by a slit of width $a$. The particle is all the more localized as the slit is thin. The larger the diffraction spot, the higher the indeterminacy of the linear momentum $p$. Let us designate by $\theta$ the *angular half-width* of the central diffraction spot (Figure 4.8).

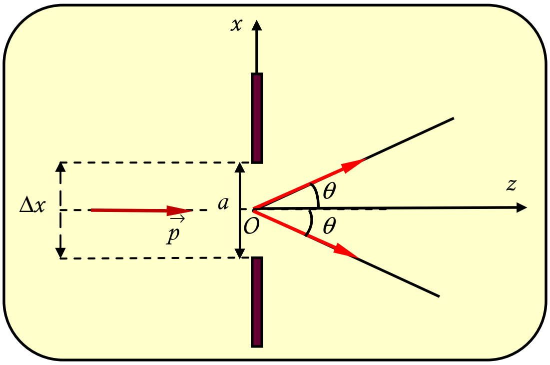

**Figure 4.8.** *Single-slit diffraction of a particle of linear momentum p*

Let us place the observer at the level of the central spot, which concentrates the majority of the diffracted particles. The uncertainty of position $x$ is of the order of magnitude of the diffraction slit. Moreover, due to diffraction, the component $p_x$ of the linear momentum along direction $Ox$ varies between $+p\sin\theta$ and $-p\sin\theta$. The uncertainty of linear momentum $p_x$ is then of the order of $p\sin\theta$. To summarize:

$$\Delta x \approx a;\ \Delta p_x \approx p\sin\theta \Rightarrow \Delta x\Delta p_x \approx ap\sin\theta \qquad [4.56]$$

Using the lattice formula [4.45] and admitting that the central spot corresponds to $n = 1$, we obtain:

$$a\sin\theta = \lambda = \frac{h}{p} \Rightarrow \sin\theta = \frac{h}{ap} \qquad [4.57]$$

Using [4.57], expression [4.56] is written (*circular permutation is subsequently applied*) as:

$$\Delta x\Delta p_x \approx h;\ \Delta y\Delta y_x \approx h;\ \Delta z\Delta p_z \approx h \qquad [4.58]$$

Results [4.58] provide only the orders of magnitude for $\Delta q\Delta p_q$ products. The uncertainty relations established by Heisenberg are generally written as follows:

$$\Delta x\Delta p_x \geq \frac{\hbar}{2}\ ;\ \Delta y\Delta p_y \geq \frac{\hbar}{2}\ ;\ \Delta z\Delta p_z \geq \frac{\hbar}{2} \qquad [4.59]$$

According to [4.59], if, for example, $\Delta x \to 0$, then $\Delta p_x \to \infty$ and vice versa. The uncertainty relations express the impossibility to simultaneously measure with precision the position $q$ and the linear momentum $p$ of a particle. However,

$\Delta q_i \Delta p_j$ ($i, j = x, y$ or $z$) does not admit a non-zero lower limit for $i \neq j$ ($\Delta x \Delta p_y = 0$). Moreover, relations [4.59] reject the classical notion of a trajectory, for which a particle's position and velocity are perfectly determined at every instant.

If the requirement is to confine the particles at a given point in space, their velocities (*therefore their linear momenta*) will be dispersed. Reciprocally, if the requirement is to have particles with well-determined velocities, the indeterminacy of their location is high; particles are then delocalized. Relations [4.59] are found using the quadratic deviations [4.55] and the momentum operator (see Chapter 5).

**APPLICATION 4.6.**

Figure 4.8 is reconsidered by adding a second slit of width $a$. Explain the interest of using a highly monokinetic beam of particles in order to observe an interference figure. Specify the order of magnitude of the quadratic deviation $\Delta x$ with respect to the distance between the two slits.

**Solution.** For a beam of monokinetic particles, their velocity is very well-defined. Component $\Delta v_x$ (hence $\Delta p_x$) is consequently small. According to Heisenberg's uncertainty relations [4.57], $\Delta x \approx \hbar / 2\Delta p_x$. A significant quadratic deviation $\Delta x$ is then obtained. This is a necessary condition for being able to observe an interference figure. However, $\Delta x$ must be larger than the distance between the two slits.

### 4.2.5. *Time–energy uncertainty relation, width of lines*

Bohr's theory has introduced the notion of stationary states. Consequently, the *lifetime* of a stationary state is infinite. Or, according to experiments, a given spectral line has a *natural width* (Figure 4.9), which is incompatible with the notion of stationary states. Indeed, the unit of the Planck constant $h$ (J · s) can be used to deduce that time $t$ and energy $E$ are complementary quantities. Heisenberg's fourth *time–energy uncertainty relation* is written as follows:

$$\Delta t \Delta E \geq \frac{\hbar}{2} \qquad [4.60]$$

Let $E$ be the energy of a physical system in a given stationary state and $\Delta t = \tau$ the system's lifetime in this state. Using the uncertainty relation [4.60], the lifetime of the stationary state can be written as follows:

$$\tau \approx \frac{\hbar}{2\Delta E} \qquad [4.61]$$

The energy of the system in a stationary state is perfectly determined. Consequently, $\Delta E = 0$. Hence according to [4.61], the lifetime of the stationary state is $\tau \rightarrow \infty$. However, the lifetimes of quantum states are actually finite. For atoms, they range between $10^{-6}$ s and $10^{-8}$ s. Let us note that for a stable atomic level, the natural width is zero. Consequently, for the ground level, $\Delta E = 0$.

The experimental measurement of $\Delta E$ is rendered difficult by the influences due, on the one hand, to interactions between atoms, and, on the other hand, to the *Doppler effect* (see Appendix 5.5).

### 4.2.6. *Heisenberg's microscope*

Heisenberg's microscope is in fact a thought experiment. It was elaborated by Heisenberg, as an argument in support of his uncertainty principle [PÈR 86, BEL 03, ATT 05].

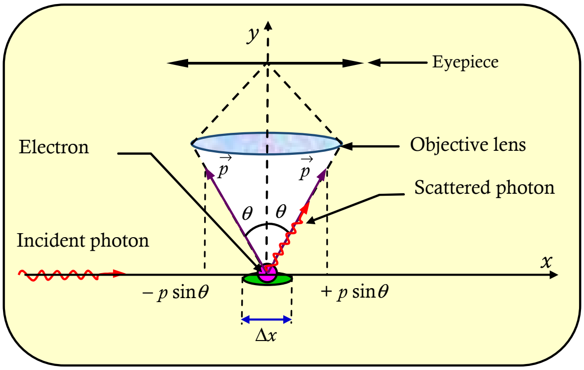

**Figure 4.9.** *Measurement of position x and linear momentum p of an electron using Heisenberg's microscope. The objective lens is limited by a cone whose opening is 2$\theta$*

In summary, this microscope is constituted of an *objective lens* and an *eyepiece* (Figure 4.9).

A monochromatic beam of photons $\gamma$ is sent to light an electron located on the $Ox$ axis of the spatial frame of reference employed. The measurement of the electron of position $x$ is possible provided that at least one photon is scattered and enters the objective lens of the microscope. Photons that enter the eyepiece deviate from the vertical $Oy$ by an angle $\theta$ and impart a momentum $p'$ to the electron during their scattering. Let $p$ be the momentum of a photon. As indicated by Figure 4.9, the momenta of the scattered photons vary between $-p\sin\theta$ and $+p\sin\theta$ along *the Ox axis*.

Let us write the law of momentum conservation (*the electron is at rest before scattering*) considering the two limits of the projection $p_{\mathrm{dx}}$ of the momentum of the scattered photon:

$$\begin{cases} p = p_x^{'} + p_{dx} = p_x^{'} + p\sin\theta \\ p = p_x^{''} - p_{dx} = p_x^{''} - p\sin\theta \end{cases} \qquad [4.62]$$

Relation [4.62] can be used to obtain the uncertainty of the electron momentum, which is:

$$\Delta p_x = p_x^{''} - p_x^{'} = 2p\sin\theta \qquad [4.63]$$

The width $\Delta x$ of the diffraction spot has the same order of magnitude as the interplanar spacing ($\Delta x \approx d$). Using [4.37] and the wavelength formula [4.4], we have (for the central spot $n = 1$):

$$2\Delta x\sin\theta = \lambda = \frac{h}{p} \Rightarrow \sin\theta = \frac{h}{2p\Delta x} \qquad [4.64]$$

Considering [4.63] and [4.64], we finally have [BEL 03, ATT 05]:

$$\Delta x\,\Delta p_x \approx h \qquad [4.65]$$

As already mentioned above, a proper representation of a localized particle is obtained if the *resolving power* $\delta x$ of the measurement devices is above $\Delta x$. To achieve this, one can choose to increase $\delta x$ or decrease $\Delta x$ using X or γ photons (decreasing $\Delta x$ amounts to decreasing the wavelength according to the first equality [4.64]).

REFRESHER ON THE MICROSCOPE.– The microscope is essentially composed of two converging optical systems that can be equated with two thin lenses:

– the *objective* is a converging lens whose focal distance is of the order of several millimeters. The objective gives a real, reversed and highly magnified image of a very small object located in front of it;

– the *eyepiece* is also a converging lens whose focal distance is of several centimeters. The eyepiece operates as a magnifier when examining the image provided by the objective.

The objective $L_1$ and the eyepiece $L_2$ are centered on the same axis; the distance between their optical centers $O$ and $O'$ ranges between 15 and 20 cm. The distance between the image focal point $F_1^{'}$ of the objective and the object focal point $F_2$ of the eyepiece is known as the *optical range* (sometimes denoted by Δ). Figure 4.10 illustrates the path of light rays through a microscope.

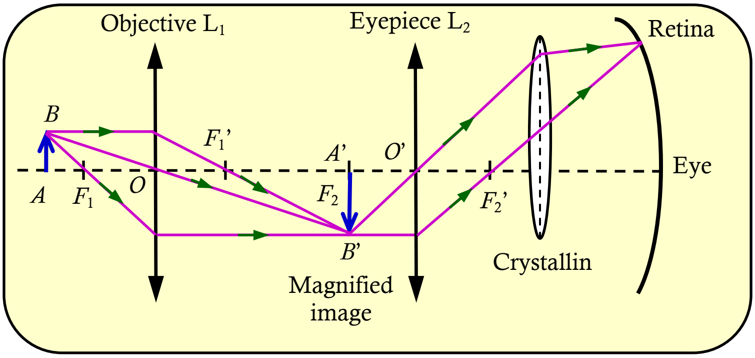

**Figure 4.10.** *Path of light rays in a microscope*

**Werner Heisenberg** was a German physicist. In 1925, in parallel to **Schrödinger** (see Chapter 5), he developed the first theory of quantum mechanics using the matrix formalism (while Schrödinger adopted a more wave-like approach, which involved the resolution of differential equations). In 1927, Heisenberg formulated the indeterminacy principle, rejecting the notion of the trajectory of a microscopic particle. He was awarded the Nobel Prize for physics in 1933 for his work in the field of quantum mechanics.

**Box 4.4.** *Heisenberg (1901–1976)*

## 4.3. Exercises

*Numerical data.*

– elementary charge: $e = 1.602 \times 10^{-19}$ C

– Planck constant: $h = 6.626 \times 10^{-34}$ J · s

– mass of electron: $m = 9.109 \times 10^{-31}$ kg

– Bohr radius: $a_0 = 0.53$ Å

– range of optical waves: 400–800 nm

### 4.3.1. *Group velocity of de Broglie waves in the relativistic case*

Let us consider a relativistic particle whose rest energy is $m_0c^2$. The particle is moving with velocity $v$ with respect to a fixed observer. The Lorentz factor is given by the expression:

$$\gamma = \frac{1}{\sqrt{1 - v^2 / c^2}}$$

(1) Express the total energy of a relativistic particle as a function of its rest energy and the Lorentz factor.

(2) Prove that group velocity can be written in the following form:

$$v_{gr} = m_0 c^2 \frac{d\gamma}{dp}$$

In this relation, $p$ designates the linear momentum of the relativistic particle.

(3) Prove that the group velocity of the de Broglie wave associated with a relativistic particle is equal to its translational velocity $v$. Draw a conclusion.

### 4.3.2. *Observing an atom with an electron microscope*

The possibility to observe an atom by means of an *electron microscope* is one of the interesting applications of Heisenberg's spatial uncertainty relations. This microscope uses an electron beam to light a sample and form its highly magnified image. By comparison with an *optical microscope*, an electron microscope has a higher *resolving power*. It makes it possible to obtain much higher magnifications of up to 5 million times, while the best optical microscopes do not go beyond 2,000 times magnification.

In an electron microscope, electromagnetic lenses (*instead of the glass lenses in an optical microscope*) are used to form the image created by the controlled electron beam that converges on a well-defined plane with respect to the studied sample. The principle of an electron microscope is presented below.

Electrons are emitted by a heated tungsten or lanthanum hexaboride filament. They are afterwards accelerated under a voltage of about 200 kV in the high vacuum tube of the microscope. The resulting electron beam is focused by magnetic lenses constituted of an iron-core coil. Focal distance variation leads to magnification variation. The image captured by the camera can be visually observed.

Figure 4.11 shows a simplified representation of an electron microscope.

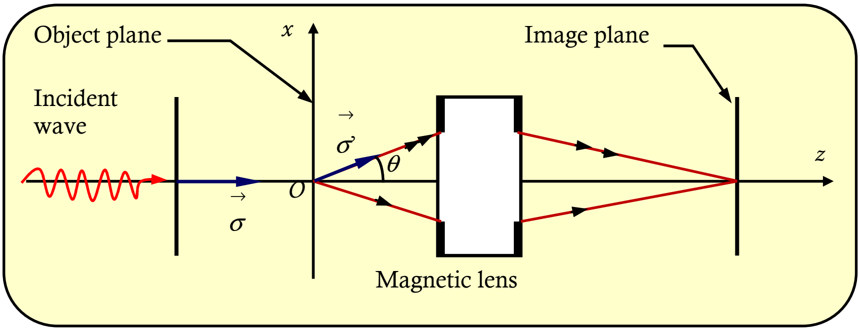

**Figure 4.11.** *Simplified representation of an electron microscope*

Let us consider an atom located at point $O$ of the object plane of the microscope. A plane wave associated with an electron is sent along the $Oz$ direction. This wave interacts with the atom in $O$ and is scattered in all directions. Scattered waves are distributed within a cone whose opening angle is $2\theta$. Let $\sigma$ be the spectroscopic wave number.

*Given data.* $\theta \approx 10^{-2}$ rad.

(1) Prove that component $\sigma'_x$ of $\vec{\sigma}'$ vector ranges between two extrema. Deduce $\Delta\sigma_x$ as a function of $\theta$ and $\lambda$.

(2) The wave group that can be detected in the image plane is such that $\Delta x \Delta\sigma_x \geq 1$. Find the expression of $\Delta x_0$ size of the smallest detail discernible by the electron microscope.

(3) The accelerating voltage of the electron beam is 100 kV. Calculate $\Delta x_0$.

(4) Is it possible to see an atom with an electron microscope? Provide a justification.

(5) Answer the same question (4) for an optical microscope.

## 4.4. Solutions

### 4.4.1. *Group velocity of de Broglie waves in the relativistic case*

The Lorentz factor is given by:

$$\gamma = \frac{1}{\sqrt{1 - v^2/c^2}} \qquad [4.66]$$

(1) *Expression of total energy*

The energy $E = mc^2$ of a particle of relativistic mass $m = \gamma m_0$ and rest energy $m_0c^2$ can be written as follows:

$$E = \gamma m_0 c^2 \tag{4.67}$$

(2) *Proof*

Using [4.67] and the definition of group velocity, we have:

$$v_{gr} = \frac{dE}{dp} \Rightarrow v_{gr} = m_0 c^2 \frac{d\gamma}{dp} \tag{4.68}$$

(3) *Expression of group velocity*

The linear momentum of the relativistic particle is $p = mv = \gamma m_0 v$. Using [4.66], we have:

$$v = \frac{p}{\gamma m_0} \Rightarrow \gamma = \frac{1}{\sqrt{1 - p^2/\gamma^2 m_0^2 c^2}} \tag{4.69}$$

Squaring and rearranging the above relation, we have:

$$\gamma^2 = 1 + \frac{p^2}{m_0^2 c^2} \Rightarrow \gamma\, d\gamma = \frac{p\, dp}{m_0^2 c^2}$$

Hence:

$$\frac{d\gamma}{dp} = \frac{p}{\gamma m_0^2 c^2} = \frac{\gamma m_0 v}{\gamma m_0^2 c^2} \Rightarrow \frac{d\gamma}{dp} = \frac{v}{m_0 c^2} \tag{4.70}$$

Using [4.68] and [4.70], we have:

$$v_{gr} = m_0 c^2 \times \frac{v}{m_0 c^2} \Rightarrow v_{\mathrm{gr}} = v$$

CONCLUSION.– de Broglie’s theory of matter waves is valid in both classical mechanics, for which $\gamma = 1$, and relativistic mechanics, for which $\gamma > 1$.

### 4.4.2. *Observing an atom with an electron microscope*

(1) *Proof*

The incident wave and the wave scattered by the atom have the same wavelength. Therefore, the wave number $\sigma' = \sigma$. Figure 4.11 shows that the projections of $\vec{\sigma}'$ on the $Ox$ axis take all the values ranging between $-\sigma\sin\theta$ and $+\sigma\sin\theta$. Hence:

$$-\sigma\sin\theta \leq \sigma'_x \leq +\sigma\sin\theta \qquad [4.71]$$

Using the extreme values and knowing that $\theta$ is very small, we have:

$$\Delta\sigma_x = 2\sigma\sin\theta \approx \frac{2\theta}{\lambda} \qquad [4.72]$$

(2) *Expression of* $\Delta x_0$

Knowing that $\Delta x \Delta\sigma_x \geq 1$, the size $\Delta x_0$ of the smallest detail discernible by the electron microscope is given by the expression according to [4.72].

$$\Delta x_0 \approx \frac{\lambda}{2\theta} \qquad [4.73]$$

(3) *Calculation of* $\Delta x_0$

In relation [4.73], the wavelength is the only unknown. According to the work–energy theorem, we have:

$$eU = \frac{1}{2}mv^2 = \frac{p^2}{2m} \qquad [4.74]$$

Using de Broglie's relation $\lambda = h/p$, we have:

$$eU = \frac{h^2}{2m\lambda^2} \Rightarrow \lambda = \frac{h}{\sqrt{2meU}} \qquad [4.75]$$

Inserting the wavelength expression [4.75] in [4.73], we find:

$$\Delta x_0 \approx \frac{h}{\theta\sqrt{8meU}} \qquad [4.76]$$

N.A.– $U = 100\text{ kV} \Rightarrow \Delta x_0 \approx 1.94 \times 10^{-10}\text{ m}$

(4) *Observing an atom with an electron microscope*

The radius of a hydrogen atom in ground state is $a_0 = 0.53$ Å. Knowing that the size of the smallest detail discernible by an electron microscope is $\Delta x_0 \approx 1.94$ Å, we obtain:

$$\Delta x_0/a_0 \approx 3.66 \Rightarrow \Delta x_0 \approx 4\, a_0 \qquad [4.77]$$

Result [4.77] actually indicates that an atom (except for the hydrogen atom, since $\Delta x_0 > a_0$) can be observed with an electron microscope. Many heavy atoms (nitrogen, boron, etc.) bound in organic molecules have been observed nowadays. Atom observation nevertheless requires proper interpretation of the images obtained, as well as a good understanding of the processes of interaction between electrons and the studied object.

(5) *Observing an atom with an optical microscope*

Let us calculate $\Delta x_0$ using [4.73] for the extreme wavelengths of the optical spectrum (400–800 nm). For $\theta \approx 10^{-2}$ rad we have:

$$20\ \mu\text{m} \leq \Delta x_0 \leq 40\ \mu\text{m} \qquad [4.78]$$

Result [4.78] indicates that the size of the smallest detail discernible by the optical microscope is of the order of several dozen micrometers. Atomic dimensions of the order of angström are 10,000 times smaller. Therefore, it is not possible to observe an atom with an optical microscope. This is due to the fact that *optical wavelengths are longer than the wavelengths of waves associated with electrons*.

# Appendices

*Introduction to Quantum Mechanics 1: Thermal Radiation and Experimental Facts Regarding the Quantization of Matter,* First Edition. Ibrahima Sakho.

# Appendix 1

# Planck's Law

## A1.1. Photon gas

The study of the distribution of black body electromagnetic radiation was the point of departure for **Max Planck** formulating the law of variation of *spectral density of electromagnetic energy* known as *Planck's law*. To establish the expression of this law, let us consider an enclosure of volume $V$ as a black body simulation.

Consider a cavity whose walls are maintained at constant temperature $T$. Due to *thermal agitation motion*, the particles that compose the walls emit and absorb photons. This is how the *photon gas* is generated in the cavity enclosure. Each time a photon of energy $E$ is absorbed or reflected by the wall, the latter receives a momentum $p$. The wall in turn bounces back upon photon emission. As result of all these processes, the photon gas exerts a *radiation pressure* on the cavity walls.

For an enclosure of volume $V$ containing $N$ particles, the pressure $P$ exerted by the $N$ particles on the walls of the enclosure is given by the following relation [HUL 86]:

$$P = \frac{1}{3}\frac{N}{V}\left\langle \vec{v} \cdot \vec{p} \right\rangle = \frac{1}{3} n \left\langle \vec{v} \cdot \vec{p} \right\rangle \qquad [A1.1]$$

where $n = N/V$ is the density of particles, and $\vec{v}$ and $\vec{p}$ are, respectively, the velocity and momentum vectors of the particle that hits the wall.

For the photon, $v = c$. Moreover, the relation between the energy $E$ and the momentum $p$ of the photon is $E = pc$. Taking this relation into account, [A1.1] leads to:

$$PV = \frac{1}{3}\left\langle NE \right\rangle \qquad [A1.2]$$

---

For color versions of the figures in this book, see www.iste.co.uk/sakho/quantum1.zip.

In this relation, $N$ designates the number of photons in the enclosure.

In contrast with a gas of $N$ classical particles that can be neither created nor destroyed, the number $N$ of photons is a variable quantity due to photon annihilation and creation processes in the cavity. Denoting $\overline{E} = \langle NE \rangle$ the *mean energy of the photon gas*, the radiation pressure verifies the following relation:

$$PV = \frac{1}{3}\overline{E} \qquad [A1.3]$$

The 1/3 factor in equation [A1.3] accounts for the isotropic propagation of the electromagnetic radiation in the cavity.

## A1.2. Photon spin and polarization

In 1889, the Russian physicist **A.I. Sadovski** theoretically proved that circularly or elliptically polarized light had an angular momentum. This phenomenon, known as *Sadovski effect*, made it possible to observe the photon *spin* $s = 1$ [SIV 86]. The *magnetic spin quantum number* is then $m_s = \pm s$, hence: $m_s = -1$, 0 or + 1, which amounts to $(2s + 1)$ values.

Moreover, the quantum number $m_s$ indicates the various directions of photon propagation. When the projection of photon spin $\vec{s}$ on the propagation axis is equal to + 1 (spin parallel to the direction of propagation), the light wave has a right hand polarization (*right-handed helicity*). Otherwise ($m_s = -1$: spin antiparallel to the direction of propagation), the polarization is left hand (*left-handed helicity*). These two states of polarization of the photon are illustrated in Figure A.1.

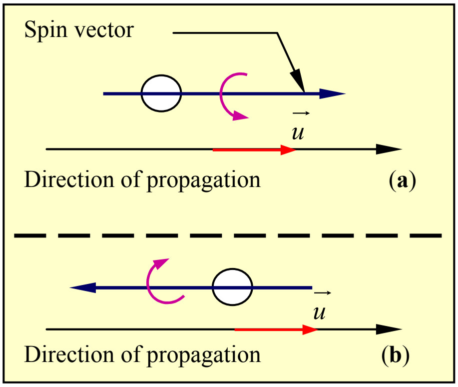

**Figure A1.1.** *The two possible states of polarization of the photon. (a) Right-handed helicity (right-hand circular polarization). (b) Left-handed helicity (left-hand circular polarization)*

The state in which the photon had the spin vector projection equal to $m_s = 0$ was a puzzling question. According to the current state of knowledge, quantum electrodynamics proves that such a state does not exist. Since electromagnetic waves are constituted of a flow of photons and the electromagnetic field can be described by two directions of propagation, the photon has two possible polarizations:

– a right-hand polarization ($m_s = +1$) corresponding to the right-handed helicity $\left|\vec{k}, m_s = +1\right\rangle$ (Figure A1.1(a));

– a left-hand polarization ($m_s = -1$) corresponding to the left-handed helicity $\left|\vec{k}, m_s = -1\right\rangle$ (Figure A1.1(b)).

The norm of the wave vector is $k = \omega / c$. If $\vec{u}$ designates the light propagation direction, then:

$$\vec{k} = \frac{\omega}{c}\vec{u} = \frac{2\pi}{\lambda}\vec{u} \qquad [A1.4]$$

## A1.3. Decomposition of electromagnetic radiation field

Let us consider an enclosure of volume $V$ that simulates a black body and is filled with electromagnetic radiation. This radiation is assumed to be generated by the vibration of a large number of *virtual quantum harmonic oscillators*. Each energy level is characterized by the quantum number $n$. Let us formally consider that $n$ designates also the average number of photons per oscillator. As presented, each oscillator is assimilated to a monochromatic electromagnetic wave of angular frequency $\omega$ and wave vector of norm $k = \omega / c$.

Let us consider that the electromagnetic wave propagates along $Ox$ axis. The wave vector is then written according to [A1.4]:

$$\vec{k} = \frac{\omega}{c}\vec{i} \qquad [A1.5]$$

Moreover, for an electromagnetic wave, the vector potential $\vec{A}$ is given by the relation in complex notation [ANN 74, SAK 18]:

$$\vec{A}(\vec{r},t) = R\left[\vec{A}_0^{\,*}\, e^{-i(\vec{k}\cdot\vec{r} - \omega t)}\right] \qquad [A1.6]$$

In this relation, $\overrightarrow{A}_0^{\,*} = \overrightarrow{A}_0\, e^{i\varphi}$ designates the *complex amplitude* of the vector potential and $\varphi$ is the wave phase.

Along the propagation direction, the vector potential is:

$$\overrightarrow{A}(x,t) = R\left[\overrightarrow{A}_0\, e^{-i(kx-\omega t-\varphi)}\right] \qquad [A1.7]$$

Considering the real part of [A1.7], we have:

$$\overrightarrow{A}(x,t) = \overrightarrow{A}_0 \cos(kx-\omega t-\varphi) \qquad [A1.8]$$

Let us write [A1.8] in the following form:

$$\overrightarrow{A}(x,t) = \overrightarrow{A}_0 \cos\left[(kx-\varphi)+(-\omega t)\right] \qquad [A1.9]$$

Considering the trigonometric transformation

$$\cos\,(a+b) = \cos a \,\cos b - \sin a \,\sin b$$

relation [A1.9] is written in the form:

$$\overrightarrow{A}(x,t) = \overrightarrow{A}_0\left[\cos\omega t\cos(kx-\varphi)+\sin\omega t\sin(kx-\varphi)\right]$$

Hence:

$$\overrightarrow{A}(x,t) = \overrightarrow{A'}_0(t)\cos(kx-\varphi)+\overrightarrow{A''}_0(t)\sin(kx-\varphi) \qquad [A1.10]$$

In relation [A1.10], we have considered:

$$\overrightarrow{A'}_0(t) = \overrightarrow{A}_0\cos\omega t\,;\ \overrightarrow{A''}_0(t) = \overrightarrow{A}_0\sin\omega t$$

Let us then write [A1.10] in the form:

$$\overrightarrow{A}(x,t) = \overrightarrow{A'}(x,t)+\overrightarrow{A''}(x,t) \qquad [A1.11]$$

with

$$\overrightarrow{A'}(x,t) = \overrightarrow{A'}_0(t)\cos(kx-\varphi)\,;\ \overrightarrow{A''}(x,t) = \overrightarrow{A'}_0(t)\sin(kx-\varphi) \qquad [A1.12]$$

Each of [A1.12] terms is a vector potential oscillating along *Ox* axis, and the two terms characterize a plane electromagnetic wave.

Let us consider one of the vector potentials [A1.12], for example $\overrightarrow{A'}(x,t)$. This amounts to considering an elementary volume $dV$ in the wall containing electromagnetic waves characterized by the vector potential $\overrightarrow{A'}(x,t)$.

Let us then consider the particular case of a one-dimensional oscillator. *Oy* axis is arbitrarily chosen. In other terms, we consider an elementary volume $dV$ containing the electromagnetic waves whose polarizations are such that the vector potential $\overrightarrow{A'}(x,t)$ oscillates along *Oy*. As indicated by [A1.3], radiation pressure is isotropic, so there is no privileged direction. The choice of *Oy* axis does not influence the final result. We therefore have (changing *A'* in *A*):

$$\vec{A}(x,t) = A_y(x,t)\vec{j} = A_0(t)\cos(k\,x - \varphi)\vec{j} \qquad \text{[A1.13]}$$

In electromagnetism, electric and magnetic field vectors are defined by the following relations [ANN 74, SAK 18]:

$$\vec{E} = -\frac{\partial \vec{A}}{\partial t} - \vec{\nabla} V \;\; ; \;\; \vec{B} = \vec{\nabla} \wedge \vec{A} \qquad \text{[A1.14]}$$

As photons are not subjected to any field of forces, scalar potential is zero. We therefore have along *Oy* axis:

$$\begin{aligned}
E_y(x,t) &= -\frac{\partial A_y(x,t)}{\partial t} \\
B_x(x,t) &= \frac{\partial A_z(x,t)}{\partial y} - \frac{\partial A_y(x,t)}{\partial z} = 0 \\
B_y(x,t) &= \frac{\partial A_x(x,t)}{\partial z} - \frac{\partial A_z(x,t)}{\partial x} = 0 \\
B_z(x,t) &= \frac{\partial A_y(x,t)}{\partial x} - \frac{\partial A_x(x,t)}{\partial y} = \frac{\partial A_y(x,t)}{\partial x}
\end{aligned} \qquad \text{[A1.15]}$$

Using [A1.13], equations [A1.15] lead to:

$$\begin{cases} E_y(x,t) = -\dfrac{\partial A_0}{\partial t}\cos(k\,x - \varphi) \\ B_z(x,t) = -\,kA_0\sin(k\,x - \varphi) \end{cases} \qquad \text{[A1.16]}$$

Moreover, within volume $dV$, the *density of electromagnetic energy* $u$ can be written in the form [ANN 74, SAK 18]:

$$u = \varepsilon_0 \frac{E^2}{2} + \frac{B^2}{2\mu_0} \qquad \text{[A1.17]}$$

The *total mean energy of the electromagnetic field* throughout volume $V$ is:

$$\langle E \rangle = \int_V u dV = \int_V \left( \varepsilon_0 \frac{\overline{E}^2}{2} + \frac{\overline{B}^2}{2\mu_0} \right) dV \qquad \text{[A1.18]}$$

Using [A1.16], the mean energy [A1.18] can be written as:

$$\langle E \rangle = \int_V \left\{ \frac{\varepsilon_0}{2} \left( \frac{dA_0}{dt} \right)^2 \cos^2(kx - \varphi) + \frac{k^2 A_0^2}{2\mu_0} \sin^2(kx - \varphi) \right\} dV \qquad \text{[A1.19]}$$

therefore:

$$\langle E \rangle = \int_V \left\{ \frac{\varepsilon_0}{2} \left( \frac{dA_0}{dt} \right)^2 \left[ 1 - \sin^2(kx - \varphi) \right] + \frac{k^2 A_0^2}{2\mu_0} \left[ 1 - \cos^2(kx - \varphi) \right] \right\} dV$$

And:

$$\langle E \rangle = \int_V \left\{ \frac{\varepsilon_0}{2} \left( \frac{dA_0}{dt} \right)^2 + \frac{k^2 A_0^2}{2\mu_0} - \left[ \frac{\varepsilon_0}{2} \left( \frac{\partial A_0}{\partial t} \right)^2 \sin^2(kx - \varphi) + \frac{k^2 A_0^2}{2\mu_0} \cos^2(kx - \varphi) \right] \right\} dV$$

Hence:

$$\langle E \rangle = \left\{ \frac{\varepsilon_0}{2} \left( \frac{dA_0}{dt} \right)^2 + \frac{k^2 A_0^2}{2\mu_0} \right\} V + \langle E_0 \rangle \qquad \text{[A1.20]}$$

In relation [A1.19], we have considered:

$$\langle E_0 \rangle = - \int_V \left\{ \frac{\varepsilon_0}{2} \left( \frac{dA_0}{dt} \right)^2 \sin^2(kx - \varphi) + \frac{k^2 A_0^2}{2\mu_0} \cos^2(kx - \varphi) \right\} dV \qquad \text{[A1.21]}$$

Knowing that in vacuum $k = \omega/c$, equation [A1.20] can be written as:

$$\langle E\rangle = \left\{\frac{\varepsilon_0}{2}\left(\frac{dA_0}{dt}\right)^2 + \frac{\omega^2 A_0^2}{2c^2\mu_0}\right\}V + \langle E_0\rangle$$

But in vacuum $\mu_0\varepsilon_0 c^2 = 1$. Therefore, after arrangement the above expression can be written as follows:

$$\langle E\rangle = \frac{\varepsilon_0}{2}V\left\{\left(\frac{dA_0}{dt}\right)^2 + \omega^2 A_0^2\right\} + \langle E_0\rangle \qquad \text{[A1.22]}$$

Let us consider $q = A_0$. This equation is then written in the form:

$$\langle E\rangle = \frac{\varepsilon_0}{2}V\left\{\left(\frac{dq}{dt}\right)^2 + \omega^2 q^2\right\} + \langle E_0\rangle \qquad \text{[A1.23]}$$

If $E_q(\omega) = \langle E\rangle - \langle E_0\rangle$, then [A1.23] becomes:

$$E_q(\omega) = \frac{\varepsilon_0}{2}V\left\{\left(\frac{dq}{dt}\right)^2 + \omega^2 q^2\right\} \qquad \text{[A1.24]}$$

But the energy of a classical harmonic oscillator of mass $m$ and angular frequency $\omega$ is given by the expression:

$$E_q(\omega) = \frac{1}{2}mv^2 + \frac{1}{2}kq^2 \qquad \text{[A1.25]}$$

Since:

$$v = \frac{dq}{dt} \quad \text{and} \quad \omega = \sqrt{\frac{k}{m}}$$

then after arrangement and factorization equation [A1.25] can be written as:

$$E_q(\omega) = \frac{m}{2}\left\{\left(\frac{dq}{dt}\right)^2 + \omega^2 q^2\right\} \qquad \text{[A1.26]}$$

The differential equation [A1.26] is analogous to equation [A1.24]. Black body radiation can therefore be considered as a set of virtual quantum harmonic oscillators of "mass" $m = \varepsilon_0 V$ (obviously, the dimension of this quantity is not that of a mass; this explains why, among others, the fact that the quantum harmonic oscillators in this study are qualified as "virtual").

It should, nevertheless, be kept in mind that comparing [A1.19] and [A1.21] leads to $\langle E\rangle = -\langle E_0\rangle$. Hence: $E_q(\omega) = \langle E\rangle - \langle E_0\rangle = 2\langle E\rangle$. If we had considered $E_q(\omega) = 2\langle E\rangle$, then $-\langle E_0\rangle = 2\langle E\rangle$. The use of $E_q(\omega) = 2\langle E\rangle$ in equation [A1.22] should be avoided. Otherwise, a 1/4 factor would be obtained in equation [A1.24], which would then differ from the classical equation [A1.26] that contains a 1/2 factor.

## A1.4. Definition of spectral density of energy

Let us consider a closed enclosure of volume $V$ whose walls are maintained at constant temperature $T$. This enclosure is assimilated to a black body. At thermal equilibrium, the enclosure is filled with a large number of photons that taken as a whole form the black body radiation. Let us delimit in this enclosure a sphere of volume $V$, filled with electromagnetic radiation, and of radius equal to the norm $k$ of the wave vector. In this sphere, the wave vector is defined by its three components $k_x$, $k_y$ and $k_z$ (Figure A1.2).

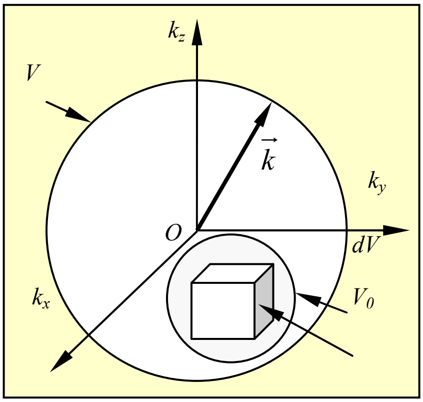

**Figure A1.2.** *Enclosure of volume V in the three-dimensional space of wave vectors*

By definition, the spectral density of electromagnetic energy denoted $\rho(\omega)$ is given by the following relation:

$$du = \rho(\omega)d\omega \tag{A1.27}$$

In this relation, $du$ designates the density of energy per unit volume.

Let $\langle dE\,(\omega,T)\rangle$ be the mean energy of the set of quantum oscillators present in the volume $V$ whose walls are maintained at temperature $T$, then:

$$du = \frac{\langle dE(\omega,T)\rangle}{V} \qquad \text{[A1.28]}$$

Using this relation, we have:

$$\rho(\omega)d\omega = \frac{\langle dE(\omega,T)\rangle}{V} \qquad \text{[A1.29]}$$

If $\langle dE\,(\omega, T)\rangle$ is known, we can express $\rho\,(\omega)$. For this purpose, let us find the number of harmonic oscillators or the number of electromagnetic waves contained in volume $V$.

## A1.5. Number of quantum harmonic oscillators

### A1.5.1. *Elementary volume in the space of wave vectors*

In the sphere of radius $k$, let us cut an element of volume $dV$ (Figure A1.2) containing a small cube of edge $a$ and volume $V_0 = a^3$. The edge $a$ is chosen in such a way that the volume $V_0$ contains only two waves that differ by their polarization. One of the waves has a *right-hand polarization* ($\left|\vec{k}, m_s = +1\right\rangle$ state) and the other one has a *left-hand polarization* ($\left|\vec{k}, m_s = -1\right\rangle$ state).

Because photons are *bosons* (*integer spin particles*), each state $\left|\vec{k}, m_s = \pm 1\right\rangle$ contains a very large number of photons. Moreover, volume $V_0$ being chosen in the space of $\vec{k}$, any "length" will be defined on one of the three axes $Ok_x$, $Ok_y$ and $Ok_z$. Intuitively, the edge $a$ is a function of the norm of the wave vector. Let us consider: $a = a(k)$. But the photon cannot be confined in a space whose dimension is below $\lambda^3$, where $\lambda$ is the wavelength of the photon. Hence:

$$a = a\,(k) > \lambda \qquad \text{[A1.30]}$$

Moreover, the number of waves contained in a one centimeter long interval is referred to as spectroscopic wave number denoted by $\bar{\nu}$. By definition, $\bar{\nu}=1/\lambda$.

Since $a\,(k) < k\,(V_0 < V)$, let us consider $a(k) = k/\bar{\nu} = k\lambda$

Volume $V_0$ is therefore equal to:

$$V_0 = a^3(k) = (k\lambda)^3 \quad \text{[A1.31]}$$

### A1.5.2. *Number of waves with angular frequencies ranging between $\omega$ and $\omega + d\omega$*

Since volume $V_0$ contains only two waves, there will be twice as many waves as elements of volume $V_0$ in $dV$ (see Figure A1.2). Therefore, the number of waves $dn_\omega$ in $dV$ is equal to:

$$dn_\omega = 2 \times \frac{dV}{V_0} \quad \text{[A1.32]}$$

The volume $V$ being that of a sphere of radius $k = \omega/c$, we have:

$$V = \frac{4}{3}\pi k^3 = \frac{4}{3c^3}\pi\omega^3 \quad \text{[A1.33]}$$

The elementary volume $dV$ is then given by the expression:

$$dV = \frac{4\pi}{c^3}\omega^2\, d\omega \quad \text{[A1.34]}$$

Inserting result [A1.34] in [A1.32], we obtain:

$$dn_\omega = \frac{8\pi}{V_0 c^3}\omega^2\, d\omega \quad \text{[A1.35]}$$

The total number of waves $dN_\omega$ or still the total number of harmonic oscillators whose angular frequencies range between $\omega$ and $\omega + d\omega$ present throughout the volume $V$ of the enclosure is $dN_\omega = V dn_\omega$. Knowing that $k = 2\pi/\lambda$, then $V_0 = (k\lambda)^3 = 8\pi^3$ and using relation [A1.35] we have:

$$dN_\omega = \frac{V}{\pi^2 c^3}\omega^2\, d\omega \quad \text{[A1.36]}$$

Let us consider:

$$f(\omega) = \frac{V}{\pi^2 c^3}\omega^2 \quad \text{[A1.37]}$$

In this case, expression [A1.36] can be written in the form:

$$dN_\omega = f(\omega)d\omega \qquad \text{[A1.38]}$$

This expression shows that $dN_\omega$ actually designates the total number of waves with angular frequencies ranging between $\omega$ and $\omega + d\omega$ present throughout volume $V$. The function $f(\omega)$ is then interpreted as density of these waves in the angular frequency interval $d\omega$.

## A1.6. Expression of Planck's law

Each electromagnetic wave is interpreted as a set of quantum harmonic oscillators. If $\langle E(\omega,T)\rangle$ designates the mean energy of one of these oscillators, then the total mean energy $\langle dE(\omega,T)\rangle$ of the set of quantum oscillators present in the volume $dV$ whose walls are maintained at temperature $T$ is equal to $dN_\omega \langle E(\omega,T)\rangle$. Hence:

$$\langle dE(\omega, T)\rangle = dN_\omega \langle E(\omega, T)\rangle$$

This leads to:

$$\langle dE(\omega,T)\rangle = \langle E(\omega,T)\rangle f(\omega)d\omega \qquad \text{[A1.39]}$$

Using relations [A1.29] and the last relation [A1.39], we have:

$$\rho(\omega)\,d\omega = \frac{\langle E(\omega,T)\rangle}{V} f(\omega)d\omega \qquad \text{[A1.40]}$$

The *spectral density of electromagnetic energy* $\rho(\omega)$ is then written as follows:

$$\rho(\omega) = \frac{\langle E(\omega,T)\rangle}{V} f(\omega) \qquad \text{[A1.41]}$$

Using [A1.37], expression [A1.41] can be written as:

$$\rho(\omega) = \frac{\omega^2}{\pi^2 c^3}\langle E(\omega,T)\rangle \qquad \text{[A1.42]}$$

For a classical harmonic oscillator, the mean energy of thermal agitation is $\langle E(\omega,T)\rangle = kT$. It can immediately be noted that this classical energy does not depend on the angular frequency $\omega$. Expression [A1.42] gives in this case the following:

$$\rho(\omega) = \frac{\omega^2}{\pi^2 c^3} kT \qquad [A1.43]$$

This corresponds to the classical Rayleigh-Jeans law [1.23] in which spectral density is denoted by $u(\omega)$. The mean energy of thermal agitation of a quantum harmonic oscillator is given by [1.48] (we have considered $\langle E_\omega \rangle (T) = \langle E(\omega, T) \rangle$):

$$\langle E(\omega,T) \rangle = \frac{\hbar\omega}{e^{\hbar\omega/kT} - 1} \text{ or } \langle E(\nu,T) \rangle = \frac{h\nu}{e^{h\nu/kT} - 1} \qquad [A1.44]$$

It is worth noting that the mean energy [A1.44] depends on the angular frequency $\omega$ or frequency $\nu$. Inserting expression [A1.44] in [A1.42], we obtain Planck's law [1.25], which is:

$$\rho(\omega) = \frac{\hbar\omega^3}{\pi^2 c^3} \frac{1}{e^{\hbar\omega/kT} - 1} \qquad [A1.45]$$

Planck's law can also be expressed as a function of frequency $\nu$. Let us note that by replacing $\omega = 2\pi\nu$ in [A1.45], we do not obtain the correct expression of spectral density $\rho(\nu)$. To establish the correct expression of $\rho(\nu)$, [A1.36] must be used for deducing the total number of waves $dN_\nu$ with frequencies ranging between $\nu$ and $\nu + d\nu$ present throughout volume $V$, hence:

$$dN_\nu = \frac{8\pi V}{c^3} \nu^2 d\nu \qquad [A1.46]$$

The *wave density* $f(\nu)$ in the angular frequency interval $d\nu$ is then:

$$f(\nu) = \frac{8\pi V}{c^3} \nu^2 \qquad [A1.47]$$

The spectral density of electromagnetic energy $\rho(\nu)$ can be written using [A1.41]:

$$\rho(\nu) = \frac{\langle E(\nu,T) \rangle}{V} f(\nu) \qquad [A1.48]$$

Inserting [A1.47] in [A1.48], we have:

$$\rho(\nu) = \frac{8\pi}{c^3}\left\langle E(\nu,T)\right\rangle \nu^{\,2} \qquad [A1.49]$$

Using the second expression in [A1.44], relation [A1.49] gives:

$$\rho(\nu) = \frac{8\pi h\nu^3}{c^3}\,\frac{1}{e^{h\nu/kT}-1} \qquad [A1.50]$$

We have therefore deduced Planck's law.

# Appendix 2

# Planck's Law and Einstein's Theory

Planck's law has its well-deserved place in Einstein's theory on the absorption and emission of electromagnetic radiation by quantum systems. One of its most remarkable consequences is the possibility to use *stimulated emission* for light amplification for the generation of laser radiation, with myriad applications, both in industry and in fundamental research. The objective of this appendix is to review the main processes of interaction between optical radiation and matter [TAR 79, FRI 85]. This offers the opportunity to introduce Einstein $B_{12}$ coefficient of *stimulated absorption* and $B_{21}$ coefficient of *stimulated emission*, as well as the $A_{21}$ coefficient of *spontaneous emission*.

## A2.1. The main processes of interaction between optical radiation and matter

The term *optical radiation* covers the range of electromagnetic waves emitted in the visible range. The corresponding wavelengths are therefore in the (400 nm < $\lambda$ < 780 nm) range.

### A2.1.1. *Stimulated absorption and emission, and spontaneous emission*

Let us consider an enclosure containing quantum systems (atoms, ions, nuclei, etc.) at thermodynamic equilibrium at temperature $T$. Let $E_1$ and $E_2$ be two non-degenerate discrete electron levels that can be filled by one of these systems. When radiation interacts with the quantum systems, light absorption and emission processes take place, in accordance with Bohr's theory (Figure A2.1).

---

For color versions of the figures in this book, see www.iste.co.uk/sakho/quantum1.zip.

*Introduction to Quantum Mechanics 1: Thermal Radiation and Experimental Facts Regarding the Quantization of Matter,* First Edition. Ibrahima Sakho.

According to Bohr frequency condition, we have:

$$\hbar\omega_{12} = E_2 - E_1 = \hbar\omega_{21} = |E_1 - E_2| \qquad [A2.1]$$

Relation [A2.1] shows that within Bohr's theory, a quantum system emits exactly the same amount of energy it has absorbed. Moreover, if the absorption process (Figure A2.1(a)) is *stimulated* (*induced*) by the incident photon of energy $\hbar\omega_{12}$, at a first analysis, nothing justifies the emission process (Figure A. 2.1(b)).

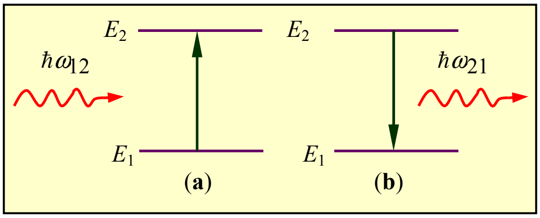

**Figure A2.1.** *Absorption (a) and emission (b) of optical radiation*

Assuming that $E_1$ represents the fundamental level, the excited level $E_2$ is characterized by a certain lifetime $\tau$. Consequently, there must be a relation between the *lifetime* $\tau$ and the de-excitation of quantum systems from a higher level of energy $E_2$. This relation cannot be explained within Bohr's semiclassical theory.

### A2.1.2. *Spontaneous emission*

In 1917, Albert Einstein shed light on the relation between the *lifetime of an excited state* and the de-excitation from this state by describing the absorption and emission of radiation in terms of *probability of transition*. He introduced the notion of *stimulated emission*. Taking into account stimulated emission makes it possible to consistently explain the lifetime of a quantum system in an excited state and the possibility (probability) for this system to move to a lower level by emitting electromagnetic radiation.

Spontaneous emission plays a fundamental role in light generation by laser systems, in which certain excited states referred to as *metastable* have an abnormally long lifetime (compared to the mean lifetime ranging from $10^{-7}$ s to $10^{-8}$ s). Figure A2.2 [SAK 13] illustrates a laser example (*optical fiber* doped with erbium ions $\text{Er}^{3+}$).

Electrons that are initially on the ground level $E_1$ are driven to the higher level $E_3$ (group of very close levels or energy band) by a mechanism known as *optical pumping*. Lifetime $\tau_{32}$ being very short (1 µs) compared to that of the metastable intermediary level of energy $E_2$ (lifetime $\tau_{21}$ = 1 ms), electrons consequently move to level 2, where they accumulate.

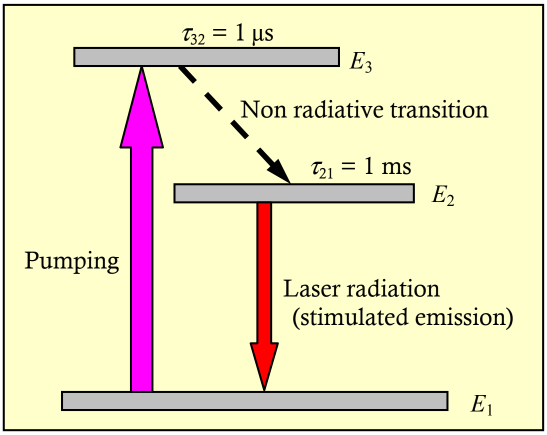

**Figure A2.2.** *Laser operating levels in an optical fiber doped with Er $^{3+}$ ions*

This "stand by" of electrons on level $E_2$ proves the *random character of* the de-excitation (*stimulated emission*) toward the ground level. The relation between the stimulated light emission from excited state $E_2$ and the lifetime of electrons in this state can be easily understood. Let us note that *non-radiative transitions* $E_3 \rightarrow E_2$ (without light emission) generate what is known as *population inversion*. Absorption of an incident photon is therefore sufficient to trigger the stimulated emission of laser radiation (*laser effect*) corresponding to $E_2 \rightarrow E_1$ transition. Finally, it is worth noting that the energy absorbed ($E_3 - E_1$) by the erbium ions is not equal to the energy ($|E_1 - E_2|$) emitted by laser effect, contrary to Bohr's theory, which predicts the same energy according to relation [A2.1].

## A2.2. Einstein's theory of absorption and emission processes

### A2.2.1. *Einstein coefficients*

Let us consider a quantum system with two discrete levels (1) and (2), whose respective energies are $E_1$ and $E_2$. The probability of absorption of the quantum system in the time unit *dt* from level (1) to level (2) is proportional to the spectral density of electromagnetic radiation $\rho(\omega_{12})$ [TAR 79, FRI 85]:

$$dP_{12} = B_{12}\,\rho(\omega_{12})\,dt \qquad \text{[A2.2]}$$

In this relation, $B_{12}$ is a coefficient.

For the emission process, two cases can be distinguished according to *Einstein's theory*:

– a stimulated emission process, whose probability of transition is proportional to the spectral density of electromagnetic energy $\rho(\omega_{12})$:

$$dP'_{21} = B_{21}\,\rho(\omega_{12})\,dt \qquad \text{[A2.3]}$$

where $B_{21}$ is a coefficient;

– a spontaneous (not induced by radiation) emission process whose probability of transition is given by the expression:

$$dP''_{21} = A_{21}\,dt \qquad \text{[A2.4]}$$

where $A_{21}$ is a coefficient.

The overall probability of transition of the quantum system in the time unit *dt* from level (2) to level (1) is then written as follows:

$$dP_{21} = [A_{21} + B_{21}\,\rho(\omega_{12})]\,dt \qquad \text{[A2.5]}$$

*In summary, the transition probabilities* that govern the processes of radiation absorption and emission by quantum systems are written as follows:

$$\begin{cases} dP_{12} = B_{12}\,\rho(\omega_{12})dt \\ dP_{21} = [A_{21} + B_{21}\,\rho(\omega_{12})]\,dt \end{cases} \qquad \text{[A2.6]}$$

Coefficients $A_{21}$, $B_{21}$ and $B_{12}$ are known as *Einstein coefficients*, and are independent of temperature and spectral density of electromagnetic energy $\rho(\omega_{12})$.

Unlike the stimulated absorption and emission processes, the spontaneous emission process is purely random. Consequently, it has no relation with the stimulated emission process (no correlation). This explains why transition probabilities [A2.5] are added. Nevertheless, Einstein coefficients $A_{21}$, $B_{21}$ and $B_{12}$ are not independent. The relations between them are deduced in the following section.

### A2.2.2. *Populations $N_1$ and $N_2$ of the levels of a quantum system*

Let $N_1$ and $N_2$ be the *populations of levels* (1) and (2) of a quantum system. Let $g_i$ be the degree of degeneracy of the level $i$ considered. The population $N_i$ of level $i$ of energy $E_i$ is given by *Boltzmann statistics*:

$$N_i = N \frac{g_i \, e^{-\beta E_i}}{\sum\limits_i g_i \, e^{-\beta E_i}} \qquad [A2.7]$$

In relation [A2.7], $N = \sum\limits_i N_i$ is the total number of quantum systems in the unit volume and $\beta = 1/kT$, where $k$ is Boltzmann constant and $T$ is the absolute temperature. Populations of levels (1) and (2) considered can be deduced from [A2.7] as follows:

$$N_1 = N \frac{g_1 \, e^{-\beta E_1}}{\sum\limits_{i=1}^{2} g_i e^{-\beta E_i}} \qquad [A2.8]$$

$$N_2 = N \frac{g_2 \, e^{-\beta E_2}}{\sum\limits_{i=1}^{2} g_i e^{-\beta E_i}} \qquad [A2.9]$$

Let us consider:

$$N_0 = \frac{N}{\sum\limits_{i=1}^{2} g_i \, e^{-\beta E_i}} \quad (N_0 \text{ is constant})$$

Expressions [A2.8] and [A2.9] are simplified as follows:

$$\begin{cases} N_1 = N_0 \, g_1 \, e^{-\beta E_1} \\ N_2 = N_0 \, g_2 \, e^{-\beta E_2} \end{cases} \qquad [A2.10]$$

### A2.2.3. *Number of transitions between energy levels*

Since $N_i$ designates the number of quantum systems present on level $i$ of energy $E_i$ and $dP_{ij}$ is the probability of $i \rightarrow j$ transition of one of the quantum systems in the time unit $dt$, the number of transitions $N_{i \rightarrow j}$ is then given by the expression:

$$N_{i \rightarrow j} = N_i \frac{dP_{ij}}{dt} \tag{A2.11}$$

Using [A2.6], we have:

$$\begin{cases} N_{1 \rightarrow 2} = N_1 B_{12} \rho(\omega_{12}) \\ N_{2 \rightarrow 1} = N_2 \left[A_{21} + B_{21} \rho(\omega_{12})\right] \end{cases} \tag{A2.12}$$

Using relations [A2.10] and [A2.11] and applying the *principle of microscopic reversibility* also known as *law of detailed balance*, the relations between Einstein coefficients are established.

### A2.2.4. *Relation between B₁₂ and B₂₁ coefficients*

Using [A2.10], we have (replacing $\beta$ by $1/kT$):

$$\frac{N_2}{N_1} = \frac{g_2}{g_1} e^{-\frac{(E_2 - E_1)}{kT}} \tag{A2.13}$$

Moreover, according to the principle of microscopic reversibility, *in thermodynamic equilibrium state, the number of direct transitions, whatever their nature, must be equal to the number of inverse transitions* [CHP 78]. Hence:

$$N_{1 \rightarrow 2} = N_{2 \rightarrow 1} \tag{A2.14}$$

Consequently, according to [A2.12] we have:

$$N_2[A_{21} + B_{21} \rho(\omega_{12})] = N_1 B_{12} \rho(\omega_{12})$$

Hence:

$$\frac{N_2}{N_1} = \frac{B_{12} \rho(\omega_{12})}{A_{21} + B_{21} \rho(\omega_{12})} \tag{A2.15}$$

Since Einstein coefficients $A_{21,}$ $B_{21}$ and $B_{12}$ are independent of temperature, relation [A2.13] is verified irrespective of *T*. In particular, for $T \to \infty$ , we have:

$$\lim_{T\to\infty}\left(\frac{N_2}{N_1}\right)=\lim_{T\to\infty}\left[\frac{g_2}{g_1}e^{-\frac{(E_2-E_1)}{kT}}\right]\to\frac{g_2}{g_1}$$

Hence:

$$\frac{N_2}{N_1}=\frac{g_2}{g_1} \qquad [A2.16]$$

Similarly, Einstein coefficients $A_{21}$, $B_{21}$ and $B_{12}$ are independent of the spectral density of electromagnetic energy $\rho$ ($\omega_{12}$). When density $\rho$ ($\omega_{12}$) is very high, expression [A2.15] is reduced to:

$$\frac{N_2}{N_1}=\frac{B_{12}}{B_{21}} \qquad [A2.17]$$

Using [A2.13] and [A2.13], the relation between coefficients $B_{21}$ and $B_{12}$ is found. Hence:

$$g_1 B_{12}=g_2 B_{21} \qquad [A2.18]$$

For simple (non-degenerate) levels, Einstein coefficients $B_{21}$ and $B_{12}$ are equal: $B_{12} = B_{21}$ (since *statistical weights* $g_1 = g_2 = 1$).

## A2.2.5. *Relation verified by $A_{21}$ coefficient*

For large values of angular frequency, the spectral density of electromagnetic energy satisfies the *Rayleigh–Jeans law* [A.1.43], which is:

$$\rho(\omega)=\frac{\omega^2}{\pi^2 c^3}kT$$

Moreover, combining [A2.15] and [A2.13], we have:

$$\frac{N_2}{N_1}=\frac{B_{12}\rho(\omega_{12})}{A_{21}+B_{21}\rho(\omega_{12})}=\frac{g_2}{g_1}e^{-\frac{(E_2-E_1)}{kT}}$$

Hence:

$$\rho(\omega_{12})\left(g_1B_{12}-g_2B_{21}e^{-\frac{(E_2-E_1)}{kT}}\right)=g_2A_{21}e^{-\frac{(E_2-E_1)}{kT}}$$

which leads to:

$$\rho(\omega_{12})=\frac{g_2A_{21}}{\left(g_1B_{12}e^{(E_2-E_1)/kT}-g_2B_{21}\right)} \qquad [A2.19]$$

The classical Rayleigh–Jeans law is valid at low angular frequencies, therefore when condition $kT>>(E_2-E_1)=\hbar\omega_{12}$ is verified. The expansion up to second order of the exponential in [A2.19] following powers of $\hbar\omega_{12}/kT$ leads to:

$$\rho(\omega_{12})=\frac{g_2A_{21}}{g_1B_{12}\left(1+\frac{(E_2-E_1)}{kT}\right)-g_2B_{21}}=\frac{g_2A_{21}}{g_1B_{12}\left(1+\frac{\hbar\omega}{kT}\right)-g_2B_{21}}$$

Taking [A2.18] into account, we have after arrangement:

$$\rho(\omega_{12})=\frac{g_2}{g_1}\frac{A_{21}}{B_{12}}\frac{kT}{\hbar\omega} \qquad [A2.20]$$

But expression [A2.20] coincides with the Rayleigh–Jeans law [A.1.43]. Hence:

$$\rho(\omega_{12})=\frac{g_2A_{21}}{g_1B_{12}}\frac{kT}{\hbar\omega}=\frac{\omega^2}{\pi^2c^3}kT$$

Taking [A2.18] into account, the above leads to:

$$A_{21}=\frac{\hbar\omega^3}{\pi^2c^3}B_{21} \qquad [A2.21]$$

# Appendix 3

# Stefan–Boltzmann Law

In 1879, Joseph Stefan (1835–1893) discovered experimentally the law according to which *radiant exitance* $M_0$ (radiated power) per unit surface of a black body is proportional to the fourth power of temperature $T$:

$$M^0 = \sigma T^4 \qquad \text{[A3.1]}$$

In the law [A3.1], $\sigma$ designates *Stefan constant*. In 1884, Ludwig Boltzmann, a PhD student under Stefan's supervision, provided the theoretical proof for the empirical law [A3.1]. This is why it is often referred to as *Stefan–Boltzmann law*. The objective in what follows is to prove the law [A3.1] using first a thermodynamic approach and then Boltzmann's approach.

## A3.1. Thermodynamic approach to establishing Stefan's law

Let us consider a black enclosure of volume $V$ whose walls maintained at temperature $T$ emit in the vacuum an electromagnetic radiation that constitutes the black body radiation. Let $u$ be the *density of electromagnetic energy per unit volume*. The *internal energy* is $U = uV$. Hence:

$$dU = udV + Vdu \qquad \text{[A3.2]}$$

According to the *first law of thermodynamics* [HUL 86]:

$$dU = \partial Q + \partial W \qquad \text{[A3.3]}$$

In relation [A3.3], $\partial Q$ and $\partial W$ designate, respectively, the amounts of heat and work exchanged by the system with its environment.

---

For color versions of the figures in this book, see www.iste.co.uk/sakho/quantum1.zip.

*Introduction to Quantum Mechanics 1: Thermal Radiation and Experimental Facts Regarding the Quantization of Matter,* First Edition. Ibrahima Sakho.

As already explained in Appendix A1, the emergence of a photonic gas in the enclosure induces a radiation pressure of the gas on the walls of the cavity, according to expression [A.1.3]. In this expression, we have [HUL 86, NGÔ 08]:

$$P = \frac{1}{3}\frac{\overline{E}}{V} \qquad \text{[A3.4]}$$

Since $\overline{E}$ designates the total mean energy radiated throughout volume *V*, the $\overline{E}/V$ ratio represents the density of electromagnetic energy per unit volume *u*. Therefore, the electromagnetic radiation pressure is written as:

$$P = \frac{u}{3} \qquad \text{[A3.5]}$$

Moreover, due to the pressure exerted on the walls, an elementary work is done:

$$\partial W = -\,PdV$$

Using [A3.5], we have:

$$\partial W = -\frac{u}{3}dV \qquad \text{[A3.6]}$$

Furthermore, the elementary work [A3.6] is correlated with an exchange of heat between walls and radiation. This amount of heat is related to the *entropy of the photonic gas* by the relation:

$$dS = \frac{\partial Q}{T} \qquad \text{[A3.7]}$$

Using [A3.3], relation [A3.7] can be written as:

$$dS = \frac{1}{T}\left(dU - \partial W\right)$$

Considering [A3.2] and [A3.6], we have:

$$dS = \frac{1}{T}\left(udV + Vdu + \frac{u}{3}dV\right)$$

Hence:

$$dS = \frac{4}{3}\frac{u}{T}dV + \frac{V}{T}du \qquad [A3.8]$$

### A3.1.1. *Mathematics refresher*

Let *f* (*x*, *y*) be a *function of two independent variables x* and *y*. Its differential *df* is written as:

$$df = \frac{\partial f}{\partial x}dx + \frac{\partial f}{\partial y}dy$$

Let us consider $A(x,y) = \frac{\partial f}{\partial x}$ and $B(x,y) = \frac{\partial f}{\partial y}$. We have:

$$df = A(x,y)dx + B(x,y)dy$$

Differential *df* is a *total exact differential* and it verifies the *property of equality of cross-derivatives*:

$$\left.\frac{\partial A(x,y)}{\partial y}\right|_x = \left.\frac{\partial B(x,y)}{\partial x}\right|_y \qquad [A3.9]$$

Given that variables *u* (density of electromagnetic energy per unit volume) and *V* are independent, and in thermodynamics the only variations of *state functions* (internal energy *U*, entropy *S*, enthalpy *H*, etc.) are total differentials, using [A3.8] and [A3.9] leads to:

$$\frac{\partial}{\partial V}\left(\frac{V}{T}\right)_u = \frac{4}{3}\frac{\partial}{\partial u}\left(\frac{u}{T}\right)_V \qquad [A3.10]$$

Knowing that the internal energy *U* = *uV*, then the density of electromagnetic energy per unit volume depends on temperature similarly to *U* (e.g., the internal energy of a perfect gas depends only on temperature according to *Joule's first law*). Equation [A3.10] is then transformed as follows:

$$\frac{1}{T} = \frac{4}{3}\frac{1}{T} + \frac{4}{3}u\frac{d}{du}\left(\frac{1}{T}\right)$$

which is:

$$\frac{1}{T}=\frac{4}{3}\frac{1}{T}-\frac{4}{3}\frac{u}{T^2}\frac{dT}{du} \qquad [A3.11]$$

After separation of variables $u$ and $T$, we have:

$$\frac{du}{u}=4\frac{dT}{T} \qquad [A3.12]$$

The integration of differential equation [A3.12] leads to:

$$\ln\left(\frac{u}{C^{te}}\right)=4\ln T=\ln\left(T^4\right) \qquad [A3.13]$$

If in [A3.13] we have $C^{te} = a$, then:

$$u=aT^4 \qquad [A3.14]$$

CAUTION.– Result [A3.14] does not correspond to Stefan–Boltzmann law. The relation between the density of electromagnetic energy per unit volume $u$ and the *radiance* $L_0$ *of the black body* must be expressed. For this purpose, let us consider a luminous body radiating through a surface $dS$ in the solid angle $d\Omega$ (Figure A3.1).

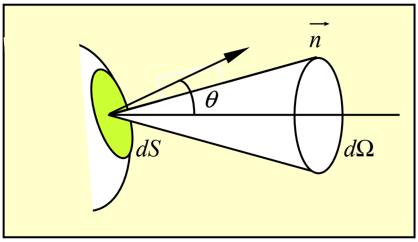

**Figure A3.1.** *Body radiating through an elementary surface dS in the solid angle dΩ*

Let $\vec{n}$ be the vector perpendicular to $dS$. The energy $d^3E$ radiated in the time interval $dt$ by the surface $dS$ in the solid angle $d\Omega$ is proportional to the product $dSd\Omega$. Since the radiative surface $dS$ follows *Lambert's law*, we have:

$$d^3E = L\cos\theta\, dSd\Omega dt \qquad [A3.15]$$

It is worth recalling that $L$ is the *radiance* of the radiative surface corresponding to the *light flux* (*light output*) emitted in the solid angle by the unit of radiative surface.

Let us now assume that the radiative surface is that of a black body of radiance $L_0$. Since the black body radiation is isotropic, let us consider the specific case of $\theta = 0$. The energy exiting a cylinder of base area $dS$ and length $l = cdt$ and generators parallel to the direction of propagation (Figure A3.6) is considered to be:

$$d^3E = L_0 dS d\Omega dt \qquad [A3.16]$$

Moreover, the energy contained in the cylinder is:

$$d^3E = dudV = dudScdt \qquad [A3.17]$$

In [A3.17], $du$ is the fraction of the density of electromagnetic energy contained in the cylinder and in the solid angle $d\Omega$.

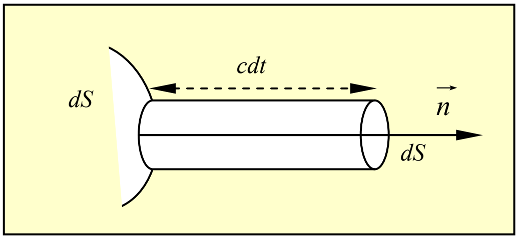

**Figure A3.2.** *Black body radiating in a cylinder of base dS and length cdt*

Equalizing [A3.16] and [A3.17], we have:

$$du = \frac{L_0}{c} d\Omega \qquad [A3.18]$$

Moreover, the solid angle $\Omega = 2\pi\,(1 - \cos\theta)$. For all the space, $\theta = \pi$ and $\Omega = 4\pi$. Integrating [A3.18] along all the directions in space, we then have:

$$u = \frac{4\pi}{c} L_0 \qquad [A3.19]$$

Using [A3.13], relation [A3.19] leads to:

$$\pi L_0 = \frac{ca}{4} T^4$$

Let us then consider that $\sigma = ca/4$. In this case, we have:

$$\pi L_0 = \sigma T^4 \qquad \text{[A3.20]}$$

Result [A3.20] actually corresponds to *Stefan–Boltzmann law* knowing that the *radiant exitance of the black body* $M^0 = \pi L_0$. It now remains to deduce the law [A3.20] following the approach adopted by Boltzmann. This will make it possible to theoretically express Stefan constant $\sigma$.

## A3.2. Stefan's law according to Boltzmann approach

Several mathematical formulae will prove useful in what follows, so they are summarized below.

(1) For a gamma integral ($\Gamma_n$), we have:

$$\Gamma_n = \int_0^\infty q^n \, e^{-aq} \, dx = \frac{n!}{a^{n+1}}, \ a \text{ is a positive constant.}$$

(2) Let us consider the following integral:

$$I_n = \int_0^\infty s^n \, e^{-bs^2} ds \ , \ b \text{ is a positive constant.}$$

Integrals $I_n$ verify a recurrence relation, as follows:

$$I_{n+2} = \frac{n+1}{2b} I_n ; \ I_0 = \frac{1}{2b}\sqrt{\frac{\pi}{b}} \ ; I_1 = \frac{1}{2b}$$

(3) *Riemann series* have the form: $\sum \frac{1}{n^\alpha}$. They are convergent if $\alpha > 1$.

(4) A *geometric progression*:

$$U_n = \sum_{k=0}^{n} U_0 q^k$$

is convergent if $|q| < 1$

Its sum $S_n$ is:

$$S_n = U_0 \frac{1-q^{n+1}}{1-q}, q \neq 1$$

$n$ is the number of terms in the progression whose common ratio is $q$ and first term is $U_0$.

(5) For a function $f(x)$, the *Taylor series expansion* around $x_0$ is written as:

$$f(x) = f(x_0) + \frac{(x-x_0)}{1!} f'(x_0) + \frac{(x-x_0)^2}{2!} f''(x_0) + ..... + \frac{(x-x_0)^n}{n!} f^n(x_0)$$

The *binomial expansion* around $x_0 = 0$ ($\alpha$ is a real number) can be deduced from the above:

$$(1+x)^\alpha = 1 + \alpha x + \alpha(\alpha-1)\frac{x^2}{2!} + \alpha(\alpha-1)(\alpha-2)\frac{x^3}{3!} + ...... + \alpha! \frac{x^n}{n!} + ......$$

(6) Finally, *Bernoulli coefficients* are denoted by $B_\text{k}$ and they have the following mathematical properties:

$$\sum_{n=1}^{\infty} \frac{1}{n^{2k}} = \frac{(2\pi)^{2k}}{2(2k)!} B_k, \; B_1 = \frac{1}{6}; B_2 = \frac{1}{30}; B_3 = \frac{1}{43}$$

These six points reviewed above are sufficient for proving Stefan–Boltzmann law.

The volume density of electromagnetic energy is related to the spectral density of energy by relation [A1.27], as follows:

$$du = \rho(\omega) d\omega)$$

Let us replace $\rho(\omega)$ by its expression [A1.45] in [A1.27], which leads to:

$$u = A \int_0^\infty \frac{\omega^3}{e^{\beta\hbar\omega} - 1} d\omega \qquad \text{[A3.21]}$$

where

$$A = \frac{\hbar}{\pi^2 c^3} \tag{A3.22}$$

Let us highlight in [A3.21] an integral of $\Gamma_{\mathrm{n}}$ type. We then obtain:

$$u = A\int_0^\infty \frac{\omega^3 e^{-\beta\hbar\omega}}{\left(e^{\beta\hbar\omega} - 1\right)\, e^{-\beta\hbar\omega}} d\omega = A\int_0^\infty \frac{\omega^3 e^{-\beta\hbar\omega}}{\left(1 - e^{-\beta\hbar\omega}\right)} d\omega$$

Hence:

$$u = A\int_0^\infty \omega^3 e^{-\beta\hbar\omega}\left(1 - e^{-\beta\hbar\omega}\right)^{-1} d\omega \tag{A3.23}$$

Let us consider: $x = -\, e^{-\beta\hbar\omega}$ $\alpha = -1$. Hence:

$$\left(1 - e^{-\beta\hbar\omega}\right)^{-1} = (1 + x)^{\alpha}$$

The Taylor series expansion of the term between parentheses in integral [A3.23] leads to:

$$\left(1 - e^{-\beta\hbar\omega}\right)^{-1} = 1 + e^{-\beta\hbar\omega} + \frac{2}{2!} e^{-2\beta\hbar\omega} + \frac{6}{3!} e^{-3\beta\hbar\omega} + \ldots\ldots + \frac{(-1)!}{n!} e^{-n\beta\hbar\omega}$$

Hence:

$$\left(1 - e^{-\beta\hbar\omega}\right)^{-1} = 1 + e^{-\beta\hbar\omega} + e^{-2\beta\hbar\omega} + e^{-3\beta\hbar\omega} + \ldots\ldots + e^{-n\beta\hbar\omega} \tag{A3.24}$$

Considering $q = e^{-\beta\hbar\omega}$, we have:

$$\left(1 - e^{-\beta\hbar\omega}\right)^{-1} = \sum_{k=0}^{n} U_0 q^k = 1 + q + q^2 + q^3 + \ldots\ldots qn \; ; U_0 = 1$$

This is a convergent series, therefore its sum is:

$$S_n = \frac{1 - e^{-(n+1)\beta\hbar\omega}}{1 - e^{-\beta\hbar\omega}}$$

At infinity, we have:

$$\left(1-e^{-\beta\hbar\omega}\right)^{-1} = \sum_{k=0}^{n} e^{-k\beta\hbar\omega} = \lim_{n\to\infty}\left[\frac{1-e^{-(n+1)\beta\hbar\omega}}{1-e^{-\beta\hbar\omega}}\right] = \frac{1}{1-e^{-\beta\hbar\omega}} \qquad [A3.25]$$

Result [A3.25] shows that the series $\left(1-e^{-\beta\hbar\omega}\right)^{-1}$ in equation [A3.23] is convergent. It can therefore be written as a Taylor series expansion to which the *cut-off condition* is applied at $n-1$ order (from 0 to $n-1$, there are actually $n$ terms). We then obtain:

$$u = A\int_0^\infty \omega^3 e^{-\beta\hbar\omega} d\omega\left[1+e^{-\beta\hbar\omega}+e^{-2\beta\hbar\omega}+...+e^{-(n-1)\beta\hbar\omega}\right]$$

Hence:

$$u = A\left[\int_0^\infty \omega^3 e^{-\beta\hbar\omega}d\omega+\int_0^\infty \omega^3 e^{-2\beta\hbar\omega}d\omega+....+\int_0^\infty \omega^3 e^{-n\beta\hbar\omega}d\omega\right] \qquad [A3.26]$$

Each integral in [A3.26] is of $\Gamma_n$ type (considering $a_n = n\beta\hbar$ ). Hence:

$$u = A\left[\frac{6}{1^4}\times\left(\frac{1}{\beta\hbar}\right)^4+\frac{6}{2^4}\times\left(\frac{1}{\beta\hbar}\right)^4+\frac{6}{3^4}\times\left(\frac{1}{\beta\hbar}\right)^4+....+\frac{6}{n^4}\times\left(\frac{1}{\beta\hbar}\right)^4\right]$$

Therefore:

$$u = 6\left(\frac{1}{\beta\hbar}\right)^4 A\left[\frac{1}{1^4}+\frac{1}{2^4}+\frac{1}{3^4}+....+\frac{1}{n^4}\right]$$

or:

$$u = 6\left(\frac{1}{\beta\hbar}\right)^4 A\sum_{n=1}^{\infty}\frac{1}{n^4} \qquad [A3.27]$$

The *Riemann series* in relation [A3.27] is convergent because $\alpha > 1$. Moreover, it can be noted that [A3.27] can be written in the form (considering $k = 2$):

$$u = 6\left(\frac{1}{\beta\hbar}\right)^4 A\sum_{n=1}^{\infty}\frac{1}{n^{2k}} \qquad [A3.28]$$

Or as a function of Bernoulli coefficients:

$$u = 6\left(\frac{1}{\beta\hbar}\right)^4 A \times \frac{(2\pi)^{2k}}{2(2k)!} B_k \bigg|_{k=2}$$

Hence:

$$u = 6\left(\frac{1}{\beta\hbar}\right)^4 A \times \frac{(2\pi)^4}{2(4)!} B_2 \qquad [A3.29]$$

Knowing that $B_2 = 1/30$, $\beta = 1\ /kT$ and $A = \hbar/\pi^2 c^3$ [A3.22], result [A3.29] is written as:

$$u = \frac{\pi^2 k^4}{15\hbar^3 c^3} T^4 \qquad [A3.30]$$

Using [A3.19], we have:

$$\frac{4\pi}{c} L_0 = \frac{\pi^2 k^4}{15\hbar^3 c^3} T^4$$

Hence:

$$\pi L_0 = \frac{\pi^2 k^4}{60\hbar^3 c^2} T^4 \qquad [A3.31]$$

Result [A3.31] actually leads to *Stefan–Boltzmann* law:

$$\pi L_0 = \sigma_{théo} T^4$$

In this relation:

$$\sigma_{théo} = \frac{\pi^2 k^4}{60\hbar^3 c^2} \qquad [A3.32]$$

We actually get the theoretical expression of Stefan–Boltzmann constant [1.35] if in [A3.32] we consider $\hbar = h/2\pi$.

**Ludwig Boltzmann** was an Austrian philosopher and physicist. In 1884, Boltzmann provided a theoretical proof of Stefan's empirical law (see Box 1.3). He is considered as the founder of statistical physics. In 1860, the Scottish physicist James Clerk Maxwell (1831–1879) established the distribution of molecular velocities in a gas at thermal equilibrium. Boltzmann generalized Maxwell's results. This led to the establishment of Maxwell–Boltzmann distribution law in the kinetic theory of gases. Constant $k$ in this law was named Boltzmann constant in his honor. Moreover, in 1877, Boltzmann formulated the relation between the entropy of a system in a given macroscopic state and the number of microscopic states that are consistent with it (Boltzmann formula). This led to the formulation of the second law of thermodynamics.

**Box A3.1.** *Boltzmann (1844–1906)*

# Appendix 4

# Dirac's Relativistic Theory

## A4.1. Fine structure perturbing Hamiltonian

Dirac's theory aims to unify quantum mechanics and the special theory of relativity. The formalism leading to the establishment of *Dirac's relativistic wave equation* is quite complex. Several notes related to this subject can be found in the references [DIR 67, COH 92, BIÉ 06, ASL 06]. The focus here will be on the analysis of the solution of Dirac's wave equation applied to *hydrogen-like systems* in the weakly relativistic domain. The Hamiltonian for weakly relativistic systems can be written as follows:

$$H = mc^2 + H_0 + W \qquad [A4.1]$$

In equation [A4.1], $mc^2$ is the rest energy of the electron, $H_0$ designates the Hamiltonian of a hydrogen-like system in the Coulomb field of potential energy $V(r) = -Ze^2/r$ and $W$ is the set of relativistic effects that have been ignored in Bohr's theory. The term $W$ is known as *fine structure Hamiltonian*. In Dirac's theory, the fine structure Hamiltonian appears in the power expansion of $v/c$ of the *relativistic Hamiltonian* $H$:

$$H = mc^2 + \frac{\vec{P}^2}{2m} + V(\vec{R}) - \frac{\vec{P}^4}{8m^3c^2} + \frac{1}{2m^2c^2}\frac{1}{R}\frac{dV(\vec{R})}{dR}\vec{L}\cdot\vec{S} + \frac{\hbar^2}{8m^2c^2}\Delta V(\vec{R}) + \ldots \qquad [A4.2]$$

This expansion features the rest energy of the electron $mc^2$ and the *non-relativistic Hamiltonian* $H_0$ (also known as *unperturbed Hamiltonian*):

$$H_0 = \frac{\vec{P}^2}{2m} + V(\vec{R})$$

---

For color versions of the figures in this book, see www.iste.co.uk/sakho/quantum1.zip.

*Introduction to Quantum Mechanics 1: Thermal Radiation and Experimental Facts Regarding the Quantization of Matter,* First Edition. Ibrahima Sakho.

The fine structure Hamiltonian can then be written according to [A4.1] and [A4.2]:

$$W = -\frac{\vec{P}^4}{8m^3c^2} + \frac{1}{2m^2c^2}\frac{1}{R}\frac{dV(\vec{R})}{dR}\vec{L}\cdot\vec{S} + \frac{\hbar^2}{8m^2c^2}\Delta V(\vec{R}) + \ldots \qquad [A4.3]$$

The terms featuring in this expansion are known as *fine structure terms* and their significance is explained below:

1) The term related to the electron's mass variation with velocity:

$$W_{mv} = -\frac{\vec{P}^4}{8m^3c^2}$$

2) The term related to the *spin-orbit interaction*:

$$W_{SO} = \frac{1}{2m^2c^2}\frac{1}{R}\frac{dV(\vec{R})}{dR}\vec{L}\cdot\vec{S}$$

3) *Darwin's term* taking into account the fact that the nucleus is not a point charge; it is also known as *contact term*:

$$W_D = \frac{\hbar^2}{8m^2c^2}\Delta V(\vec{R})$$

Considering these terms, the fine structure Hamiltonian [A4.3] can be written in the following form:

$$W = W_{mv} + W_{SO} + W_D + \ldots\ldots \qquad [A4.4]$$

The effects of these various terms are the following:

– $W_{mv}$ and $W_D$ make it possible to account for the global downward shift of the energy levels of the hydrogen-like systems with respect to Bohr semiclassic levels of energy;

– $W_{SO}$ makes it possible to remove the degeneracy of the energy levels characterized by the same value of the angular momentum quantum number $\ell$, but with a different value of the total quantum number $j = \ell \pm s$, $s$ is the spin of the electron.

## A4.2. Energy of the weakly relativistic hydrogen-like systems

Finding the exact solution of *Dirac's relativistic wave equation*, we have:

$$E_{nj} = mc^2 \left[ 1 + \left( \frac{Z\alpha}{n - \left( j + \frac{1}{2} \right) + \sqrt{\left( j + \frac{1}{2} \right)^2 - (Z\alpha)^2}} \right)^2 \right] \qquad [A4.5]$$

Expanding expression [A4.5] as powers of $Z\alpha$, we have:

$$E_{nj} = mc^2 \left\{ 1 - \frac{1}{2} \frac{(Z\alpha)^2}{n^2} \left[ 1 + \frac{1}{2} \frac{(Z\alpha)^2}{n} \left( \frac{1}{j + \frac{1}{2}} - \frac{3}{4n} \right) \right] + \ldots \right\} \qquad [A4.6]$$

Solution [A4.6] includes the rest energy $mc^2$ of the *optical electron* of hydrogen-like systems. Moreover, the *relativistic correction* introduces a term that is proportional to $(Z\alpha)^4$, compared to Bohr energy $-(Z\alpha)^2/2n^2$.

Dirac's theory makes it possible to account for many phenomena that are not explained within Bohr theory, such as the *spin of the electron*, the *fine structure* of the hydrogen atom, etc., but it is not a complete description of the hydrogen atom. For example, it cannot explain the *hyperfine structure* of the hydrogen atom requiring the consideration of the nuclear spin ignored in Dirac's theory or *Lamb shift* due to *zero-point oscillations* ($T = 0$K) of the *phonic vacuum*.

## A4.3. Effects of the fine structure perturbing Hamiltonian

Compared to the rest energy $mc^2$ of the electron, the total energy of hydrogen-like systems in the weakly relativistic domain is provided by the truncated expression according to Dirac's formula [A4.6]:

$$E_{nj} = -\frac{Z^2\alpha^2 mc^2}{2n^2} - \frac{Z^4\alpha^4 mc^2}{2n^3} \left( \frac{1}{j + 1/2} - \frac{3}{4n} \right) \qquad [A4.7]$$

Similarly, compared to the rest energy $mc^2$ of the electron, the relativistic Hamiltonian of hydrogen-like systems can be written in the following form:

$$H = H_0 + W_j^{mv} \qquad [A4.8]$$

In expression [A4.8], $W_j^{mv}$ is known as fine structure Hamiltonian or perturbing Hamiltonian, whose mean value is written according to [A4.8]:

$$\left\langle W_{n,j}^{mv} \right\rangle = -\frac{Z^4\alpha^4 mc^2}{2n^3}\left(\frac{1}{j+1/2} - \frac{3}{4n}\right) \qquad [A4.9]$$

The mean values of the fine structure Hamiltonian for $1s_{1/2}$, $2s_{1/2}$, $2p_{1/2}$, $2p_{3/2}$, $3s_{1/2}$, $3p_{1/2}$, $3p_{3/2}$, $3d_{3/2}$ and $3d_{5/2}$ quantum levels are the following:

– $1s_{1/2}$ level: $\left\langle W_{1,1/2}^{mv} \right\rangle = -\frac{1}{8}Z^4\alpha^4 mc^2$

– $2s_{1/2}$ and $2p_{1/2}$ levels: $\left\langle W_{2,1/2}^{mv} \right\rangle = -\frac{5}{128}Z^4\alpha^4 mc^2$

– $2p_{3/2}$ level: $\left\langle W_{2,3/2}^{mv} \right\rangle = -\frac{1}{128}Z^4\alpha^4 mc^2$ [A4.10]

– $3s_{1/2}$ and $3p_{1/2}$ levels: $\left\langle W_{3,1/2}^{mv} \right\rangle = -\frac{1}{72}Z^4\alpha^4 mc^2$

– $3p_{3/2}$ and $3d_{3/2}$ levels: $\left\langle W_{3,3/2}^{mv} \right\rangle = -\frac{1}{216}Z^4\alpha^4 mc^2$

– For $3d_{5/2}$ level: $\left\langle W_{3,5/2}^{mv} \right\rangle = -\frac{1}{648}Z^4\alpha^4 mc^2$

Results [A4.10] indicate a degeneracy of the energy levels having the same value of the internal quantum number $j$ but with a different value of the angular momentum quantum number $\ell$.

The effect of the fine structure Hamiltonian $W_j^{mv}$ on the levels for which $n = 1$ and $n = 2$ of the hydrogen atom can be illustrated using diagrams. Under the effect of the fine structure Hamiltonian, the ground level of the hydrogen atom shifts downwards with an amount equal to $-(1/8)\alpha^4 mc^2$ (Figure A4.1). It is worth noting that the Hamiltonian $W_j^{mv}$ features no fine structure on the ground level. Its effect is a shift of 1 $s_{1/2}$ level as a whole.

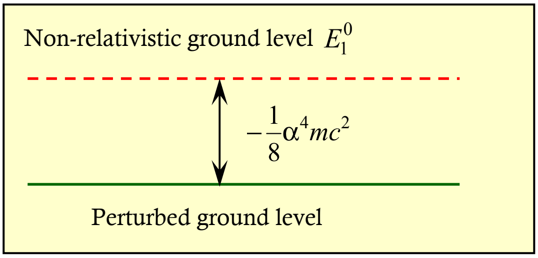

**Figure A4.1.** *Effect of the fine structure Hamiltonian on the ground level of the hydrogen atom*

As for the first excited level $n = 2$, the Hamiltonian $W_j^{mv}$ generates its split into three sublevels $2s_{1/2}$, $2p_{1/2}$ and $2p_{3/2}$, all shifted downwards with respect to level $n = 2$, as predicted by Bohr theory. These relative shifts are indicated in Figure A4.2.

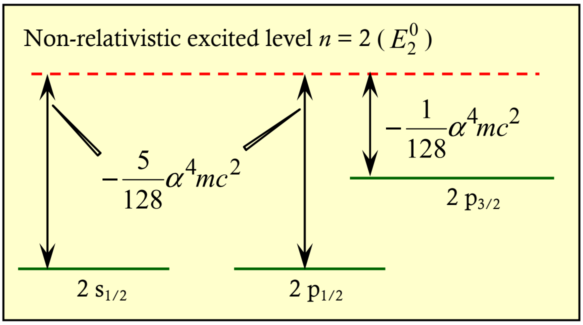

**Figure A4.2.** *Effect of the fine structure Hamiltonian on the first excited level of the hydrogen atom. This level splits into three sublevels. The degeneracy of $2s_{1/2}$ and $2p_{1/2}$ is worth noting*

Figure A4.2 indicates that the perturbing Hamiltonian $W_j^{mv}$ does not lift the degeneracy of $2\ s_{1/2}$ and $2\ p_{1/2}$ levels. Taking into consideration the zero-point oscillations of the photonic vacuum removes this degeneracy. This point will be clarified in Appendix A5.

# Appendix 5

# Fine and Hyperfine Structures, Natural Width

## A5.1. Lamb shift, physical vacuum

As already noted, all the quantum states of the hydrogen atom characterized by the same value of the principal quantum number $n$ and the total quantum number $j$ are degenerate and have therefore the same energy. This is due to the fact that, according to Dirac's relativistic theory, the energy of the hydrogen-like atom does not depend on the angular momentum quantum number $\ell$ .

Furthermore, in accordance with Dirac's theory, $2s_{1/2}$ and $2p_{1/2}$ levels overlap, and so do $3s_{1/2}$ and $3p_{1/2}$ levels, and $3p_{3/2}$ and $3\ d_{3/2}$ levels, as indicated by the mean values [A4.10]. To confirm **Dirac's** predictions, the degeneracy of $2s_{1/2}$ and $2p_{1/2}$ levels has been verified by analyzing the fine structure of the $H_\alpha$ line of the hydrogen atom.

In 1947, **Willis Eugene Lamb** and his student Robert Retherford conducted the first experiments related to the *electron excitation* of hydrogen atoms at the ground state [SIV 86]. The initial idea in *Lamb and Retherford experiments* was that the excited $2p_{1/2}$ level is unstable, while $2s_{1/2}$ level is *metastable* (*the lifetime of the hydrogen atom on* $2s_{1/2}$ *level being approximately* $10^8$ *times longer than in* $2p_{1/2}$ state).

Moreover, $2p_{1/2} \rightarrow 1s_{1/2}$ electron transition is allowed by the *selection rule* $\Delta\ell = \pm 1$, whereas $2s_{1/2} \rightarrow 1s_{1/2}$ transition is forbidden, since $\Delta\ell = 0$. Therefore, $2p_{1/2} \rightarrow 1s_{1/2}$ electron transition is $10^8$ faster than $2s_{1/2} \rightarrow 1s_{1/2}$ transition (*given that the lifetime of an atom in an excited state is equal to the inverse of the probability of spontaneous transition between the excited state and the underlying state*).

---

For color versions of the figures in this book, see www.iste.co.uk/sakho/quantum1.zip.

*Introduction to Quantum Mechanics 1: Thermal Radiation and Experimental Facts Regarding the Quantization of Matter,* First Edition. Ibrahima Sakho.

The simplified experimental set-up used by Lamb and Retherford is schematically shown in Figure A5.1.

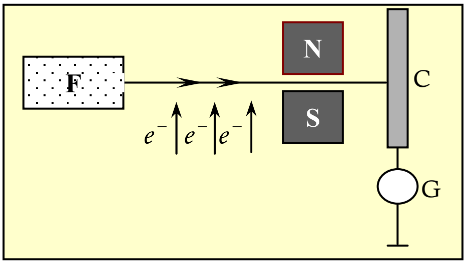

**Figure A5.1.** *Lamb and Retherford experimental setup*

Dihydrogen molecules are thermally dissociated in furnace *F*. The resulting hydrogen atoms are all in ground state $1s_{1/2}$. The atoms with horizontal velocities escape and hit a metallic target *C* that is connected to a galvanometer *G*. In this case, the galvanometer indicates no passage of electric current. This proves that the atoms are actually in the ground state, hence there is no energy transfer between these atoms and the free electrons in target *C*.

Making the junction of the atom beam with an electron beam some atoms are excited and pass to $2s_{1/2}$ and $2p_{1/2}$ states. Atoms that are in $2p_{1/2}$ state de-excite almost instantaneously and never reach the target. Only the atoms brought to metastable $2s_{1/2}$ state can reach the target. When they hit the target, they transfer an excitation energy of 10.2 eV (13.6 – 3.4 eV) to the free electrons in the target. This generates a flow of electrons and consequently the presence of an electric current that is sensed by the galvanometer. Assuming that $2s_{1/2}$ and $2p_{1/2}$ states do not overlap, the action of a magnetic field (of cyclic variation) on the hydrogen atoms that are in metastable $2s_{1/2}$ state generates stimulated transitions between $2s_{1/2}$ and $2p_{1/2}$ states.

When the rotational frequency of the magnetic field is equal to the frequency of the line of transition between $2s_{1/2}$ and $2p_{1/2}$ states, *magnetic resonance* takes place (*as result of the magnetic moment constantly directing the total angular momentum of the atom in parallel or antiparallel direction with respect to the magnetic field*). Since $2s_{1/2}$ levels are above $2p_{1/2}$ level, excited hydrogen atoms pass from $2s_{1/2}$ level to $2p_{1/2}$ level, then instantaneously to ground level $1s_{1/2}$. This is why some atoms that are in metastable state $2s_{1/2}$ de-excite to $2p_{1/2}$ state and never manage to reach the target. This leads to a decrease in the current intensity measured by the galvanometer. The minimum current intensity is then observed at resonance or when the speed of transitions between $2s_{1/2}$ and $2p_{1/2}$ states stimulated by the acting magnetic field is maximal.

Noting the minimum of this intensity enables us to determine the resonance frequency of the magnetic field, as well as the energy gap between the two quantum states $2s_{1/2}$ and $2p_{1/2}$. Lamb and Retherford experiments have shown that subshells $2s_{1/2}$ and $2p_{1/2}$ of the hydrogen atom are distinct and separated by a distance of 1,057.845 ± 0.09 MHz (Figure A5.2). This difference, and more generally any frequency difference between fine structure levels characterized by the same value of the principal quantum number $n$ and internal quantum number $j$, but by different values of the angular momentum quantum number $\ell$ is known as *Lamb shift*.

Let us note that since $2s_{1/2}$ level is above $2p_{1/2}$ level, $2s_{1/2} \to 2p_{1/2}$ transitions that are allowed by the selection rule $\Delta\ell = \pm 1$ can take place in the absence of any external field. Nevertheless, knowing that the probability of spontaneous transition is proportional to the cube of the frequency of the transition between the respective levels (see [A5.25]), then $2s_{1/2} \to 2p_{1/2}$ transition has an extremely weak probability to occur, given that the difference between these two levels is very small.

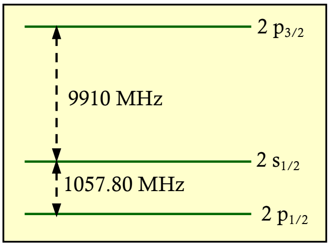

**Figure A5.2.** *Lamb shift of $2s_{1/2}$ and $2p_{1/2}$ levels*

In general, the *mean lifetime* of the excited states of atomic systems is of about $10^{-6}$–$10^{-8}$ s. The $2s_{1/2}$ state has a lifetime of $10^{-4}$ *s*. This is 100 to 10,000 times longer than the *mean lifetime of an excited state*. The $2s_{1/2}$ level is thus described as *metastable state*. Figure A5.3 illustrates the relative position of $2s_{1/2}$, $2p_{1/2}$ and $2p_{3/2}$ levels observed in Lamb and Retherford experiments.

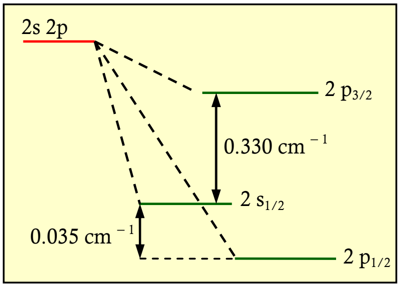

**Figure A5.3.** *Relative positions of $2s_{1/2}$, $2p_{1/2}$ and $2p_{3/2}$ levels into which the $n$ = 2 excited level of the hydrogen atom splits*

The degeneracy of 2s2p levels, its lifting under the *effect of the fine structure Hamiltonian* and the Lamb shift of $2s_{1/2}$ and $2p_{1/2}$ levels are particularly worth noting in this figure.

**Willis Eugene Lamb** was an American physicist. In 1947, Lamb and his student Robert Retherford observed the Lamb shift. He was awarded half of the 1955 Nobel Prize for physics "for his discoveries related to the fine structure of the hydrogen atom spectrum". The other half was awarded to the German-American physicist **Polykarp Kusch (1911–1993)** for having very precisely determined the magnetic moment of the electron.

**Box A5.1.** *Lamb (1913–2008)*

## A5.2. Hyperfine interaction, nuclear spin of the hydrogen atom

If the finite dimensions of the atomic nucleus and its motion-related effects are ignored, the energy of an atom is influenced only by the Coulombian nucleus – electrons and electron – electron interactions, as well as by the mutual interactions between electron spins (*spin-spin coupling*), the interaction between the orbital and spin magnetic moments of the electrons (*spin-orbit coupling*) and the dependence of electron mass on velocity, which is significant for the inner electrons of heavy atoms. If the nuclear spin denoted by $I$ is non-zero, the spin magnetic moment of the nucleus and the orbital and spin magnetic moments of the electron interact. This interaction generates what is known as *hyperfine structure*.

In 1928, the Russian physicists **Dobretsov** and **Terenin**, and independently the German physicist **Schüler,** discovered the hyperfine structure of sodium $^{23}$Na [FRI 85] when studying the radiative transition $3\ ^2S_{1/2} \rightarrow 3\ ^2P_{1/2,3/2}$. This transition corresponds to doublets denoted $D_1$ and $D_2$ of respective wavelengths $\lambda_1 = 589.5930$ nm ($3\ ^2P_{1/2} \rightarrow 3\ ^2S_{1/2}$ transition) and $\lambda_2 = 588.9963$ nm ($3\ ^2P_{3/2} \rightarrow 3\ ^2S_{1/2}$ transition). According to these studies, each of $D_1$ and $D_2$ lines splits into two other lines distanced by 2.3 pm and 2.1 pm, respectively (Figure A5.4) [SAK 08]. However, given the improvement of spectroscopic measurements, it was noted that in fact line $D_1$ splits into four components (*quadruplet*) and line $D_2$ into six components (*sextuplet*).

Taking the nuclear spin into consideration makes it possible to explain the split of $D_1$ and $D_2$ lines into several components or the hyperfine structure of the yellow line D of sodium. The electron configuration of the ground state of sodium $^{23}$Na is: $1s^2\,2s^2\,2p^6\,3s^1$. Knowing that the valence electron occupies the state $3s^1$ ($n = 3$, $\ell = 0$, 1 or 2), using the spectroscopic notation $^{2S+1}L_J$, the following spectral terms are obtained: $S = 1/2 \Rightarrow$ level multiplicity $2S + 1 = 2$; for $\ell = 0$, $J = 1/2$: the spectral term 3 $^2S_{1/2}$ is obtained; for $\ell = 1$, $J = 1/2$ or $3/2$: two spectral terms 3 $^2P_{1/2}$ and 3 $^2P_{3/2}$ are obtained.

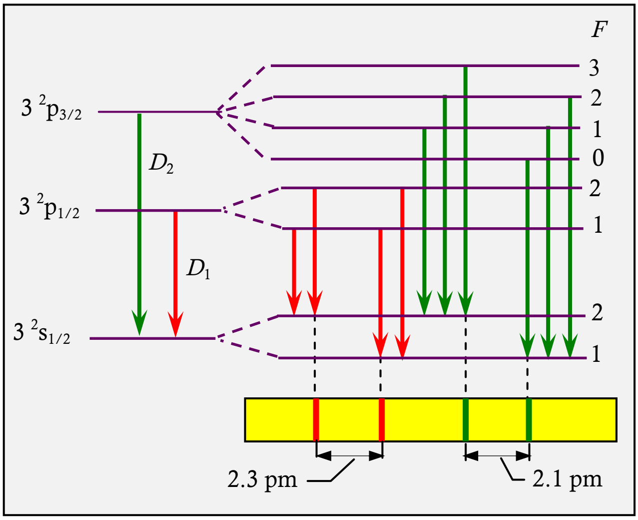

**Figure A5.4.** *Hyperfine structure of sodium $D_1$ and $D_2$ lines*

Moreover, if $\vec{J}$ is the total angular momentum summing the orbital and spin angular momenta of the valence electrons and $\vec{I}$ is the spin nuclear momentum, then the total angular momentum $\vec{F}$ of the atom is defined by the following relation:

$$\vec{F} = \vec{J} + \vec{I} \qquad [A5.1]$$

The quantum number $F$ takes all the values ranging between $J + I$ and $|J - I|$, therefore a total of $(2I + 1)$ values (if $J \geq I$). If $J \leq I$, $F$ takes a total of $(2J + 1)$ values.

For sodium 23, the *nuclear spin* is $I = 3/2$.

– for 3 $^2S_{1/2}$ and 3 $^2P_{1/2}$ terms, $J = 1/2$, therefore there are $2J + 1 = 2$ values for $F$, hence: $F = 3/2 + 1/2 = 2$ and $F = 3/2 - 1/2 = 1$

– for 3 $^2P_{3/2}$ term, $J = 3/2$; therefore $2J + 1 = 2I + 1 = 4$ values for $F$; hence: $F = 3/2 + 3/2 = 3$; $F = 3/2 + 3/2 - 1 = 2$ ; $F = 3/2 + 3/2 - 2 = 1$ and finally $F = 3/2 - 3/2 = 0$

In addition, for the hydrogen atom, the nuclear spin is $I = 1/2$ and the total quantum number is $J = 1/2$. Then the quantum number $F$ takes the values 0 and 1. The *hyperfine transition* 1 → 0 then generates the 21 cm wavelength (1,420 MHz; $5.9 \times 10^{-6}$ eV) line emitted by hydrogen in interstellar space. This line discovered in 1951 by **Edward Mills Purcell** and **Harold Ewen** marked the beginning of *radio astronomy*. The development in 1963 of the *hydrogen maser* made it possible to measure with excellent precision the frequency of 1 → 0 transition, hence:

$$\nu = 1420405751.768 \pm 0.001 \text{ Hz}$$

**Edward Mills Purcell** was an American physicist. He is especially well-known for his works on nuclear magnetic resonance. He shared the 1952 Nobel Prize for physics with the Swiss physicist Felix Bloch (1905–1983) “for their development of new methods for fine nuclear magnetic measurements and the subsequent discoveries”.

**Harold Ewen** was an American radio astronomer. He is especially known for his discovery together with Purcell of the 21 cm wavelength line of the hydrogen atom.

**Box A5.2.** *Purcell (1912–1997); Ewen (1922–2015)*

## A5.3. Anomalous Zeeman effect on the yellow line of sodium

Taking the electron spin into account, the experiments show that when a sodium atom is exposed to a uniform magnetic field, $D_1$ line splits into four components and $D_2$ line into six components. Our objective here is to theoretically verify these observations. A sodium atom in a magnetic field has the following energy:

$$E = E_0 - \overrightarrow{\mathcal{M}_J} \cdot \overrightarrow{B} \qquad [A5.2]$$

In [A5.2], the magnetic moment $\overrightarrow{\mathcal{M}_J}$ of the atom is given by:

$$\overrightarrow{\mathcal{M}_J} = g\gamma\overrightarrow{J} \qquad [A5.3]$$

In [A5.3], the quantity $g$ designates what is known as *Landé factor*, defined by the following expression:

$$g = \frac{g_s + g_\ell}{2} + \frac{g_s - g_\ell}{2} \times \frac{S(S+1) - L(L+1)}{J(J+1)} \qquad [A5.4]$$

Knowing that $g_\ell = 1$ and $g_s = 2$, Landé factor [A5.4] can be written in the following form:

$$g = \frac{3}{2} + \frac{S(S+1) - L(L+1)}{2J(J+1)} \qquad \text{[A5.5]}$$

Inserting [A5.3] in [A5.2] and considering that the projection of the angular momentum on the direction of the magnetic field is quantified, we obtain:

$$E = E_0 - gm_J \gamma B\hbar \qquad \text{[A5.6]}$$

Inserting Larmor frequency Ω in this relation, we have:

$$E = E_0 + gm_J \Omega\hbar \qquad \text{[A5.7]}$$

Formula [A5.7] determines the fine structure of the energy levels of the sodium atom and, consequently, the number of sublevels into which each level splits under the action of the magnetic field (assumed weak, to avoid the emergence of *Paschen–Back effect*). *Radiative transitions* between sublevels are governed by the selection rules:

$$\Delta m_J = \pm 1, 0 \qquad \text{[A5.8]}$$

Let us now theoretically explain the *anomalous Zeeman effect* on sodium $D_1$ and $D_2$ lines corresponding, respectively, to $3^2P_{1/2} \rightarrow 3^2S_{1/2}$ and $3^2P_{3/2} \rightarrow 3\ ^2S_{1/2}$ electron transitions. We first evaluate the Landé factor for each of these three sublevels $3^2P_{3/2}$, $3^2P_{1/2}$ and $3^2S_{1/2}$. Using [A5.11], we find:

– for $3^2P_{3/2}$ : $L = 1, S = 1/2, J = 3/2 \Rightarrow g = 4/3$

– for $3^2P_{1/2}$ : $L = 1, S = 1/2, J = 1/2 \Rightarrow g = 2/3$

– for $3^2S_{1/2}$: $L = 0, S = 1/2, J = 1/2 \Rightarrow g = 2$

According to [A5.13], the frequencies of the emitted lines are given by the relation:

$$\Delta E = \Delta E_0 + \Delta(gm_J)\Omega\hbar \qquad \text{[A5.9]}$$

It is worth noting that in [A5.9] Landé factor is not constant, therefore the variation of ($gm_J$) product should be taken into account. We therefore obtain:

$$\omega = \omega_0 + \Delta\,(gm_J)\Omega \qquad \text{[A5.10]}$$

The values of quantities $m_J$ and $gm_J$ relative to the three sublevels $3^2P_{3/2}$, $3^2P_{1/2}$ and $3^2S_{1/2}$ of the fine structure are grouped in Table A5.1 (in this table, the total magnetic quantum number $m_J$ takes values from $-J$ to $+J$).

|  | $^2P_{3/2}$ |  |  |  | $^2P_{1/2}$ |  | $^2S_{1/2}$ |  |
|---|---|---|---|---|---|---|---|---|
| $m_J$ | − 3/2 | − 1/2 | + 1/2 | + 3/2 | − 1/2 | +1/2 | − 1/2 | +1/2 |
| $gm_J$ | − 2 | − 2/3 | + 2/3 | + 2 | − 1/3 | +1/3 | − 1 | +1 |

**Table A5.1.** *Values of quantities $m_J$ and $gm_J$ relative to levels $3\ ^2P_{3/2}$, $3\ ^2P_{1/2}$ and $3\ ^2S_{1/2}$ of the sodium atom*

Using formula [A5.10] and the results summarized in Table A5.1, we determine the frequencies of the allowed lines resulting from the transitions between the fine structure sublevels of the sodium atom. The results summarized in Table A5.2 show that the $3^2P_{1/2} \to 3^2S_{1/2}$ line splits into four components, while the $3^2P_{3/2} \to 3^2S_{1/2}$ line splits into six components, which confirms the experimental observations.

| Transition | Line: $3\ ^2P_{1/2} \to 3\ ^2S_{1/2}$ |  |
|---|---|---|
| $m_J^{(1)} \to m_J^{(2)}$ | $(gm_J)^1 \to (gm_J)^2$ | Frequency |
| − 1/2 → +1/2 | −1/3 − 1 = − 4/3 | $\omega_0 - (4/3)\Omega$ |
| − 1/2 → − ½ | −1/3 + 1 = 2 /3 | $\omega_0 + (2/3)\Omega$ |
| +1/2 → +1/2 | 1/3 − 1 = − 2/3 | $\omega_0 - (2/3)\Omega$ |
| +1/2 → − ½ | −1/3 +1 = 4/3 | $\omega_0 + (4/3)\Omega$ |
| − 1/2 → +1/2 | −1/3 − 1 = − 4/3 | $\omega_0 - (4/3)\Omega$ |
| − 3/2 → +1/2 | Forbidden | – |
| − 3/2 → − 1/2 | −2 + 1 = −1 | $\omega_0 - \Omega$ |
| − 1/2 → +1/2 | −2 /3 − 1 = − 5/3 | $\omega_0 - (5/3)\Omega$ |
| − 1/2 → −1/2 | −2/3 + 1 = 1/3 | $\omega_0 + (1/3)\Omega$ |
| +1/2 → +1/2 | 2/3 − 1 = − 1/3 | $\omega_0 - (1/3)\Omega$ |
| +1/2 → −1/2 | 2/3 + 1 = 5/3 | $\omega_0 + (5/3)\Omega$ |
| +3/2 → +1/2 | 2 − 1 = 1 | $\omega_0 + \Omega$ |
| +3/2 → −1/2 | Forbidden | – |

**Table A5.2.** *Frequencies of allowed lines corresponding to transitions between the $3^2P_{3/2}$, $3^2P_{1/2}$ and $3^2S_{1/2}$ fine structure sublevels of the sodium atom*

Figure A5.5 presents a schematic illustration of the *anomalous Zeeman effect* on sodium $D_1$ and $D_2$ lines. Theoretical predictions (Cal) are compared to experimental data (Obs) [CHP 78, SAK 08].

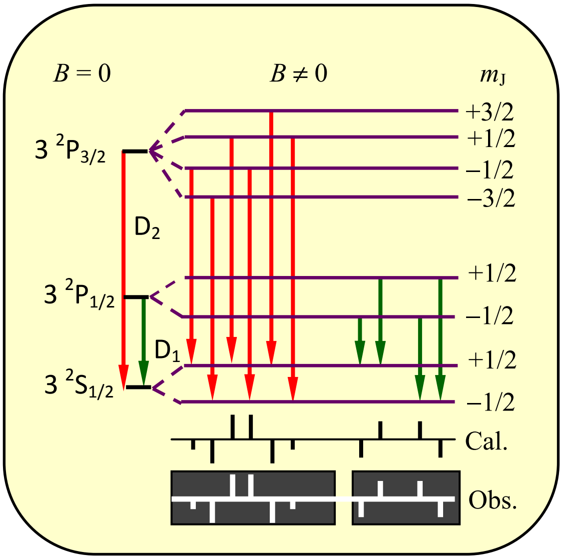

**Figure A5.5.** *Anomalous Zeeman effect on sodium $D_1$ and $D_2$ lines*

## A5.4. Lifetime of excited states

As already explained in Chapter 4, the experiments show that a given spectral line has a *natural width* (Figure 4.9) that can be explained based on the fourth Heisenberg's *time-energy uncertainty relation* [4.60].

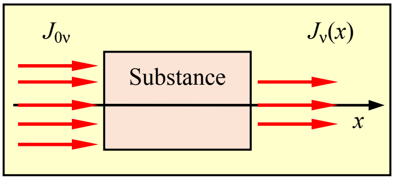

**Figure A5.6.** *Light beam of frequency $\nu$ crossing a substance of thickness dx*

One of the indirect methods for determining lifetime relies on the study of absorption lines. For this purpose, let us consider a light beam of frequency $\nu$ and initial intensity $J_{0\nu}$ penetrating a given substance of thickness $dx$ (Figure A5.6).

Light is partly absorbed when crossing through the substance, which results in an attenuation of intensity $J_\nu$.

The decrease in intensity $dJ_\nu$ is then written as:

$$dJ_\nu = -\, a_\nu J_\nu dx \qquad [A5.11]$$

In this expression, $a_\nu$ designates the *coefficient of absorption* of the studied substance. The variation of the coefficient of absorption as a function of frequency in the range of the absorbed line is shown in Figure A5.7.

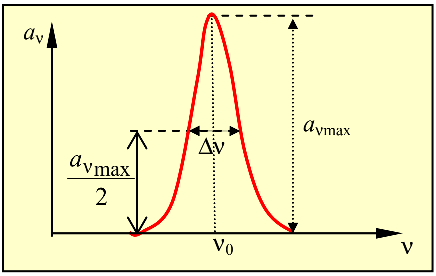

**Figure A5.7.** *Variation of the coefficient of absorption $a_\nu$ of a substance as a function of frequency*

The area enclosed by the contour of the line of *width at half-height* $\Delta\nu$ and the abscissa axis is given by the following integral relation:

$$\int a_\nu d\nu = \frac{\lambda_0^2}{8\pi} \cdot \frac{g_2}{g_1} \cdot \frac{N}{\tau} \qquad [A5.12]$$

In relation [A5.12], $\lambda_0$ designates the light wavelength corresponding to the maximum of absorption ($\nu_0 = c/\lambda_0$), $g_1$ and $g_2$ are the statistical weights of the energy levels between which absorption occurs, $N$ is the number of atoms in 1 $cm^3$ of substance and $\tau$ is the *mean lifetime* of atoms in the considered excited state. Determining the area enclosed by the absorption curve (Figure A5.7) makes it possible to measure the *natural width* of the spectral line, since $\Delta\nu = \Delta E/\hbar \sim 1/\tau$.

In the general case, the lifetime is of the order of $10^{-8}$ to $10^{-7}$ s and in some cases it can reach $10^{-6}$ s, as for example in the case of the $5^1S_0 - 5^3P_1$ transition line of cadmium Cd (Table A5.3).

Appendix A2 has introduced *Einstein integral coefficient of spontaneous emission* $A_{21}$ [A2.16] reflecting the *probability of spontaneous transition* $2 \rightarrow 1$

(Figure A2.1) per time unit of the considered quantum system $\mu$. This coefficient is therefore expressed in $s^{-1}$. In what follows, we shall prove that the lifetime of an excited state is the inverse of coefficient $A_{21}$.

Let $N_2(t)$ be the number of quantum systems filling the higher level 2 (Figure A2.1) at the moment $t$. The number $dN_2$ of transitions of the quantum systems toward the lower level 1 between $t$ and $t + dt$ is given by the expression:

$$-dN_2(t) = A_{21}N_2(t)dt \qquad [A5.13]$$

The "–" sign before the left term of equation [A5.13] reflects the decrease in time of population $N_2(t)$. The integration of [A5.13] between the limits $t = 0$ and $t$ leads to:

$$N_2(t) = N_{20}\, e^{-A_{21}t} \qquad [A5.14]$$

As already specified in Chapter 4, the lifetime of an excited state cannot be rigorously determined due to the randomness of the de-excitation of the levels of quantum systems.

A quantum system that is in excited state at moment $t$ can deexcite at moment $t + dt$ or remain in excited state for an infinitely long duration. This is why the *overall lifetime* of the quantum system is first determined and then the *mean lifetime* is deduced.

In the time interval between $t$ and $t + dt, -dN_2$ quantum systems have de-excited. Each of these quantum systems has therefore lived a duration $t$ in excited state. The lifetime $dT$ of $-dN_2$ quantum systems is then:

$$dT = -\, t dN_2(t) \qquad [A5.15]$$

Using [A5.13] and [A5.14], relation [A5.15] is written as:

$$dT = A_{21}N_{20}\, t\, e^{-A_{21}t}\, dt \qquad [A5.16]$$

The overall lifetime is obtained by integrating equation [A5.16] between the time limits 0 and ∞, hence:

$$T = A_{21}N_{20}\int_0^{\infty} te^{-A_{21}t}dt \qquad [A5.17]$$

Integral [A5.17] is of the type:

$$\int_0^\infty x^n e^{-\alpha x} dx = \frac{n!}{\alpha^{n+1}}$$

This then gives:

$$T = A_{21} N_{20} \times \frac{1}{(A_{21})^2}$$

Hence:

$$T = \frac{N_{20}}{A_{21}} \qquad [A5.18]$$

The mean lifetime is then $T/N_{20}$, which according to [A5.18] is:

$$\tau = \frac{1}{A_{21}} \qquad [A5.19]$$

CONCLUSION.– The mean lifetime of a quantum system is inversely proportional to the probability of spontaneous transitions.

As an example, let us estimate the lifetime in the visible range.

Einstein coefficient $A_{21}$ depends on the squares of the *matrix elements* $|d_{21}|^2$ *of (electric or magnetic) dipole transitions* of the quantum system $\mu$ and on the cubes of the *dipole transition frequency* $\omega_{21}$. According to quantum electrodynamics [CHP 78], we have:

$$A_{21} = \frac{4|d_{21}|^2 \omega_{21}^3}{3\hbar c^3} \qquad [A5.20]$$

Knowing that $\omega = 2\pi c/\lambda$, expression [A5.20] can be written as:

$$A_{21} = \frac{32\pi^3 |d_{21}|^2}{3\hbar \lambda_{21}^3} \qquad [A5.21]$$

*Given data*. $\lambda_{21}$ = 500 nm, $d_{21}$ = 1 D (*Debye symbol*, 1D = $10^{-18}$ uemcgs); $c = 3 \times 10^{10}$ cm · s$^{-1}$; $\hbar = 1.05 \times 10^{-27}$ erg · s

Relation [A5.21] gives:

$$A_{21} = 2.52 \times 10^{6}\,\mathrm{s}^{-1}\mathrm{s}$$

Or according to [A5.19]:

$$\tau \approx 4.0 \times 10^{-7}\,\mathrm{s}$$

Table A5.3 summarizes several values of the mean lifetime in excited states of a certain number of atomic systems.

| Atom | Transition | Wavelength (Å) | Lifetime (s) |
|---|---|---|---|
| H | $2\,^2P — 1\,^2S_{1/2}$ | 1,216 | $1.2 \times 10^{-8}$ |
| Na | $3\,^2P — 3\,^2S_{1/2}$ | 5,896.59 | $1.6 \times 10^{-8}$ |
| K | $4\,^2P — 4\,^2S_{1/2}$ | 7,699.76 | $2.7 \times 10^{-8}$ |
| Cd | $5\,^3P_1 — 5\,^1S_0$ | 3,261 | $2.5 \times 10^{-6}$ |
| Hg | $6\,^3P_1 — 6\,^1S_0$ | 2,537 | $1.0 \times 10^{-7}$ |

**Table A5.3.** *Mean lifetime of the excited states of several atomic systems*

NOTE.– Let us estimate the natural width $\Delta E$ of the ultraviolet line $\lambda = 253.7$ nm of the mercury atom. The lifetime of the excited state is $\tau = 1.0 \times 10^{-7}$ s (see Table A5.3). According to Heisenberg's fourth uncertainty relation:

$$\Delta E/\hbar \sim 1/\tau \Rightarrow \Delta E \sim \hbar/\tau = h/(2\pi\tau)$$

N.A.– $\Delta E = 6.63 \times 10^{-34}/(2 \times \pi \times 10^{-7} \times 1.6 \times 10^{-19}) = 6.6 \times 10^{-9}$ eV

## A5.5. Doppler effect, broadening of lines

From an experimental perspective, it is difficult to measure width $\Delta\nu$ or $\Delta E$ ($\Delta E = h\Delta\nu$) because of the influences due, on the one hand, to interactions between atoms and, on the other hand, to *Doppler effect*. By definition, the Doppler effect is the variation of the frequency of a light signal when the source and the emitter are in relative motion. If quantum systems in gaseous state collide, their mean lifetimes become shorter than their natural lifetimes. This generates an additional broadening known as *collisional broadening* $\Delta\omega_{\mathrm{col}}$ [CHP 78]. This collisional broadening increases with the pressure of the gas constituting the quantum systems. Consequently, the stronger the gas rarefaction, the more we have $\Delta\omega_{\text{col}} \to 0$.

Moreover, the dispersion of quantum systems velocities generates a broadening of the spectral lines by Doppler effect. To explain this effect, let us consider a quantum system $S$ at rest with respect to a reference frame $R_0$ that is in uniform rectilinear motion with velocity $v$ with respect to an observer $O$ attached to a fixed reference frame $R$ (Figure A5.8). According to the laws of transformation of the *wave four-vector* $\left(\vec{k}\,,\,\omega/c\right)$, we have [GRO 85]:

$$\begin{cases} k_{0x} = \gamma_{(v)}\left(k_x - \beta\omega/c\right) \\ k_{0y} = k_y \\ k_{0z} = k_z \\ \omega_0/c = \gamma_{(v)}\left(\omega/c - \beta k_x\right) \end{cases} \qquad [\text{A5.22}]$$

In the transformation relations [A5.22],

$$\beta = v/c \text{ and } \gamma_{(v)} = \left(1-\beta^2\right)^{-1/2}. \qquad [\text{A5.23}]$$

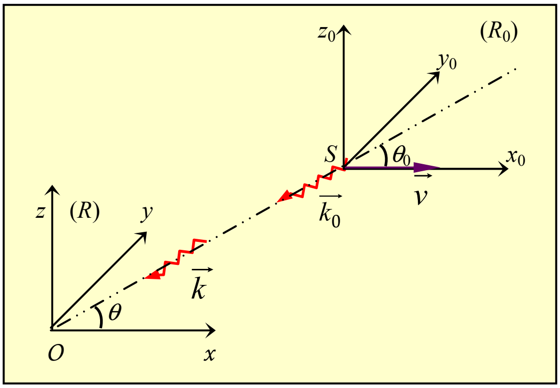

**Figure A5.8.** *A quantum system S emits a wave whose wave vector is $\vec{k}_0$ in the reference frame $R_0$. With respect to the reference frame R attached to the fixed observer O, the wave vector is denoted by $\vec{k}$*

Knowing that the projection $k_x$ of the wave vector along the axis $Ox$ in the reference frame $R$ is equal to $k_x = -k\cos\theta$, the fourth relation among the transformation relations [A5.22] gives:

$$\omega_0/c = \gamma_{(v)}\left(\omega/c + \beta k \cos\theta\right) \qquad [\text{A5.24}]$$

Knowing that $k = \omega/c$, this leads to:

$$\omega_0 = \gamma_{(v)}\omega(1 + \beta \cos\theta) \qquad \text{[A5.25]}$$

Replacing $\gamma_{(v)}$ and $\beta$ by their expressions [A5.22], we finally get:

$$\omega = \omega_0 \frac{\sqrt{1 - v^2/c^2}}{1 + \frac{v}{c}\cos\theta} \qquad \text{[A5.26]}$$

For *weakly relativistic quantum systems*, expression [A5.26] becomes:

$$\omega \cong \omega_0 \left(1 - \frac{v}{c}\cos\theta\right) \qquad \text{[A5.27]}$$

Expression [A5.27] shows that *Doppler broadening* disappears if radiation is emitted perpendicularly to the observation direction ($\theta = \pi/2$).

# References

[ANN 74] Annequin R., Boutigny J., *Électricité* 2, Librairie Vuibert, Paris, 1974.

[ASL 08] Aslangul C., *Mécanique quantique 2*, *développements et applications à basse énergie*, Éditions De Boeck Université, Brussels, 2008.

[ATT 05] Attaourti Y., *Mécanique quantique*, *une approche analytique*, Volume I, Afrique Orient, Casablanca, 2005.

[BAR 06] Barisien T., "Fil quantique idéal", available at: www.cnrs.fr/publications/imagesdelaphysique/couv.../15_Fil_ quantique_ ideal.pdf, 2006.

[BAS 17] Basdevant J.-L., *Introduction à la mécanique quantique*, 2nd ed., Éditions De Boeck Université, Brussels, 2017.

[BAY 17] Baye D., Dufour M., Fuks B., *Mécanique quantique, une introduction générale illustrée par des exercices résolus*, Ellipses Éditions Marketing S.A., Paris, 2017.

[BEL 03] Belorizky E., *Initiation à la mécanique quantique, approche élémentaire et applications*, Dunod, Paris, 2003.

[BIÉ 06] Biémont E., *Spectroscopie atomique,* Éditions De Boeck, Brussels, 2006.

[BLI 15] Blinder R., Étude par résonance magnétique nucléaire de nouveaux états quantiques induits sous champ magnétique : condensation de Bose-Einstein dans le composé DTN, Thesis, Grenoble Alpes University, 2015.

[CAR 79] Caratini R., *Physique, Chimie, Bordas Encyclopédie*, Bordas, Paris, 1979.

[CHP 78] Chpolski E., *Fondement de la mécanique quantique et structure de l'enveloppe électronique de l'atome*, Éditions Mir, Moscow, 1978.

[COH 77] Cohen-Tanoundji C., Diu B., Laloe F., *Mécanique quantique* 1, Hermann, Paris, 1977.

[COH 92] Cohen-Tanoundji C., Diu B., Laloe F., *Mécanique quantique* 2, Hermann, Paris, 1992.

*Introduction to Quantum Mechanics 1: Thermal Radiation and Experimental Facts Regarding the Quantization of Matter,* First Edition. Ibrahima Sakho.

[DAV 27] DAVISSON C., GERMER L.H., “Diffraction of electrons by a crystal of nickel”, *Physical Review*, vol. 30, no. 705, 1927.

[DEB 25] DE BROGLIE L., Recherches sur la théorie des Quanta, Annales de Physique, series 10, vol. 3, Paris, 1925.

[DIR 67] DIRAC P.A., *Les principes de la mécanique quantique*, Presses Polytechniques et Universitaires Romandes, Lausanne, 1967.

[DUA 08] DUARTE J.M.C., *The Photoelectric Effect: Determination of Planck’s Constant*, Massachusetts Institute of Technology, Massachusetts, 2008.

[DUB 04] DUBIN F., Exciton dans un fil quantique organique, Thesis, Paris VI University, Paris, 2004.

[DUT 16] DUTOIT C.-E., Étude par résonance paramagnétique électronique des composés organiques (TMTTF) 2X (X=AsF6, PF6 et SbF6), Thesis, Aix-Marseille University, 2016.

[END 07] ENDERLIN A., Contrôle cohérent des excitations électroniques dans une boîte quantique unique, Internship Report, Institut des NanoSciences de Paris, Paris, 2007.

[FRI 85] FRIDRINE S., MOVNINE S., *Bases physiques de la technique électronique*, Éditions Mir, Moscow, 1985.

[GRI 95] GRIFFITHS D.J., *Introduction to Quantum Mechanics*, Prentice Hall Inc., Upper Saddle River, 1995.

[GRI 08] GRIBON J.R., *Le chat de Schrödinger*, *la physique quantique et le réel*, Éditions Alphée, Jean-Paul Bertrand, Monaco, 2008.

[GRO 85] GROSSETETTE C.H., *Relativité restreinte et structure atomique de la matière,* Ellipses Éditions Marketing S.A., Paris, 1985.

[GUY 03] GUYMONT M., *Structure de la matière*, Belin Sup, Paris, 2003.

[HAM 90] HAMON M., PELLERIN F., GUERNET M., MAHUZIER G., *Chimie analytique, méthodes spectrales et analyse organique*, Volume 3, Masson, Paris, 1990.

[HLA 00] HLADIK J., CHRYSOS M., *Introduction à la mécanique quantique*, Dunod, Paris, 2000.

[HUL 86] HULIN M., MAURY J.-P., *Thermodynamique. Les deux principes*, Armand Colin, Paris, 1986.

[LAH 17] LAHOUAL M., Étude des propriétés optoélectroniques d’une diode laser à puits quantique à base du $Mg_xZn_{1-x}Se$, Thesis, University of Biskra, Algeria, 2017.

[MAR 00] MARCHILDON L., *Mécanique quantique*, Éditions De Boeck, Brussels, 2000.

[MIL 14] MILLOT N., NIÉPCE J.-C., *Cristallographie géométrique, cours, exercices et problèmes corrigés*, Lavoisier, Paris, 2014.

[MOI 16] MOISAN M., KÉROACK D., STAFFORD L., *Physique atomique et spectroscopie optique*, EDP Sciences, Grenoble, 2016.

[NGÔ 08] NGÔ C., NGÔ H., *Physique statistique*, Dunod, Paris, 2008.

[PAI 82] PAIS A., *"Subtle is the Lord...". The Science and the Life of Albert Einstein*, Oxford University Press, Oxford, 1982.

[PAR 01] PARKER M.P., *The Bohr-Sommerfeld Model of the Atom*, Project PHYSNET, Michigan State University, East Lansing, 2001.

[PAR 15] PARKS J.E., *The Compton Effect: Compton Scattering and Gamma Ray Spectroscopy*, The University of Tennessee, Knoxville, 2015.

[PÉR 86] PÉREZ J.-P., CHÉRY NICOLE S.-C., *Relativité et Quantification*, Masson, Paris, 1986.

[PER 11] PERROT O., Cours de rayonnement, I.U.T. de Saint-Omer, Department of Thermal Engineering and Energy, Dunkirk, 2011.

[PHI 03] PHILLIPS A C., *Introduction to Quantum Mechanics*, John Wiley & Sons Ltd., USA, 2003.

[PLO 16] PLOTNITSKY A., *The Principles of Quantum Theory, From Planck's Quanta to the Higgs Boson*, Springer International Publishing, Switzerland, 2016.

[RAP 06] RAPIOR G., SENGSTOCK K., BAEV V., *New Features of the Franck-Hertz Experiment*, American Association of Physics Teachers, College Park, Maryland, 2006.

[SAK 08] SAKHO I., Cours de Physique Atomique, Institut de Technologie Nucléaire Appliquée, Cheikh Anta Diop University, Dakar, 2008.

[SAK 11] SAKHO I., *Histoire de l'atome, de l'insécabilité au modèle probabiliste*, Éditions Publibook, Paris, 2011.

[SAK 12] SAKHO I., *Mécanique Quantique* 1, *exercices corrigés et commentés*, Hermann, Paris, 2012.

[SAK 13] SAKHO I., Formalisme général de la méthode de la constante d'écran par unité de charge nucléaire appliqué à l'étude de la photoionisation résonante des systèmes atomiques à plusieurs électrons, Thesis, Institut de Technologie Nucléaire Appliquée, Cheikh Anta Diop University, 2013.

[SAK 15] SAKHO I., Cours de propriétés électroniques liées au confinement, Master de Physique des Matériaux, UFR Sciences et Technologies, Ziguinchor University, Ziguinchor, 2015.

[SAK 16] SAKHO I., *Physique Terminales S*, Nouvelles Éditions Africaines du Sénégal, Dakar, 2016.

[SAK 18a] SAKHO I., *Screening Constant by Unit Nuclear Charge Method, Description & Application to the Photoionization of Atomic Systems*, ISTE Ltd, London and John Wiley & Sons, Inc., New York, 2018.

[SAK 18b] SAKHO I., *Electrostatique, magnétostatique & induction électromagnétique : Résumés de cours & 120 exercices corrigés*, Editions Ellipses, Paris, 2018.

[SIV 86] SIVOUKHINE D., *Cours de Physique Générale, Tome V : Physique Atomique et Nucléaire*, Éditions Mir, Moscow, 1986.

[STA 08] ST-AMAND A., *Physique des ondes*, Presses de l'Université du Québec, Quebec, 2008.

[STÖ 07] STÖCKER H., JUNDT F., GUILLAUME G., *Toute la physique*, Dunod, Paris, 2007.

[TAR 79] TARRASSOV L., *Bases physiques de l'électronique quantique*, Éditions Mir, Moscow, 1979.

[THA 08] THALLET R., VILLAIN L., FEBVRE P., *Dictionnaire de physique*, Éditions De Boeck, Brussels, 2008.

[THO 10] THORNTON S.T., Rex A., *Physique moderne*, De Boeck, Brussels, 2010.

[WIK 17] WIKIPÉDIA, "Règle de Klechkowski", available at: https://fr.wikipedia.org/wiki/Règle_de_Klechkowski, 2017.

[WIK 18] WIKIPÉDIA, "Chat de Schrödinger", available at: https://fr.wikipedia.org/wiki/Chat_de_Schrödinger, 2018.

# Index

*Introduction to Quantum Mechanics 1: Thermal Radiation and Experimental Facts Regarding the Quantization of Matter,* First Edition. Ibrahima Sakho.

# Other titles from

# ISTE

# in

# Waves

## 2019

DAHOO Pierre-Richard, LAKHLIFI Azzedine
*Infrared Spectroscopy of Triatomics for Space Observation*
*(Infrared Spectroscopy Set – Volume 2)*

RÉVEILLAC Jean-Michel
*Electronic Music Machines: The New Musical Instruments*

ROMERO-GARCIA Vicente, HLADKY-HENNION Anne-Christine
*Fundamentals and Applications of Acoustic Metamaterials: From Seismic to Radio Frequency*
*(Metamaterials Applied to Waves Set – Volume 1)*

## 2018

SAKHO Ibrahima
*Screening Constant by Unit Nuclear Charge Method: Description and Application to the Photoionization of Atomic Systems*

## 2017

DAHOO Pierre-Richard, LAKHLIFI Azzedine
*Infrared Spectroscopy of Diatomics for Space Observation*
*(Infrared Spectroscopy Set – Volume 1)*

PARET Dominique, HUON Jean-Paul
*Secure Connected Objects*

PARET Dominque, SIBONY Serge
*Musical Techniques: Frequencies and Harmony*

RÉVEILLAC Jean-Michel
*Analog and Digital Sound Processing*

STAEBLER Patrick
*Human Exposure to Electromagnetic Fields*

## 2016

ANSELMET Fabien, MATTEI Pierre-Olivier
*Acoustics, Aeroacoustics and Vibrations*

BAUDRAND Henri, TITAOUINE Mohammed, RAVEU Nathalie
*The Wave Concept in Electromagnetism and Circuits: Theory and Applications*

PARET Dominique
*Antennas Designs for NFC Devices*

PARET Dominique
*Design Constraints for NFC Devices*

WIART Joe
*Radio-Frequency Human Exposure Assessment*

## 2015

PICART Pascal
*New Techniques in Digital Holography*

## 2014

APPRIOU Alain
*Uncertainty Theories and Multisensor Data Fusion*

JARRY Pierre, BENEAT Jacques N.
*RF and Microwave Electromagnetism*

LAHEURTE Jean-Marc
*UHF RFID Technologies for Identification and Traceability*

SAVAUX Vincent, LOUËT Yves
*MMSE-based Algorithm for Joint Signal Detection, Channel and Noise Variance Estimation for OFDM Systems*

THOMAS Jean-Hugh, YAAKOUBI Nourdin
*New Sensors and Processing Chain*

TING Michael
*Molecular Imaging in Nano MRI*

VALIÈRE Jean-Christophe
*Acoustic Particle Velocity Measurements using Laser: Principles, Signal Processing and Applications*

VANBÉSIEN Olivier, CENTENO Emmanuel
*Dispersion Engineering for Integrated Nanophotonics*

## 2013

BENMAMMAR Badr, AMRAOUI Asma
*Radio Resource Allocation and Dynamic Spectrum Access*

BOURLIER Christophe, PINEL Nicolas, KUBICKÉ Gildas
*Method of Moments for 2D Scattering Problems: Basic Concepts and Applications*

GOURE Jean-Pierre
*Optics in Instruments: Applications in Biology and Medicine*

LAZAROV Andon, KOSTADINOV Todor Pavlov
*Bistatic SAR/GISAR/FISAR Theory Algorithms and Program Implementation*

LHEURETTE Eric
*Metamaterials and Wave Control*

PINEL Nicolas, BOURLIER Christophe
*Electromagnetic Wave Scattering from Random Rough Surfaces: Asymptotic Models*

SHINOHARA Naoki
*Wireless Power Transfer via Radiowaves*

TERRE Michel, PISCHELLA Mylène, VIVIER Emmanuelle
*Wireless Telecommunication Systems*

## 2012

LALAUZE René
*Chemical Sensors and Biosensors*

LE MENN Marc
*Instrumentation and Metrology in Oceanography*

LI Jun-chang, PICART Pascal
*Digital Holography*

## 2011

BECHERRAWY Tamer
*Mechanical and Electromagnetic Vibrations and Waves*

BESNIER Philippe, DÉMOULIN Bernard
*Electromagnetic Reverberation Chambers*

GOURE Jean-Pierre
*Optics in Instruments*

GROUS Ammar
*Applied Metrology for Manufacturing Engineering*

LE CHEVALIER François, LESSELIER Dominique, STARAJ Robert
*Non-standard Antennas*

## 2010

BEGAUD Xavier
*Ultra Wide Band Antennas*

MARAGE Jean-Paul, MORI Yvon
*Sonar and Underwater Acoustics*

## 2009

BOUDRIOUA Azzedine
*Photonic Waveguides*

BRUNEAU Michel, POTEL Catherine
*Materials and Acoustics Handbook*

DE FORNEL Frédérique, FAVENNEC Pierre-Noël
*Measurements using Optic and RF Waves*

FRENCH COLLEGE OF METROLOGY
*Transverse Disciplines in Metrology*

## 2008

FILIPPI Paul J.T.
*Vibrations and Acoustic Radiation of Thin Structures*

LALAUZE René
*Physical Chemistry of Solid-Gas Interfaces*

## 2007

KUNDU Tribikram
*Advanced Ultrasonic Methods for Material and Structure Inspection*

PLACKO Dominique
*Fundamentals of Instrumentation and Measurement*

RIPKA Pavel, TIPEK Alois
*Modern Sensors Handbook*

## 2006

BALAGEAS Daniel *et al.*
*Structural Health Monitoring*

BOUCHET Olivier *et al.*
*Free-Space Optics*

BRUNEAU Michel, SCELO Thomas
*Fundamentals of Acoustics*

FRENCH COLLEGE OF METROLOGY
*Metrology in Industry*

GUILLAUME Philippe
*Music and Acoustics*

GUYADER Jean-Louis
*Vibration in Continuous Media*